Modeling and mathematical analysis of complex systems: Kinetic and macroscopic approaches and applications in biology and vehicular traffic

Mohamed Zagour

UNIVERSITY CADI AYYAD

DOCTORAL THESIS

Modeling and mathematical analysis of complex systems: Kinetic and macroscopic approaches and applications in biology and vehicular traffic

Author:
Mohamed Zagour

Supervisors:
Prof. Mostafa Bendahmane
Prof. Fahd Karami
Prof. Driss Meskine

A thesis submitted in fulfillment of the requirements
for the degree of Doctor of Philosophy in applied mathematics

in the

Mathematics and modelling of complex systems
High School of Technology of Essaouira

Examiners:
Ali Souissi, Université Mohammed V, Rabat
Lahcen Maniar, Université Cadi Ayyad, Marrakech
Mouhcine Tilioua, Université Moulay Ismail , Meknes
Noureddine Alaa, Université Cadi Ayyad, Marrakech
Abdelghafour Atlas, Université Cadi Ayyad, Marrakech

04/23/2019

"People who wish to analyze nature without using mathematics must settle for a reduced understanding".

Richard Phillips Feynman

UNIVERSITY CADI AYYAD

Abstract

High School of Technology of Essaouira

Doctor of Philosophy in applied mathematics

Modeling and mathematical analysis of complex systems: Kinetic and macroscopic approaches and applications in biology and vehicular traffic

by Mohamed Zagour

This thesis deals with modeling and mathematical analysis of complex systems on the basis of kinetic and macroscopic approaches. The ultimate aims are to propose and to study a new kinetic and macroscopic-fluid models. Moreover, we show the possibility of passing from kinetic to macroscopic regimes. Specifically, we are concerned with the modeling and the mathematical analysis of the biological interacting populations living in a complex fluid medium in the first place. For this, we propose two new cross-diffusion-fluid systems. Next, we derive these systems from a new kinetic-fluid models by adopting micro-macro decomposition method. In the second place, we are interested to the modeling and mathematical analysis of vehicular traffic according to a kinetic theory for active particles approach. We propose a general mathematical structure which includes the features of the complex system under consideration and which appears to be the most important aspects of the dynamics to be retained by the modeling approach. Namely heterogeneity of the driver-vehicle subsystem, aggregation dynamics for vehicles with closed each other velocity, passing probability, variable properties of the road-environment where the dynamics occur and role of the external actions. To cut it short, each field of application contains three main parts:

- **Part of modeling and derivation:** In the first application, we propose a suitable kinetic-fluid models describing the evolution of the competing populations living in a complex fluid medium. We derive our proposed cross-diffusion-fluid systems from these models by using micro-macro decomposition method. In the second application, we propose a general mathematical kinetic structure accounting for all different possible type of interactions. Modeling each appeared terms in these mathematical structures leads to a derived models which permit to obtained macroscopic quantities such as the density, the flux and the mean velocity.
- **Part of mathematical analysis:** This part is devoted to prove the existence of weak solutions of the cross-diffusion-fluid systems by using Schauder fixed-point method for the first proposed system and nonlinear Galerkin method for the second proposed system.
- **Part of computational analysis:** Here, we adopt a suitable numerical methods and we present different simulations toward the validation of our proposed models and methods.

Keywords: *Kinetic-fluid derivation, cross-diffusion, Brinkman equations, Navier-Stokes systems, micro-macro decomposition, asymptotic preserving scheme, Schauder's fixed-point, nonlinear Galerkin method, finite volume method, finite element method, vehicular traffic, kinetic theory for active particles, games theory, local and mean field interactions.*

Résumé:

Cette thèse porte sur la modélisation et l'analyse mathématique de systèmes complexes sur la base d'approches cinétiques et macroscopiques. Les objectifs ultimes sont de proposer et d'étudier de nouveaux modèles cinétiques et macroscopiques-fluides. De plus, nous montrons la possibilité de passer de régimes cinétiques à macroscopiques. Nous nous intéressons plus particulièrement à la modélisation et à l'analyse mathématique des populations en interaction biologique qui vivent dans un milieu fluide complexe. Pour cela, nous proposons deux nouveaux systèmes de fluide à diffusion croisée. Ensuite, nous dérivons ces systèmes d'un nouveau modèle cinétique-fluide en adoptant la méthode de décomposition micro-macro. En second lieu, nous nous intéressons à la modélisation et à l'analyse mathématique du trafic vehiculaire selon une approche cinétique des particules actives. Nous proposons une structure mathématique générale qui inclut les caractéristiques du système complexe considéré et qui semble être l'aspect le plus important de la dynamique à retenir par l'approche de modélisation. Notament, l'hétérogénéité du sous-système conducteur-véhicule, la dynamique d'agrégation pour les véhicules dont les vitesses sont proches les unes des autres, la probabilité de dépassement, les propriétés variables de l'environnement routier où la dynamique se produit et le rôle des actions externes. Pour faire court, chaque application contient trois parties principales:

•**Partie de la modélisation et de la dérivation:** dans la première application, nous proposons un modèle cinétique-fluide approprié décrivant l'évolution des populations en interactions vivant dans un milieu fluide complexe. Nous avons dérivé les systèmes de diffusion croisée proposés à partir de ces modèles en utilisant la méthode de décomposition micro-macro. Dans la seconde application, nous proposons une structure mathématique générale prenant en compte tous les types d'interactions possibles. La modélisation de chacun des termes apparus dans ces structures mathématiques conduit à des modèles dérivés qui permettent d'obtenir des quantités macroscopiques telles que la densité, le flux et la vitesse moyenne.

•**Partie de l'analyse mathématique:** Cette partie est dédiée à la preuve de l'existence de solutions faibles des systèmes de diffusion-croisée-fluide en utilisant la méthode des points fixes de Schauder pour le premier système proposé et la méthode de Galerkin non linéaire pour le deuxième système proposé.

•**Partie de l'analyse numerique:** nous adoptons ici des méthodes numériques appropriées et présentons différentes simulations pour la validation des modèles/ méthodes que nous proposons.

Contents

Acknowledgements **xi**

1 General Introduction **1**
1.1 Introduction to the complex system in biology . . . 1
1.2 Introduction to the complex system in vehicular traffic . . . 3
1.3 Organization of the report . . . 5

I Kinetic-fluid derivation and mathematical analysis of cross-diffusion-fluid models **9**

2 Kinetic-fluid derivation and mathematical analysis of cross-diffusion-Brinkman system **11**
2.1 Introduction . . . 11
2.2 Derivation of cross-diffusion-Brinkman systems . . . 13
2.2.1 The kinetic-fluid model . . . 13
2.2.2 The equivalent micro-macro formulation . . . 15
2.2.3 Derivation of macroscopic systems . . . 18
2.2.4 Derivation of cross-diffusion-Brinkman system . . . 19
2.3 Mathematical analysis of the cross-diffusion-Brinkman system . . . 21
2.3.1 Existence of solutions for the approximate problems . . . 23
2.3.2 Existence result to the fixed problem . . . 24
2.3.3 The fixed-point method . . . 24
2.3.4 Existence of weak solutions . . . 26
2.4 Numerical analysis of micro-macro cross-diffusion-Brinkman system . . . 28
2.4.1 A time semi-implicit discretization . . . 28
2.4.2 Full discretization . . . 30
2.4.3 Boundary conditions . . . 31
2.4.4 Numerical results . . . 32
2.5 Conclusion and perspectives . . . 33

3 Kinetic-fluid derivation and mathematical analysis of nonlocal cross-diffusion-fluid system **37**
3.1 Introduction . . . 37
3.2 From improved kinetic-fluid model to generalized nonlocal cross-diffusion-fluid systems . . . 39
3.2.1 The improved kinetic-fluid model . . . 39
3.2.2 Micro-macro formulation . . . 40
3.2.3 Derivation of general macroscopic models . . . 42
3.2.4 Derivation of nonlocal cross-diffusion-fluid system . . . 43
3.3 Mathematical analysis . . . 44
3.4 Computational analysis . . . 51
3.4.1 A time semi-implicit discretization . . . 51

3.4.2 Computational analysis 1D . . . 52
Boundary layers conditions . . . 53
Numerical simulations . . . 54
3.4.3 Computational analysis 2D . . . 61
Effect of the nonlocal cross-diffusion-fluid . . . 61
Effect of external forces on the fluid dynamic and on the distribution of populations . . . 66
3.5 Conclusion . . . 67

II Mathematical modeling of vehicular traffic by kinetic theory approach of active particles 71

4 Representation and mathematical structures for one lane flow 73
4.1 Kinetic theory approach . . . 73
4.2 On the kinetic theory representation . . . 74
4.3 Mathematical structures . . . 75
4.3.1 Boltzmann models with binary interactions . . . 76
4.3.2 Models with Enskog-like interactions . . . 76
4.3.3 Boltzmann models with averaged binary interactions . . . 77
4.4 Discrete velocity models . . . 78
4.5 Kinetic Theory of Active Particles . . . 80
4.6 A fully-discrete-state kinetic model by Fermo and Tosin . . . 82

5 Multiscale continuum-velocity kinetic model for vehicular traffic with local and mean field interactions 85
5.1 Introduction . . . 85
5.2 Mathematical structures . . . 86
5.2.1 Representation . . . 86
5.2.2 Interaction domains and perceived quantities . . . 87
5.2.3 Mean field interactions . . . 87
5.2.4 Short range interactions . . . 88
5.2.5 Interactions with the external actions . . . 88
5.2.6 A mathematical structure toward modeling . . . 88
5.2.7 Critical analysis . . . 89
5.3 From mathematical structures to models . . . 89
5.3.1 Modeling accelerations . . . 89
5.3.2 Modeling the perceived density . . . 90
5.3.3 Modeling the encounter rate . . . 90
5.3.4 Modeling short range interactions . . . 91
Interaction with faster particles . . . 91
Interaction with slower particles . . . 91
5.3.5 Modelling external action . . . 93
5.3.6 Parameters and critical analysis . . . 93
5.4 Simulations toward validation of models . . . 94
5.4.1 Spatially homogeneous problem . . . 94
5.4.2 Spatially inhomogeneous problem . . . 97
Application: emerging of two clusters . . . 98

6 Conclusion and perspectives **101**
6.1 Summary 101
6.2 Looking ahead for perspectives 102

A Mathematical analysis of the spatially homogeneous problem **103**
A.1 Local existence 104
A.2 Global existence 105

List of Figures

1.1 Food chain of land and sea species 2
1.2 Illustration of asymptotic preserving schemes. 2
1.3 The three observation scales. 3
1.4 Vehicular traffic congestion in Casablanca city 4

2.1 Convergence order of the method for $\varepsilon \in \{1, 10^{-2}, 10^{-3}, 10^{-6}\}$ at time $t = 0.01$ ($M = 1$) for the density c in the left and the density s in the right obtained from micro-macro scheme. 33
2.2 The Subfigures (a), (b), (c), (d) present time dynamics of predators densities $c(t;x)$, while Subfigures (e), (f), (g), (h) present time dynamics of preys densities $s(t;x)$ at $t = 0.02, 0.04, 0.07, 0.1$ obtained from the AP scheme with $\varepsilon = 10^{-k}, k = 0;1;2;3;6$ and comparison with cross-diffusion-Brinkman system on the domain $[-1;1]$ and initial conditions are given by $c_0 = 0.65$ and $s_0 = \exp(30x^2)$ in the case: $u = 0$. 34
2.3 The Subfigures (a), (b), (c), (d) present time dynamics of predators densities $c(t;x)$, while Subfigures (e), (f), (g), (h) present time dynamics of preys densities $s(t;x)$ at $t = 0.02, 0.04, 0.07, 0.1$ obtained from the AP scheme with $\varepsilon = 10^{-k}, k = 0;1;2;3;6$ and comparison with cross-diffusion-Brinkman system on the domain $[-1;1]$ and initial conditions are given by $c_0 = 0.65$ and $s_0 = \exp(30(x+0.5)^2)$ in the case: $u = 1$. 35
2.4 Evolution of the densities $c(t;x)$ and $s(t;x)$ using micro-macro scheme for $\varepsilon = 10^{-6}$ in the case $u = 0$. 36
2.5 Evolution of the densities $c(t;x)$ and $s(t;x)$ using micro-macro scheme for $\varepsilon = 10^{-6}$ in the case $u = 1$ 36
2.6 Evolution of the densities $c(t;x)$ and $s(t;x)$ using micro-macro scheme for $\varepsilon = 10^{-6}$ in the case $u = -1$. 36

3.1 Test with local diffusitive functions: The first and second columns present, respectively, the dynamics of the densities $u_1(t;x)$ and $u_2(t;x)$ obtained from local micro-macro scheme with $\varepsilon = 10^{-k}$, $k = 0$, 1, 2, 3, 6, 9 against local cross-diffusion scheme with $v = 0$ at $t = 0.001, 0.003, 0.005, 0.007$. . . 56
3.2 Test with nonlocal diffusitive functions: The first and second columns present, respectively, the dynamics of the densities $u_1(t;x)$ and $u_2(t;x)$ obtained from nonlocal micro-macro scheme with $\varepsilon = 10^{-k}, k = 0$, 1, 2, 3, 6, 9 against nonlocal cross-diffusion scheme with $v = 0$ at successive time $t = 0.001, 0.003, 0.005, 0.007$. 57
3.3 Test with fluid effect: The first and second columns present, respectively, the dynamics of the densities $u_1(t;x)$ and $u_2(t;x)$ obtained from local micro-macro scheme with $\varepsilon = 10^{-k}, k = 0$, 1, 2, 3, 6, 9 against local cross-diffusion-fluid scheme with $v = 2.5$ at successive time $t = 0.001, 0.002, 0.003, 0.005$. . 58

3.4 From left to right column, the obtained numerical solutions of u_1, u_2, u_3 from the nonlocal (AP) scheme with $\varepsilon = 10^{-k}$, $k = 0, 1, 2, 3, 6, 9$, against of the nonlocal cross-diffusion model with $v = 0$ at successive time $t = 0.001, 0.005, 0.01, 0.06$. 60
3.5 Test 1: snapshot of the three densities u_1, u_2 and u_3 at successive time $t = 0, 0.2, 0.4, 0.6$ with $\mathbf{v} = \mathbf{0}$. 63
3.6 Cross-diffusion effect: patterns of the three interacting populations with different cross-diffusion parameters at final time $t = 0.1$. 64
3.7 Test 2: snapshot of the three densities u_1, u_2 and u_3 at successive time $t = 0, 0.2, 0.4, 0.6$ with $\mathbf{v}(x, y) = (1 - x)(1 + x)(1 - y)(1 + y)$. 65
3.8 Schematic of the spatial domain Ω with boundary conditions. 66
3.9 Evolution of the three interacting populations and snapshot of the fluid velocity and the pressure in the case: $\nabla\phi = (0, 0)$. 68
3.10 Evolution of the three interacting populations and snapshot of the fluid velocity and the pressure in the case: $\nabla\phi = (0, 1)$. 69

5.1 The probability density (discrete velocity) proposed by [21] vs our probability density (continuous velocity) in the case: $0.3 = v_* < v^* = 0.7$, $u = 1$ and $\rho^p = 0.6$. 92
5.2 The probability density (discrete velocity) proposed by [21] vs our probability density (continuous velocity) in the case: $0.7 = v_* > v^* = 0.3$, $u = 1$ and $\rho^p = 0.6$. 92
5.3 Fundamental diagram: flux q vs density ρ. 95
5.4 Free flow phase and fundamental diagram: flux q vs density ρ. 95
5.5 Fundamental diagram: kinetic energy E vs density ρ. 96
5.6 Fundamental diagram: mean velocity ξ vs density ρ. 96
5.7 Evolution of two clusters in the case of bad road condition ($\alpha = 0.3$). . . . 99
5.8 Evolution of two clusters in the case of good road condition ($\alpha = 0.95$). . 99

Acknowledgements

I would like to thank some people who accompanied me on this unforgettable experience. How not to start with my thesis supervisors, Prof. Mostafa Bendahmane, Prof. Fahd Karami and Prof. Driss Meskine, for their unconditional support throughout these years of thesis. I measure well my chance to have been supervised by three exceptional people on the human and professional levels.

My deepest sense of gratitude to Abdelghani Bellouquid, passed away on August 31, 2015, who introduced me into the fascinating research field of kinetic theories. It was a great honour to be able to take my first steps in research in contact with such a mathematician. He has been a great man, so kind and so modest. I need to thank him for make me change my view over several things in my life. I will never forget you. Rest in peace dear Abdel.

I would like to thank Prof. Lahcen Maniar, Prof. Ali Souissi and Prof. Mouhcine Tilioua for their interest in this work by agreeing to report on this manuscript. I also thank Prof. Noureddine Alaa, Prof. Abdelghafour Atlas and Prof. Mostafa Bendahmane who accepted to be examiners in my thesis jury.

I need to thank Prof. Nicola Bellomo, who always offered a continuous advice and encouragement throughout the course of this thesis. I thank him for the systematic guidance.

I have to thank Prof. Abdelghafour Atlas for his continuous support and advices. I thank him also for the many numerical tricks he shared with me.

As part of the Erasmus international mobility project between the University of Cadi Ayyad and the University of Granada, I had the opportunity to meet great people. I begin by thanking Prof. Juan Solar for the invitation, Prof. Juanjo Nieto and Prof. Juan Calvo for the collaboration that led to the writing of an article. I express my gratitude for their valuable explanations. Finally, I would like to thank my friend David Poyato for the good times spent together in Granada and wish him good luck with his thesis.

I acknowledge my gratitude to the Director of High School of Technology of Essaouira, Mr Belaïd Bougadir for giving me the access to the laboratory and who offered me an opportunity to be part of his team. Many thanks to Mr Khalid Elkalay the assistant director for his continuous support and his encouragements.

I also thank my friends for their presence and support during these years of hard work. Thanks to Mohamed Ben Marzoug, Mohamed El Guide, Brahim Rafik, Khadija Sadik and Lamia Ziad. Thanks to PhD students: Omar, Elmahdi, Sanae, Farah, Ahmed, Hassan, Hanane, Sara... and everyone else.

I deeply thank my family who has always supported me throughout these long years studies. Specially, my mother and my brother Abderrahmane who took care of me during those years, to cheer me up when it was needed and just to be here today...

Finally, I thank the National Center for Scientific and Technical Research for the financial support it gave me to carry out this research project and also the National Institute for Research in Computer Science and Automation of France for the invitation to visit Prof. Bendahmane in Bordeaux.

To the memory of my father Ahmed Zagour
and Abdelghani Bellouquid

Chapter 1

General Introduction

"Mathematical modeling is the art of translating problems from an application area into tractable mathematical formulations whose theoretical and numerical analysis provides insight answers and guidance useful for the originating application "[1]*. Thus, in the last few decades modeling of complex systems has been the subject of many investigations leading to an increasing number of research scientific papers. Furthermore, a wide set of possible applications, such as cross-diffusion systems, vehicular traffic and others, has directed the attention of mathematicians towards research domains usually populated by engineers, biologists or researchers with other expertise. Bearing these facts in mind, this thesis attempts to propose a new kinetic and macroscopic models leading to a much more better explanations and realistic results for the interacting populations living in complex flow and vehicular traffic applications.*

1.1 Introduction to the complex system in biology

During the last few decades, cross-diffusion systems have attracted a growth intention of mathematicians and biologists. Mainly for their ability to predict some interesting features in the studied field, for instance population dynamic in ecology. In mathematical biology applications, cross diffusion systems arise to model segregation phenomena between competing species. In real life, we observe that prey (for e.g. phytoplankton) has the tendency to keep away from predator (for e.g. zooplankton) at the same time predator has the tendency to get closer to the prey, see Figure 1.1-(a) and the following references [77, 84, 59] for more details. We observe also that many species live in complex flow so that species are transported in direction of the flow. Conversely, the velocity of the flow is under the influence of external forces including the density of species,see Figure 1.1-(b). Thus, it is interesting to study the dynamic of the interacting species on the basis of the coupled cross-diffusion-fluid model. In this thesis, we propose two new models: a nonlinear cross-diffusion system coupled with augmented Brinkman problem and nonlocal cross-diffusion system for multi-populations coupled within the incompressible Navier-Stokes. More in details, we deals with three main parts to study the aforesaid models:

- **kinetic-fluid derivation:** This first part aims to derive a general macroscopic models from kinetic-fluid equations. We start by presenting the kinetic-fluid models with a suitable scaling and their properties. Next, we perform the micro-macro decomposition method to obtain the equivalent formulation to the kinetic-fluid equations. Finally, we derive a general macroscopic models from the equivalent micro-macro formulation. Then by the suitable choices of different operators, we get the purpose cross-diffusion-fluid models.
- **Mathematical analysis:** This part deals with the proof of existence of weak solutions to the derived models. For the nonlinear cross-diffusion model coupled with Brinkman

[1] Prof. Dr. Arnold Neumaier, Fakultät für Mathematik, Universität Wien

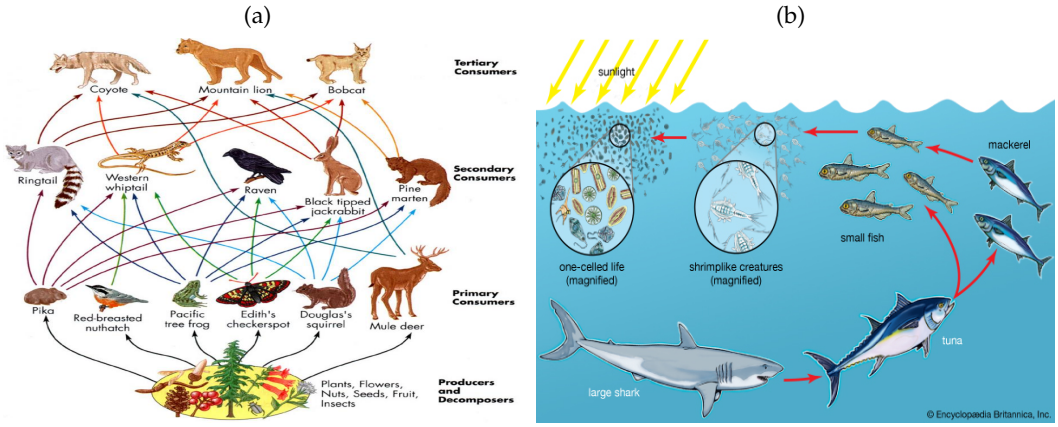

FIGURE 1.1: Food chain of land (a) and sea (b) species.[2]

problem, we use Schauder fixed-point. For the nonlocal cross-diffusion system for multi-populations coupled within the incompressible Navier-Stokes, we use the nonlinear Galerkin method.

• **Computational analysis:** Here, we deal with the discrete asymptotic preserving scheme. Indeed, we propose a numerical scheme uniformly stable along the transition from kinetic to macroscopic regimes (thus their computational complexity does not depend on the Knudsen parameter which models the distance between species). On the other hand, we show various numerical results which reflect some biological phenomena. For instance, interactions between preys and predators, fluid effect on the interacting species and external forces effects on the fluid dynamic and on the interacting species...

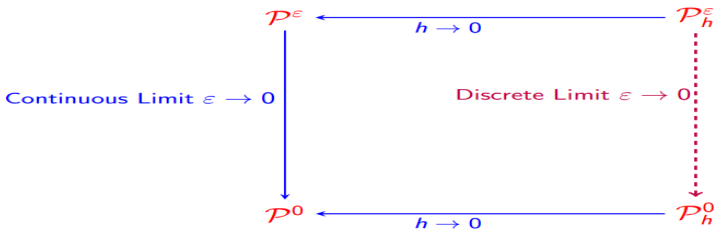

FIGURE 1.2: Illustration of asymptotic preserving schemes.

We mention that this thesis deals with the asymptotic preserving (AP) schemes. The idea of AP can be illustrated in Figure 1.2. Assume we start with a multi-scale kinetic model $\mathcal{P}^\varepsilon$ depending on Knudsen parameter ε. As Knudsen parameter tends to zero the model is approximated by a macroscopic model $\mathcal{P}^0$ which is independent of ε. Denote by $\mathcal{P}_h^\varepsilon$ the numerical discretization of $\mathcal{P}^\varepsilon$, where $h = (\Delta t, \Delta x, \Delta v)$ is the numerical parameter such as mesh size and or time step. The asymptotic limit of $\mathcal{P}_h^\varepsilon$, as ε tends to zeros with h fixed, if exists, is denoted by $\mathcal{P}_h^0$. The scheme $\mathcal{P}_h^\varepsilon$ is called AP if $\mathcal{P}_h^0$ is a good (consistent and stable) approximation of $\mathcal{P}^0$. In this thesis, we adopt micro-macro decomposition method. The idea of this technique is to write the unknown distribution function as a sum of an equilibrium and a deviation. It permits to reformulate the singularly perturbed kinetic system into an equivalent micro-macro formulation which is

[2]Source: (a) www.pltwa.com/uploads/2/7/8/2/27828107/food_webs_activity_plan.pdf
(b) Encyclopidia Britanica, Inc.

a regular perturbation of the derivative model. Thus, solving numerically the equivalent micro-macro formulation instead of the perturbed kinetic system will permit to shift automatically the limit problem, if the perturbation parameter ε is too small.

1.2 Introduction to the complex system in vehicular traffic

Nowadays, prediction and control of traffic attracts the intention of mathematicians researchers and engineers. With the increasing number of vehicles, the urban traffic system faces many problems, like, e.g., cities congestion and environmental pollution, see Figure 1.4. Indeed, traffic congestion induces not only long wasted time lost by users but also additional pollution of various kinds. In fact, it generates both an economic cost and environmental damage. An additional problem worth mentioning is the need to reduce car crashes, a human and social cost that is related not only to inadequate driving, but also to the planning of the flow conditions.

We believe that mathematical models can help to understand the dynamics of the traffic and give insight into questions like-what causes congestion, what determines the time and location of traffic break down, how does a congestion propagate. Thus, the aims of applied mathematicians and engineers has been to develop traffic models in order to predict the evolution of traffic flow. This in turn helps in answering how to handle urgent traffic issues and supports strategies of organizing traffic flow. Moreover, the organized traffic may reduce the travel time due to an optimized traffic distribution.

The existing literature of traffic flow is vast and characterized by various contributions taking into account modeling aspects, qualitative analysis of the existing models and simulations related to applications. Various types of models of traffic vehicular differing on the level of description can be found in the literature, see the reviews [18, 17, 66, 57]. The mathematical approach can be developed at the three observation and representation scales, namely microscopic, macroscopic, and statistical over the microscopic state, see Figure 1.3. Different mathematical structures correspond to each type of representation:

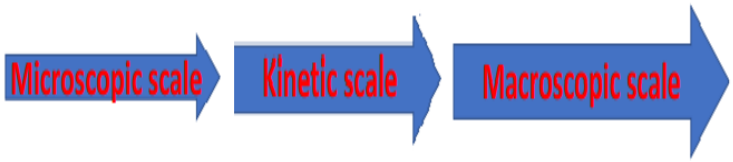

FIGURE 1.3: The three observation scales.

• **Microscopic models** focus on the behavior of individual vehicles, and study how one vehicle dynamically interacts with another. These models attempt to describe the overall characteristics of the system by integrating the characteristic of each individual vehicle. Mathematical models at the microscopic scale have a structure analogous to that of Newtonian dynamics. The model describes the acceleration of vehicles as the output of the action of surrounding vehicles. Microscopic models have three categories: car-following models, cellular automata models and sub-microscopic models. Car-following models analyze the vehicle following behavior in one lane. Cellular automata models view individual vehicles as self-driven particles, which is a collection of particles respond to a random perturbation by the motion of the other nearby particles. Sub-microscopic models describe more details, such as driver's psychological reactions, response to the traffic

(a) (b)

FIGURE 1.4: Vehicular traffic congestion in Casablanca city, Morocco.[3]

and car lights, etc.

• **Macroscopic models** mainly describe the spatio-temporal association rules of the traffic flow features, including traffic flow rate, velocity and density. The theoretical basis of dynamic macroscopic models is the fluid dynamics model, which is also known as the continuum model of traffic flow. Equations in fluid dynamics are a set of partial differential equations known as the Euler equations, expressing the conservation of mass, momentum and energy. The basic idea is to look at large scales so to consider cars as small particles and their density as the main quantity to be considered. They are especially used in the modeling framework of the large networks. Their current applications cover the traffic simulation for planning and infrastructure design.

• **Kinetic models** named also mesoscopic or statistical models present an intermediate step between the above two approach of model, they specific vehicle behavior in probabilistic terms. Thus, traffic is represented by small groups of vehicle for which the activities and interactions are described at a low level of detail. Mesoscopic models consist in the derivation of a Boltzmann type evolution equation for the statistical distribution function on the position and velocity of vehicles within a framework close to that of gas-kinetic theory. More details about kinetic models in next Chapter 4.

Thereafter, we focus on the kinetic approach due to its several advantages versus microscopic and macroscopic models. Indeed, kinetic theory is able to capture the complexity problems of vehicular traffic like the assumption of continuity of the distribution function and the assumption of homogeneity of the behavior of the driver, which have been criticized by [40]. Moreover, on the one hand they can be more fundamentally justified than the standard macroscopic models, leading to a better justification of the macroscopic models and potentially to more accurate results. On the other hand, compared to microscopic models, kinetic theory requires a lower number of equations, which makes them more accessible by computational and mathematical analysis.

It is worth stating three key aspects of the complexity of vehicular traffic flow that models should cope with.

• **Ability to express strategy**. Systems driver-vehicle have a *self-organization* abilities affected by the state of surrounding environment. The individual behavior of the driver-vehicle is heterogeneously distributed among vehicles.

[3]Source: (a) www.actu-maroc.com/embouteillages-attendus-pour-les-departs-en-vacances
(b) www.aujourdhui.ma/societe/circulation-et-stationnement-dans-les-grandes-villes

• **Interactions and multiscale effects**. Interactions among vehicles are microscopic interactions. Probably the most striking effect of these interactions is the spontaneous emergence of self-organized flow patterns, that can be clearly seen at larger scales. The influence of smaller on larger scales can be viewed as *micro-to-macro* scaling. The opposite influence is possible. This induces *outer-to-inner* multiscale couplings, which make vehicles interactions nonlinearly additive.
• **Large deviations and loss of determinism**. The expression of the strategic ability and the characteristics of the interactions among vehicles described above can be considered under either a *deterministic* or a *stochastic* perspective. The former is appropriate in normal conditions, when a standard rational attitude can be identified, over which large deviations are not expected. Conversely, the latter is particularly suited for addressing cases in which irrational behaviors cannot be excluded, which might induce large deviations.

1.3 Organization of the report

The thesis is organized in two main parts: Each part contains two chapters and each chapter will be introduced by a short motivational section.

First part: This part deals with the biological interacting populations application.

Chapter 2. We summarize the results published in the paper [24]. As it mentioned above, several competing species are living in a complex fluid medium. Thus, it is so important to model this real observation. This is in fact the main objective in [24], where we propose and we study a new nonlinear model describing dynamical interaction of two species within viscous flow. Our proposed model is a nonlinear cross-diffusion system coupled with Brinkman problem written in terms of velocity fluid $\boldsymbol{u}$, vorticity $\boldsymbol{\omega}$, pressure p, and describing the flow patterns driven by an external source depending on the densities of species c and s. Our proposed system is as follows

$$
\textit{System } 1 \begin{cases}
c_t + \boldsymbol{u}\cdot\nabla c - \operatorname{div}\Big[\big(D_c(c) + 2\,a_{11}\,c + a_{12}\,s\big)\,\nabla c + a_{12}\,c\,\nabla s\Big] = H_c(c,s), & \text{in } \Omega_T,\\
s_t + \boldsymbol{u}\cdot\nabla s - \operatorname{div}\Big[\big(D_s(s) + a_{21}\,c + 2\,a_{22}\,s\big)\,\nabla s + a_{21}\,s\,\nabla c\Big] = H_s(c,s), & \text{in } \Omega_T,\\
\mathbb{K}^{-1}\boldsymbol{u} + \sqrt{\mu}\,\mathbf{curl}\,\boldsymbol{\omega} + \nabla p = Q(c,s)\boldsymbol{g} + \mathbf{F}, & \text{in } \Omega_T,\\
\boldsymbol{\omega} - \sqrt{\mu}\,\mathbf{curl}\,\boldsymbol{u} = \mathbf{0}, & \text{in } \Omega_T,\\
\operatorname{div}\boldsymbol{u} = 0, & \text{in } \Omega_T,\\
\Big(c\boldsymbol{u} - (D_c(c) + 2\,a_{11}\,c + a_{12}\,s)\nabla c - a_{12}\,c\nabla s\Big)\cdot\eta = 0, & \text{on } \partial\,\Omega_T,\\
\Big(s\boldsymbol{u} - (D_s(s) + a_{21}\,c + 2\,a_{22}\,s)\nabla s - a_{21}\,s\nabla c\Big)\cdot\eta = 0, & \text{on } \partial\,\Omega_T,\\
\boldsymbol{u}\cdot\eta = u_\partial,\ \boldsymbol{\omega}\times\eta = \boldsymbol{\omega}_\partial, & \text{on } \partial\,\Omega_T,\\
c(t=0,x) = c_0(x), \quad s(t=0,x) = s_0(x), & \text{in } \Omega,
\end{cases}
$$

where $D_c(c)$, $D_s(s)$ are the nonlinear diffusitive functions and $a_{ij} > 0$ for $i,j = 1,2$ is known as self and cross-diffusion rates. The parameter μ is the fluid viscosity in the considered regime, it is assumed independent of the densities of species c and s, $\mathbb{K}(x)$ is the permeability tensor rescaled with viscosity, $Q(c,s)\boldsymbol{g}$ represents the force exerted by the densities on the fluid motion, and $\mathbf{F}(t,x)$ is an external force applied to the porous medium. The functions H_c and H_s are the reaction terms. A typical example of H_c and H_s is given by Lotka-Voltera (logistic) type growth term.

In the first part, we derive a macroscopic models from the following kinetic-fluid equations by using the micro-macro decomposition method:

$$\textit{Model}\,1\begin{cases}\big(\varepsilon\partial_t+\xi\cdot\nabla_x\big)f_1^\varepsilon=\frac{1}{\varepsilon}\mathcal{T}_1[f_2^\varepsilon](f_1^\varepsilon)+G_1(f_1^\varepsilon,f_2^\varepsilon,\boldsymbol{u},\xi),\\[2mm]\big(\varepsilon\partial_t+\xi\cdot\nabla_x\big)f_2^\varepsilon=\frac{1}{\varepsilon}\mathcal{T}_2[f_1^\varepsilon](f_2^\varepsilon)+G_2(f_1^\varepsilon,f_2^\varepsilon,\boldsymbol{u},\xi),\\[2mm]\mathbb{K}^{-1}\boldsymbol{u}+\sqrt{\mu}\,\mathbf{curl}\,\boldsymbol{\omega}+\nabla p=Q\Big(\int_V f_1^\varepsilon d\xi,\int_V f_2^\varepsilon d\xi\Big)\,\boldsymbol{g}+\mathbf{F},\\\boldsymbol{\omega}-\sqrt{\mu}\,\mathbf{curl}\,\boldsymbol{u}=\mathbf{0},\\\operatorname{div}\boldsymbol{u}=0,\end{cases}$$

where f_1, f_2 are the generalized distribution functions which depend on time t, position $x\in\Omega\subset\mathbb{R}^d$ and velocity $\xi\in V\subset\mathbb{R}^d$. The Knudsen parameter ε measures the distance of the system to its equilibrium. Specifically, when ε is small, the system is close to an equilibrium state, while for large ε, the system is far from equilibrium. Moreover, $\mathcal{T}_1[f_2]$, $\mathcal{T}_2[f_1]$ and $G_i, i=1,2$ are, respectively, the turning and interaction operators. Comparing to the work by [11], the novelty in our work is that we derive the cross-diffusion system with nonlinear diffusitive functions instead of a diffusion with constants. Moreover, our system is coupled to the augmented Brinkman problem.

On the basis of Schauder fixed-point theory, we prove the existence of weak solutions for the derived model in the second part. The last part is devoted to develop a one dimensional finite volume approximation for the kinetic-fluid model, which are uniformly stable along the transition from kinetic to macroscopic regimes. Our computation method is validated with various numerical tests.

Chapter 3. We summarize the results in our paper [7]. Motivated by our work in [24], here we propose and we study a generalized system. Our proposed system is contains a nonlocal diffusion and a nonlinear cross-diffusion describing the dynamic of interacting multi-populations living in a complex medium governed with the incompressible Navier-Stokes equation (non-stationary fluid flow). Our proposed system is written as follows

$$\textit{System}\,2\begin{cases}\partial_t u_i+\mathbf{v}.\nabla_x u_i-\operatorname{div}_x\Big(d_{u_i}\Big(\int_\Omega u_i dx\Big)\nabla_x u_i+\sum_{j=1}^n\mathcal{A}_i^j(u_1,...,u_n)\nabla_x u_j\Big)=F_i, & \text{in }\Omega_T,\\[2mm]\partial_t\mathbf{v}-\nu\Delta\mathbf{v}+(\mathbf{v}.\nabla_x)\mathbf{v}+\nabla_x p+Q(u_1,...,u_n)\nabla_x\phi=\mathbf{0},\ \operatorname{div}_x\mathbf{v}=0, & \text{in }\Omega_T,\\[2mm]\mathbf{v}=\mathbf{0}\text{ and }\Big(d_{u_i}\Big(\int_\Omega u_i dx\Big)\nabla_x u_i+\sum_{j=1}^n\mathcal{A}_i^j(u_1,...,u_n)\nabla_x u_j\Big)\cdot\eta=0, & \text{on }\partial\Omega_T,\\[2mm]u_i(t=0,x)=u_{i,0}(x),\ \mathbf{v}(t=0,x)=\mathbf{v}_0(x), & \text{in }\Omega,\end{cases}$$

for $i=1,...,n$. u_i is the density of $i-th$ population, d_{u_i} is the nonlocal diffusivitie functions assumed to be depend on the whole of each population in the domain rather than on the local density, $\mathcal{A}_i^j$ $(i,j=1,...,n)$ is the nonlinear cross-diffusion matrix elements, $\mathbf{v}$ is the fluid velocity, p is the fluid pressure, ν is the fluid viscosity, $Q(u_1,...,u_n)\nabla\phi$ represents the external force applied to the incompressible fluid and $\boldsymbol{n}$ is the unit outward normal to Ω on $\partial\Omega$. Finally, F_i is the reaction terms for $i=1,...,n$.

The first part of this chapter is devoted to the derivation of the proposed system from the following nonlocal kinetic-fluid model

$$\textit{Model } 2 \begin{cases} \varepsilon \partial_t f_i^\varepsilon + \xi \cdot \nabla_x \mathcal{F}_i(f_i^\varepsilon) = \frac{1}{\varepsilon} \mathcal{T}_i[f_1^\varepsilon, ..., f_{i-1}^\varepsilon, f_{i+1}^\varepsilon, ..., f_n^\varepsilon](f_i) + G_i(f_1^\varepsilon, ..., f_n^\varepsilon, \xi, \mathbf{v}), \\ \partial_t \mathbf{v} - \nu \Delta_x \mathbf{v} + (\mathbf{v} \cdot \nabla_x)\mathbf{v} + \nabla_x p + Q\big(\int_V f_1^\varepsilon d\xi, ..., \int_V f_n^\varepsilon d\xi\big)\nabla_x \phi = \mathbf{0}, \ \ \mathrm{div}_x \mathbf{v} = \mathbf{0}, \\ f_i^\varepsilon(t=0, x, \xi) = f_{i,0}^\varepsilon(x, \xi), \quad \mathbf{v}(t=0, x) = \mathbf{v}_0(x). \end{cases}$$

The derivation is based on micro-macro decomposition method which leads to an equivalent system coupled the microscopic and macroscopic equations. Comparing with [24], here we deal with the derivation from a nonlocal kinetic-fluid model for multi-interacting populations living in a fluid generated by the incompressible Navier-Stokes equations.

In the second part, we prove the existence of weak solutions of the proposed nonlocal cross-diffusion-fluid system. The proof is based on the nonlinear Galerkin method, a priori estimates and compactness arguments. We develop numerical approximations for the equivalent model of the kinetic-fluid system and for the macroscopic model in the next part in order to show the asymptotic preserving scheme property. In other words, when the distance between species (mean free path) is too small, the profiles of the densities given by the two schemes (micro-macro and macroscopic schemes) are almost the same. On the other hand, we reproduce some numerical results of phenomena taking into account the effects of non-locality of diffusivity functions and of the fluid. The last part is devoted to the computational analysis of the nonlocal cross-diffusion-fluid model in two dimension.

Second part: This part is devoted to vehicular traffic flow application.

Chapter 4. We begin with a detailed review of the main vehicular traffic kinetic models available in the pertinent literature.

Chapter 5. We summarize the results proposed in the paper [28]. We propose and we study a new general mathematical structure for vehicular traffic according to a kinetic theory approach. The mathematical structure proposed in this work includes the features of the complex system under consideration which, according to the authors' opinion, appear to be the most important aspects of the dynamics to be retained by the modeling approach. Namely heterogeneity of the driver-vehicle subsystem, aggregation dynamics for vehicles with closed each other velocity, passing probability, variable properties of the road-environment where the dynamics occur and role of the external actions. Our proposed model is as follows

$$\begin{aligned} &\partial_t f(t,x,v,u) + v\partial_x f(t,x,v,u) + \partial_v(\mathcal{F}[f](t,x,v,u) f(t,x,v,u)) \\ &\quad = \int_{[0,1]^3} \eta[f] \mathcal{A}[f;\alpha](v_* \to v | v_*, v^*, u)\, f(t,x,v_*,u)\, f(t,x,v^*,u^*) dv_*\, dv^*\, du^* \\ &\qquad - f(t,x,v,u) \int_{[0,1]^2} \eta[f]\, f(t,x,v^*,u^*) dv^*\, du^* \\ &\qquad\quad + \mu[f]\big(f_e(x, v_e(x)) - f(t,x,v,u)\big), \end{aligned}$$

where x and v are the dimensionless position and velocity variables, and u is a variable which denotes the quality of the micro-system. f is the distribution function over the

state at the microscopic scale. The remained terms in the above model are

- $\mathcal{F}[f]$ is the overall acceleration of all vehicles which obtained by integration corresponding to the action of all vehicles in the sensitive zone Ω_ℓ.
- $\eta[f]$ is the encounter rate which models the number of interactions per unit time between candidate and test particles with field particles;
- $\mathcal{A}[f](v_* \to v|u)$ is the transition probability density which defines the probability density that a candidate particle falls into the state of with the field particles;
- $\mu[f]$ models the intensity of the action while $v_e(x)$ is the speed imposed by the external action.

We model the interactions at the microscopic scale by methods of game theory, thus leading to the derivation of mathematical models within the framework of the kinetic theory. Short and long range interactions are modeled to depict change of velocity related to passing and clustering phenomena. Numerical results are provided to compute the fundamental diagrams predicted by the spatially homogeneous problem and emerging of two clusters predicted by the spatially inhomogeneous problem.

Part I

Kinetic-fluid derivation and mathematical analysis of cross-diffusion-fluid models

Chapter 2

Kinetic-fluid derivation and mathematical analysis of cross-diffusion-Brinkman system

This chapter aims to summarize our work [24] in which we propose a new nonlinear system describing dynamical interaction of two species within viscous flow. The proposed system is a cross-diffusion system coupled with Brinkman problem written in terms of velocity fluid, vorticity and pressure, and describing the flow patterns driven by an external source depending on the distribution of species. In the first part, we derive a macroscopic systems from the kinetic-fluid equations by using the micro-macro decomposition method. Basing on Schauder fixed-point theory, we prove the existence of weak solutions for the derived system in the second part. The last part is devoted to develop a one dimensional finite volume approximation for the kinetic-fluid model, which are uniformly stable along the transition from kinetic to macroscopic regimes. Our computation method is validated with various numerical tests.

2.1 Introduction

In this paper [24], we are interested to the viscous flow in porous medium which is always modelled by Brinkman equations stating momentum and the conservation of mass of the fluid. We note that Brinkman problem is a parameter dependent combination of Darcy and Stokes models, so that the flow is dominated by Darcy regime and by Stokes elsewhere. Motivated by this phenomena, we propose a nonlinear cross-diffusion system include additional terms accounting for the advection of each species with the fluid velocity, coupled with Brinkman problem written in terms of fluid velocity, vorticity and pressure, and describing the flow patterns driven by an external source depending on the distribution of species.

In order to state our problem, let $\Omega \subset \mathbb{R}^3$ be a simply connected, and bounded porous domain saturated with a Newtonian incompressible fluid, where also the two species are present. The physical scenario of interest can be therefore described by a coupled system written in terms of the fluid velocity $\boldsymbol{u}$, the rescaled fluid vorticity $\boldsymbol{\omega}$, the fluid pressure p, and the densities of two species c and s. The cross-diffusion-Brinkman system can be written for (t,x) in $\Omega_T := (0,T)\times\Omega$:

$$\begin{cases} c_t + \boldsymbol{u}\cdot\nabla_x c - \Delta_x\Big[\big(D_c(c) + a_{11}\,c + a_{12}\,s\big)c\Big] = H_c(c,s), \\ s_t + \boldsymbol{u}\cdot\nabla_x s - \Delta_x\Big[\big(D_s(s) + a_{21}\,c + a_{22}\,s\big)s\Big] = H_s(c,s), \\ \mathbb{K}^{-1}\boldsymbol{u} + \sqrt{\mu}\,\mathbf{curl}\,\boldsymbol{\omega} + \nabla_x p = Q(c,s)\boldsymbol{g} + \mathbf{F}, \\ \boldsymbol{\omega} - \sqrt{\mu}\,\mathbf{curl}\,\boldsymbol{u} = \mathbf{0}, \\ \operatorname{div}\boldsymbol{u} = 0, \end{cases} \tag{2.1.1}$$

where $D_c(c)$, $D_s(s)$ are the nonlinear diffusitive functions and $a_{ij} > 0$ for $i,j = 1,2$ is known as self and cross-diffusion rates. The parameter μ is the fluid viscosity in the considered regime, it is assumed independent of the densities of species c and s, $\mathbb{K}(x)$ is the permeability tensor rescaled with viscosity, $Q(c,s)\boldsymbol{g}$ represents the force exerted by the densities on the fluid motion, and $\mathbf{F}(t,x)$ is an external force applied to the porous medium. The functions H_c and H_s are the reaction terms. A typical example of H_c and H_s is given by Lotka-Voltera (logistic) type growth term:

$$\begin{cases} H_c(c,\, s) = c(a_1 - b_1\, c - d_1\, s), \\ \\ H_s(c,\, s) = s(a_2 - b_2\, c - d_2\, s), \end{cases} \tag{2.1.2}$$

where a_1 and a_2 are the Malthusian growth coefficients, and b_1, d_2 and b_2, d_1 are the coefficients of intra- and inter-species competition, respectively. Note that our system reads for suitably smooth functions c and s as follows

$$\begin{cases} c_t + \boldsymbol{u}\cdot\nabla_x c - \operatorname{div}_x\Big[\Big(D_c(c) + 2\,a_{11}\,c + a_{12}\,s\Big)\,\nabla c + a_{12}\,c\,\nabla_x s\Big] = H_c(c,s), & \text{in } \Omega_T, \\ s_t + \boldsymbol{u}\cdot\nabla_x s - \operatorname{div}_x\Big[\Big(D_s(s) + a_{21}\,c + 2a_{22}\,s\Big)\,\nabla s + a_{21}\,s\,\nabla_x c\Big] = H_s(c,s), & \text{in } \Omega_T, \\ \mathbb{K}^{-1}\boldsymbol{u} + \sqrt{\mu}\,\mathbf{curl}\,\boldsymbol{\omega} + \nabla_x p = Q(c,s)\boldsymbol{g} + \mathbf{F}, & \text{in } \Omega_T, \\ \boldsymbol{\omega} - \sqrt{\mu}\,\mathbf{curl}\,\boldsymbol{u} = \mathbf{0}, & \text{in } \Omega_T, \\ \operatorname{div}\boldsymbol{u} = 0, & \text{in } \Omega_T. \end{cases} \tag{2.1.3}$$

Our system (2.1.3) is complemented with the following boundary conditions in $\Sigma_T := (0,T)\times\partial\Omega$ and initial data:

$$\begin{aligned} \big(c\boldsymbol{u} - (D_c(c) + 2\,a_{11}\,c + a_{12}\,s)\nabla_x c - a_{12}\,c\nabla_x s\big)\cdot\eta = 0, \quad & (t,x)\in\Sigma_T, \\ \big(s\boldsymbol{u} - (D_s(s) + a_{21}\,c + 2a_{22}\,s)\nabla_x s - a_{21}\,s\nabla_x c\big)\cdot\eta = 0, \quad & (t,x)\in\Sigma_T, \\ \boldsymbol{u}\cdot\eta = u_\partial,\ \boldsymbol{\omega}\times\eta = \boldsymbol{\omega}_\partial, \quad & (t,x)\in\Sigma_T, \\ c(t=0,x) = c_0(x), \quad s(t=0,x) = s_0(x), \quad & x\in\Omega, \end{aligned} \tag{2.1.4}$$

where η is the unit outward normal to Ω on $\partial\Omega$. Note that in the case $(a_{i,j})_{1\le i,j\le 2} := 0$, our system can be reduced to the recent system by [2], in which the authors proposed reaction-diffusion system representing the bacteria-chemical mass exchange, coupled with Brinkman problem.

To the best of our knowledge, there are few papers proposing the augmented velocity-vorticity-pressure formulation (augmented Brinkman model) without reaction-diffusion system coupling. It was initially proposed in [89], where the authors added vorticity as a new unknown variable. In [1, 5], the authors proposed the analysis of this system using mixed finite element method for standard and non-standard boundary conditions, respectively. Later, in [72], the authors have studied numerically an advection-diffusion-reaction system coupled with an incompressible viscous flow. When the fluid is at rest ($\boldsymbol{u} = 0$), several works have been proposed in the literature to investigate the theoretical and numerical analysis of the cross-diffusion system. For instance, the works in [23, 92] include the analysis of the weak solution and the global existence of solution. Moreover, the authors in [87] specified the conditions for the existence of unstable equilibrium points. On the other hand, many numerical methods are proposed to approximate the solution. We refer the reader to finite difference method in [33], finite element method in [9], deterministic particle method in [49], finite volume method in [6, 3, 4] and positivity-preserving Euler-Galerkin method in [34]. We want to mention here that this is the first attempt to derive macroscopic system with nonlinear diffusitive terms. Moreover, in our contribution we present a new system (Cross-diffusion-Brinkman system) that combine

interaction of the species in the presence of fluid.

In this chapter, we derive a general cross-diffusion systems coupled with the Brinkman problem from the kinetic-fluid using micro-macro decomposition method. In particular, we are interesting to derive our cross-diffusion-Brinkman system (3.1.1). The idea of micro-macro decomposition is to write the unknown distribution function as a sum of an equilibrium and a deviation. We note that this method permits to reformulate the singularly perturbed kinetic system into an equivalent micro-macro formulation which is a regular perturbation of the derivative system. Thus, solving numerically the equivalent micro-macro formulation instead of the perturbed kinetic system will permit to shift automatically the limit problem, if the perturbation parameter (Knudsen parameter or sometimes it refers as mean free path) is too small. Several contributions have investigated the asymptotic limit in the following cases: diffusion limit in [71, 26, 22], anomalous diffusion limit in [39, 35], hyperbolic system in [78] and Keller-Segel systems of pattern formation in biological tissues in [11, 16, 27]. Note that there are different approaches to construct such scheme for kinetic systems in various contexts. For instance, the authors in [13, 14] developed the approach of continuum mechanics based on micro-macro derivation in biological tissue and [20] for incompressible Navier-Stokes, (see the interesting overview [8] for more details). Another approach can be found in [52, 65], where the authors used the domain decomposition method for the linear transport equation.

The outline of this Chapter is the following: In Section 2.2, we present the kinetic model and its properties. Next, we perform the micro-macro formulation, which is the ingredient key in the construction of our numerical method. Section 2.3 is devoted to proving the existence of weak solutions for derived macroscopic system. Our numerical method is demonstrated in Section 2.4 with various numerical tests.

2.2 Derivation of cross-diffusion-Brinkman systems

This section aims to derive general macroscopic systems using micro-macro decomposition method following the line of the paper [11]. Note that the authors in this paper have derived a macroscopic systems of Keller-Segel type, which describe the chemotaxis phenomenon [62]. First, we present the properties of the kinetic system which lead to an equivalent micro-macro formulation. Next, we derive formally a general macroscopic nonlinear coupled system. We finish this subsection by deriving our cross-diffusion-Brinkman system (2.1.3). We want to mention here that the novelty in this first part is that we derive the cross-diffusion system with nonlinear diffusitive functions coupled with Brinkman problem.

2.2.1 The kinetic-fluid model

In order to derive a general macroscopic cross-diffusion-Brinkman system from the kinetic-fluid model, we consider the parabolic-parabolic scaling. Thus, the kinetic-fluid model is as follows

$$\begin{cases} \big(\varepsilon\partial_t + \xi\cdot\nabla_x\big) f_1^\varepsilon = \frac{1}{\varepsilon}\mathcal{T}_1[f_2^\varepsilon](f_1^\varepsilon) + G_1(f_1^\varepsilon, f_2^\varepsilon, \boldsymbol{u}, \xi), \\ \big(\varepsilon\partial_t + \xi\cdot\nabla_x\big) f_2^\varepsilon = \frac{1}{\varepsilon}\mathcal{T}_2[f_1^\varepsilon](f_2^\varepsilon) + G_2(f_1^\varepsilon, f_2^\varepsilon, \boldsymbol{u}, \xi), \\ \mathbb{K}^{-1}\boldsymbol{u} + \sqrt{\mu}\,\mathbf{curl}\,\boldsymbol{\omega} + \nabla_x p = Q\Big(\int_V f_1^\varepsilon d\xi, \int_V f_2^\varepsilon d\xi\Big)\,\boldsymbol{g} + \mathbf{F}, \\ \boldsymbol{\omega} - \sqrt{\mu}\,\mathbf{curl}\,\boldsymbol{u} = \mathbf{0}, \\ \operatorname{div}\boldsymbol{u} = 0, \end{cases} \tag{2.2.1}$$

where f_1, f_2 are the generalized distribution functions which depend on time t, position $x \in \Omega \subset \mathbb{R}^d$ and velocity $\xi \in V \subset \mathbb{R}^d$ (V assumed to be bounded and symmetric). The remaining macroscopic variables and parameters, namely $\boldsymbol{u}$, μ, $\boldsymbol{\omega}$, p, Q, $\boldsymbol{g}$, and $\mathbf{F}$, are defined in the introduction. The Knudsen parameter ε measures the distance of the system to its equilibrium. Specifically, when ε is small, the system is close to an equilibrium state, while for large ε, the system is far from equilibrium. Moreover, $\mathcal{T}_1[f_2]$, $\mathcal{T}_2[f_1]$ and $G_i, i = 1, 2$ are, respectively, the turning and interaction operators, assumed to satisfy the following properties:

- The turning operators are decomposed as follows

$$\mathcal{T}_1[f_2](h) = \mathcal{T}_1^1(h) + \varepsilon \mathcal{T}_1^2[f_2](h), \quad \mathcal{T}_2[f_1](h) = \mathcal{T}_1^2(h) + \varepsilon \mathcal{T}_2^2[f_1](h), \tag{2.2.2}$$

  where $\mathcal{T}_j^i$ for $i, j = 1, 2$ are given by

$$\mathcal{T}_j^i(h) = \int_V \left[T_j^i(\xi^*, \xi) h(t, x, \xi^*) - T_j^i(\xi, \xi^*) h(t, x, \xi) \right] d\xi^*, \tag{2.2.3}$$

  where $T_j^i(\xi, \xi^*)$ is the probability kernel for the new velocity $\xi \in V$, given that the previous velocity was ξ^*. The dependence on f_2 (resp. f_1) of the operator $\mathcal{T}_1^2[f_2]$ (resp. $\mathcal{T}_2^2[f_1]$) stems from T_2^1 (resp. T_2^2). We assume that $\mathcal{T}_1^1$ is independent on f_2 and $\mathcal{T}_2^1$ is independent on f_1. In what follows, we shall consider $\mathcal{T}_1^1(h) = \mathcal{L}_1(h)$ and $\mathcal{T}_2^1(h) = \mathcal{L}_2(h)$.

- We assume that

$$\int_V \mathcal{L}_1(h) d\xi = \int_V \mathcal{T}_1^2[f_2](h) d\xi = \int_V \mathcal{L}_2(h) d\xi = \int_V \mathcal{T}_2^2[f_1](h) d\xi = 0. \tag{2.2.4}$$

- There exists a bounded velocity distribution $M_i(\xi) > 0$, $(i = 1, 2)$ independent of t and x, such that

$$T_1^1(\xi, \xi^*) M_1(\xi^*) = T_1^1(\xi^*, \xi) M_1(\xi), \quad T_2^1(\xi, \xi^*) M_2(\xi^*) = T_2^1(\xi^*, \xi) M_2(\xi) \tag{2.2.5}$$

  holds. Furthermore, M_i are normalized and the flow produced by these equilibrium distributions vanishes

$$\int_V M_i(\xi) d\xi = 1, \quad \int_V \xi\, M_i(\xi) d\xi = 0, \quad i = 1, 2. \tag{2.2.6}$$

  The probability kernels $T_1^1(\xi, \xi^*)$ and $T_2^1(\xi, \xi^*)$ are bounded, and there exist constants $\sigma_i > 0$, $i = 1, 2$, such that

$$T_1^1(\xi, \xi^*) \geq \sigma_1 M_1(\xi), \quad T_2^1(\xi, \xi^*) \geq \sigma_2 M_2(\xi), \tag{2.2.7}$$

  for all $(\xi, \xi^*) \in V \times V$.

- Moreover, we assume that the interaction operators G_i $(i = 1, 2)$ satisfy the following properties:

$$G_i(f_1, f_2, \boldsymbol{u}, \xi) = G_{i1}(f_1, f_2, \boldsymbol{u}, \xi) + \varepsilon G_{i2}(f_1, f_2, \xi), \tag{2.2.8}$$

  where

$$\int_V G_{i1}(f_1, f_2, \boldsymbol{u}, \xi) d\xi = 0, \tag{2.2.9}$$

for $i = 1, 2$.

Thanks to technical calculations in [30], the operators $\mathcal{L}_i$ $(i = 1, 2)$ have the following properties (the proof of the following lemma can be found in [11]):

Lemma 2.2.1 *Assume that the hypothesis (3.2.6), (3.2.7) and (3.2.8) hold. Then, the following properties of the operators $\mathcal{L}_1$ and $\mathcal{L}_2$ hold true:*

1) *The operator $\mathcal{L}_i$ is self-adjoint in the space $\mathrm{L}^2\left(V, \frac{d\xi}{M_i}\right)$.*

2) *For $h \in \mathrm{L}^2$, the equation $\mathcal{L}_i(g) = h$, $(i = 1, 2)$ has a unique solution $g \in \mathrm{L}^2\left(V, \frac{d\xi}{M_i}\right)$, satisfying*
$$\int_V g(\xi)\, d\xi = 0 \quad \text{if and only if} \quad \int_V h(\xi)\, d\xi = 0.$$

3) *The equation $\mathcal{L}_i(g) = \xi\, M_i(\xi)$, has a unique solution which be denoted by $\theta_i(\xi)$, for $i = 1, 2$.*

4) *The kernel of $\mathcal{L}_i$ is $N(\mathcal{L}_i) = vect(M_i(\xi))$, $i = 1, 2$.*

2.2.2 The equivalent micro-macro formulation

In this subsection, we rewrite each kinetic equation in (2.2.1) as an equivalent system coupling a hydrodynamic part with a kinetic part. For this, we decompose f_i, $(i = 1, 2)$ into a main part that is close to the equilibrium in diffusive regimes, and another part that vanishes in its limit, i.e

$$f_1(t, x, \xi) = M_1(\xi)c(t, x) + \varepsilon g_1(t, x, \xi), \quad f_2(t, x, \xi) = M_2(\xi)s(t, x) + \varepsilon g_2(t, x, \xi),$$

where
$$c(t, x) = \int_V f_1(t, x, \xi)d\xi, \quad s(t, x) = \int_V f_2(t, x, \xi)d\xi.$$

We will use frequently the notation $\langle . \rangle$ which denote the integral with respect to the variable ξ. We observe that $\langle g_i \rangle = 0$, for $i = 1, 2$. Inserting f_1 and f_2 in the kinetic model (2.2.1) and using the properties of the kernel operators, we get

$$\begin{aligned}\partial_t(M_1 c) + \varepsilon\partial_t g_1 + \frac{1}{\varepsilon}\xi M_1 \cdot \nabla_x c + \xi \cdot \nabla_x g_1 = \frac{1}{\varepsilon}\mathcal{L}_1(g_1) + \frac{1}{\varepsilon}\mathcal{T}_1^2[f_2](M_1(\xi)c) \\ + \mathcal{T}_1^2[f_2](g_1) + \frac{1}{\varepsilon}G_{11}(f_1, f_2, \boldsymbol{u}, \xi) + G_{12}(f_1, f_2, \xi), \quad (2.2.10)\end{aligned}$$

$$\begin{aligned}\partial_t(M_2 s) + \varepsilon\partial_t g_2 + \frac{1}{\varepsilon}\xi M_2 \cdot \nabla_x s + \xi \cdot \nabla_x g_2 = \frac{1}{\varepsilon}\mathcal{L}_2(g_2) + \frac{1}{\varepsilon}\mathcal{T}_2^2[f_1](M_2(\xi)s) \\ + \mathcal{T}_2^2[f_1](g_2) + \frac{1}{\varepsilon}G_{21}(f_1, f_2, \boldsymbol{u}, \xi) + G_{22}(f_1, f_2, \xi), \quad (2.2.11)\end{aligned}$$

$$\mathbb{K}^{-1}\boldsymbol{u} + \sqrt{\mu}\,\mathbf{curl}\,\boldsymbol{\omega} + \nabla_x p = Q(c, s)\boldsymbol{g} + \mathbf{F}, \quad \boldsymbol{\omega} - \sqrt{\mu}\,\mathbf{curl}\,\boldsymbol{u} = \mathbf{0}, \quad \mathrm{div}\,\boldsymbol{u} = 0. \quad (2.2.12)$$

The micro-macro formulation equivalent to system (3.2.1) is obtained by two steps. In the first step, we use a projection technique to separate the macroscopic densities $(c(t, x)$,

$s(t,x)$) and microscopic quantities ($g_1(t,x,\xi)$, $g_2(t,x,\xi)$). For that, let P_{M_i} denote the orthogonal projection onto $N(\mathcal{L}_i)$, for $i=1,2$. It follows

$$P_{M_i}(h) = \langle h\rangle M_i, \quad \text{for any} \quad h \in \mathrm{L}^2\left(V, \frac{d\xi}{M_i}\right),$$

for $i=1,2$. Regarding the orthogonal projections P_{M_1}, P_{M_2}, we have the following result:

Lemma 2.2.2 *(cf. [11]) For the projection P_{M_1}, P_{M_2}, we have the following properties :*

$$(I-P_{M_1})(M_1 c) = (I-P_{M_2})(M_2 s) = P_{M_1}(g_1) = P_{M_2}(g_2) = 0,$$

$$(I-P_{M_1})(\xi M_1\cdot\nabla_x c) = \xi M_1\cdot\nabla_x c, \qquad (I-P_{M_2})(\xi M_2\cdot\nabla_x s) = \xi M_2\cdot\nabla_x s,$$

$$(I-P_{M_1})(\mathcal{T}_1^2[f_2](M_1(\xi)c) = \mathcal{T}_1^2[f_2](M_1(\xi)c),$$

$$(I-P_{M_2})(\mathcal{T}_2^2[f_1](M_2(\xi)s)) = \mathcal{T}_2^2[f_1](M_2(\xi)s),$$

$$(I-P_{M_2})(\mathcal{T}_2^2[f_1](h)) = \mathcal{T}_2^2[f_1](h), \quad (I-P_{M_1})(\mathcal{T}_1^2[f_2](h)) = \mathcal{T}_1^2[f_2](h),$$

$$(I-P_{M_1})(\mathcal{L}_i(h)) = \mathcal{L}_i(h), \quad (I-P_{M_i})(G_{i1}(f_1,f_2,\boldsymbol{u},\xi)) = G_{i1}(f_1,f_2,\boldsymbol{u},\xi), \quad i=1,2.$$

Taking the operators $I-P_{M_1}$ and $I-P_{M_2}$ into (2.2.10) and (2.2.11), respectively, and using Lemma 2.2.2, yield the following microscopic equations:

$$\begin{aligned}\varepsilon\partial_t g_1 + \frac{1}{\varepsilon}\xi M_1\cdot\nabla_x c + (I-P_{M_1})(\xi\cdot\nabla_x g_1) = \frac{1}{\varepsilon}\mathcal{L}_1(g_1) + \frac{1}{\varepsilon}\mathcal{T}_1^2[f_2](M_1(\xi)c) \\ +\mathcal{T}_1^2[f_2](g_1) + \frac{1}{\varepsilon}G_{11}(f_1,f_2,\boldsymbol{u},\xi) + (I-P_{M_1})G_{12}(f_1,f_2,\xi),\end{aligned} \tag{2.2.13}$$

$$\begin{aligned}\varepsilon\partial_t g_2 + \frac{1}{\varepsilon}\xi M_2\cdot\nabla_x s + (I-P_{M_2})(\xi\cdot\nabla_x g_2) = \frac{1}{\varepsilon}\mathcal{L}_2(g_2) + \frac{1}{\varepsilon}\mathcal{T}_2^2[f_1](M_2(\xi)s) \\ +\mathcal{T}_2^2[f_1](g_2) + \frac{1}{\varepsilon}G_{21}(f_1,f_2,\boldsymbol{u},\xi) + (I-P_{M_1})G_{22}(f_1,f_2,\xi).\end{aligned} \tag{2.2.14}$$

For the second step, we integrate (2.2.10) with respect to ξ

$$\begin{aligned}\partial_t c\int_V M_1 d\xi + \varepsilon\partial_t\int_V g_1 d\xi + \frac{1}{\varepsilon}\int_V \xi M_1 d\xi\cdot\nabla_x c + \int_V \xi\cdot\nabla_x g_1 d\xi = \frac{1}{\varepsilon}\int_V \mathcal{L}_1(g_1)d\xi \\ +\frac{1}{\varepsilon}\int_V \mathcal{T}_1^2[f_2](M_1(\xi)c)d\xi \ + \int_V \mathcal{T}_1^2[f_2](g_1)d\xi \\ +\frac{1}{\varepsilon}\int_V G_{11}(f_1,f_2,\boldsymbol{u},\xi)d\xi + \int_V G_{12}(f_1,f_2,\xi)d\xi.\end{aligned}$$

Thanks to (2.2.4), (2.2.6) and (2.2.9) and the fact that $\langle g_1\rangle = \langle g_2\rangle = 0$, we obtain the following macroscopic equation:

$$\partial_t c + \langle\xi\cdot\nabla_x g_1\rangle = \langle G_{12}(f_1,f_2,\xi)\rangle. \tag{2.2.15}$$

Similarly to (2.2.15), we obtain from (2.2.11)

$$\partial_t s + \langle\xi\cdot\nabla_x g_2\rangle = \langle G_{22}(f_1,f_2,\xi)\rangle. \tag{2.2.16}$$

Finally, thanks to (2.2.13), (2.2.14), (2.2.15), and (2.2.16), the micro-macro formulation reads

$$
\begin{cases}
\varepsilon\partial_t g_1 + \frac{1}{\varepsilon}\xi M_1\cdot\nabla_x c + (I-P_{M_1})(\xi\cdot\nabla_x g_1) = \frac{1}{\varepsilon}\mathcal{L}_1(g_1) \\
\qquad\qquad + \frac{1}{\varepsilon}\mathcal{T}_1^2[f_2](M_1(\xi)c) + \mathcal{T}_1^2[f_2](g_1) \\
\qquad\qquad + \frac{1}{\varepsilon}G_{11}(f_1,f_2,\boldsymbol{u},\xi) + (I-P_{M_1})G_{12}(f_1,f_2,\xi), \\
\partial_t c + \langle \xi\cdot\nabla_x g_1\rangle = \langle G_{12}(f_1,f_2,\xi)\rangle, \\
\varepsilon\partial_t g_2 + \frac{1}{\varepsilon}\xi M_2\cdot\nabla_x s + (I-P_{M_2})(\xi\cdot\nabla_x g_2) = \frac{1}{\varepsilon}\mathcal{L}_2(g_2) \\
\qquad\qquad + \frac{1}{\varepsilon}\mathcal{T}_2^2[f_1](M_2(\xi)s) + \mathcal{T}_2^2[f_1](g_2) \\
\qquad\qquad + \frac{1}{\varepsilon}G_{21}(f_1,f_2,\boldsymbol{u},\xi) + (I-P_{M_2})G_{22}(f_1,f_2,\xi), \\
\partial_t s + \langle \xi\cdot\nabla_x g_2\rangle = \langle G_{22}(f_1,f_2,\xi)\rangle, \\
\mathbb{K}^{-1}\boldsymbol{u} + \sqrt{\mu}\,\mathbf{curl}\,\boldsymbol{\omega} + \nabla_x p = Q(c,s)\boldsymbol{g} + \mathbf{F}, \\
\boldsymbol{\omega} - \sqrt{\mu}\,\mathbf{curl}\,\boldsymbol{u} = \mathbf{0}, \\
\operatorname{div}\boldsymbol{u} = 0.
\end{cases}
\tag{2.2.17}
$$

Note that system (2.2.17) is the micro-macro formulation of the kinetic-fluid model (2.2.1). The following proposition shows that system (2.2.17) and the model (2.2.1) are equivalent.

Proposition 2.2.1 *i) Let $(f_1, f_2, \boldsymbol{u}, \boldsymbol{\omega}, p)$ be a solution of the kinetic system (2.2.1). Then the functions $(c, g_1, s, g_2, \boldsymbol{u}, \boldsymbol{\omega}, p)$ (where $c = \langle f_1\rangle$, $s = \langle f_2\rangle$, $g_1 = \frac{1}{\varepsilon}(f_1 - M_1 c)$, $g_2 = \frac{1}{\varepsilon}(f_2 - M_2 s)$) are a solution to coupled system (2.2.17) with the associated initial data*

$$
c(t=0) = c_0 = \langle f_{10}\rangle, \quad g_1(t=0) = g_{10} = \frac{1}{\varepsilon}(f_{10} - M_1 c_0), \tag{2.2.18}
$$

$$
s(t=0) = s_0 = \langle f_{20}\rangle, \quad g_2(t=0) = g_{20} = \frac{1}{\varepsilon}(f_{20} - M_2 s_0), \tag{2.2.19}
$$

ii) Conversely, if $(c, g_1, s, g_2, \boldsymbol{u}, \boldsymbol{\omega}, p)$ satisfies system (2.2.17) with initial data $(c_0, g_{10}, s_0, g_{20})$ such that $\langle g_{10}\rangle = \langle g_{20}\rangle = 0$, then $(f_1 = M_1 c + \varepsilon g_1$, $f_2 = M_2 s + \varepsilon g_2$, $\boldsymbol{u}$, $\boldsymbol{\omega}$, $p)$ is a solution to kinetic model (2.2.1) with initial data $f_{10} = M_1 c_0 + \varepsilon g_{10}$, $f_{20} = M_2 s_0 + \varepsilon g_{20}$ and we have $c = \langle f_1\rangle$, $s = \langle f_2\rangle$ and $\langle g_1\rangle = \langle g_2\rangle = 0$.

Remark 2.2.1 *The proof of i) is already detailed above. For the proof of ii) we refer the reader to proof of Theorem 1 in [11].*

In order to derive the macroscopic systems from the micro-macro formulation (2.2.17), we need more assumptions on the turning operators $\mathcal{T}_1^2$, $\mathcal{T}_2^2$ (recall that $\mathcal{T}_1^2$ and $\mathcal{T}_2^2$ are given in (2.2.3)-(2.2.7)) and the interactions terms G_{i1}, G_{i2}. Moreover, we assume that these terms satisfy the following asymptotic behavior when $\varepsilon \to 0$:

$$\mathcal{T}_1^2[M_2(\xi)s+\varepsilon g_2]=\mathcal{T}_1^2[M_2(\xi)s]+O(\varepsilon),\quad \mathcal{T}_2^2[M_1(\xi)c+\varepsilon g_1]=\mathcal{T}_2^2[M_1(\xi)c]+O(\varepsilon), \tag{2.2.20}$$

and for $i=1,2$,

$$G_{i1}(M_1(\xi)c+\varepsilon g_1,M_2(\xi)s+\varepsilon g_2,\boldsymbol{u},\xi)=G_{i1}(M_1(\xi)c,M_2(\xi)s,\boldsymbol{u},\xi)+O(\varepsilon), \tag{2.2.21}$$

$$G_{2i}(M_1(\xi)c+\varepsilon g_1,M_2(\xi)s+\varepsilon g_2,\xi)=G_{2i}(M_1(\xi)c,M_2(\xi)s,\xi)+O(\varepsilon). \tag{2.2.22}$$

2.2.3 Derivation of macroscopic systems

This subsection is devoted to derive a macroscopic systems from the micro-macro formulation (2.2.17) of the kinetic-fluid system (2.2.1) as ε goes to 0. First, we use (2.2.20)-(2.2.22) and (2.2.17), to obtain

$$\mathcal{L}_1(g_1)=\xi M_1\cdot\nabla_x c-\mathcal{T}_1^2[M_2(\xi)s](M_1(\xi)c)-G_{11}(M_1c,M_2s,\boldsymbol{u},\xi)+O(\varepsilon),$$

$$\mathcal{L}_2(g_2)=\xi M_2\cdot\nabla_x s-\mathcal{T}_2^2[M_1(\xi)c](M_2(\xi)s)-G_{21}(M_1c,M_2s,\boldsymbol{u},\xi)+O(\varepsilon).$$

Observe that from Lemma 2.2.1, (2)), $\mathcal{L}_1$ and $\mathcal{L}_2$ are and invertible. This implies

$$\begin{aligned} g_1 &= (\mathcal{L}_1)^{-1}(\xi M_1\cdot\nabla_x v)-(\mathcal{L}_1)^{-1}(\mathcal{T}_1^2[M_2(\xi)s](M_1(\xi)c)) \\ &\quad -(\mathcal{L}_1)^{-1}(G_{11}(M_1c,M_2s,\boldsymbol{u},\xi))+O(\varepsilon), \end{aligned} \tag{2.2.23}$$

and

$$\begin{aligned} g_2 &= (\mathcal{L}_2)^{-1}(\xi M_2\cdot\nabla_x s)-(\mathcal{L}_2)^{-1}(\mathcal{T}_2^2[M_1(\xi)c](M_2(\xi)s)) \\ &\quad -(\mathcal{L}_2)^{-1}(G_{21}(M_1c,M_2s,\boldsymbol{u},\xi))+O(\varepsilon). \end{aligned} \tag{2.2.24}$$

Inserting (2.2.23) and (2.2.24) into the second and the fourth equations in (2.2.17), yield the following coupled macroscopic system:

$$\begin{cases} \partial_t c+\Big\langle \xi.\nabla_x(\mathcal{L}_1)^{-1}(\xi M_1\cdot\nabla_x c)\Big\rangle-\Big\langle \xi.\nabla_x(\mathcal{L}_1)^{-1}(\mathcal{T}_1^2[M_2(\xi)s](M_1(\xi)c))\Big\rangle \\ \qquad -\Big\langle \xi.\nabla_x(\mathcal{L}_1)^{-1}(G_{11}(M_1c,M_2s,\boldsymbol{u},\xi))\Big\rangle=\Big\langle G_{12}(M_1c,M_2s,\xi)\Big\rangle+O(\varepsilon), \\ \partial_t s+\Big\langle \xi.\nabla_x(\mathcal{L}_2)^{-1}(\xi M_2\cdot\nabla_x s)\Big\rangle-\Big\langle \xi.\nabla_x(\mathcal{L}_2)^{-1}(\mathcal{T}_2^2[M_1(\xi)c](M_2(\xi)s))\Big\rangle \\ \qquad -\Big\langle \xi.\nabla_x(\mathcal{L}_2)^{-1}(G_{21}(M_1c,M_2s,\boldsymbol{u},\xi))\Big\rangle=\Big\langle G_{22}(M_1c,M_2s,\xi)\Big\rangle+O(\varepsilon), \\ \mathbb{K}^{-1}\boldsymbol{u}+\sqrt{\mu}\,\mathbf{curl}\,\boldsymbol{\omega}+\nabla_x p=Q(c,s)\boldsymbol{g}+\mathbf{F},\quad \boldsymbol{\omega}-\sqrt{\mu}\,\mathbf{curl}\,\boldsymbol{u}=\mathbf{0},\quad \operatorname{div}\boldsymbol{u}=0. \end{cases} \tag{2.2.25}$$

The next lemma gives the calculations of the terms with the inverse of the operators $\mathcal{L}_1$ and $\mathcal{L}_2$ appearing in system (2.2.25).

Lemma 2.2.3 *(cf. [11]) Assume that the operators $\mathcal{L}_1$, $\mathcal{L}_2$, G_{11} and G_{21} are satisfy the assumptions above. Then, we have the following identities :*

$$\Big\langle \xi.\nabla_x(\mathcal{L}_1)^{-1}(\xi M_1\cdot\nabla_x c)\Big\rangle=\operatorname{div}_x\Big(\langle\xi\otimes\theta_1(\xi)\rangle\cdot\nabla_x c\Big),$$

$$\Big\langle \xi.\nabla_x(\mathcal{L}_2)^{-1}(\xi M_2\cdot\nabla_x s)\Big\rangle = \operatorname{div}_x\Big(\langle \xi\otimes\theta_2(\xi)\rangle\cdot\nabla_x s\Big),$$

$$\Big\langle \xi.\nabla_x(\mathcal{L}_1)^{-1}(\mathcal{T}_1^2[M_2(\xi)s](M_1(\xi)c))\Big\rangle = \operatorname{div}_x\Big\langle \frac{\theta_1(\xi)}{M_1(\xi)}c\mathcal{T}_1^2[M_2(\xi)s](M_1(\xi))\Big\rangle,$$

$$\langle \xi.\nabla_x(\mathcal{L}_i)^{-1}(G_{i1}(M_1c,M_2s,\boldsymbol{u},\xi))\rangle = \operatorname{div}_x\Big\langle \frac{\theta_i(\xi)}{M_i(\xi),\xi}G_{i1}(M_1c,M_2s,\boldsymbol{u},\xi)\Big\rangle, \quad i=1,2.$$

In addition, here we need the following identity

$$\Big\langle \xi.\nabla_x(\mathcal{L}_2)^{-1}(\mathcal{T}_2^2[M_1(\xi)c](M_2(\xi)s))\Big\rangle = \operatorname{div}_x\Big\langle \frac{\theta_2(\xi)}{M_2(\xi)}s\mathcal{T}_2^2[M_1(\xi)c](M_2(\xi))\Big\rangle,$$

where θ_1 and θ_2 are given in Lemma 2.2.1.

Finally, thanks to system (2.2.25) and Lemma 2.2.3 we get the following macroscopic system:

$$\begin{cases} \partial_t c + \operatorname{div}_x(c\,\alpha_1(s) + \Gamma_1(c,s,\boldsymbol{u}) - d_c\cdot\nabla_x c) - H_1(c,s) + O(\varepsilon) = 0,\\ \partial_t s + \operatorname{div}_x(s\,\alpha_2(c) + \Gamma_2(c,s,\boldsymbol{u}) - d_s\cdot\nabla_x s) - H_2(c,s) + O(\varepsilon) = 0,\\ \mathbb{K}^{-1}\boldsymbol{u} + \sqrt{\mu}\,\mathbf{curl}\,\boldsymbol{\omega} + \nabla_x p = Q(c,s)\boldsymbol{g} + \mathbf{F}, \quad \boldsymbol{\omega} - \sqrt{\mu}\,\mathbf{curl}\,\boldsymbol{u} = \mathbf{0}, \quad \operatorname{div}\boldsymbol{u} = 0, \end{cases} \tag{2.2.26}$$

where d_c, d_s, $\alpha_1(s)$, $\alpha_2(c)$, $\Gamma_1(c,s,\boldsymbol{u})$, $\Gamma_2(c,s,\boldsymbol{u})$, $H_1(c,s)$ and $H_2(c,s)$ are given by

$$d_c = -\int_V \xi\otimes\theta_1(\xi)d\xi, \quad d_s = -\int_V \xi\otimes\theta_2(\xi)d\xi, \tag{2.2.27}$$

$$\alpha_1(s) = -\int_V \frac{\theta_1(\xi)}{M_1(\xi)}\mathcal{T}_1^2[M_2(\xi)s](M_1(\xi))d\xi, \quad \alpha_2(c) = -\int_V \frac{\theta_2(\xi)}{M_2(\xi)}\mathcal{T}_2^2[M_1(\xi)c](M_2(\xi))d\xi, \tag{2.2.28}$$

$$\Gamma_i(c,s,\boldsymbol{u}) = -\int_V \frac{\theta_i(\xi)}{M_i(\xi)}G_{i1}(M_1c,M_2s,\boldsymbol{u},\xi)d\xi, \quad i=1,2, \tag{2.2.29}$$

$$H_1(c,s) = \int_V G_{12}(M_1c,M_2s,\xi)d\xi, \quad H_2(c,s) = \int_V G_{22}(M_1c,M_2s,\xi)d\xi. \tag{2.2.30}$$

2.2.4 Derivation of cross-diffusion-Brinkman system

In this subsection, we consider the case where the set for velocity is the sphere of radius $r>0$, $V = rS^{d-1}$ and $x\in\Omega\subset\mathbb{R}^2$. We assume that the probability kernel T_i^1 is given by

$$T_i^1 = \frac{\sigma_i}{|V|}, \text{ for } i=1,2.$$

This implies

$$\mathcal{L}_i(f) = -\frac{\sigma_i}{|V|}\Big(f|V| - \langle f\rangle\Big), \text{ for } i=1,2.$$

Observe that $M_i(\xi) = \frac{1}{|V|}$ satisfies (2.2.6). For this choice of M_i, $\theta_i(\xi) = -\frac{\xi}{\sigma_i|V|}$ is a solution of $\mathcal{L}_i(\theta_i(\xi)) = \xi M_i(\xi)$, for $i=1,2$. Now, we let $T_1^2[g]$ and $T_2^2[g]$ such that

$$T_1^2[g] = a_{12}\frac{\beta_1}{|V|}\xi.\nabla_x g \quad \text{and} \quad T_2^2[g] = a_{21}\frac{\beta_2}{|V|}\xi.\nabla_x g,$$

where $\beta_1 = \frac{\sigma_1}{r^2}\, d\,|V|$ and $\beta_2 = \frac{\sigma_2}{r^2}\, d\,|V|$. It follows

$$\mathcal{T}_1^2[M_2 s](M_1) = -a_{12}\frac{\beta_1 M_2}{|V|^2}\xi\cdot\ \nabla_x s \quad \text{and} \quad \mathcal{T}_2^2[M_1 c](M_2) = -a_{21}\frac{\beta_2 M_1}{|V|^2}\xi\cdot\ \nabla_x c.$$

Therefore, we get

$$\alpha_1(s) = -\frac{\beta_1\, a_{12}}{\sigma_1|V|^2}\left(\int_V \xi\otimes\xi d\xi\right)\cdot\ \nabla_x s,\ = -a_{12}\,\nabla_x s,$$

and

$$\alpha_2(v) = -\frac{\beta_2\, a_{21}}{\sigma_2|V|^2}\left(\int_V \xi\otimes\xi d\xi\right)\cdot\ \nabla_x c\ = -a_{21}\,\nabla_x c.$$

Moreover, we use (2.2.27) to obtain

$$d_c = \frac{1}{\sigma_1|V|}\left(\int_V \xi\otimes\xi d\xi\right) = \frac{r^2}{d\sigma_1}I, \quad d_s = \frac{1}{\sigma_2|V|}\left(\int_V \xi\otimes\xi d\xi\right) = \frac{r^2}{d\sigma_2}I. \tag{2.2.31}$$

Now, we define $G_{i,1}$, for $i = 1, 2$ by

$$\begin{cases} G_{1\,1}(M_1 c,\, M_2 s,\, \boldsymbol{u}, \xi) = \dfrac{d\sigma_1}{r^2|V|}\Big(M_1\, c\, \boldsymbol{u} - M_1(2a_{11}c + \tilde{d}_c(c))\ - a_{12}M_2 s\Big)\,\xi.\ \nabla_x c, \\ G_{2\,1}(M_1 c,\, M_2 s,\, \boldsymbol{u}, \xi) = \dfrac{d\sigma_2}{r^2|V|}\Big(M_2\, s\, \boldsymbol{u} - a_{21}M_1 c\ -\ M_2(2a_{22}s + \tilde{d}_s(s))\Big)\,\xi.\ \nabla_x s, \end{cases} \tag{2.2.32}$$

where $\tilde{d}_c(c)$ and $\tilde{d}_s(s)$ are a nonlinear positive functions. It is not difficult to see that $\int_V G_{i1}d\xi = 0$ and therefore satisfies condition (2.2.9) (recall that $\langle \xi M_i\rangle = 0$), for $i = 1, 2$. Next, we use the definitions of Γ_1 and Γ_2 in (2.2.29), to obtain from (2.2.32) and (2.2.31) (recall that $\theta_i = -\frac{\xi}{\sigma_i|V|}$)

$$\begin{aligned} \Gamma_1(c, s, \boldsymbol{u}) &= \tfrac{d}{r^2|V|^2}\left(\int_V \xi\otimes\xi d\xi\right)\cdot\ \Big(c\boldsymbol{u} - (2a_{11}c + a_{12}s + \tilde{d}_c(c))\nabla_x c\Big) \\ &= c\boldsymbol{u} - (2a_{11}c + a_{12}s + \tilde{d}_c(c))\nabla_x c, \end{aligned} \tag{2.2.33}$$

$$\begin{aligned} \Gamma_2(c, s, \boldsymbol{u}) &= \tfrac{d}{r^2|V|^2}\left(\int_V \xi\otimes\xi d\xi\right)\cdot\ \Big(s\boldsymbol{u} - (a_{21}c + 2a_{22}s + \tilde{d}_s(s))\nabla_x s\Big) \\ &= s\boldsymbol{u} - (a_{21}c + 2a_{22}s + \tilde{d}_s(s))\nabla_x s. \end{aligned} \tag{2.2.34}$$

Now collecting the previous results with $\mathrm{div}_x\, \boldsymbol{u} = 0$ and (2.2.26), we arrive to the macroscopic cross-diffusion-Brinkman system of the order $O(\varepsilon)$

$$\begin{cases} c_t + \boldsymbol{u}\cdot\nabla c - \mathrm{div}_x\left((D_c(c) + 2a_{11}c + a_{12}s)\nabla_x c + a_{12}c\nabla_x s\right) = H_1(c, s) + O(\varepsilon), \\ s_t + \boldsymbol{u}\cdot\nabla s - \mathrm{div}_x\left((D_s(s) + a_{21}c + 2a_{22}s)\nabla_x s + a_{21}s\nabla_x c\right) = H_2(c, s) + O(\varepsilon), \\ \mathbb{K}^{-1}\boldsymbol{u} + \sqrt{\mu}\,\mathbf{curl}\,\boldsymbol{\omega} + \nabla_x p = Q(c, s)\boldsymbol{g} + \mathbf{F}, \quad \boldsymbol{\omega} - \sqrt{\mu}\,\mathbf{curl}\,\boldsymbol{u} = \mathbf{0}, \quad \mathrm{div}_x \boldsymbol{u} = 0, \end{cases} \tag{2.2.35}$$

where $D_c(c) = \frac{r^2}{d\,\sigma_1} + \tilde{d}_c(c)$ and $D_s(s) = \frac{r^2}{d\,\sigma_2} + \tilde{d}_s(s)$. In order to derive cross-diffusion-Brinkman system with the explicit form of H_c, H_s, we define the interactions operators

G_{12} and G_{22} by

$$\begin{cases} G_{12}(M_1 c,\, M_2 s\,, \xi) = \dfrac{H_1(c,s)}{|V|}, \\ G_{22}(M_1 c,\, M_2 s\,, \xi) = \dfrac{H_2(c,s)}{|V|}. \end{cases} \tag{2.2.36}$$

Finally, we use (2.2.30) to deduce $H_1 = H_c$ and $H_2 = H_s$. Note that we can choose different explicit forms depending on the field of interest (for example, Lotka-Voltera reaction terms as in [6]).

2.3 Mathematical analysis of the cross-diffusion-Brinkman system

Before stating our result concerning the weak solutions, we collect some preliminary material, including relevant notations and conditions imposed on the data of our problem. Let Ω be a bounded, open subsets of $\mathbb{R}^3$ with a smooth boundary $\partial\Omega$; η is the unit outward normal to Ω on $\partial\Omega$. Next, $|\Omega|$ is the Lebesgue measure of Ω. We denote by $\mathrm{H}^1(\Omega)$ the Sobolev space of functions $u : \Omega \to \mathbb{R}$ for which $u \in \mathrm{L}^2(\Omega)$ and $\nabla_x u \in \mathrm{L}^2(\Omega;\mathbb{R}^3)$. For $1 \le p \le +\infty$, $\|\cdot\|_{\mathrm{L}^p(\Omega)}$ is the usual norm in $L^p(\Omega)$; then

$$\mathrm{L}^p_+(\Omega) = \{u : \Omega \longrightarrow \mathbb{R}_+ \text{ measurable and } \int_\Omega |u(x)|^p \,\mathrm{d}\mathbf{x} < +\infty\},$$

$$\mathrm{L}^\infty_+(\Omega) = \{u : \Omega \longrightarrow \mathbb{R}_+ \text{ measurable and } \sup_{x\in\Omega} |u(x)| < +\infty\}.$$

If X is a Banach space, $a < b$ and $1 \le p \le +\infty$, $\mathrm{L}^p(a,b;X)$ denotes the space of all measurable functions $u : (a,b) \longrightarrow X$ such that $\| u(\cdot) \|_X$ belongs to $\mathrm{L}^p(a,b)$.
Next T is a positive number and

$$\Omega_t := \Omega \times (0,t) \text{ and } \Sigma_t := \partial\Omega \times (0,t),$$

for $0 < t \le T$.
Regarding the permeability tensor, we suppose that $\mathbb{K} \in [C(\bar{\Omega})]^{3\times 3}$ is symmetric and uniformly positive definite. Moreover, there exists $C > 0$ such that

$$\mathbf{v}^{\mathrm{t}}\mathbb{K}^{-1}(x)\mathbf{v} \ge C|\mathbf{v}|^2 \quad \forall\, \mathbf{v} \in \mathbb{R}^3,\ \forall\, x \in \Omega. \tag{2.3.1}$$

The diffusivities are assumed positive, coercive, and continuous

$$D_i : [0,1] \mapsto \mathbb{R}^+ \text{ is continuous}, \quad 0 < D^{\min} \le D_i(u) \le D^{\max} < \infty, \quad u \in \mathbb{R}, \tag{2.3.2}$$

for $i \in \{s,c\}$. In addition we assume that Q is a continuous function and there exists constant a $C_Q > 0$ such that

$$|Q(c,s)| \le C_Q(1 + |c| + |s|) \text{ for all } c,s \in \mathbb{R}. \tag{2.3.3}$$

Initial data are assumed nonnegative and in L^2

$$c_0, s_0 \ge 0, \quad c_0, s_0 \in \mathrm{L}^2(\Omega). \tag{2.3.4}$$

In the proof of the existence of the weak solution, we will use the following assumption (ellipticity condition)

$$8a_{11}a_{21} \ge a_{12}^2 \text{ and } 8a_{22}a_{12} \ge a_{21}^2. \tag{2.3.5}$$

Next, we consider the kernel of the bilinear form $\int_\Omega q \operatorname{div} \boldsymbol{u}\,\mathrm{d}\mathbf{x}$, that is

$$\mathrm{X} := \{\mathbf{v} \in \mathbf{H}_0(\operatorname{div};\Omega) : \int_\Omega q \operatorname{div} \mathbf{v}\,\mathrm{d}\mathbf{x} = 0,\ \forall q \in \mathrm{L}^2_0(\Omega)\}$$

$$= \{\mathbf{v} \in \mathbf{H}_0(\operatorname{div};\Omega) : \operatorname{div} \mathbf{v} = 0 \text{ a.e. in } \Omega\}.$$

We endow the space $\mathbf{H}(\mathbf{curl};\Omega)$ with the following μ-dependent norm:

$$\|\boldsymbol{z}\|^2_{\mathbf{H}(\mathbf{curl};\Omega)} := \|\boldsymbol{z}\|^2_{0,\Omega} + \mu\|\mathbf{curl}\,\boldsymbol{z}\|^2_{0,\Omega}.$$

Moreover, we recall the following inf-sup condition (see for e.g. [50] for more details): there exists $C_\Omega > 0$ only depending on Ω, such that

$$\sup_{\substack{\mathbf{v}\in\mathbf{H}(\operatorname{div};\Omega)\\ \mathbf{v}\neq 0}} \frac{\left|\int_\Omega q \operatorname{div}\mathbf{v}\,\mathrm{d}\mathbf{x}\right|}{\|\mathbf{v}\|_{\mathbf{H}(\operatorname{div};\Omega)}} \geq C_\Omega \|q\|_{0,\Omega} \quad \forall q \in \mathrm{L}^2_0(\Omega). \tag{2.3.6}$$

Now we define what we mean by weak solutions of the system (2.1.3). We also supply our main existence result.

Definition 2.3.1 *We say that $(c, s, \boldsymbol{u}, \boldsymbol{\omega}, p)$ is a weak solution to problem (2.1.3), if c and s are nonnegative,*

$$c, s \in \mathrm{L}^\infty(0,T;\mathrm{L}^2(\Omega)) \cap \mathrm{L}^2(0,T;\mathrm{H}^1(\Omega))$$

$$\boldsymbol{u} \in \mathbf{L}^2(0,T;\mathbf{H}(\operatorname{div};\Omega)), \quad \boldsymbol{\omega} \in \mathbf{L}^2(0,T;\mathbf{H}(\mathbf{curl};\Omega)), p \in \mathrm{L}^2(0,T;\mathrm{L}^2_0(\Omega))$$

and

$$\int_0^T \langle \partial_t c, \varphi_c\rangle\,\mathrm{d}t + \iint_{\Omega_T} \Big[\big(D_c(c) + 2a_{11}\,c + a_{12}\,s\big)\nabla_x c + a_{12}\,c\,\nabla_x s - c\boldsymbol{u}\Big]\cdot\nabla_x\varphi_c\,\mathrm{d}\mathbf{x}\,\mathrm{d}t = \iint_{\Omega_T} H_c(c,s)\varphi_c\,\mathrm{d}\mathbf{x}\,\mathrm{d}t,$$

$$\int_0^T \langle \partial_t s, \varphi_s\rangle\,\mathrm{d}t + \iint_{\Omega_T} \Big[\big(D_s(s) + a_{21}\,c + 2a_{22}\,s\big)\nabla_x s + a_{21}\,s\,\nabla_x c - s\boldsymbol{u}\Big]\cdot\nabla_x\varphi_s\,\mathrm{d}\mathbf{x}\,\mathrm{d}t = \iint_{\Omega_T} H_s(c,s)\varphi_s\,\mathrm{d}\mathbf{x}\,\mathrm{d}t,$$

$$\iint_{\Omega_T} \mathbb{K}^{-1}\boldsymbol{u}\cdot\mathbf{v}\,\mathrm{d}\mathbf{x}\,\mathrm{d}t + \sqrt{\mu}\iint_{\Omega_T}\mathbf{curl}\,\boldsymbol{\omega}\cdot\mathbf{v}\,\mathrm{d}\mathbf{x}\,\mathrm{d}t - \iint_{\Omega_T} p\operatorname{div}_x\mathbf{v}\,\mathrm{d}\mathbf{x}\,\mathrm{d}t = \iint_{\Omega_T}(Q(c,s)\boldsymbol{g} + \boldsymbol{F})\cdot\mathbf{v}\,\mathrm{d}\mathbf{x}\,\mathrm{d}t,$$

$$\sqrt{\mu}\iint_{\Omega_T}\mathbf{curl}\,\boldsymbol{z}\cdot\boldsymbol{u}\,\mathrm{d}\mathbf{x}\,\mathrm{d}t - \iint_{\Omega_T}\boldsymbol{\omega}\cdot\boldsymbol{z}\,\mathrm{d}\mathbf{x}\,\mathrm{d}t = 0,$$

$$-\iint_{\Omega_T} q\operatorname{div}_x\boldsymbol{u}\,\mathrm{d}\mathbf{x}\,\mathrm{d}t = 0,$$

for all $\varphi_c,\ \varphi_s \in \mathrm{L}^2(0,T;W^{1,\infty}(\Omega))$, $\mathbf{v} \in \mathbf{L}^2(0,T;\mathbf{H}_0(\operatorname{div};\Omega))$, $\boldsymbol{z} \in \mathbf{L}^2(0,T;\mathbf{H}_0(\mathbf{curl};\Omega))$, $q \in \mathrm{L}^2(0,T;\mathrm{L}^2_0(\Omega))$. $\langle\cdot,\cdot\rangle$ denotes the duality pairing between $W^{1,\infty}(\Omega)$ and $(W^{1,\infty}(\Omega))'$.

Theorem 2.3.1 *Assume conditions (2.3.1), (2.3.2), (2.3.5) and (2.3.6) hold. If $c_0 \in \mathrm{L}^2_+(\Omega)$, $s_0 \in \mathrm{L}^2_+(\Omega)$, then the problem (2.1.3) possesses a weak solution.*

To prove Theorem 2.3.1, we first prove existence of solutions to the approximate problem (2.3.7) below by applying the Schauder fixed-point theorem (in an appropriate functional setting). Then, having proved existence for the aproximate system, the final goal is to send the regularization parameter ε to zero to fabricate weak solutions of the original systems (2.1.3). Convergence is achieved by means of a priori estimates and compactness arguments.

Remark 2.3.1 *Note that a major difficulty for our system (2.1.3) is the strong coupling in the highest derivatives. Therefore, standard parabolic theory is not directly applicable to our system due to the cross-diffusion-Brinkman terms. We point out that this system is strongly nonlinear and so no maximum principle applies. Moreover, we have not been able to prove uniqueness of weak solutions because of the presence of nonlinear lower-order terms (cross-diffusion terms).*

2.3.1 Existence of solutions for the approximate problems

This subsection is devoted to proving existence of solutions to the approximate problem (2.3.7) below of system (2.1.3). The existence proof is based on the Shauder fixed-point theorem, a priori estimates, and the compactness method. The approximation systems read for $(t,x) \in (0,T] \times \Omega$:

$$\begin{cases} c_t + \boldsymbol{u}\cdot\nabla_x c - \operatorname{div}_x\Big[\big(D_c(c) + 2\,a_{11}\,f_\varepsilon^+(c) + a_{12}\,f_\varepsilon^+(s)\big)\,\nabla_x c + a_{12}\,f_\varepsilon^+(c)\,\nabla_x s\Big] = H_{c,\varepsilon}(c^+,s^+), \\ s_t + \boldsymbol{u}\cdot\nabla_x s - \operatorname{div}_x\Big[\big(D_s(s) + a_{21}\,f_\varepsilon^+(c) + 2a_{22}\,f_\varepsilon^+(s)\big)\,\nabla_x s + a_{21}\,f_\varepsilon^+(s)\,\nabla_x c\Big] = H_{s,\varepsilon}(c^+,s^+), \\ \mathbb{K}^{-1}\boldsymbol{u} + \sqrt{\mu}\,\mathbf{curl}\,\boldsymbol{\omega} + \nabla_x p = Q(s,c)\boldsymbol{g} + \mathbf{F}, \quad \boldsymbol{\omega} - \sqrt{\mu}\,\mathbf{curl}\,\boldsymbol{u} = \mathbf{0}, \quad \operatorname{div}_x \boldsymbol{u} = 0, \end{cases} \tag{2.3.7}$$

subject to the boundary conditions and initial data given by (2.1.4). Herein, $\varepsilon > 0$ is a small number,

$$\begin{cases} H_{c,\varepsilon}(a) = \dfrac{H_c}{1+\varepsilon\,|H_c|} \text{ and } H_{s,\varepsilon}(a) = \dfrac{H_s}{1+\varepsilon\,|H_s|}\,, \\ f_\varepsilon(a) = \dfrac{a}{1+\varepsilon\,|a|} \text{ and } b^+ = \max(0,b) \text{ for any } a,b \in \mathbb{R}. \end{cases}$$

Note that under condition (2.3.5), the matrix

$$M(c,s) = \begin{pmatrix} \Big(2\,a_{11}\,f^+(c) + a_{12}\,f^+(s)\Big)\,Id_3 & \dfrac{1}{2}\Big(a_{12}\,f^+(c) + a_{21}\,f^+(s)\Big)\,Id_3 \\ \dfrac{1}{2}\Big(a_{12}\,f^+(c) + a_{21}\,f^+(s)\Big)\,Id_3 & \Big(a_{21}\,f^+(c) + 2\,a_{22}\,f^+(s)\Big)\,Id_3 \end{pmatrix}$$

is uniformly nonnegative. Indeed, its characteristic polynomial factors out

$$P(\lambda) = \frac{1}{4^3}\Big(4\lambda^2 - 4\big(2a_{11}f^+(c) + a_{12}f^+(s) + a_{21}f^+(c) + 2a_{22}f^+(s)\big)\lambda + R\Big)^3.$$

Setting $f^+(s) = \kappa f^+(c)$, $\kappa \geq 0$, one gets $R = 4f^+(c)^2 Q(\kappa)$, where

$$Q(\kappa) = (8a_{11}a_{21} - a_{12}^2) + (16a_{11}a_{22} + 2a_{12}a_{21})\kappa + (8a_{22}a_{12} - a_{21}^2)\kappa^2.$$

We conclude that if $8a_{11}a_{21} \geq a_{12}^2$ and $8a_{22}a_{12} \geq a_{21}^2$, then $M(c,s)$ is uniformly nonnegative. Hence the utility of assumption (2.3.5). (see [25] for more details). We shall frequently use this to prove the existence (and nonnegativity) of weak solutions.

2.3.2 Existence result to the fixed problem

In this subsection, we omit the dependence of the solutions on the parameter ε. We prove, for each fixed $\varepsilon > 0$, the existence of solutions to the fixed problem (2.3.7), by applying the Schauder fixed-point theorem. Since we use Schauder fixed-point theorem, we need to introduce the following closed subset of the Banach space $\mathrm{L}^2(\Omega_T, \mathbb{R}^n)$:

$$\mathcal{A} = \{U = (c, s) \in \mathrm{L}^2(\Omega_T, \mathbb{R}^2) : \|U\|_{\mathrm{L}^\infty(0,T;\mathrm{L}^2(\Omega,\mathbb{R}^2))\cap \mathrm{L}^2(0,T;\mathrm{H}^1(\Omega,\mathbb{R}^2))} \leq C_{\mathcal{A}}\}, \tag{2.3.8}$$

where $C_{\mathcal{A}} > 0$ is a constant that will be defined below. With $(\bar{c}, \bar{s}) \in \mathcal{A}$ fixed, let $(c, s, \boldsymbol{u}, \boldsymbol{\omega}, p)$ be the unique solution of the system in Ω_T

$$\begin{cases} c_t + \boldsymbol{u}\cdot\nabla_x c - \operatorname{div}_x\Big[\big(D_c(\bar{c}) + 2\,a_{11}\,f_\varepsilon^+(\bar{c}) + a_{12}\,f_\varepsilon^+(\bar{s})\big)\,\nabla_x c + a_{12}\,f_\varepsilon^+(\bar{c})\,\nabla_x s\Big] = H_{c,\varepsilon}(\bar{c}^+, \bar{s}^+), \\ s_t + \boldsymbol{u}\cdot\nabla_x s - \operatorname{div}_x\Big[\big(D_s(\bar{s}) + a_{21}\,f_\varepsilon^+(\bar{c}) + 2a_{22}\,f_\varepsilon^+(\bar{s})\big)\,\nabla_x s + a_{21}\,f_\varepsilon^+(\bar{s})\,\nabla_x c\Big] = H_{s,\varepsilon}(\bar{c}^+, \bar{s}^+), \\ \mathbb{K}^{-1}\boldsymbol{u} + \sqrt{\mu}\,\mathbf{curl}\,\boldsymbol{\omega} + \nabla_x p = Q(\bar{c}, \bar{s})\boldsymbol{g} + \mathbf{F}, \quad \boldsymbol{\omega} - \sqrt{\mu}\,\mathbf{curl}\,\boldsymbol{u} = \mathbf{0}, \quad \operatorname{div}_x \boldsymbol{u} = 0. \end{cases} \tag{2.3.9}$$

2.3.3 The fixed-point method

Now, we introduce a map $\mathrm{L} : \mathcal{A} \to \mathcal{A}$ such that $\mathrm{L}(\bar{c}, \bar{s}) = (c, s)$, where (c, s) solve (2.3.9). By using the Schauder fixed-point theorem, we prove that the map L have a fixed point for (2.3.9).

We start with the following result where the proof can be found in [50] Theorem 1.3:

Theorem 2.3.2 *Let $(\mathcal{X}, \langle\cdot,\cdot\rangle_{\mathcal{X}})$ be a Hilbert space. Let $\mathcal{A} : \mathcal{X}\times\mathcal{X} \to \mathbb{R}$ be a bounded symmetric bilinear form, and let $\mathcal{G} : \mathcal{X} \to \mathbb{R}$ be a bounded functional. Assume that there exists $\bar{\beta} > 0$ such that*

$$\sup_{\substack{y\in\mathcal{X}\\ y\neq 0}} \frac{\mathcal{A}(x,y)}{\|y\|_{\mathcal{X}}} \geq \bar{\beta}\,\|x\|_{\mathcal{X}} \quad \forall\, x \in \mathcal{X}.$$

Then, there exists a unique $x \in \mathcal{X}$, such that

$$\mathcal{A}(x,y) = \mathcal{G}(y) \quad \forall\, y \in \mathcal{X}.$$

Moreover, there exists $C > 0$, independent of the solution, such that

$$\|x\|_{\mathcal{X}} \leq C\|\mathcal{G}\|_{\mathcal{X}'}.$$

Observe that from Brinkman equation in (2.3.9) we solve the following problem: Find $(\boldsymbol{u}, \boldsymbol{\omega}) \in \mathrm{X}\times\mathbf{H}(\mathbf{curl};\Omega)$ such that

$$\begin{aligned} \int_\Omega \mathbb{K}^{-1}\boldsymbol{u}\cdot\mathbf{v}\,\mathrm{d}\mathbf{x} + \sqrt{\mu}\int_\Omega \mathbf{curl}\,\boldsymbol{\omega}\cdot\mathbf{v}\,\mathrm{d}\mathbf{x} &= \int_\Omega (Q(\bar{c},\bar{s})\boldsymbol{g} + \mathbf{F})\cdot\mathbf{v}\,\mathrm{d}\mathbf{x}, \qquad \forall \mathbf{v}\in \mathrm{X}, \\ \sqrt{\mu}\int_\Omega \mathbf{curl}\,\boldsymbol{z}\cdot\boldsymbol{u}\,\mathrm{d}\mathbf{x} - \int_\Omega \boldsymbol{\omega}\cdot\boldsymbol{z}\,\mathrm{d}\mathbf{x} &= 0, \qquad \forall \boldsymbol{z}\in\mathbf{H}_0(\mathbf{curl};\Omega). \end{aligned}$$

Next we exploit Theorem 2.3.2 and we work exactly as in the proofs of [1, Theorem 2.2 and Corollary 2.1] to get the following lemma for a fixed $(\bar{c}, \bar{s}) \in \mathcal{A}$ and for any $t > 0$.

Lemma 2.3.1 *Assume that $(\bar{c}, \bar{s}) \in \mathcal{A}$. Then, the variational problem*

$$\begin{aligned} \int_\Omega \mathbb{K}^{-1}\boldsymbol{u}\cdot\mathbf{v}\,\mathrm{d}\mathbf{x} + \sqrt{\mu}\int_\Omega \mathbf{curl}\,\boldsymbol{\omega}\cdot\mathbf{v}\,\mathrm{d}\mathbf{x} - \int_\Omega p\,\operatorname{div}_x\mathbf{v}\,\mathrm{d}\mathbf{x} &= \int_\Omega (Q(\bar{c},\bar{s})\boldsymbol{g} + \boldsymbol{F})\cdot\mathbf{v}\,\mathrm{d}\mathbf{x}, \\ \sqrt{\mu}\int_\Omega \mathbf{curl}\,\boldsymbol{z}\cdot\boldsymbol{u}\,\mathrm{d}\mathbf{x} - \int_\Omega \boldsymbol{\omega}\cdot\boldsymbol{z}\,\mathrm{d}\mathbf{x} &= 0, \\ -\int_\Omega q\,\operatorname{div}_x\boldsymbol{u}\,\mathrm{d}\mathbf{x} &= 0, \end{aligned} \tag{2.3.10}$$

admits a unique solution $(\boldsymbol{u},\boldsymbol{\omega},p)\in \mathbf{H}(\mathrm{div};\Omega)\times\mathbf{H}(\mathbf{curl};\Omega)\times \mathrm{L}^2_0(\Omega)$. *Moreover, there exists* $C>0$ *independent of* μ *such that*

$$\begin{aligned}\|\boldsymbol{u}\|_{\mathbf{H}(\mathrm{div};\Omega)}+\|\boldsymbol{\omega}\|_{\mathbf{H}(\mathbf{curl};\Omega)}+\|p\|_{0,\Omega}\leq C\big((1+\|\overline{c}\|_{0,\Omega}+\|\overline{s}\|_{0,\Omega})\|\boldsymbol{g}\|_{\infty,\Omega}+\|\boldsymbol{F}\|_{0,\Omega}\\ +\|u_\partial\|_{-1/2,\partial\Omega}+\|\boldsymbol{\omega}_\partial\|_{-1/2,\partial\Omega}\big).\end{aligned}\tag{2.3.11}$$

Now, let us show that L is a continuous mapping. For this, letting $(\overline{c}_\ell,\overline{s}_\ell)_\ell$ be sequence in $\mathcal{A}$. Next, we let $(\overline{c},\overline{s})\in\mathcal{A}$ be such that $(\overline{c}_\ell,\overline{s}_\ell)_\ell\to(\overline{c},\overline{s})$ in $\mathrm{L}^2(\Omega_T,\mathbb{R}^2)$ as $\ell\to\infty$. Define $(c_\ell,s_\ell)=\mathrm{L}(\overline{c}_\ell,\overline{s}_\ell)$. The goal is to show that (c_ℓ,s_ℓ) converges to $\mathrm{L}(\overline{c},\overline{s})$ in $\mathrm{L}^2(\Omega_T,\mathbb{R}^3)$. Next, we need the following lemma:

Lemma 2.3.2 *The solution* (c_ℓ,s_ℓ) *to system (2.3.9) satisfies:*

(i) *The sequence* $(c_\ell,s_\ell)_\ell$ *is bounded in* $\mathrm{L}^2(0,T;\mathrm{H}^1(\Omega,\mathbb{R}^2))\cap\mathrm{L}^\infty(0,T;\mathrm{L}^2(\Omega,\mathbb{R}^2))$.

(ii) *The sequence* $(c_\ell,s_\ell)_\ell$ *is relatively compact in* $\mathrm{L}^2(\Omega_T,\mathbb{R}^3)$.

Proof 2.3.1 *(i) We multiply the first and the second in (2.3.9) by* c_ℓ *and* s_ℓ *respectively, integrate over* Ω *and using the uniform nonnegativity of* $M(\overline{c}_\ell,\overline{s}_\ell)$, *yields*

$$\begin{aligned}&\frac{1}{2}\frac{d}{dt}\int_\Omega\Big(|c_\ell|^2+|s_\ell|^2\Big)\,\mathrm{d}\mathbf{x}+D^{\min}\int_\Omega\Big(|\nabla_x c_\ell|^2+|\nabla_x s_\ell|^2\Big)\,\mathrm{d}\mathbf{x}\\ &+\int_\Omega\Big[2\,a_{11}\,|\nabla_x c_\ell|^2+a_{12}\,\nabla_x c_\ell\cdot\nabla s_\ell+a_{21}\,|\nabla s_\ell|^2\Big]\,f_\varepsilon^+(c_\ell)\,\mathrm{d}\mathbf{x}\\ &+\int_\Omega\Big[a_{12}\,|\nabla_x c_\ell|^2+a_{21}\,\nabla_x c_\ell\cdot\nabla_x s_\ell+2\,a_{22}\,|\nabla_x s_\ell|^2\Big]\,f_\varepsilon^+(s_\ell)\,\mathrm{d}\mathbf{x}\\ &=\frac{1}{2}\frac{d}{dt}\int_\Omega\Big(|c_\ell|^2+|s_\ell|^2\Big)\,\mathrm{d}\mathbf{x}+D^{\min}\int_\Omega\Big(|\nabla_x c_\ell|^2+|\nabla_x s_\ell|^2\Big)\,\mathrm{d}\mathbf{x}\\ &+\int_\Omega(\nabla_x c_\ell,\nabla_x s_\ell)^T\,M(c_\ell,s_\ell)\,(\nabla_x c_\ell,\nabla_x s_\ell)\,\mathrm{d}\mathbf{x}=\int_\Omega H_{c,\varepsilon}(\overline{c}_\ell^+,\overline{s}_\ell^+)c_\ell\,\mathrm{d}\mathbf{x}+\int_\Omega H_{s,\varepsilon}(\overline{c}_\ell^+,\overline{s}_\ell^+)s_\ell\,\mathrm{d}\mathbf{x}\\ &\leq C\int_\Omega\Big(|c_\ell|^2+|s_\ell|^2\Big)\,\mathrm{d}\mathbf{x},\end{aligned}\tag{2.3.12}$$

for some constant $C>0$. *Herein, we have used assumption (2.3.2) and*

$$\int_\Omega c_\ell\,\boldsymbol{u}\cdot\nabla_x c_\ell\,\mathrm{d}\mathbf{x}+\int_\Omega s_\ell\,\boldsymbol{u}\cdot\nabla_x s_\ell\,\mathrm{d}\mathbf{x}=\frac{1}{2}\int_\Omega\boldsymbol{u}\cdot\nabla_x(c_\ell)^2\,\mathrm{d}\mathbf{x}+\frac{1}{2}\int_\Omega\boldsymbol{u}\cdot\nabla_x(s_\ell)^2\,\mathrm{d}\mathbf{x}=0.$$

In view of (2.3.5) (recall that the matrix $M(c_\ell,s_\ell)$ *is nonnegative under condition (2.3.5)) and Gronwall's inequality it follows from (2.3.12) that,*

$$\sup_{t\in(0,T)}\int_\Omega\Big(|c_\ell|^2+|s_\ell|^2\Big)\,\mathrm{d}\mathbf{x}\leq\exp(CT)\|c_0+s_0\|_{\mathrm{L}^2(\Omega)},\tag{2.3.13}$$

which proves the first part of (i).
From (2.3.12) and (2.3.13) we may also conclude that,

$$\int\int_{\Omega_T}(|\nabla_x c_\ell|^2+|\nabla_x s_\ell|^2)\,\mathrm{d}\mathbf{x}\,\mathrm{d}t\leq\frac{T\exp(CT)}{D^{\min}}\|c_0+s_0\|_{\mathrm{L}^2(\Omega)},\tag{2.3.14}$$

yielding (i).

(ii) Finally multiplying the first, the second and the third equation (2.3.9) by $\varphi_c,\varphi_s\in\mathrm{L}^2(0,T;\mathrm{H}^1(\Omega))$, *respectively and using the boundedness of* f_ε^+, $H_{c,\varepsilon}$, $H_{s,\varepsilon}$, *and (2.3.14) there exists a constant* $C(\varepsilon)>0$ *such that*

$$\left|\int_0^T\langle\,\partial_t c_\ell,\varphi_c\,\rangle\,\mathrm{d}t\right|+\left|\int_0^T\langle\,\partial_t s_\ell,\varphi_s\,\rangle\,\mathrm{d}t\right|\leq C(\varepsilon)\Big(\|\varphi_c\|_{\mathrm{L}^2(0,T;\mathrm{H}^1(\Omega))}+\|\varphi_s\|_{\mathrm{L}^2(0,T;\mathrm{H}^1(\Omega))}\Big),\tag{2.3.15}$$

so we get (ii). Then, (ii) is a consequence of (i) and the uniform boundedness (2.3.15) of $(c_\ell,s_\ell)_\ell$ *in* $\mathrm{L}^2(0,T;(\mathrm{H}^1(\Omega,\mathbb{R}^2))')$

Remark 2.3.2 *Note that it is easy to deduce from Lemma 2.3.2 that the constant $C_{\mathcal{A}} > 0$ (consult (2.3.8)) is defined as follows:*

$$C_{\mathcal{A}} = \frac{(D^{\min} + T)\exp(CT)}{D^{\min}} \|c_0 + s_0\|_{\mathrm{L}^2(\Omega)}$$

for some constant $C > 0$.

From Lemma 2.3.2, there exist functions $(c_\ell, s_\ell) \in \mathrm{L}^2(0,T;\mathrm{H}^1(\Omega,\mathbb{R}^2))$ such that, up to extracting subsequences if necessary,

$$(c_\ell, s_\ell) \to (c,s) \text{ in } (\mathrm{L}^2(\Omega_T))^2 \text{ strongly},$$

and from this the continuity of L on $\mathcal{A}$ follows. We observe that, from Lemma 2.3.2, $\mathrm{L}(\mathcal{A})$ is bounded in the set

$$\mathcal{E} = \left\{ u \in \mathrm{L}^2(0,T;\mathrm{H}^1(\Omega,\mathbb{R}^2)) \ : \ \partial_t u \in \mathrm{L}^2(0,T;(\mathrm{H}^1(\Omega,\mathbb{R}^2))') \right\}. \tag{2.3.16}$$

By a standard Aubin-Lions-Simon compactness lemma (see for e.g. [85],Theorem 5 or [74]), $\mathcal{E} \hookrightarrow \mathrm{L}^2(\Omega_T,\mathbb{R}^2)$ is compact, thus L is compact. Now, by the Schauder fixed point theorem, the operator L has a fixed point $(c_\varepsilon, s_\varepsilon)$ such that $\mathrm{L}(c_\varepsilon, s_\varepsilon) = (c_\varepsilon, s_\varepsilon)$. Then there exists a solution $(c_\varepsilon, s_\varepsilon, \boldsymbol{u}_\varepsilon, \boldsymbol{\omega}_\varepsilon, p_\varepsilon)$ of

$$\begin{aligned}
\int_0^T \langle \partial_t c_\varepsilon, \varphi_c \rangle \,\mathrm{d}t + \iint_{\Omega_T} \Big[\left(D_c(c_\varepsilon) + 2\,a_{11}\, f_\varepsilon^+(c_\varepsilon) + a_{12}\, f_\varepsilon^+ s_\varepsilon)\right) \nabla_x c_\varepsilon + a_{12}\, f_\varepsilon^+(c_\varepsilon)\, \nabla_x s \\
- c_\varepsilon \boldsymbol{u}_\varepsilon \Big] \cdot \nabla_x \varphi_c \,\mathrm{d}\mathbf{x}\,\mathrm{d}t = \iint_{\Omega_T} H_{c,\varepsilon}(c_\varepsilon^+, s_\varepsilon^+)\varphi_c \,\mathrm{d}\mathbf{x}\,\mathrm{d}t, \\
\int_0^T \langle \partial_t s_\varepsilon, \varphi_s \rangle \,\mathrm{d}t + \iint_{\Omega_T} \Big[\left(D_s(s_\varepsilon) + a_{21}\, f_\varepsilon^+(c_\varepsilon) + 2a_{22}\, f_\varepsilon^+(s_\varepsilon)\right) \nabla_x s_\varepsilon + a_{21}\, f_\varepsilon^+(s_\varepsilon)\, \nabla_x c_\varepsilon \\
- c_\varepsilon \boldsymbol{u}_\varepsilon \Big] \cdot \nabla_x \varphi_s \,\mathrm{d}\mathbf{x}\,\mathrm{d}t = \iint_{\Omega_T} H_{s,\varepsilon}(c_\varepsilon^+, s_\varepsilon^+)\varphi_s \,\mathrm{d}\mathbf{x}\,\mathrm{d}t, \\
\iint_{\Omega_T} \mathbb{K}^{-1} \boldsymbol{u}_\varepsilon \cdot \mathbf{v} \,\mathrm{d}\mathbf{x}\,\mathrm{d}t + \sqrt{\mu} \iint_{\Omega_T} \mathbf{curl}\, \boldsymbol{\omega}_\varepsilon \cdot \mathbf{v} \,\mathrm{d}\mathbf{x}\,\mathrm{d}t - \iint_{\Omega_T} p_\varepsilon \,\mathrm{div}_x\, \mathbf{v} \,\mathrm{d}\mathbf{x}\,\mathrm{d}t \\
= \iint_{\Omega_T} (Q(c_\varepsilon, s_\varepsilon)\boldsymbol{g} + \mathbf{F}) \cdot \mathbf{v} \,\mathrm{d}\mathbf{x}\,\mathrm{d}t, \\
\sqrt{\mu} \iint_{\Omega_T} \mathbf{curl}\, \boldsymbol{z} \cdot \boldsymbol{u}_\varepsilon \,\mathrm{d}\mathbf{x}\,\mathrm{d}t - \iint_{\Omega_T} \boldsymbol{\omega}_\varepsilon \cdot \boldsymbol{z} \,\mathrm{d}\mathbf{x}\,\mathrm{d}t = 0, \\
- \iint_{\Omega_T} q \,\mathrm{div}_x\, \boldsymbol{u}_\varepsilon \,\mathrm{d}\mathbf{x}\,\mathrm{d}t = 0,
\end{aligned} \tag{2.3.17}$$

for all $\varphi_c,\ \varphi_s \in \mathrm{L}^2(0,T;\mathrm{H}^1(\Omega))$, $\mathbf{v} \in \mathbf{L}^2(0,T;\mathbf{H}_0(\mathrm{div};\Omega))$, $\boldsymbol{z} \in \mathbf{L}^2(0,T;\mathbf{H}_0(\mathbf{curl};\Omega))$, $q \in \mathrm{L}^2(0,T;\mathrm{L}^2_0(\Omega))$.

2.3.4 Existence of weak solutions

Note that from Subsection 2.3.3, we know there exist sequences $(c_\varepsilon, s_\varepsilon, \boldsymbol{u}_\varepsilon, \boldsymbol{\omega}_\varepsilon, p_\varepsilon)_{\varepsilon>0}$ solution to (2.3.7). We have now the following series of a priori estimates.

Lemma 2.3.3 *Assume conditions (2.3.1), (2.3.2) and (2.3.5) hold. If $c_0, s_0 \in L^2_+(\Omega)$ then the solution $(c_\varepsilon, s_\varepsilon, \boldsymbol{u}_\varepsilon, \boldsymbol{\omega}_\varepsilon, p_\varepsilon)$ is nonnegative. Moreover, there exist constants $c_1, \ldots, c_5 > 0$ not depending on ε such that*

$$\|(c_\varepsilon, s_\varepsilon)\|_{\mathrm{L}^\infty(0,T;\mathrm{L}^2(\Omega,\mathbb{R}^2))} \le c_1, \tag{2.3.18}$$

$$\|H_{c,\varepsilon}(c_\varepsilon, s_\varepsilon)\|_{\mathrm{L}^1(\Omega_T)} + \|H_{s,\varepsilon}(c_\varepsilon, s_\varepsilon)\|_{\mathrm{L}^1(\Omega_T)} \le c_2, \tag{2.3.19}$$

$$\|\nabla_x c_\varepsilon\|_{\mathrm{L}^2(\Omega_T)} + \|\nabla_x s_\varepsilon\|_{\mathrm{L}^2(\Omega_T)} \le c_3, \tag{2.3.20}$$

$$\|\boldsymbol{u}_\varepsilon\|_{\mathbf{H}(\mathrm{div};\Omega)} + \|\boldsymbol{\omega}_\varepsilon\|_{\mathbf{H}(\mathbf{curl};\Omega)} + \|p_\varepsilon\|_{0,\Omega} \le c_4, \tag{2.3.21}$$

$$\|\partial_t c_\varepsilon\|_{\mathrm{L}^2(0,T;(W^{1,\infty}(\Omega))')} + \|\partial_t s_\varepsilon\|_{\mathrm{L}^2(0,T;(W^{1,\infty}(\Omega))')} \le c_5. \tag{2.3.22}$$

Proof.
In the weak formulation (2.3.17) we take $\varphi_c = -c_\varepsilon^-$, $\varphi_s = -s_\varepsilon^-$, and we integrate over Ω instead Ω_T, we get from (2.3.2) and (2.3.5)

$$\frac{1}{2}\frac{d}{dt}\int_\Omega \left(|c_\varepsilon^-|^2 + |s_\varepsilon^-|^2\right) \mathrm{d}\mathbf{x} \leq 0. \tag{2.3.23}$$

Herein, we used

$$-\int_\Omega c_\varepsilon^- \boldsymbol{u}_\varepsilon \cdot \nabla_x c_\varepsilon \,\mathrm{d}\mathbf{x} - \int_\Omega s_\varepsilon^- \boldsymbol{u}_\varepsilon \cdot \nabla_x s_\varepsilon \,\mathrm{d}\mathbf{x} = \frac{1}{2}\int_\Omega \boldsymbol{u}_\varepsilon \cdot \nabla_x (c_\varepsilon^-)^2 \,\mathrm{d}\mathbf{x} + \frac{1}{2}\int_\Omega \boldsymbol{u}_\varepsilon \cdot \nabla_x (s_\varepsilon^-)^2 \,\mathrm{d}\mathbf{x} = 0.$$

This yields the nonnegativity of $(c_\varepsilon, s_\varepsilon)$.
By the (weak) lower semicontinuity properties of norms, the estimates (2.3.13) and (2.3.14) hold with (c_ℓ, c_ℓ) replaced by $(c_\varepsilon, s_\varepsilon)$. Moreover, the constants c_1, c_3 are independent of ε (consult the proof of Lemma 2.3.2). Observe that for $j = c, s$

$$\left|H_{j,\varepsilon}(c_\varepsilon, s_\varepsilon)\right| \leq C(|c_\varepsilon|^2 + |s_\varepsilon|^2),$$

for some constant $C > 0$. Using this, (2.3.19) is a consequence of (2.3.18).
Next, we use (2.3.18) and Lemma 2.3.1 to deduce (2.3.21). Finally using the weak formulation (2.3.17), we deduce from (2.3.18) and (2.3.20): for all $\varphi_c \in \mathrm{L}^2(0,T;W^{1,\infty}(\Omega))$

$$\begin{aligned}
&\left|\int_0^T \langle \partial_t c_\varepsilon, \varphi_c\rangle \,\mathrm{d}t\right| \\
&\quad\leq D^{\max}\|\nabla_x c_\varepsilon\|_{\mathrm{L}^2(\Omega_T)}\|\nabla_x \varphi_c\|_{\mathrm{L}^2(\Omega_T)} + \|c_\varepsilon\|_{\mathrm{L}^\infty(0,T;\mathrm{L}^2(\Omega))}\|\boldsymbol{u}_\ell\|_{\mathrm{L}^2(\Omega_T)}\|\nabla_x \varphi_c\|_{\mathrm{L}^2(0,T;W^{1,\infty}(\Omega))} \\
&\qquad + C\Big(\|c_\varepsilon\|_{\mathrm{L}^\infty(0,T;\mathrm{L}^2(\Omega))} + \|s_\varepsilon\|_{\mathrm{L}^\infty(0,T;\mathrm{L}^2(\Omega))}\Big) \\
&\qquad\quad \times \Big(\boldsymbol{u}_\ell + \|\nabla_x s_\varepsilon\|_{\mathrm{L}^2(\Omega_T)}\Big)\|\nabla_x \varphi_c\|_{\mathrm{L}^2(0,T;\mathrm{L}^\infty(\Omega))} \\
&\qquad\quad + C'\Big(1 + \|c_\varepsilon\|_{\mathrm{L}^\infty(0,T;\mathrm{L}^2(\Omega))} + \|s_\varepsilon\|_{\mathrm{L}^\infty(0,T;\mathrm{L}^2(\Omega))}\Big) \\
&\qquad\quad \times \Big(1 + \|c_\varepsilon\|_{\mathrm{L}^2(\Omega_T)} + \|s_\varepsilon\|_{\mathrm{L}^2(\Omega_T)}\Big)\|\varphi_c\|_{\mathrm{L}^2(0,T;\mathrm{L}^\infty(\Omega))} \\
&\quad\leq C''\|\varphi_c\|_{\mathrm{L}^2(0,T;W^{1,\infty}(\Omega))},
\end{aligned} \tag{2.3.24}$$

for some constant $C, C', C'' > 0$ independent of ε. From this we deduce the bound

$$\|\partial_t c_\varepsilon\|_{\mathrm{L}^2(0,T;(W^{1,\infty}(\Omega))')} \leq C''. \tag{2.3.25}$$

Reasoning along the same lines for c_ε yields (2.3.25) for s_ε .

■

In view of Lemma 2.3.3 and Aubin-Lions-Simon compactness lemma, we can assume there exist limit functions (c, s) such that as $\varepsilon \to 0$ the following convergences hold (modulo extraction of subsequences, which we do not bother to relabel):

$$\begin{cases}
(c_\varepsilon, s_\varepsilon) \to (c, s) \text{ a.e. in } \Omega_T, \text{ strongly in } \mathrm{L}^2(\Omega_T, \mathbb{R}^2) \text{ and weakly in } \mathrm{L}^2(0,T;\mathrm{H}^1(\Omega,\mathbb{R}^2)), \\
H_{j,\varepsilon}(c_\varepsilon, s_\varepsilon) \to H_{j,c}(c, s) \text{ a.e. in } \Omega_T \text{ and strongly in } \mathrm{L}^1(\Omega_T), \\
\boldsymbol{u}_\varepsilon \to \boldsymbol{u} \text{ weakly in } \mathbf{L}^2(0,T;\mathbf{H}_0(\mathrm{div};\Omega)), \\
\boldsymbol{\omega}_\varepsilon \to \boldsymbol{\omega} \text{ weakly in } \mathbf{L}^2(0,T;\mathbf{H}_0(\mathbf{curl};\Omega)), \\
p_\varepsilon \to p \text{ weakly in } \mathrm{L}^2(0,T;\mathrm{L}^2_0(\Omega)).
\end{cases} \tag{2.3.26}$$

for $j = c, s$. Additionally, $(\partial_t c_\varepsilon, \partial_t s_\varepsilon,) \to (\partial_t c, \partial_t s)$ weakly in $\mathrm{L}^2(0,T;(W^{1,\infty}(\Omega,\mathbb{R}^2))')$ as $\varepsilon \to 0$. An application of Young and Hölder inequalities we get

$$\begin{aligned}\|f_\varepsilon(c_\varepsilon) - c\|_{L^2(\Omega_T)} &\leq \sqrt{2}\|c_\varepsilon - c\|_{\mathrm{L}^2(\Omega_T)} + \sqrt{2}\|\frac{\varepsilon c_\varepsilon c}{1+\varepsilon c_\varepsilon}\|_{\mathrm{L}^2(\Omega_T)} \\ &\leq \sqrt{2}\|c_\varepsilon - c\|_{\mathrm{L}^2(\Omega_T)} + \sqrt{2}\|\frac{\varepsilon c_\varepsilon c}{(1+\varepsilon c_\varepsilon)^{2/3}(\varepsilon c_\varepsilon)^{1-2/3}}\|_{\mathrm{L}^2(\Omega_T)} \\ &\leq \sqrt{2}\|c_\varepsilon - c\|_{L^2(\Omega_T)} + \sqrt{2}\varepsilon^{2/3}\|c_\varepsilon^{2/3} c\|_{\mathrm{L}^2(\Omega_T)} \\ &\leq \sqrt{2}\|c_\varepsilon - c\|_{\mathrm{L}^2(\Omega_T)} + \sqrt{2}\varepsilon^{2/3}\|c_\varepsilon\|^{2/3}_{\mathrm{L}^\infty(0,T;\mathrm{L}^2(\Omega))} \\ &\qquad \times \|c\|_{\mathrm{L}^2(0,T;L^6(\Omega))}.\end{aligned} \tag{2.3.27}$$

Thanks to the Sobolev embedding $(H^1(\Omega) \subset \mathrm{L}^6(\Omega))$ we deduce from (2.3.27)

$$f_\varepsilon(c_\varepsilon) \to c \text{ a.e. in } \Omega_T \text{ and strongly in } \mathrm{L}^2(\Omega_T). \tag{2.3.28}$$

In the same way we get

$$f_\varepsilon(s_\varepsilon) \to s \text{ a.e. in } \Omega_T \text{ and strongly in } \mathrm{L}^2(\Omega_T). \tag{2.3.29}$$

Finally, by passing to the limit $\varepsilon \to 0$ in the weak formulation (2.3.17), with $\varphi_c, \varphi_s \in \mathrm{L}^2(0,T;W^{1,\infty}(\Omega))$, $\mathbf{v} \in \mathbf{L}^2(0,T;\mathbf{H}_0(\mathrm{div};\Omega))$, $\boldsymbol{z} \in \mathbf{L}^2(0,T;\mathbf{H}_0(\mathbf{curl};\Omega))$ and $q \in \mathrm{L}^2(0,T;\mathrm{L}^2_0(\Omega))$, we obtain in this way that the limit $(c, s, \boldsymbol{u}, \boldsymbol{\omega}, p)$ is a solution of system problem (2.1.3) in the sense of Definition 2.3.1.

2.4 Numerical analysis of micro-macro cross-diffusion-Brinkman system

In this section we develop an asymptotic preserving scheme (AP). We propose a numerical scheme uniformly stable along the transition from kinetic to macroscopic regimes. Inspired by the continuous derivation, we use the time semi-implicit discretization for the micro-macro formulation (2.2.17) which is equivalent to the kinetic-fluid model (2.2.1). After the full discretization of (2.2.17), we show various numerical tests to validate the proposed approach.

2.4.1 A time semi-implicit discretization

First, we present a time discretization to our coupled system (2.2.17). We denote by Δt a fixed time step and by $t_k := k\Delta t$ a discrete time with $k \in \mathbb{N}$. The approximations of $c(t,x)$, $s(t,x)$, $g_1(t,x,\xi)$, $g_2(t,x,\xi)$, $\boldsymbol{u}(t,x)$, $\boldsymbol{\omega}(t,x)$ and $p(t,x)$ at the time step t_k are denoted by $c^k := c(t_k,x)$, $s^k := s(t_k,x)$, $g_i^k := g_i(t_k,x,\xi)$, $\boldsymbol{u}^k := \boldsymbol{u}(t_k,x)$, $\boldsymbol{\omega}^k := \boldsymbol{\omega}(t_k,x)$ and $p^k := p(t_k,x)$ for $i = 1,2$. The semi-implicit scheme for microscopic equations in system (2.2.17) reads

$$\begin{cases} \dfrac{g_1^{k+1} - g_1^k}{\Delta t} + \dfrac{1}{\varepsilon^2}\xi M_1 \cdot \nabla_x c^k + \dfrac{1}{\varepsilon}(I - P_{M_1})(\xi \cdot \nabla_x g_1^k) = \dfrac{1}{\varepsilon^2}\mathcal{L}_1(g_1^{k+1}) \\ \quad + \dfrac{1}{\varepsilon^2}\mathcal{T}_1^2[M_2(\xi)s^k](M_1(\xi)c^k) + \dfrac{1}{\varepsilon}\mathcal{T}_1^2[M_2(\xi)s^k](g_1^k) \\ \quad + \dfrac{1}{\varepsilon^2}G_{11}(M_1(\xi)c^k, M_2(\xi)s^k, \boldsymbol{u}^k, \xi) + \dfrac{1}{\varepsilon}(I - P_{M_1})G_{12}(M_1(\xi)c^k, M_2(\xi)s^k, \xi), \\ \dfrac{g_2^{k+1} - g_2^k}{\Delta t} + \dfrac{1}{\varepsilon^2}\xi M_2 \cdot \nabla_x s^k + \dfrac{1}{\varepsilon}(I - P_{M_2})(\xi \cdot \nabla_x g_2^k) = \dfrac{1}{\varepsilon^2}\mathcal{L}_2(g_2^{k+1}) \\ \quad + \dfrac{1}{\varepsilon^2}\mathcal{T}_2^2[M_1(\xi)c^k](M_2(\xi)s^k) + \dfrac{1}{\varepsilon}\mathcal{T}_2^2[M_1(\xi)c^k](g_2^k) \\ \quad + \dfrac{1}{\varepsilon^2}G_{21}(M_1(\xi)c^k, M_2(\xi)s^k, \boldsymbol{u}^k, \xi) + \dfrac{1}{\varepsilon}(I - P_{M_2})G_{22}(M_1(\xi)c^k, M_2(\xi)s^k, \xi). \end{cases} \tag{2.4.1}$$

In the hydrodynamic equations of system (2.2.17), we take g_1 and g_2 at the time t_{k+1}. The result is

$$\begin{cases} \dfrac{c^{k+1}-c^k}{\Delta t} + \langle \xi \cdot \nabla_x g_1^{k+1} \rangle = \langle G_{12}(M_1(\xi)c^k, M_2(\xi)s^k, \xi) \rangle, \\ \dfrac{s^{k+1}-s^k}{\Delta t} + \langle \xi \cdot \nabla_x g_2^{k+1} \rangle = \langle G_{22}(M_1(\xi)c^{k+1}, M_2(\xi)s^k, \xi) \rangle. \\ \mathbb{K}^{-1}\boldsymbol{u}^{k+1} + \sqrt{\mu}\,\mathbf{curl}\,\boldsymbol{\omega}^{k+1} + \nabla_x p^{k+1} = Q(c^{k+1}, s^{k+1})\boldsymbol{g} + \mathbf{F}, \\ \boldsymbol{\omega}^{k+1} - \sqrt{\mu}\,\mathbf{curl}\,\boldsymbol{u}^{k+1} = \mathbf{0}, \quad \mathrm{div}_x \boldsymbol{u}^{k+1} = 0. \end{cases} \tag{2.4.2}$$

Proposition 2.4.1 *The numerical scheme given by (2.4.1)-(2.4.2) is consistent with equations (2.2.25) when ε goes to 0.*

Proof 2.4.1 *The asymptotic behavior of scheme (2.4.1)-(2.4.2) is obtained similarly as the continuous case. Since the operator $-\mathcal{L}_i$ is self-adjoint and positive, the operator $(I - \frac{\Delta t}{\varepsilon^2}\mathcal{L}_i)$ is also invertible for all $\Delta t \geq 0$ for $i = 1, 2$. Hence (2.4.1) gives*

$$\begin{aligned} g_1^{k+1} = \Big(I - \frac{\Delta t}{\varepsilon^2}\mathcal{L}_1\Big)^{-1}\Big[g_1^k + \frac{\Delta t}{\varepsilon^2}\big(\mathcal{T}_1^2[M_2 s^k](M_1 c^k + \varepsilon g_1^k) + G_{11}(M_1 c^k, M_2 s^k, \boldsymbol{u}^k, \xi) \\ -\xi M_1 \cdot \nabla_x c^k\big) + \frac{\Delta t}{\varepsilon}(I - P_{M_1})\big(G_{12}(M_1 c^k, M_2 s^k, \xi) - \xi \cdot \nabla_x g_1^k\big)\Big] \end{aligned} \tag{2.4.3}$$

and

$$\begin{aligned} g_2^{k+1} = \Big(I - \frac{\Delta t}{\varepsilon^2}\mathcal{L}_2\Big)^{-1}\Big[g_2^k + \frac{\Delta t}{\varepsilon^2}\big(\mathcal{T}_2^2[M_1 c^k](M_2(\xi)s^k + \varepsilon g_2^k) + G_{21}(M_1 c^k, M_2 s^k, \boldsymbol{u}^k, \xi) \\ -\xi M_2 \cdot \nabla_x s^k\big) + \frac{\Delta t}{\varepsilon}(I - P_{M_2})\big(G_{22}(M_1 c^k, M_2 s^k, \xi) - \xi \cdot \nabla_x g_2^k\big)\Big]. \end{aligned} \tag{2.4.4}$$

We use the limited development with respect to ε to get $\big(I - \frac{\Delta t}{\varepsilon^2}\mathcal{L}_i\big)^{-1} = -\frac{\varepsilon^2}{\Delta t}\mathcal{L}_i^{-1} + O(\varepsilon^3)$, for $i = 1, 2$ and the fact that $\mathcal{L}_1$ and $\mathcal{L}_2$ are linear and invertible. Then, we develop the right hand side of (2.4.3) and (2.4.4) with regard to ϵ when $\epsilon \to 0$ and we take the same order of ε. We have:

$$g_1^{k+1} = \mathcal{L}_1^{-1}\Big(\xi M_1 \cdot \nabla_x c^k - \mathcal{T}_1^2[M_2 s^k](M_1 c^k) - G_{11}(M_1 c^k, M_2 s^k, \boldsymbol{u}^k, \xi)\Big) + O(\varepsilon),$$

and

$$g_2^{k+1} = \mathcal{L}_2^{-1}\Big(\xi M_2 \cdot \nabla_x s^k - \mathcal{T}_2^2[M_1 c^k](M_2 s^k)\Big) - G_{21}(M_1 c^k, M_2 s^k, \boldsymbol{u}^k, \xi)\Big) + O(\varepsilon).$$

Inserting g_1^{k+1} and g_2^{k+1} into (2.4.2), we obtain

$$\begin{aligned} \frac{c^{k+1}-c^k}{\Delta t} + \Big\langle \xi \cdot \nabla_x \mathcal{L}_1^{-1}\big[\xi M_1 \cdot \nabla_x c^k - \mathcal{T}_1^2[M_2 s^k](M_1 c^k) - G_{11}(M_1 c^k, M_2 s^k, \boldsymbol{u}^k, \xi)\big]\Big\rangle \\ = \Big\langle G_{12}(M_1 c^k, M_2 s^k, \xi)\Big\rangle + O(\varepsilon), \end{aligned} \tag{2.4.5}$$

and

$$\begin{aligned} \frac{s^{k+1}-s^k}{\Delta t} + \Big\langle \xi \cdot \nabla_x \mathcal{L}_2^{-1}\big[\xi M_2 \cdot \nabla_x s^k - \mathcal{T}_2^2[M_1 c^k](M_2 s^k) - G_{21}(M_1 c^k, M_2 s^k, \boldsymbol{u}^k, \xi)\big]\Big\rangle \\ = \Big\langle G_{22}(M_1 c^{k+1}, M_2 s^k, \xi)\Big\rangle + O(\varepsilon), \end{aligned} \tag{2.4.6}$$

which is consistent with system (2.2.25) when ε goes to 0.

2.4.2 Full discretization

In this subsection, we present our method in one-dimensional case into the domain $[-a,a]$ for fixed $a \in \mathbb{R}$. Let $\mathbb{T} = \{K_j, \quad j = 1,\dots,N_x\}$ be an admissible mesh in the meaning of Definition 5.5 page 125 in Ref. [46]. The control volume is given by $K_j =]x_{j-\frac{1}{2}}, x_{j+\frac{1}{2}}[$ with $x_j = \frac{1}{2}(x_{j-\frac{1}{2}} + x_{j+\frac{1}{2}})$ and its length is denoted by $h_j = x_{j+\frac{1}{2}} - x_{j-\frac{1}{2}}$ for $j = 1,\dots,N_x$. For the velocity space, we consider $\xi_\ell = \xi_{\min} + \ell\Delta\xi$, for $\ell = 0,...,N_\xi - 1$ where $\Delta\xi = \frac{1}{N_\xi}(\xi_{\max} - \xi_{\min})$ with $\xi_{\max} = -\xi_{\min}$. We shall assume that $g = \mathbf{F} = 0$. Thus, the fluid velocity is a given function depending only on time, namely $u(t) = \partial_x p$. The methodology is as follow: the macroscopic equations in (2.4.2) are computed in the control volume K_j while the microscopic equations in (2.4.1) should be computed in the interface of K_j. Precisely, the macroscopic densities are as follows

$$c(t_k,x)|_{K_j} \approx c_j^k, \qquad s(t_k,x)|_{K_j} \approx s_j^k,$$

and the microscopic ones are given by

$$g_1(t_k,x_{j+\frac{1}{2}},\xi_\ell)|_{\partial K_j} \approx g^k_{1,j+\frac{1}{2},\ell}, \qquad g_2(t_k,x_{j+\frac{1}{2}},\xi_\ell)|_{\partial K_j} \approx g^k_{2,j+\frac{1}{2},\ell}$$

for $j = 1,...,N_x$ and $\ell = 1,...,N_\xi$. Now, we integrate the macroscopic equations in (2.4.2) over the control volume K_j, we approximate the time derivatives by differential quotients and using an upwind choice for g_1 and g_2 to arrive to

$$\begin{cases} \frac{c_j^{k+1}-c_j^k}{\Delta t} + \left\langle \xi_\ell \frac{g^{k+1}_{1,j+\frac{1}{2},\ell} - g^{k+1}_{1,j-\frac{1}{2},\ell}}{h_j} \right\rangle = \langle G_{12}(M_{1,\ell}c_j^k, M_{2,\ell}s_j^k, \xi_\ell)\rangle, \\ \frac{s_j^{k+1}-s_j^k}{\Delta t} + \left\langle \xi_\ell \frac{g^{k+1}_{2,j+\frac{1}{2},\ell} - g^{k+1}_{2,j-\frac{1}{2},\ell}}{h_j} \right\rangle = \langle G_{22}(M_{1,\ell}c_j^{k+1}, M_{2,\ell}s_j^k, \xi_\ell)\rangle, \\ \frac{p_{j+1}^k - p_j^k}{h_j} = u^k. \end{cases} \tag{2.4.7}$$

For the microscopic equations in (2.4.1), we compute the unknowns functions g_1 and g_2 in the interface of K_j (or integrating over the control volume $I_{j+\frac{1}{2}}$):

$$\begin{cases} \frac{g^{k+1}_{1,j+\frac{1}{2},\ell} - g^k_{1,j+\frac{1}{2},\ell}}{\Delta t} + \frac{1}{\varepsilon}(I - P_{M_{1,j}})\left(\xi_\ell^+ \frac{g^k_{1,j+\frac{1}{2},\ell} - g^k_{1,j-\frac{1}{2},\ell}}{h_j} + \xi_\ell^- \frac{g^k_{1,j+\frac{3}{2},\ell} - g^k_{1,j+\frac{1}{2},\ell}}{h_j}\right) \\ \quad = \frac{1}{\varepsilon^2}\left[\mathcal{L}_{1,\ell}(g^{k+1}_{1,j+\frac{1}{2},\ell}) - \xi_\ell M_{1,\ell}\frac{c_{j+1}^k - c_j^k}{h_j} + \mathcal{T}^2_{1,\ell}[M_{2,\ell}s^k_{j+\frac{1}{2}}](M_{1,\ell}c^k_{j+\frac{1}{2}})\right. \\ \qquad \left. + G_{11,\ell}(M_{1,\ell}c^k_{j+\frac{1}{2}}, M_{2,\ell}s^k_{j+\frac{1}{2}}, u^k, \xi_\ell)\right] \\ \qquad + \frac{1}{\varepsilon}\left[\mathcal{T}^2_{1,\ell}[M_{2,\ell}s^k_{j+\frac{1}{2}}](g^k_{1,j+\frac{1}{2},\ell}) + (I - P_{M_{1,\ell}})G_{12,\ell}(M_{1,\ell}c^k_{j+\frac{1}{2}}, M_{2,\ell}s^k_{j+\frac{1}{2}}, \xi_\ell)\right], \\ \frac{g^{k+1}_{2,j+\frac{1}{2},\ell} - g^k_{2,j+\frac{1}{2},\ell}}{\Delta t} + \frac{1}{\varepsilon}(I - P_{M_{2,\ell}})\left(\xi_\ell^+ \frac{g^k_{2,j+\frac{1}{2},\ell} - g^k_{2,j-\frac{1}{2},\ell}}{h_j} + \xi_\ell^- \frac{g^k_{2,j+\frac{3}{2},\ell} - g^k_{2,j+\frac{1}{2},\ell}}{h_j}\right) \\ \quad = \frac{1}{\varepsilon^2}\left[\mathcal{L}_{2,\ell}(g^{k+1}_{2,j+\frac{1}{2},\ell}) - \xi_\ell M_{2,\ell}\frac{s_{j+1}^k - s_j^k}{h_j} + \mathcal{T}^2_{2,\ell}[M_{1,\ell}c^k_{j+\frac{1}{2}}](M_{2,\ell}s^k_{j+\frac{1}{2}})\right. \\ \qquad \left. + G_{21,\ell}(M_{1,\ell}c^k_{j+\frac{1}{2}}, M_{2,\ell}s^k_{j+\frac{1}{2}}, u^k, \xi_\ell)\right] \\ \qquad + \frac{1}{\varepsilon}\left[\mathcal{T}^2_{2,\ell}[M_{1,\ell}c^k_{j+\frac{1}{2}}](g^k_{2,j+\frac{1}{2},\ell}) + (I - P_{M_{2,\ell}})G_{22}(M_{1,\ell}c^k_{j+\frac{1}{2}}, M_{2,\ell}s^k_{j+\frac{1}{2}}, \xi_\ell)\right]. \end{cases} \tag{2.4.8}$$

In the following proposition, we show that our scheme proposed in the micro-macro formulation (2.4.8)-(2.4.7) is uniformly stable along the transition from kinetic to macroscopic regimes.

Proposition 2.4.2 *The time and space approximations (2.4.8)-(2.4.7) of the micro-macro formulation in the limit (ε goes to zero), satisfy the following discretization:*

$$\begin{aligned}
&\frac{c_j^{k+1}-c_j^k}{\Delta t}+\frac{1}{h_j}\Big\langle \xi_\ell\Big[\mathcal{L}_{1,\ell}^{-1}\Big(\xi_\ell M_{1,\ell}\frac{c_{j+1}^k-c_j^k}{h_j}\Big)-\mathcal{L}_{1,\ell}^{-1}\Big(\xi_\ell M_{1,\ell}\frac{c_j^k-c_{j-1}^k}{h_j}\Big)\Big]\Big\rangle\\
&+\frac{1}{h_j}\Big\langle \xi_\ell\Big[\mathcal{L}_{1,\ell}^{-1}\Big(\mathcal{T}_1^2[M_{2,\ell}s^k_{j+\frac12}](M_{1,\ell}c^k_{j+\frac12})\Big)-\mathcal{L}_{1,\ell}^{-1}\Big(\mathcal{T}_{1,\ell}^2[M_{2,\ell}s^k_{j-\frac12}](M_{1,\ell}c^k_{j-\frac12})\Big)\Big]\Big\rangle\\
&+\frac{1}{h_j}\Big\langle \xi_\ell\Big[\mathcal{L}_{1,\ell}^{-1}\Big(G_{11,\ell}(M_{1,\ell}c^k_{j+\frac12},M_{2,\ell}s^k_{j+\frac12},u^k,\xi_\ell)\Big)-\mathcal{L}_{1,\ell}^{-1}\Big(G_{11,\ell}(M_{1,\ell}c^k_{j-\frac12},M_{2,\ell}s^k_{j-\frac12},u^k,\xi_\ell)\Big)\Big]\Big\rangle\\
&\qquad=\Big\langle G_{12,\ell}(M_{1,\ell}c_j^k,M_{2,\ell}s_j^k,\xi_\ell)\Big\rangle+O(\varepsilon),
\end{aligned}\tag{2.4.9}$$

and

$$\begin{aligned}
&\frac{s_j^{k+1}-s_j^k}{\Delta t}+\frac{1}{h_j}\Big\langle \xi_\ell\Big[\mathcal{L}_{2,\ell}^{-1}\Big(\xi_\ell M_{2,\ell}\frac{s_{j+1}^k-s_j^k}{h_j}\Big)-\mathcal{L}_{2,\ell}^{-1}\Big(\xi_\ell M_{2,\ell}\frac{s_j^k-s_{j-1}^k}{h_j}\Big)\Big]\Big\rangle\\
&+\frac{1}{h_j}\Big\langle \xi_\ell\Big[\mathcal{L}_{2,\ell}^{-1}\Big(\mathcal{T}_{2,\ell}^2[M_{1,\ell}c^k_{j+\frac12}](M_{2,\ell}s^k_{j+\frac12})\Big)-\mathcal{L}_{2,\ell}^{-1}\Big(\mathcal{T}_{2,\ell}^2[M_{1,\ell}c^k_{j-\frac12}](M_{2,\ell}s^k_{j-\frac12})\Big)\Big]\Big\rangle\\
&+\frac{1}{h_j}\Big\langle \xi_\ell\Big[\mathcal{L}_{2,\ell}^{-1}\Big(G_{21,\ell}(M_{1,\ell}c^k_{j+\frac12},M_{2,\ell}s^k_{j+\frac12},u^k,\xi_\ell)\Big)-\mathcal{L}_{2,\ell}^{-1}\Big(G_{21,\ell}(M_{1,\ell}c^k_{j-\frac12},M_{2,\ell}s^k_{j-\frac12},u^k,\xi_\ell)\Big)\Big]\Big\rangle\\
&\qquad=\Big\langle G_{22,\ell}(M_{2,\ell}c_j^{k+1},M_{2,\ell}s_j^k,\xi_\ell)\Big\rangle+O(\varepsilon),
\end{aligned}\tag{2.4.10}$$

which is consistent with system (2.2.25).

2.4.3 Boundary conditions

For the numerical solution of the kinetic equation (2.2.1), the following inflow boundary conditions are usually prescribe for the distribution functions f_1 and f_2:

$$f_i(t,x_{\min},\xi)=f_{i,l}(\xi),\quad \xi>0\qquad f_i(t,x_{\max},\xi)=f_{i,r}(\xi),\quad \xi<0,\ \text{for } i=1,2.$$

We shall denote $w_1=c$ and $w_2=s$. The inflow boundary conditions can be rewritten in the micro-macro formulation by

$$w_i(t,x_0)M_i+\frac{\varepsilon}{2}(g_i(t,x_{\frac12},\xi)+g_i(t,x_{-\frac12},\xi))=f_{i,l}(\xi),\quad \xi>0,$$

$$w_i(t,x_{N_x})M_i+\frac{\varepsilon}{2}(g_i(t,x_{N_x+\frac12},v)+g_i(t,x_{N_x-\frac12},\xi))=f_{i,r}(\xi),\quad \xi<0,$$

for $i=1,2$. For the other velocities, we consider the following artificial Neumann boundary conditions:

$$g_i(t,x_{\frac12},\xi_\ell)=g_i(t,x_{-\frac12},\xi_\ell),\quad \xi_\ell<0,$$
$$g_i(t,x_{N_x+\frac12},\xi_\ell)=g_i(t,x_{N_x-\frac12},\xi_\ell),\quad \xi_\ell>0,$$

for $i=1,2$. Furthermore, the ghost points can be computed for $i=1,2$ as follows:

$$g^{k+1}_{i,-\frac12,\ell}=\begin{cases}\frac{2}{\varepsilon}(f_{1,l}(\xi_\ell)-w_{i,0}^{k+1}M_i)-g^{k+1}_{i,\frac12,\ell},\quad \xi_\ell>0,\\ g^{k+1}_{i,\frac12,\ell},\quad \xi_\ell<0;\end{cases}\tag{2.4.11}$$

$$g^{k+1}_{i,N_x+\frac12,\ell}\begin{cases}\frac{2}{\varepsilon}(f_{i,r}(\xi_\ell)-w_{i,N_x}^{k+1}M_i)-g^{k+1}_{i,N_x-\frac12},\quad \xi_\ell<0,\\ g^{k+1}_{i,N_x-\frac12,\ell},\quad \xi_\ell>0.\end{cases}\tag{2.4.12}$$

It then follows from (2.4.7) that for $i = 1, 2$:

$$\begin{cases} (1 + \frac{2\Delta t}{\varepsilon h_0} < \xi_\ell^+ M_{i,\ell} >) w_{i,0}^{k+1} = w_{i,0}^k - \frac{\Delta t}{h_0} \big\langle (\xi_\ell + \xi_\ell^+ - \xi_\ell^-) g_{i,\frac{1}{2},\ell}^{k+1} - \frac{2\xi_\ell^+}{\varepsilon} f_{i,l}(\xi_\ell) \big\rangle \\ \qquad\qquad + \Delta t \big\langle G_{i2,\ell}(M_{1,\ell} c_0^k, M_{2,\ell} s_0^k) \big\rangle, \\ (1 - \frac{2\Delta t}{\varepsilon h_{N_x}} < \xi_\ell^- M_{i,\ell} >) w_{i,N_x}^{k+1} = w_{i,N_x}^k - \frac{\Delta t}{h_{N_x}} \big\langle \frac{2\xi_\ell^-}{\varepsilon} f_{i,r}(\xi_\ell) - (\xi_\ell - \xi_\ell^+ + \xi_\ell^-) g_{i,N_x-\frac{1}{2},\ell}^{k+1} \big\rangle \\ \qquad\qquad + \Delta t \big\langle G_{i2,\ell}(M_{1,\ell} c_{N_x}^k, M_{2,\ell} s_{N_x}^k) \big\rangle. \end{cases} \tag{2.4.13}$$

2.4.4 Numerical results

In this subsection, we present some numerical experiments in order to validate our approach. In the following tests, the computational domain in space is $[-1; 1]$ while the velocity space is $V = [-1; 1]$ with 64 discrete points, which yields good enough accuracy for numerical results [29]. We adopt a set of parameters, namely the coefficients of intra- and inter-specific competition, used in the book by [84] (adopted also by [6]): $a_1 = 0.61/year$, $a_2 = 0.82/year$, $b_1 = 0.4575$, $b_2 = 0.31$, $d_1 = 9.5$ and $d_2 = 8.2$. The diffusion coefficients are constants ($D_c = 1$ and $D_s = 1$). Moreover, we consider $a_{11} = a_{22} = 0.5$ and $a_{12} = a_{21} = 1$ which satisfy the conditions (2.3.5). The initial densities correspond to the c-predator species and the s-prey species are given by

$$c_0(x) = 0.65 \quad \text{and} \quad s_0(x) = \exp(-30x^2).$$

The initial cell distribution function is as follow

$$f_1(0; x; \xi) = c_0(x) M_1(\xi) \quad \text{and} \quad f_2(0; x; \xi) = s_0(x) M_2(\xi),$$

where $M_i(\xi) = \frac{1}{|V|}$ for $i = 1, 2$. Next, we consider the macroscopic cross-diffusion-Brinkman system in one dimension. We discretize this system by using finite volume method

$$\begin{cases} \frac{c_j^{k+1} - c_j^k}{\Delta t} = D_c \Big(\frac{c_{j+1}^k - c_j^k}{h_j h_{i+\frac{1}{2}}} - \frac{c_j^k - c_{j-1}^k}{h_{i-\frac{1}{2}} h_j} \Big) - \frac{(\partial_x^{(m)} c_{j+1}^k)(c+s)_{j+1}^k - (\partial_x^{(m)} c_{j-1}^k)(c+s)_{j-1}^k}{h_j} \\ \qquad - \frac{c_{j+1}^k - c_j^k}{h_j} u^k + 2 \frac{(\partial_x^{(m)} s_{j+1}^k) c_{j+1}^k - (\partial_x^{(m)} s_{j-1}^k) c_{j-1}^k}{h_j} + H_1(c_j^k, s_j^k), \\ \frac{s_j^{k+1} - s_j^k}{\Delta t} = D_s \Big(\frac{s_{j+1}^k - s_j^k}{h_j h_{i+\frac{1}{2}}} - \frac{s_j^k - s_{j-1}^k}{h_{i-\frac{1}{2}} h_j} \Big) - \frac{(\partial_x^{(m)} s_{j+1}^k)(c^{k+1} + s^k)_{j+1} - (\partial_x^{(m)} s_{j-1}^k)(c^{k+1} + s^k)_{j-1}}{h_j} \\ \qquad - \frac{s_{j+1}^k - s_j^k}{h_j} u^k + 0.5 \frac{(\partial_x^{(m)} c_{j+1}^{k+1}) s_{j+1}^k - (\partial_x^{(m)} c_{j-1}^{k+1}) s_{j-1}^k}{h_j} + H_2(c_j^{k+1}, s_j^k), \\ u^{k+1} = \frac{p_{j+1}^k - p_j^k}{h_j}. \end{cases} \tag{2.4.14}$$

where

$$\partial_x^{(m)} z_j^k = \frac{z_{j+1}^k - z_j^k}{h_j} \quad \text{and} \quad \partial_x^{(m)} z_0^k = \partial_x^{(m)} z_{N_x}^k = 0,$$

for $1 \le j \le N_x - 1$. In Figure 2.1, we present the plots in log scale of the error estimates given by

$$e_{\Delta x}(h) = \frac{|h_{\Delta x}(t) - h_{2\Delta x}(t)|_1}{|h_{2\Delta x}(0)|_1}$$

to test the convergence of our scheme. This can be considered as an estimation of the relative error in l^1 norm, where $h_{\Delta x}$ is the numerical solution computed from a uniform grid of size $\Delta x = \frac{x_{max} - x_{min}}{N_x}$. The computations are performed with $N_x = \{80, 160, 320, 640\}$, $\Delta t = 10^{-6}$ at $t = 0.01$ for $\varepsilon = \{1, 10^{-2}, 10^{-3}, 10^{-6}\}$.

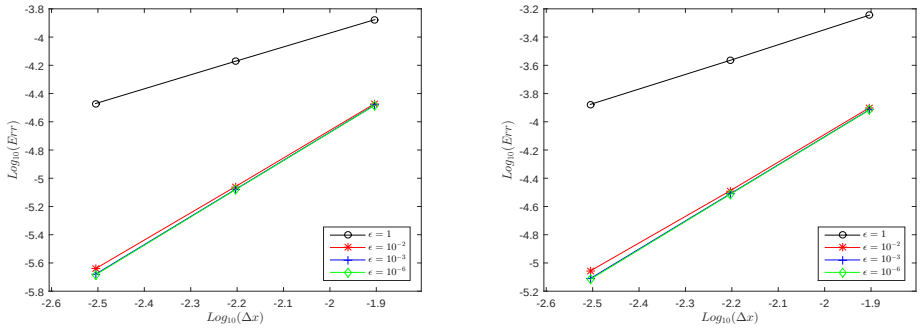

FIGURE 2.1: Convergence order of the method for $\varepsilon \in \{1, 10^{-2}, 10^{-3}, 10^{-6}\}$ at time $t = 0.01$ ($M = 1$) for the density c in the left and the density s in the right obtained from micro-macro scheme.

In Figure 2.2, we compute our numerical scheme for different values of times $t = 0.02,\ 0.03,\ 0.07,\ 0.1$ and for $\varepsilon = 10^{-k}$ where $k \in \{0, 1, 2, 3, 6\}$ against the macroscopic system in the case: $u = 0$ and $c_0 = 0.65$, $s_0 = \exp(30x^2)$. Moreover in Figure 2.3, we consider $u = 1$ and $c_0 = 0.65$, $s_0 = \exp(30(x + 0.5)^2)$. These figures show that our (AP) scheme is stable in the limit. We observe that the profile of the densities c and s given by the two schemes are almost the same when $\varepsilon \to 0$ and this illustrates the result in Proposition 2.4.2. Moreover, we observe that the cross-diffusion effect induces the formation of patterns (by using Turing mechanisms) in the presence of the fluid. Moreover, we notice that the distribution of prey and predator is affected by the fluid transport. In Figures 2.4, 2.5 and 2.6, we illustrate the evolution of the densities c and s using micro-macro scheme for $\varepsilon = 10^{-6}$ at final time $T = 0.01$ with different values of u ($u = 0,\ u = 1$ and $u = -1$). We note here that the species are diffusing according to the sign of the velocity u.

2.5 Conclusion and perspectives

In this chapter, we have proposed a new nonlinear macroscopic system coupled with the augmented Brinkman problem in a viscous flow in porous media. Specifically, the micro-macro decomposition has been applied to the kinetic system coupled with Brinkman problem (2.2.1) to derive asymptotic preserving numerical scheme. In other parts, we have proved the existence of weak solutions of the derived system (2.1.3) by using Schauder fixed-point theory. Finally, it has shown that the presented numerical scheme enjoys the asymptotic preserving property, in other words: when Knudsen parameter ε is small, our scheme is asymptotically equivalent to a standard numerical scheme for the derived macroscopic system. In this work, we developed our numerical results in one dimension using finite volume method for both macroscopic system (cross-diffusion-Brinkman) and micro-macro formulation. We believe that our technique can be extended to two dimensions. One only has to well choose the meshes, specifically for the non-structural ones.

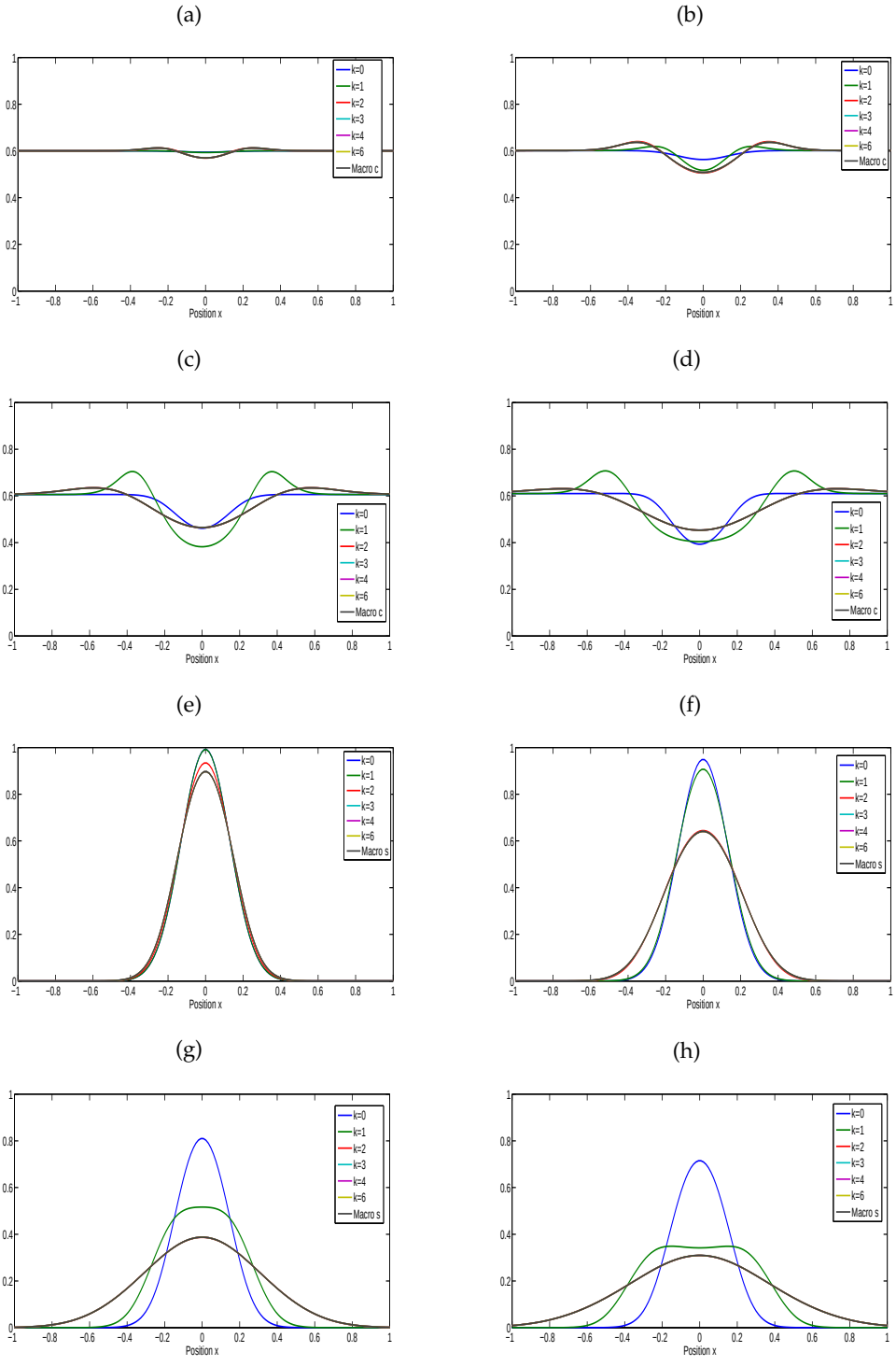

FIGURE 2.2: The Subfigures (a), (b), (c), (d) present time dynamics of predators densities $c(t;x)$, while Subfigures (e), (f), (g), (h) present time dynamics of preys densities $s(t;x)$ at $t = 0.02, 0.04, 0.07, 0.1$ obtained from the AP scheme with $\varepsilon = 10^{-k}$, $k = 0; 1; 2; 3; 6$ and comparison with cross-diffusion-Brinkman system on the domain $[-1; 1]$ and initial conditions are given by $c_0 = 0.65$ and $s_0 = \exp(30x^2)$ in the case: $u = 0$.

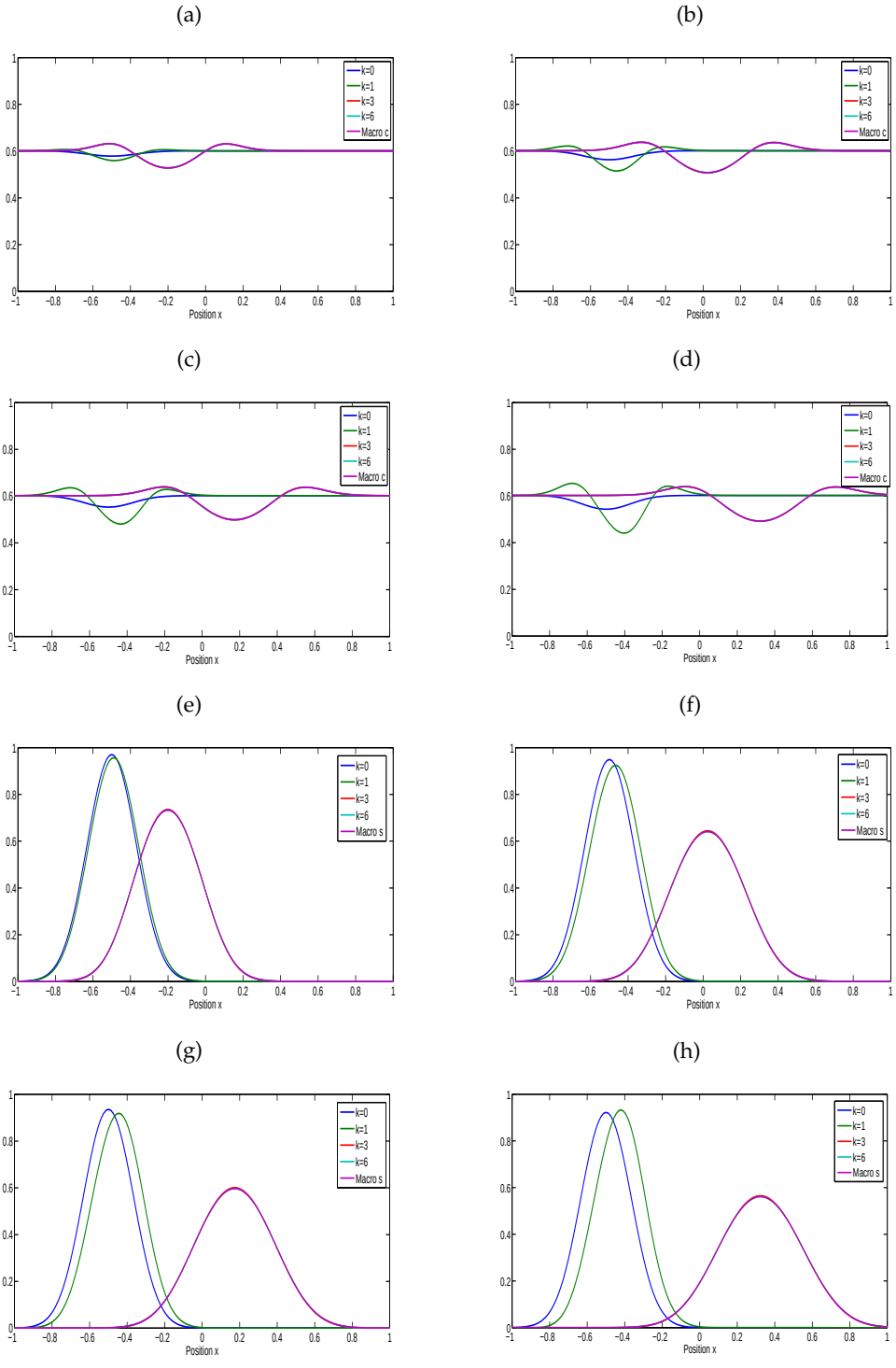

FIGURE 2.3: The Subfigures (a), (b), (c), (d) present time dynamics of predators densities $c(t;x)$, while Subfigures (e), (f), (g), (h) present time dynamics of preys densities $s(t;x)$ at $t = 0.02, 0.04, 0.07, 0.1$ obtained from the AP scheme with $\varepsilon = 10^{-k}$, $k = 0;1;2;3;6$ and comparison with cross-diffusion-Brinkman system on the domain $[-1;1]$ and initial conditions are given by $c_0 = 0.65$ and $s_0 = \exp(30(x+0.5)^2)$ in the case: $u = 1$.

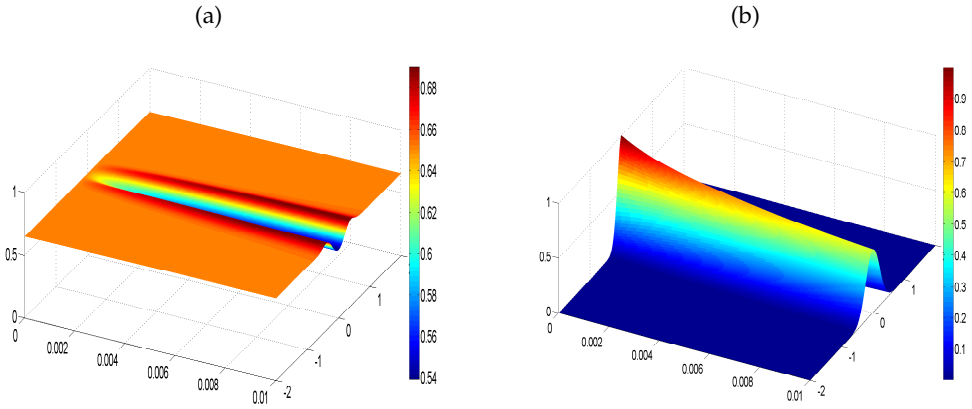

FIGURE 2.4: Evolution of the densities $c(t;x)$ and $s(t;x)$ using micro-macro scheme for $\varepsilon = 10^{-6}$ in the case $u = 0$.

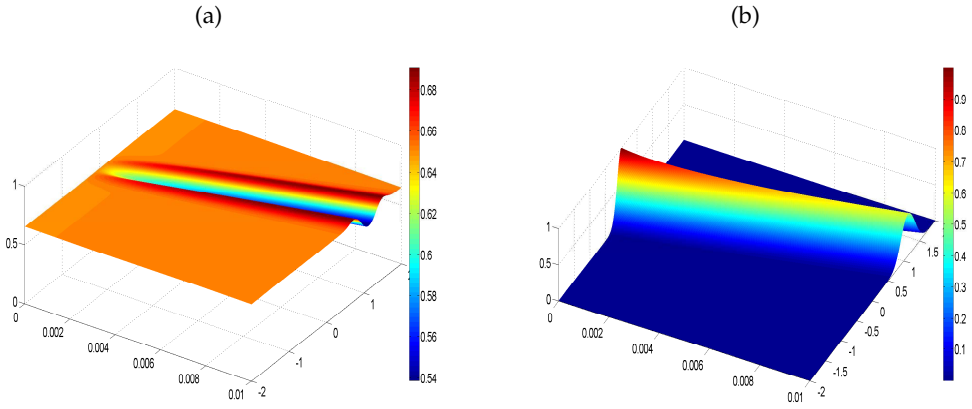

FIGURE 2.5: Evolution of the densities $c(t;x)$ and $s(t;x)$ using micro-macro scheme for $\varepsilon = 10^{-6}$ in the case $u = 1$.

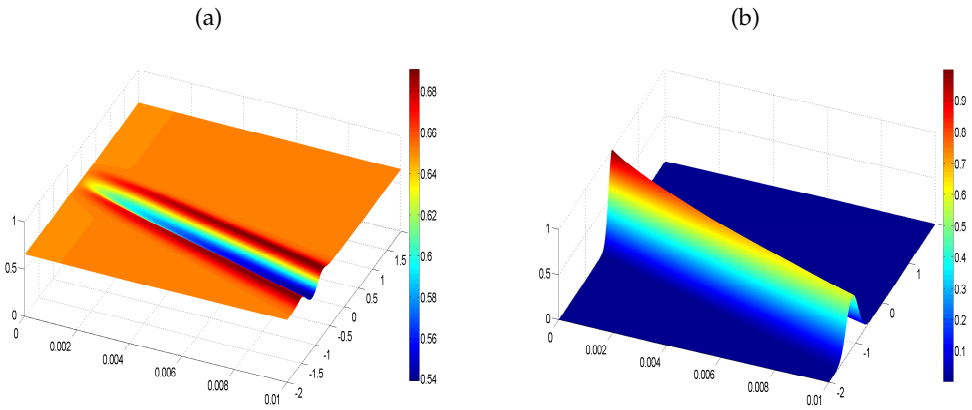

FIGURE 2.6: Evolution of the densities $c(t;x)$ and $s(t;x)$ using micro-macro scheme for $\varepsilon = 10^{-6}$ in the case $u = -1$.

Chapter 3

Kinetic-fluid derivation and mathematical analysis of nonlocal cross-diffusion-fluid system

In this chapter, we propose a generalized nonlocal cross-diffusion-fluid model describing the dynamic of interacting multi-populations living in a complex medium. First, we derive our nonlocal cross-diffusion-fluid system from a nonlocal kinetic-fluid model by performing the micro-macro decomposition method. Second, we prove the existence of weak solutions for the proposed model by applying the nonlinear Galerkin method within a priori estimates and compactness arguments. Based on micro-macro decomposition, we propose and we develop an asymptotic preserving numerical schemes. Finally, we deal with the computational results of the proposed model.

3.1 Introduction

In chapter 2, we have considered two interacting species living in the stationary fluid governed by the augmented Brinkman system. In this chapter, we mainly propose and we study a generalized nonlocal cross-diffusion-fluid system. On the one hand, our proposed system deals with nonlocal diffusitive functions and with nonlinear cross-diffusion matrix accounting for multi-interacting populations. On the other hand, it is strongly coupled to a generalized fluid governed by the incompressible Navier-Stokes equation [70, 86].

In order to state our problem, we consider $\Omega \in \mathbb{R}^d$, $d = 2, 3$, a simply connected domain saturated with a Newtonian incompressible fluid, where also the multi-populations are present. The physical scenario of interest can be described by the following coupled nonlocal cross-diffusion-fluid system

$$\begin{cases} \partial_t u_i + \mathbf{v}\cdot\nabla u_i - \operatorname{div}\left(d_{u_i}\Big(\int_\Omega u_i\,\mathrm{d}\mathbf{x}\Big)\nabla u_i + \sum_{j=1}^{n}\mathcal{A}_i^j(u_1,\dots,u_n)\nabla u_j\right) = F_i(u_1,\dots,u_n), \\ \\ \partial_t \mathbf{v} - \nu\Delta\mathbf{v} + (\mathbf{v}\cdot\nabla)\mathbf{v} + \nabla p + Q(u_1,\dots,u_n)\nabla\phi = \mathbf{0}, \quad \operatorname{div}\mathbf{v} = 0, \end{cases} \tag{3.1.1}$$

in $\Omega_T := (0,T)\times\Omega$, for $i = 1,\dots,n$. We augment this system along with the boundary conditions

$$\mathbf{v} = \mathbf{0}, \quad \Big(d_{u_i}\Big(\int_\Omega u_i\,\mathrm{d}\mathbf{x}\Big)\nabla u_i + \sum_{j=1}^{n}\mathcal{A}_i^j(u_1,\dots,u_n)\nabla u_j\Big)\cdot\eta = 0 \quad \text{on } \Sigma_T := (0,T]\times\partial\Omega, \tag{3.1.2}$$

and the initial conditions

$$u_i(t=0,\mathbf{x}) = u_{i,0}(\mathbf{x}), \quad \mathbf{v}(t=0,\mathbf{x}) = \mathbf{v}_0(\mathbf{x}) \quad \text{for } \mathbf{x}\in\Omega, \tag{3.1.3}$$

for $i = 1,\dots,n$. Herein, $u_1,\dots,u_n$ are the populations densities, $\mathbf{v}$ is the fluid velocity, p is the fluid pressure, d_{u_i} is the nonlocal diffusitive functions, $\mathcal{A}_i^j$ $(i,j = 1,\dots,n)$ is the nonlinear cross-diffusion matrix elements, F_i $(i = 1,\dots,n)$ is the reaction terms, ϕ stands for the gravitational

potential produced by the action of physical forces on the populations, $Q(u_1,\dots,u_n)\nabla\phi$ represents the external force applied to the incompressible fluid where Q is an operator depending on the populations densities, ν is the fluid viscosity and η is the unit outward normal to Ω on $\partial\Omega$. We recall that the nonlocal diffusitive functions assumed to be depend on the whole of each population in the domain rather than on the local density. In the other words, the diffusion of individuals is guided by the global state of the population in the medium. For instance, we assume that the nonlocal diffusion is an increasing function of its argument to model populations having the tendency to leave crowded zones. Otherwise, we use the nonlocal decreasing diffusitive function to model species attracted by the growing population. We want to mention that the coupling in our model (3.1.1) appears through the convection term $\mathbf{v}\cdot\nabla u_i$ and the external force $Q(u_1,\dots,u_n)\nabla\phi$.

Note that in the absence of the fluid flow i.e $\mathbf{v}=\mathbf{0}$, system (3.1.1) reduces to a classical cross-diffusion system (see for e.g [4]). In this case, if the cross-diffusion matrix is neglected, we obtain from (3.1.1) a classical nonlocal diffusion system (see for e.g [32, 37]). However, several contributions are proposed in the case of a constant diffusitive function, see for e.g [3, 6, 23, 36, 44, 60, 87, 92] where a detailed theoretical and numerical studies has been established. Indeed in [23], the authors included the analysis of the weak solutions, the paper in [87] specified the conditions for the existence of unstable equilibrium points, the authors in [92] proved the global existence of solution and recently, the global in time of weak solutions using entropy and duality methods are proved in [36, 44, 60]. Regarding the numerical study of cross-diffusion system without fluid, we refer the reader to finite difference method in [33], finite element method in [9], deterministic particle method in [49], finite volume method in [6, 3, 4] and positivity-preserving Euler-Galerkin method in [34]. Now, under the presence of fluid flow ($\mathbf{v}\neq\mathbf{0}$) we obtain reaction-diffusion-fluid models (see for e.g [45, 51, 53, 91, 13, 31, 75, 88, 94, 93]). In passing, we mention the recent work on cross-diffusion-Brinkman system in [24] (stationary fluid case). The authors in this paper proved the existence of weak solutions using Schauder fixed-point method under a specific assumptions on the cross-diffusion matrix term (ellipticity condition). Comparing to the paper [24], in this chapter we study a nonlocal cross-diffusion system of multi-populations dynamics completed by the presence of a non-stationary incompressible fluid. In this chapter, we prove the existence of weak solutions by using nonlinear Galerkin method within an a priori estimates and compactness arguments. We mention that the assumed conditions on the cross-diffusion matrix make it possible to have the existence of weak solutions of the cross-diffusion-fluid system with the elements of nonlinear matrix of power up to three of cross-diffusion.

In this chapter, we are also concerned with the derivation of macroscopic systems from kinetic models. As it is know, this can be achieved mathematically by the asymptotic analysis, see for e.g diffusion limit [26, 42, 71], derivation of hyperbolic models in [48, 78], of chemotaxis models [14, 16, 11, 27, 8], of incompressible Navier-Stokes [20], of Cucker-Smale models [80] and anomalous diffusion limit [39]. Numerically, this is a challenging question because it is too much expensive in time. However, some encouraging results are obtained overtook this drawback by adopt the asymptotic preserving scheme based on micro-macro decomposition method (see for e.g [24, 26, 71]). Note that all this works derived macroscopic systems from local kinetic models and they limited their studies to kinetic models within two components. Comparing to the existence works, in this chapter, we deal with the derivation of system (3.1.1) from a nonlocal kinetic-fluid model for multi-interacting populations living in a fluid generated by the incompressible Navier-Stokes equations. We also propose and develop an asymptotic preserving numerical schemes which is stable in the limit along the transition from kinetic to macroscopic regimes.

This chapter is organized as follows: In Section 3.2, we present our nonlocal kinetic-fluid model and its properties. We use micro-macro decomposition method to obtain an equivalent system of model (3.2.1) bellow. Moreover, we derive a general macroscopic-fluid model. We finish this section by a suitable modeling of the terms appeared in model (3.2.1) and we derive our model (3.1.1). Section 3.3 is devoted to prove the existence of weak solutions of the proposed nonlocal cross-diffusion-fluid system. The proof is based on the nonlinear Galerkin method, apriori estimates and compactness arguments. In Section 3.4, we propose and develop numerical approximations in 1D for micro-macro formulation and for the macroscopic model. The objective is to show the asymptotic preserving scheme property and simultaneously to illustrate the effects of nonlocal diffusion, of cross-diffusion and of advection terms. Finally, Motivated by the obtained

numerical simulations, we investigate the computational analysis of the proposed model in 2D.

3.2 From improved kinetic-fluid model to generalized nonlocal cross-diffusion-fluid systems

In this section, we derive a macroscopic-fluid models from a nonlocal kinetic-fluid model using micro-macro decomposition method. Firstly, we present the properties of the aforesaid model. On the basis of the micro-macro decomposition technique, we give an equivalent appropriate system. Then, we formally derive a class of macroscopic-fluid models. Herein, we consider a nonlocal kinetic-fluid model describing multi-interacting populations living in a fluid governed by the incompressible Navier-Stokes equations.

3.2.1 The improved kinetic-fluid model

This subsection is devoted to state our improved kinetic-fluid model and to present its properties. We propose the following nonlocal kinetic-fluid model for $i = 1, \dots, n$

$$\begin{cases} \varepsilon \partial_t f_i + \xi \cdot \nabla_x \mathcal{F}_i(f_i) = \dfrac{1}{\varepsilon} \mathcal{T}_i[f_1, \dots, f_{i-1}, f_{i+1}, \dots, f_n](f_i) + G_i(f_1, \dots, f_n, \xi, \mathbf{v}), \\ \partial_t \mathbf{v} - \nu \Delta \mathbf{v} + (\mathbf{v} \cdot \nabla)\mathbf{v} + \nabla p + Q\Big(\displaystyle\int_V f_1 d\xi, \dots, \int_V f_n d\xi \Big) \nabla \phi = \mathbf{0}, \ \ \operatorname{div} \mathbf{v} = 0, \\ f_i(t = 0, \mathbf{x}, \xi) = f_{i,0}(\mathbf{x}, \xi), \quad \mathbf{v}(t = 0, \mathbf{x}) = \mathbf{v}_0(\mathbf{x}), \end{cases} \tag{3.2.1}$$

where $(f_i(t, \mathbf{x}, \xi))_{i=1}^n$ is the distribution function describing the statistical evolution of species, where $t > 0$, $\mathbf{x} \in \mathbb{R}^d$ and $\xi \in V$ are respectively, time, position and velocity. The term $\mathcal{F}_i(f_i)$ is the nonlocal function, $\mathcal{T}_i$ is the stochastic operator representing a random modification of direction of species and the operator G_i $(i = 1, \dots, n)$ describing the gain-loss balance of species. The mean free path ε measures the distance between species. We recall that we adopt the parabolic-parabolic scaling limit, see for more details [16, 27]. Herein, the nonlocal function $\mathcal{F}_i$ is defined by

$$\mathcal{F}_i(f_i)(t, \mathbf{x}, \xi) = \Phi_i\Big(\int_\Omega \int_V f_i(t, \mathbf{x}, \xi)\, d\xi \ \mathrm{d}\mathbf{x} \Big) f_i(t, \mathbf{x}, \xi) \quad i = 1, \dots, n.$$

Under the assumptions that $\Phi_i = 1$ and $i = 1, 2$, the reduced model has been studied by [24, 11]. The micro-macro decomposition method is based on the following assumptions. The interaction operators G_i satisfy the following properties

$$G_i(f_1, \dots, f_n, \xi, \mathbf{v}) = G_i^1(f_1, \dots, f_n, \xi, \mathbf{v}) + \varepsilon\, G_i^2(f_1, \dots, f_n, \xi, \mathbf{v}), \tag{3.2.2}$$

where

$$\int_V G_i^1(f_1, \dots, f_n, \xi, \mathbf{v}) d\xi = 0, \ \ i = 1, \dots, n. \tag{3.2.3}$$

Next, the turning operator $\mathcal{T}_i$ is decomposed as follows

$$\mathcal{T}_i[f_1, \dots, f_{i-1}, f_{i+1}, \dots, f_n](f_i) = \mathcal{T}_i^1(f_i) + \varepsilon\, \mathcal{T}_i^2[f_1, \dots, f_{i-1}, f_{i+1}, \dots, f_n](f_i), \tag{3.2.4}$$

where $\mathcal{T}_i^1(f_i)$ represents the dominant part of the turning kernel and assumed independent of $f_1, \dots, f_{i-1}, f_{i+1}, \dots, f_n$. The operator $\mathcal{T}_i^j$ for $i = 1, \dots, n$ and $j = 1, 2$ are given by

$$\mathcal{T}_i^j(f_i) = \int_V \big(T_i^{j^*} f_i(t, \mathbf{x}, \xi^*) - T_i^j f_i(t, \mathbf{x}, \xi) \big), d\xi^*, \tag{3.2.5}$$

where T_i^j is the probability kernel for the new velocity $\xi \in V$ given that the previous velocity was ξ^*. The kernel operator $T_i^{1^*}$ is defined by $T_i^{1^*} = T_i^1(\xi^*, \xi)$ and the operator T_i^2 may depend on the distribution function $f_1, \dots, f_{i-1}, f_{i+1}, \dots, f_n$ and their derivatives. Moreover, we assume that the

operators $\mathcal{T}_i$ satisfy

$$\int_V \mathcal{T}_i \, d\xi = \int_V \mathcal{T}_i^1(f_i) d\xi = \int_V \mathcal{T}_i^2[f_1, \dots, f_{i-1}, f_{i+1}, \dots, f_n](f_i) d\xi = 0, \quad i = 1, \dots, n. \tag{3.2.6}$$

Moreover, we assume that there exists a bounded velocity distribution $M_i(\xi) > 0$ for $i = 1, \dots, n$ independent of t and x such that

$$T_i^1(\xi, \xi^*) M_i(\xi^*) = T_i^1(\xi^*, \xi) M_i(\xi), \tag{3.2.7}$$

holds. The flow produced by these equilibrium distributions vanishes and M_i are normalized, i.e.

$$\int_V \xi \, M_i(\xi) d\xi = 0, \quad \int_V M_i(\xi) d\xi = 1, \quad i = 1, \dots, n. \tag{3.2.8}$$

Regarding the probability kernels, we assume that $T_i^1(\xi, \xi^*)$ is bounded, and there exist a constant $\sigma_i > 0$ ($i \in \{1, \dots, n\}$), such that

$$T_i^1(\xi, \xi^*) \geq \sigma_i M_i(\xi), \tag{3.2.9}$$

for all $(\xi, \xi^*) \in V \times V$.
In what follows, we shall consider $\mathcal{L}_i = \mathcal{T}_i^1$ for $i = 1, \dots, n$. Using the same arguments as in [10, 30], the operator $\mathcal{L}_i$ has the following properties.

Lemma 3.2.1 *By assuming that the hypothesis (3.2.6), (3.2.7) and (3.2.8) are satisfied. Then, the following properties of the operators $\mathcal{L}_i$ for $i = 1, \dots, n$ hold true:*

i) The operator $\mathcal{L}_i$ is self-adjoint in the space $\mathrm{L}^2\left(V, \frac{d\xi}{M_i}\right)$.

ii) For $f \in \mathrm{L}^2$, the equation $\mathcal{L}_i(g) = f$ has a unique solution $g \in \mathrm{L}^2\left(V, \frac{d\xi}{M_i}\right)$, satisfying

$$\int_V g(\xi) \, d\xi = 0 \quad \Longleftrightarrow \quad \int_V f(\xi) \, d\xi = 0.$$

iii) The equation $\mathcal{L}_i(g) = \xi \, M_i(\xi)$, has a unique solution denoted by $\theta_i(\xi)$ for $i = 1, \dots, n$.

iv) The kernel of $\mathcal{L}_i$ is $N(\mathcal{L}_i) = vect(M_i(\xi))$ for $i = 1, \dots, n$.

3.2.2 Micro-macro formulation

This subsection is devoted to obtain an equivalent micro-macro system of nonlocal kinetic-fluid model (3.2.1). The obtained equivalent system contains microscopic and macroscopic components.
The main idea of the micro-macro method is to decompose the distribution function f_i for $i = 1, \dots, n$ as follows

$$f_i(t, \mathbf{x}, \xi) = M_i(\xi) u_i(t, \mathbf{x}) + \varepsilon g_i(t, \mathbf{x}, \xi),$$

where

$$u_i(t, \mathbf{x}) = \langle f_i(t, \mathbf{x}, \xi) \rangle := \int_V f_i(t, \mathbf{x}, \xi) \, d\xi.$$

We have $\langle g_i \rangle = 0$ and $\Phi_i\Big(\int_\Omega \langle f_i(t, \mathbf{x}, \xi) \rangle \, \mathrm{d}\mathbf{x}\Big) = \Phi_i\Big(\int_\Omega u_i \, \mathrm{d}\mathbf{x}\Big) := \Phi_i(u_i)$ for $i = 1, \dots, n$. Inserting f_i in nonlocal kinetic-fluid model (3.2.1) and using the above assumptions and properties of the

interaction and the turning operators, we get

$$\begin{cases} \partial_t(M_i(\xi)u_i) + \varepsilon\partial_t g_i + \dfrac{1}{\varepsilon}\xi M_i(\xi)\cdot\nabla(\Phi_i(u_i)u_i) + \xi\cdot\nabla(\Phi_i(u_i)g_i) = \dfrac{1}{\varepsilon}\mathcal{L}_i(g_i) \\ \qquad + \dfrac{1}{\varepsilon}\mathcal{T}_i^2[f_1,\dots,f_{i-1},f_{i+1},\dots,f_n](M_i(\xi)u_i) + \mathcal{T}_i^2[f_1,\dots,f_{i-1},f_{i+1},\dots,f_n](g_i) \\ \qquad + \dfrac{1}{\varepsilon}G_i^1(f_1,\dots,f_n,\xi,\mathbf{v}) + G_i^2(f_1,\dots,f_n,\xi,\mathbf{v}), \\ \partial_t\mathbf{v} - \nu\Delta\mathbf{v} + (\mathbf{v}\cdot\nabla)\mathbf{v} + \nabla p + Q(u_1,\dots,u_n)\nabla\phi = \mathbf{0}, \ \ \operatorname{div}\mathbf{v} = 0. \end{cases} \tag{3.2.10}$$

The micro-macro decomposition method is based on two steps. First, we use the projection technique to separate the macroscopic density $u_i(t,x)$ and microscopic quantity $g_i(t,x,\xi)$ for $i=1,\dots,n$. For that, we consider P_{M_i} the orthogonal projection onto $N(\mathcal{L}_i)$, for $i=1,\dots,n$. It follows

$$P_{M_i}(h) = \langle h\rangle M_i, \quad \text{for any} \quad h\in \mathrm{L}^2\left(V,\frac{d\xi}{M_i}\right), \qquad i=1,\dots,n.$$

Regarding the orthogonal projections P_{M_i} for $i=1,\dots,n$, we have the following result.

Lemma 3.2.2 *We have the following properties for the projection P_{M_i}, $i=1,\dots,n$*

$$\begin{aligned} (I-P_{M_i})\big(M_i(\xi)u_i\big) &= P_{M_i}(g_i) = 0, \\ (I-P_{M_i})\big(\xi M_i(\xi)\cdot\nabla(\Phi_i(u_i))u_i\big) &= \xi M_i(\xi)\cdot\nabla(\Phi_i(u_i)u_i), \\ (I-P_{M_i})\big(\mathcal{T}_i^2[f_1,\dots,f_{i-1},f_{i+1},\dots,f_n](M_i(\xi)u_i)\big) &= \mathcal{T}_i^2[f_1,\dots,f_{i-1},f_{i+1},\dots,f_n](M_i(\xi)u_i), \\ (I-P_{M_i})\big(\mathcal{T}_i^2[f_1,\dots,f_{i-1},f_{i+1},\dots,f_n](g_i)\big) &= \mathcal{T}_i^2[f_1,\dots,f_{i-1},f_{i+1},\dots,f_n](g_i), \\ (I-P_{M_i})(\mathcal{L}_i(g_i)) &= \mathcal{L}_i(g_i), \\ (I-P_{M_i})G_i^1(f_1,\dots,f_n,\xi,\mathbf{v}) &= G_i^1(f_1,\dots,f_n,\xi,\mathbf{v}). \end{aligned}$$

Second, we integrate (3.2.10) with respect to ξ. Thanks to these two steps, we obtain the following micro-macro formulation for $i=1,\dots,n$

$$\begin{cases} \partial_t g_i + \dfrac{1}{\varepsilon^2}\xi M_i(\xi)\cdot\nabla(\Phi_i(u_i)u_i) + \dfrac{1}{\varepsilon}(I-P_{M_i})(\xi\cdot\nabla(\Phi_i(u_i)g_i)) = \dfrac{1}{\varepsilon^2}\mathcal{L}_i(g_i) \\ \qquad + \dfrac{1}{\varepsilon^2}\mathcal{T}_i^2[f_1,\dots,f_{i-1},f_{i+1},\dots,f_n](M_i(\xi)u_i) + \dfrac{1}{\varepsilon}\mathcal{T}_i^2[f_1,\dots,f_{i-1},f_{i+1},\dots,f_n](g_i) \\ \qquad + \dfrac{1}{\varepsilon^2}G_i^1(f_1,\dots,f_n,\xi,\mathbf{v}) + \dfrac{1}{\varepsilon}(I-P_{M_i})G_i^2(f_1,\dots,f_n,\xi,\mathbf{v}), \\ \partial_t u_i + \Phi_i(u_i)\,\langle\xi\cdot\nabla g_i\rangle = \langle G_i^2(f_1,\dots,f_n,\xi,\mathbf{v})\rangle, \\ \partial_t\mathbf{v} - \nu\Delta\mathbf{v} + (\mathbf{v}\cdot\nabla)\mathbf{v} + \nabla p + Q(u_1,\dots,u_n)\nabla\phi = \mathbf{0}, \ \ \operatorname{div}\mathbf{v} = 0. \end{cases} \tag{3.2.11}$$

The following proposition shows that micro-macro formulation (3.2.11) is equivalent to nonlocal kinetic-fluid equation (3.2.1).

Proposition 1 *i) Let $(f_1,\dots,f_n,\mathbf{v},p)$ be a solution of nonlocal kinetic-fluid model (3.2.1). Then $(u_1,\dots,u_n,g_1,\dots,g_n,\mathbf{v},p)$ (where $u_i=\langle f_i\rangle$ and $g_i=\frac{1}{\varepsilon}(f_i-M_iu_i)$) is a solution to coupled system (3.2.11) associated with the following initial data for $i=1,\dots,n$*

$$u_i(t=0)=u_{i,0}=\langle f_{i,0}\rangle, \quad g_i(t=0)=g_{i,0}=\frac{1}{\varepsilon}(f_{i,0}-M_iu_{i,0}), \quad \text{and } \mathbf{v}(t=0)=\mathbf{v}_0, \tag{3.2.12}$$

ii) Conversely, if $(u_1,\dots,u_n,g_1,\dots,g_n,\mathbf{v},p)$ satisfies system (3.2.11) associated with the following initial data $(u_{1,0},\dots,u_{n,0},g_{1,0},\dots,g_{n,0},\mathbf{v}_0)$ such that $\langle g_{i,0}\rangle=0$ for $i=1,\dots,n$. Then $(f_1,\dots,f_n,\mathbf{v},p)$ (where

$f_i = M_i u_i + \varepsilon g_i$) is a solution to nonlocal kinetic-fluid model (3.2.1) with initial data $f_{i,0} = M_i u_{i,0} + \varepsilon g_{i,0}$ and we have $u_i = \langle f_i \rangle$ and $\langle g_i \rangle = 0$, for $i = 1, \dots, n$.

Next, in order to develop asymptotic analysis of system (3.2.11), we assume that $\mathcal{T}_i^2$ and G_i^j satisfy the following asymptotic behavior $\varepsilon \to 0$

$$\begin{aligned} &\mathcal{T}_i^2[M_1u_1 + \varepsilon g_1, \dots, M_{i-1}u_{i-1} + \varepsilon g_{i-1}, M_{i+1}u_{i+1} + \varepsilon g_{i+1}, \dots, M_n u_n + \varepsilon g_n] \\ &\qquad = \mathcal{T}_i^2[M_1u_1, \dots, M_{i-1}u_{i-1}, M_{i+1}u_{i+1}, \dots, M_n u_n] + O(\varepsilon) \end{aligned} \tag{3.2.13}$$

$$G_i^j(M_1(\xi)u_1 + \varepsilon g_1, \dots, M_n(\xi)u_n + \varepsilon g_n, \xi, \mathbf{v}) = G_i^j(M_1(\xi)u_1, \dots, M_n(\xi)u_n, \xi, \mathbf{v}) + O(\varepsilon), \tag{3.2.14}$$

for $i = 1, \dots, n$ and $j = 1, 2$.

3.2.3 Derivation of general macroscopic models

Here, we show that micro-macro formulation (3.2.11), which is equivalent to kinetic equation (3.2.1), allows to obtain a general macroscopic models as ε goes to 0. Indeed, using (3.2.13), (3.2.14) and (3.2.11), we obtain for $i = 1, \dots, n$

$$\mathcal{L}_i(g_i) = \xi M_i(\xi) \cdot \nabla\Big(\Phi_i(u_i)u_i\Big) - \mathcal{T}_i^2[M_1(\xi)u_1, \dots, M_{i-1}(\xi)u_{i-1}, M_{i+1}(\xi)u_{i+1}, \dots, M_n(\xi)u_n](M_i(\xi)u_i)$$

$$-G_i^1(M_1(\xi)u_1, \dots, M_n(\xi)u_n, \xi, \mathbf{v}) + O(\varepsilon).$$

From Lemma 3.2.1, property *ii*), the operator $\mathcal{L}_i$ is invertible. This implies

$$\begin{aligned} g_i \;=\; & \mathcal{L}_i^{-1}\Big(\xi M_i \cdot \nabla(\Phi_i(u_i)u_i)\Big) - \mathcal{L}_i^{-1}\Big(\mathcal{T}_i^2[M_1u_1, \dots, M_{i-1}u_{i-1}, M_{i+1}u_{i+1}, \dots, M_n u_n](M_i u_i)\Big) \\ & -\mathcal{L}_i^{-1}\Big(G_i^1(M_1u_1, \dots, M_n u_n, \xi, \mathbf{v})\Big) + O(\varepsilon), \quad i = 1, \dots, n. \end{aligned} \tag{3.2.15}$$

Next, inserting (3.2.15) into the second equation in (3.2.11) yields the following macroscopic system

$$\begin{cases} \partial_t u_i + \Phi_i(u_i)\Big\langle \xi \cdot \nabla \mathcal{L}_i^{-1}\Big(\xi M_i(\xi) \cdot \nabla(\Phi_i(u_i)u_i)\Big)\Big\rangle \\ -\Phi_i(u_i)\Big\langle \xi \cdot \nabla \mathcal{L}_i^{-1}\Big(\mathcal{T}_i^2[M_1(\xi)u_1, \dots, M_{i-1}(\xi)u_{i-1}, M_{i+1}(\xi)u_{i+1}, \dots, M_n(\xi)u_n](M_i(\xi)u_i)\Big)\Big\rangle \\ -\Phi_i(u_i)\Big\langle \xi \cdot \nabla \mathcal{L}_i^{-1}\Big(G_i^1(M_1(\xi)u_1, \dots, M_n(\xi)u_n, \xi, \mathbf{v})\Big)\Big\rangle = \Big\langle G_i^2(M_1(\xi)u_1, \dots, M_n(\xi)u_n, \xi, \mathbf{v})\Big\rangle + O(\varepsilon), \\ \partial_t \mathbf{v} - \nu\Delta\mathbf{v} + (\mathbf{v} \cdot \nabla)\mathbf{v} + \nabla p + Q(u_1, \dots, u_n)\nabla\phi = \mathbf{0}, \;\; \operatorname{div}\mathbf{v} = 0. \end{cases} \tag{3.2.16}$$

The following lemma gives the calculations of the terms with the inverse of the operators $\mathcal{L}_i$ for $i = 1, \dots, n$ appearing in system (3.2.16).

Lemma 3.2.3 *Assume that the operators $\mathcal{L}_i$ and G_i^1 for $i = 1, \dots, n$ satisfy the assumptions above. Then, we have the following identities*

$$\Big\langle \xi.\nabla \mathcal{L}_i^{-1}\Big(\xi M_i(\xi) \cdot \nabla(\Phi_i(u_i)u_i)\Big)\Big\rangle = \operatorname{div}\Big(\langle \xi \otimes \theta_i(\xi)\rangle \cdot \nabla(\Phi_i(u_i)u_i)\Big),$$

$$\begin{aligned} &\Big\langle \xi \cdot \nabla \mathcal{L}_i^{-1}\Big(\mathcal{T}_i^2[M_1(\xi)u_1, \dots, M_{i-1}(\xi)u_{i-1}, M_{i+1}(\xi)u_{i+1}, \dots, M_n(\xi)u_n](M_i(\xi)u_i)\Big)\Big\rangle \\ &= \operatorname{div}\Big\langle \frac{\theta_i(\xi)}{M_i(\xi)} u_i \mathcal{T}_i^2[M_1(\xi)u_1, \dots, M_{i-1}(\xi)u_{i-1}, M_{i+1}(\xi)u_{i+1}, \dots, M_n(\xi)u_n](M_i(\xi)u_i))\Big\rangle, \end{aligned}$$

$$\Big\langle \xi \cdot \nabla \mathcal{L}_i^{-1}\Big(G_i^1(M_1(\xi)u_1, \dots, M_n(\xi)u_n, \xi, \mathbf{v})\Big)\Big\rangle = \operatorname{div}\Big\langle \frac{\theta_i(\xi)}{M_i(\xi)} G_i^1(M_1(\xi)u_1, \dots, M_n(\xi)u_n, \xi, \mathbf{v})\Big\rangle,$$

where θ_i are given in Lemma 3.2.1 for $i = 1, \dots, n$.

Finally, thanks to system (3.2.16) and Lemma 3.2.3, we obtain the following macroscopic system

$$\begin{cases} \partial_t u_i + \operatorname{div}\Big(\beta_i(u_i)\,\alpha_i(u_1,\dots,u_{i-1},u_{i+1},\dots,u_n) + \Gamma_i(u_1,\dots,u_n,\mathbf{v}) - \Psi_i(u_i)\cdot\nabla u_i\Big) \\ \qquad\qquad = H_i(u_1,\dots,u_n,\mathbf{v}) + O(\varepsilon), \\ \partial_t \mathbf{v} - \nu\Delta\mathbf{v} + (\mathbf{v}\cdot\nabla)\mathbf{v} + \nabla p + Q(u_1,\dots,u_n)\nabla\phi = \mathbf{0}, \;\; \operatorname{div}\mathbf{v} = 0, \end{cases} \tag{3.2.17}$$

where the functions Ψ_i, β_i, α_i, Γ_i and H_i are given by

$$\Psi_i(u_i) = -\Big\langle \xi\otimes\theta_i(\xi)\Big\rangle\,(\Phi_i(u_i))^2, \tag{3.2.18}$$

$$\beta_i(u_i) = u_i\,\Phi_i(u_i), \tag{3.2.19}$$

$$\alpha_i(u_1,\dots,u_{i-1},u_{i+1},\dots,u_n) = -\Big\langle \frac{\theta_i(\xi)}{M_i}\mathcal{T}_i^2[M_1u_1,\dots,M_{i-1}u_{i-1},M_{i+1}u_{i+1},\dots,M_nu_n](M_i)\Big\rangle, \tag{3.2.20}$$

$$\Gamma_i(u_1,\dots,u_n,\mathbf{v}) = -\Big\langle \frac{\theta_i(\xi)}{M_i}G_i^1(M_1u_1,\dots,M_nu_n,\xi,\mathbf{v})\Big\rangle\,\Phi_i(u_i), \tag{3.2.21}$$

$$H_i(u_1,\dots,u_n,\mathbf{v}) = \Big\langle G_i^2(M_1u_1,\dots,M_nu_n,\xi,\mathbf{v})\Big\rangle, \text{ for } i=1,\dots,n. \tag{3.2.22}$$

3.2.4 Derivation of nonlocal cross-diffusion-fluid system

We consider the case where the set for velocity is a sphere of radius $r>0$, $V = rS^{d-1}$. We assume that $(f_1,\dots,f_n,\mathbf{v},p)$ solution of system (3.2.1) with the following nonlocal function

$$\Phi_i(s) = \sqrt{D_i(s)}, \quad i=1,\dots,n. \tag{3.2.23}$$

We mention that biologically D_i are strictly positive function for all $i=1,\dots,n$. From Eq. (3.2.18), we obtain

$$\Psi_i(u_i) = \frac{1}{\sigma_i|V|}\langle\xi\otimes\xi\rangle\,D_i\Big(\int_\Omega u_i(t,\mathbf{x})\,d\mathbf{x}\Big). \tag{3.2.24}$$

Next, we assume that the probability kernel T_i^1 is given by

$$T_i^1 = \frac{\sigma_i}{|V|}, \quad \text{for } i=1,\dots,n.$$

This implies

$$\mathcal{L}_i(g_i) = -\frac{\sigma_i}{|V|}\Big(g_i\,|V| - \langle g_i\rangle\Big) = -\sigma_i\,g_i \quad \text{for } i=1,\dots,n.$$

Notice that $M_i(\xi) = \frac{1}{|V|}$ satisfies assumption (3.2.8). For this particular choice of M_i, we have $\theta_i = -\frac{\xi}{\sigma_i|V|}$ is a solution of $\mathcal{L}_i(\theta_i(\xi)) = \xi M_i(\xi)$ for $i=1,\dots,n$. The other probability kernel T_i^2 is given by

$$T_i^2[f_1,\dots,f_{i-1},f_{i+1},\dots,f_n,\xi,\xi^*] = -\frac{\mu_i}{\Phi_i|V|^2}\sum_{j,j\neq i}\mathcal{K}_{\frac{f_j}{M_j}}(\xi,\xi^*)\cdot\nabla\Big(\frac{f_j}{M_j}\Big),$$

where $\mu_i = \frac{\sigma_i}{r^2}\,d\,|V|$ and the function $\mathcal{K}_{\frac{f_j}{M_j}}$ satisfies the following asymptotic

$$\mathcal{K}_{u_j+\varepsilon\frac{g_j}{M_j}} = \mathcal{K}_{u_j} + O(\varepsilon), \;\; \varepsilon\to 0.$$

From Eq. (3.2.5), we obtain

$$\mathcal{T}_i^2[M_1u_1,\dots,M_{i-1}u_{i-1},M_{i+1}u_{i+1},\dots,M_nu_n](M_i) = -\frac{\mu_i}{\Phi_i|V|^2}\sum_{j,j\neq i}\chi_j(\xi,u_j)\cdot\nabla u_j,$$

where

$$\chi_j(\xi,\, u_j) = \Big\langle \mathcal{K}_{u_j}(\xi,\, \xi^*) M_i(\xi) - \mathcal{K}_{u_j}(\xi^*,\, \xi) M_i(\xi^*) \Big\rangle.$$

Therefore, from Eqs. (3.2.19) and (3.2.20), we have

$$\beta_i(u_i)\, \alpha_i(u_1, \dots, u_{i-1}, u_{i+1}, \dots, u_n) = -\sum_{j, j\neq i} \mathcal{C}_i(u_i, u_j)\, \nabla u_j. \tag{3.2.25}$$

It only remains now to model G_i^1 and G_i^2 for

$$\begin{cases} G_i^1(f_1, \dots, f_n, \xi, \mathbf{v}) = -\dfrac{d\sigma_i}{\Phi_i\, r^2 |V|} \Big(\mathcal{B}_i(f_1, \dots, f_n)\, \xi\, M_i \cdot \nabla f_i - f_i\, \xi\, M_i \cdot \mathbf{v} \Big) \\ G_i^2(f_1, \dots, f_n, \xi, \mathbf{v}) = F_i\Big(\dfrac{f_1}{|V|}, \dots, \dfrac{f_n}{|V|} \Big), \quad \text{for } i = 1, \dots, n. \end{cases} \tag{3.2.26}$$

Then, we use the definitions of Γ_i in (3.2.21) and of H_i in (3.2.22) to obtain from (3.2.26)

$$\Gamma_i(u_1, \dots, u_n, \mathbf{v}) = -\frac{d}{r^2 |V|^2} \langle \xi \otimes \xi \rangle \cdot \big(\mathcal{B}_i(u_1, \dots, u_n) \nabla u_i - u_i \mathbf{v} \big) = -\mathcal{B}_i(u_1, \dots, u_n) \nabla u_i + u_i \mathbf{v}, \tag{3.2.27}$$

$$H_i(u_1, \dots, u_n) = F_i(u_1, \dots, u_n). \tag{3.2.28}$$

Finally, setting

$$d_{u_i}\Big(\int_\Omega u_i \, \mathrm{d}\mathbf{x} \Big) = \frac{1}{\sigma_i |V|} \langle \xi \otimes \xi \rangle\, D_i\Big(\int_\Omega u_i(t, \mathbf{x}) \, \mathrm{d}\mathbf{x} \Big) = \frac{r^2}{d\, \sigma_i}\, D_i\Big(\int_\Omega u_i(t, \mathbf{x}) \, \mathrm{d}\mathbf{x} \Big),$$

$$\sum_{j=1}^n \mathcal{A}_i^j(u_1, \dots, u_n) \nabla u_j = \sum_{j, j\neq i} \mathcal{C}_j(u_i, u_j)\, \nabla u_j + \mathcal{B}_i(u_1, \dots, u_n) \nabla u_i,$$

and collecting the previous results with $\operatorname{div} \mathbf{v} = 0$ and (3.2.17), we obtain the nonlocal cross-diffusion-fluid system (3.1.1) of the order $O(\varepsilon)$

$$\begin{cases} \partial_t u_i + \mathbf{v} \cdot \nabla u_i - \operatorname{div}\Big(d_{u_i}\Big(\displaystyle\int_\Omega u_i \, \mathrm{d}\mathbf{x} \Big) \nabla u_i + \sum_{j=1}^n \mathcal{A}_i^j(u_1, \dots, u_n) \nabla u_j \Big) = F_i(u_1, \dots, u_n) + O(\varepsilon), & \text{in } \Omega_T, \\ \partial_t \mathbf{v} - \nu \Delta \mathbf{v} + (\mathbf{v} \cdot \nabla)\mathbf{v} + \nabla p + Q(u_1, \dots, u_n) \nabla \phi = \mathbf{0}, \ \operatorname{div} \mathbf{v} = 0, & \text{in } \Omega_T, \\ u_i(t = 0, \mathbf{x}) = u_{i,0}(\mathbf{x}), \ \mathbf{v}(t = 0, \mathbf{x}) = \mathbf{v}_0(\mathbf{x}), & \text{in } \Omega, \\ \mathbf{v} = \mathbf{0} \quad \text{and} \quad \Big(d_{u_i}\Big(\displaystyle\int_\Omega u_i \, \mathrm{d}\mathbf{x} \Big) \nabla u_i + \sum_{j=1}^n \mathcal{A}_i^j(u_1, \dots, u_n) \nabla u_j \Big) \cdot \eta = 0, & \text{on } \Sigma_T. \end{cases} \tag{3.2.29}$$

for $i = 1, \dots, n$.

3.3 Mathematical analysis

Let Ω be a bounded, open subsets of $\mathbb{R}^d$, $d = 2, 3$ with a smooth boundary $\partial\Omega$ and $|\Omega|$ is the Lebesgue measure of Ω. We denote by $\mathrm{H}^1(\Omega)$ the Sobolev space of functions $u : \Omega \to \mathbb{R}$ for which $u \in \mathrm{L}^2(\Omega)$ and $\nabla u \in \mathrm{L}^2(\Omega; \mathbb{R}^d)$. For $1 \leq p \leq +\infty$, $\| \cdot \|_{\mathrm{L}^p(\Omega)}$ is the usual norm in $\mathrm{L}^p(\Omega)$. If X is a Banach space, $a < b$ and $1 \leq p \leq +\infty$, $\mathrm{L}^p(a, b; X)$ denotes the space of all measurable functions $u : (a, b) \longrightarrow X$ such that $\| u(\cdot) \|_X$ belongs to $\mathrm{L}^p(a, b)$. Moreover, we define the following vectorial space

$$\mathbf{L}^2(\Omega) = \big\{ \boldsymbol{u} = (u_1, \dots, u_n) \ / \ u_i \in \mathrm{L}^2(\Omega)\ \forall i \in \{1, \dots, n\} \big\},$$

$$\mathbf{H}^1(\Omega) = \big\{ \boldsymbol{u} = (u_1, \dots, u_n) \ / \ u_i \in \mathrm{H}^1(\Omega)\ \forall i \in \{1, \dots, n\} \big\},$$

$$\mathbf{D}(\Omega) = \{\boldsymbol{u} = (u_1, \dots, u_n) \ / \ u_i \in \mathcal{D}(\Omega) \ \forall i \in \{1, \dots, n\}\},$$
$$\mathbf{W}^{1,\infty}(\Omega) = \{\boldsymbol{u} = (u_1, \dots, u_n) \ / \ u_i \in W^{1,\infty}(\Omega) \ \forall i \in \{1, \dots, n\}\}.$$

Now, we introduce basic spaces in the study of the Navier-Stokes equation. Let the spaces $\mathcal{V}$, $\mathbf{V}$; $\mathbf{H}$ defined as:

$$\mathcal{V} = \{\mathbf{v} \in \mathcal{D}(\Omega), \ \operatorname{div} \mathbf{v} = 0\}, \ \mathbf{V} = \overline{\mathcal{V}}^{\mathrm{H}_0^1(\Omega)}, \ \mathbf{H} = \overline{\mathcal{V}}^{\mathrm{L}^2(\Omega)}.$$

The coupled system of interest (3.2.29) can be written as

$$\begin{cases} \partial_t \boldsymbol{u} + (\mathbf{v} \cdot \nabla)\boldsymbol{u} - \mathbf{div}\Big(D(\boldsymbol{u})\nabla \boldsymbol{u} + \mathcal{A}(\boldsymbol{u})\nabla \boldsymbol{u}\Big) = F(\boldsymbol{u}), & \text{in } \Omega_T, \\ \partial_t \mathbf{v} - \nu \Delta \mathbf{v} + (\mathbf{v}.\nabla)\mathbf{v} + \nabla p + Q(\boldsymbol{u})\nabla \phi = \mathbf{0}, \ \operatorname{div} \mathbf{v} = 0, & \text{in } \Omega_T, \\ \boldsymbol{u}(t = 0, \mathbf{x}) = \boldsymbol{u}_0(\mathbf{x}), \ \mathbf{v}(t = 0, \mathbf{x}) = \mathbf{v}_0(\mathbf{x}), & \text{in } \Omega, \\ \mathbf{v} = \mathbf{0} \quad \text{and} \ \Big(D(\boldsymbol{u})\nabla \boldsymbol{u} + \mathcal{A}(\boldsymbol{u})\nabla \boldsymbol{u}\Big)\eta = \mathbf{0}, & \text{on } \Sigma_T, \end{cases} \tag{3.3.1}$$

where $\boldsymbol{u} = (u_1, \dots, u_n)^T$ is the densities of populations, $\mathbf{v} = (v_1, \dots, v_d)^T$ is the velocity of the fluid and p is the scalar function describing the pressure of the fluid. The diagonal matrix $D(\boldsymbol{u}) = (D(\boldsymbol{u})_{i,j})_{1 \le i,j \le n}$ satisfy $D(\boldsymbol{u})_{i,i} = d_{u_i}\Big(\int_\Omega u_i \ \mathrm{d}\mathbf{x}\Big)$ for $i \in \{1, \dots, n\}$ is a nonlocal diffusion matrix and $\mathcal{A}$ is a nonlinear cross-diffusion matrix.
In the proof of the existence of weak solutions, we will use the following assumptions.
We assume that for $i \in \{1, \dots, n\}$, the function $d_{u_i} : \mathbb{R} \to \mathbb{R}^+$ is continuous and satisfying the following:

$$\underline{d_i} \le d_{u_i}(r) \le \bar{d}_i \quad \forall r \in \mathbb{R} \text{ and } \quad \forall i \in \{1, \dots, n\} \tag{3.3.2}$$

where $\underline{d_i}$ and $\bar{d}_i$ are strictly positive constants.
Regarding the cross-diffusion matrix $\mathcal{A} = (\mathcal{A}_{i,j})_{1 \le i,j \le n}$, we assume that

$$\forall u_1, \dots, u_n \ge 0 \qquad \mathcal{A}_i^j(u_1, ..u_{i-1}, 0, u_{i+1}, \dots, u_n) = 0 \quad \forall i, j \in \{1, .., n\} \ i \ne j \tag{3.3.3}$$

$$\forall u_1, \dots, u_n \ge 0 \quad \forall \mathbf{v} \in \mathbb{R}^n \qquad \Big(\mathcal{A}(u_1, .., u_n)\psi, \psi\Big) \ \ge \ \frac{1}{C} \|\mathcal{A}(u_1, .., u_n)\| \ \|\psi\|^2, \tag{3.3.4}$$

where $\Big(\cdot, \cdot\Big)$ is the usual scalar product on $\mathbb{R}^n$, and

$$\forall u_1, \dots, u_n \ge 0 \quad \|\mathcal{A}(u_1, .., u_n)\| \ \le \ C(1 + \sum_{i=1}^n |u_i|^r) \quad \text{with } r < \begin{cases} 4, & \text{if } d = 2 \\ 10/3, & \text{if } d = 3. \end{cases} \tag{3.3.5}$$

Assumptions (3.3.3), (3.3.4) allow for nonnegative solutions; assumption (3.3.4) also expresses the positivity of the cross-diffusion matrix; and (3.3.5) is a kind of growth assumption on $\mathcal{A}$. For the reaction terms F_i, we assume they are continuous functions and there exists a constant C_F such that

$$\forall u_1, \dots, u_n \ge 0, \quad F_i(u_1, \dots, u_{i-1}, 0, u_{i+1}, \dots, u_n) \ge 0 \quad \text{and} \quad \sum_{i=1}^n F_i(u_1, .., u_n)\, u_i \le C_F(1 + \sum_{i=1}^n u_i^2). \tag{3.3.6}$$

Regarding the function Q, we assume it is a continuous function and there exists constant $C_Q > 0$ such that

$$|Q(u_1, \dots, u_n)| \le C_Q(1 + \sum_{i=1}^n |u_i|) \text{ for all } u_1, \dots, u_n \in \mathbb{R}. \tag{3.3.7}$$

Moreover, we assume that

$$\nabla \phi \in \left(\mathrm{L}^{d+2}(\Omega)\right)^d \quad \text{and } \phi \text{ is independent of time}$$

stands for the gravitational potential produced by the action of physical forces on the species.

Finally, we assume that initial conditions are

$$\boldsymbol{u}_0 \geq \mathbf{0}, \quad \boldsymbol{u}_0 \in \mathbf{L}^2(\Omega), \quad \mathbf{v}_0 \in \mathbf{H}. \tag{3.3.8}$$

Now we define what we mean by weak solution of the system (3.1.1). We also supply our main existence result.

Definition 3.3.1 *We say that $(\boldsymbol{u}, \mathbf{v})$ is a weak solution to problem (3.2.29), if $\boldsymbol{u}$ is nonnegative,*

$$\boldsymbol{u} \in \mathrm{L}^\infty(0,T;\mathbf{L}^2(\Omega)) \cap \mathrm{L}^2(0,T;\mathbf{H}^1(\Omega)),$$

$$\mathbf{v} \in \mathrm{L}^2(0,T;\mathbf{V}) \cap C\big([0,\,T];\,\mathbf{H}\big), \;\; \partial_t \mathbf{v} \in \mathrm{L}^1(0,T;\mathbf{V}')$$

and the following identities hold

$$\begin{aligned} &-\iint_{\Omega_T} \boldsymbol{u}\cdot\partial_t\Psi_1 \,\mathrm{d}\mathbf{x}\,\mathrm{d}t - \iint_{\Omega_T} (\mathbf{v}\cdot\nabla)\boldsymbol{u}\cdot\Psi_1 \,\mathrm{d}\mathbf{x}\,\mathrm{d}t + \iint_{\Omega_T} D(\boldsymbol{u})\nabla\boldsymbol{u} : \nabla\Psi_1 \,\mathrm{d}\mathbf{x}\,\mathrm{d}t \\ &\quad + \iint_{\Omega_T} \mathcal{A}(\boldsymbol{u})\nabla\boldsymbol{u} : \nabla\Psi_1 \,\mathrm{d}\mathbf{x}\,\mathrm{d}t = \int_\Omega \boldsymbol{u}_0(\mathbf{x})\cdot\Psi_1(0,\mathbf{x})\,\mathrm{d}\mathbf{x} + \iint_{\Omega_T} F(\boldsymbol{u})\cdot\Psi_1 \,\mathrm{d}\mathbf{x}\,\mathrm{d}t, \end{aligned} \tag{3.3.9}$$

$$\begin{aligned} &\int_0^T \langle \partial_t\mathbf{v}, \Psi_2\rangle_{\mathbf{V}',\mathbf{V}} \,\mathrm{d}t + \nu\int_\Omega \nabla\mathbf{v} : \nabla\Psi_2 \,\mathrm{d}\mathbf{x}\,\mathrm{d}t + \iint_{\Omega_T} (\mathbf{v}\cdot\nabla)\mathbf{v}\cdot\Psi_2 \,\mathrm{d}\mathbf{x}\,\mathrm{d}t \\ &\qquad + \iint_{\Omega_T} Q(\boldsymbol{u})\nabla\phi\cdot\Psi_2 \,\mathrm{d}\mathbf{x}\,\mathrm{d}t = \mathbf{0}, \end{aligned} \tag{3.3.10}$$

for all test functions $\Psi_1 = (\psi_{1,u},\dots,\psi_{n,u})^T \in \mathbf{D}([0,T)\times\bar{\Omega})$ and $\Psi_2 = (\psi_{1,v},\dots,\psi_{d,v})^T \in C_c^0(0,T;\mathbf{V})$ where $C_c^0(0,T;\mathbf{V})$ denotes the space of continuous functions with compact support and values in $\mathbf{V}$.

Theorem 3.3.2 *Assume conditions (3.3.3)-(3.3.6) hold. If assumption (3.3.8) is satisfied, then the problem (3.3.1) has a weak solution in the sense of Definition 3.3.1.*

Proof 3.3.1 (Proof of Theorem 3.3.2) *The proof of the existence of weak solution is based on the nonlinear Galerkin method. Although we solve the problem in a finite-dimensional space firstly and we are looking estimates that allows us to pass to the limit. We decompose the proof of Theorem 3.3.2 into three parts: first, we write the approximate solution, then we give a priori estimates and finally we pass to the limit.*

First step: approximate solution. *We choose sequences $\{\psi_{1,u},\psi_{2,u},\dots\}$, $\{\psi_{1,v},\psi_{2,v},\dots\}$ in $\mathcal{D}(\Omega)$ such that $\cup_{m=1}^\infty \mathcal{V}_{m,u}$, $\cup_{m=1}^\infty \mathcal{V}_{m,v}$ with $\mathcal{V}_{m,u} = span\{\psi_{1,u},\psi_{2,u},\dots,\psi_{m,u}\}$ (resp. $\mathcal{V}_{m,v} = span\{\psi_{1,v},\psi_{2,v},\dots,\psi_{m,v}\}$) is dense in $(H^s(\Omega))^n$ (resp. $(H^s(\Omega))^d$ with s large enough such that $(H^s(\Omega))^r$ is continuously embedded in $(C^1(\overline{\Omega}))^r$ for $r>0$. We consider the following sequence for approximating solutions of the problem (3.3.1):*

$$\boldsymbol{u}^m(t,\mathbf{x}) = \sum_{k=1}^m b_k^m(t)\psi_{k,u}(\mathbf{x}), \qquad \mathbf{v}^m(t,\mathbf{x}) = \sum_{k=1}^m c_k^m(t)\psi_{k,v}(\mathbf{x}), \tag{3.3.11}$$

where for $1\leq k\leq m$ the functions $b_k^m : [0,\,T)\to\mathbb{R}$ and $c_k^m : [0,\,T)\to\mathbb{R}$ are supposed to be measurable bounded functions. For the initial conditions, we choose the coefficients as

$$b_k^m(0) := \int_\Omega \boldsymbol{u}_0\psi_{k,u}(\mathbf{x})\,\mathrm{d}\mathbf{x}, \quad c_k^m(0) := \int_\Omega \mathbf{v}_0\psi_{k,v}(\mathbf{x})\,\mathrm{d}\mathbf{x}$$

such that as $m\to\infty$, we have

$$\boldsymbol{u}^m(0,.)\to\boldsymbol{u}_0, \quad \mathbf{v}^m(0,.)\to\mathbf{v}_0 \quad \text{in } \mathbf{L}^2(\Omega). \tag{3.3.12}$$

where $\boldsymbol{u}^m(0,.) := \sum_{k=1}^m b_k^m(0)\psi_{k,u}(.)$ and $\mathbf{v}^m(0,.) := \sum_{k=1}^m c_k^m(0)\psi_{k,v}(.)$.

For $1 \le k \le m$ the coefficients b_k^m and c_k^m are obtained from the following system

$$\begin{aligned}\int_\Omega \partial_t \boldsymbol{u}^m \cdot \psi_{k,u}\,\mathrm{d}\mathbf{x} - \int_\Omega (\mathbf{v}^m \cdot \nabla)\boldsymbol{u}^m \cdot \psi_{k,u}\,\mathrm{d}\mathbf{x} + \int_\Omega D(\boldsymbol{u}^m)\nabla \boldsymbol{u}^m : \nabla \psi_{k,u}\,\mathrm{d}\mathbf{x} \\ + \int_\Omega \mathcal{A}(\boldsymbol{u}^{m,+})\nabla \boldsymbol{u}^m : \nabla \psi_{k,u}\,\mathrm{d}\mathbf{x} = \int_\Omega F(\boldsymbol{u}^{m,+}) \cdot \psi_{k,u}\,\mathrm{d}\mathbf{x},\end{aligned} \tag{3.3.13}$$

$$\int_\Omega \partial_t \mathbf{v}^m \cdot \psi_{k,v}\,\mathrm{d}\mathbf{x} + \nu \int_\Omega \nabla \mathbf{v}^m : \nabla \psi_{k,v}\,\mathrm{d}\mathbf{x} + \int_\Omega (\mathbf{v}^m \cdot \nabla)\mathbf{v}^m \cdot \psi_{k,v}\,\mathrm{d}\mathbf{x} + \int_\Omega Q(\boldsymbol{u}^m)\nabla \phi \cdot \psi_{k,v}\,\mathrm{d}\mathbf{x} = \mathbf{0}, \tag{3.3.14}$$

or equivalently (by suing the orthonormality of the bases)

$$\begin{cases} \Big(b_k^m(t)\Big)' = \mathcal{F}_k\Big(t, b_1^m(t), \ldots, b_m^m(t), c_1^m(t), \ldots, c_m^m(t)\Big), \\ \Big(c_k^m(t)\Big)' = \mathcal{G}_k\Big(t, b_1^m(t), \ldots, b_m^m(t), c_1^m(t), \ldots, c_m^m(t)\Big), \\ b_k^m(0) = \int_\Omega \boldsymbol{u}_0 \psi_k\,\mathrm{d}\mathbf{x},\ c_k^m(0) = \int_\Omega \mathbf{v}_0 \psi_k\,\mathrm{d}\mathbf{x}, \end{cases} \tag{3.3.15}$$

Herein,

$$\mathcal{A}(\boldsymbol{u}^{m,+}) = \Big(\mathcal{A}_i^j\big(\sum_{k=1}^m b_k^m(t)\psi_{k,u}(\mathbf{x})\big)^+\Big)_{1\le i,j\le n}, \qquad F(\boldsymbol{u}^{m,+}) = \Big(F_j\big(\sum_{k=1}^m b_k^m(t)\psi_{k,u}(\mathbf{x})\big)^+\Big)_{1\le j\le n},$$

and

$$\begin{aligned}\mathcal{F}_k\Big(t, b_1^m, \ldots, b_m^m, c_1^m, \ldots, c_m^m\Big) &:= \int_\Omega (\mathbf{v}^m \cdot \nabla)\boldsymbol{u}^m \cdot \psi_{k,u}\,\mathrm{d}\mathbf{x} - \int_\Omega D(\boldsymbol{u}^m)\nabla \boldsymbol{u}^m : \nabla \psi_{k,u}\,\mathrm{d}\mathbf{x} \\ &\quad - \int_\Omega \mathcal{A}(\boldsymbol{u}^{m,+})\nabla \boldsymbol{u}^m : \nabla \psi_{k,u}\,\mathrm{d}\mathbf{x} + \int_\Omega F(\boldsymbol{u}^{m,+}) \cdot \psi_{k,u}\,\mathrm{d}\mathbf{x},\end{aligned}$$

$$\begin{aligned}\mathcal{G}_k\Big(t, b_1^m, \ldots, b_m^m, c_1^m, \ldots, c_m^m\Big) &:= -\nu \int_\Omega \nabla \mathbf{v}^m : \nabla \psi_{k,v}\,\mathrm{d}\mathbf{x} - \int_\Omega (\mathbf{v}^m \cdot \nabla)\mathbf{v}^m \cdot \psi_{k,v}\,\mathrm{d}\mathbf{x} \\ &\quad - \int_\Omega Q(\boldsymbol{u}^m)\nabla \phi \cdot \psi_{k,v}\,\mathrm{d}\mathbf{x}\end{aligned}$$

for $1 \le k \le m$, where $s^+ = \max(s, 0)$. Then, thanks to the existence result of ordinary differential equations (cf. [54]), system (3.3.15) has a continuous solution $\Big(c_k^m(t), b_k^m(t)\Big)_{k=1}^m$ on an interval $(0, \tau')$, $\tau' > 0$ and may depend on m. Using a standard arguments, it is not difficult to show that the local solution constructed above can be extended to the whole interval $[0, T)$ independent of m.
Note that from (3.3.13) and (3.3.14), the Faedo-Galerkin solutions satisfy the following weak formulations for each fixed $t > 0$:

$$\begin{aligned}\int_\Omega \partial_t \boldsymbol{u}^m \cdot \psi_u\,\mathrm{d}\mathbf{x} - \int_\Omega (\mathbf{v}^m \cdot \nabla)\boldsymbol{u}^m \cdot \psi_u\,\mathrm{d}\mathbf{x} + \int_\Omega D(\boldsymbol{u}^m)\nabla \boldsymbol{u}^m : \nabla \psi_u\,\mathrm{d}\mathbf{x} \\ + \int_\Omega \mathcal{A}(\boldsymbol{u}^{m,+})\nabla \boldsymbol{u}^m : \nabla \psi_v\,\mathrm{d}\mathbf{x} = \int_\Omega F(\boldsymbol{u}^{m,+}) \cdot \psi_u\,\mathrm{d}\mathbf{x},\end{aligned} \tag{3.3.16}$$

$$\int_\Omega \partial_t \mathbf{v}^m \cdot \psi_v\,\mathrm{d}\mathbf{x} + \nu \int_\Omega \nabla \mathbf{v}^m : \nabla \psi_v\,\mathrm{d}\mathbf{x} + \int_\Omega (\mathbf{v}^m \cdot \nabla)\mathbf{v}^m \cdot \psi_v\,\mathrm{d}\mathbf{x} + \int_\Omega Q(\boldsymbol{u}^m)\nabla \phi \cdot \psi_v\,\mathrm{d}\mathbf{x} = \mathbf{0}, \tag{3.3.17}$$

for all test functions $\psi_u \in \mathbf{D}([0, T) \times \bar{\Omega})$ and $\psi_v \in C_c^0(0, T; \mathbf{V})$

To passing to the limit in (3.3.16)-(3.3.17) and proving the existence of $\boldsymbol{u}$ and $\mathbf{v}$, we need the following a priori estimates lemma.

Second step: a priori estimates

Lemma 3.3.3 *Let $\boldsymbol{u}_0 \in \mathbf{L}^2(\Omega)^+$ and $\mathbf{v}_0 \in \mathbf{H}$, then the problem (3.3.16)- (3.3.17) has a weak solution $\boldsymbol{u}^m \in \mathrm{L}^2\big(0,T;\mathbf{H}^1(\Omega)\big)$, $\mathbf{v}^m \in \mathrm{L}^2\big(0,T;\,\mathbf{V}\big)$ satisfying:*

$$\begin{aligned}
&\int_\Omega |\boldsymbol{u}^m|^2\,\mathrm{d}\mathbf{x} + \iint_{\Omega_T} |\nabla \boldsymbol{u}^m|^2\,\mathrm{d}\mathbf{x}\,\mathrm{d}t \le C,\\
&\iint_{\Omega_T} \Big(\max_{1\le i,j\le n} |\mathcal{A}_i^{j,m}(u_1^m,\dots,u_n^m)|\Big) \sum_{i=1}^n |\nabla u_i^m|^2\,\mathrm{d}\mathbf{x}\,\mathrm{d}t \le C,\\
&\int_\Omega |\mathbf{v}^m|^2\,\mathrm{d}\mathbf{x} + \nu \iint_{\Omega_T} |\nabla \mathbf{v}^m|^2\,\mathrm{d}\mathbf{x}\,\mathrm{d}t \le C,
\end{aligned} \tag{3.3.18}$$

where C is a strictly positive constant independent of m.

Proof 3.3.2 *Substituting $\psi_u = -\boldsymbol{u}^{m,-}$ in (3.3.16) and integrating over $(0,\tau)$, we get*

$$\begin{aligned}
\frac{1}{2}\int_\Omega |\boldsymbol{u}^{m,-}(\tau,\mathbf{x})|^2\,\mathrm{d}\mathbf{x} - \int_0^\tau\int_\Omega (\mathbf{v}^m\cdot\nabla)\boldsymbol{u}^m\cdot\boldsymbol{u}^{m,-}\,\mathrm{d}\mathbf{x}\,\mathrm{d}t + \int_0^\tau\int_\Omega D(\boldsymbol{u}^m)|\nabla \boldsymbol{u}^{m,-}|^2\,\mathrm{d}\mathbf{x}\,\mathrm{d}t\\
+\int_0^\tau\int_\Omega \mathcal{A}(\boldsymbol{u}^{m,+})|\nabla \boldsymbol{u}^{m,-}|^2\;\mathrm{d}\mathbf{x}\,\mathrm{d}t = \int_0^\tau\int_\Omega F(\boldsymbol{u}^{m,+})\cdot\boldsymbol{u}^{m,-}\,\mathrm{d}\mathbf{x}\,\mathrm{d}t + \frac{1}{2}\int_\Omega |\boldsymbol{u}_0^-|^2\,\mathrm{d}\mathbf{x}.
\end{aligned}$$

Since $\operatorname{div}\mathbf{v}^m = 0$ and $\mathbf{v}^m = \mathbf{0}$ on $\partial\Omega$, we have

$$-\int_\Omega (\mathbf{v}^m\cdot\nabla)\boldsymbol{u}^m\cdot\boldsymbol{u}^{m,-} = \frac{1}{2}\int_\Omega \nabla(\boldsymbol{u}^m)^2\mathbf{v}^m = -\frac{1}{2}\int_\Omega \operatorname{div}(\mathbf{v}^m)(\boldsymbol{u}^m)^2 + \frac{1}{2}\int_{\partial\Omega}\mathbf{v}^m(\boldsymbol{u}^m)^{2^T}\eta = \mathbf{0}.$$

Using the positivity conditions (3.3.2), (3.3.3) and (3.3.6) on $D(\boldsymbol{u}^m)$, $\mathcal{A}$ and F, respectively, we have

$$\int_\Omega |\boldsymbol{u}^{m,-}(\tau,\mathbf{x})|^2\,\mathrm{d}\mathbf{x} \le \int_\Omega |\boldsymbol{u}_0^-|^2\,\mathrm{d}\mathbf{x}.$$

Since $\boldsymbol{u}_0$ is nonnegative, we deduce that $\boldsymbol{u}^{m,-} = 0$. Thus the nonnegativity of $\boldsymbol{u}^m$.
Now, substituting $\psi_u = \boldsymbol{u}^m$ in (3.3.16) and integrating over $(0,\,\tau)$ with $\tau < T$ to obtain

$$\begin{aligned}
\frac{1}{2}\int_\Omega |\boldsymbol{u}^m(\tau,\mathbf{x})|^2\,\mathrm{d}\mathbf{x} - \int_0^\tau\int_\Omega (\mathbf{v}^m\cdot\nabla)\boldsymbol{u}^m\cdot\boldsymbol{u}^m\,\mathrm{d}\mathbf{x}\,\mathrm{d}t + \int_0^\tau\int_\Omega D(\boldsymbol{u}^m)|\nabla \boldsymbol{u}^m|^2\,\mathrm{d}\mathbf{x}\,\mathrm{d}t\\
+\int_0^\tau\int_\Omega \mathcal{A}(\boldsymbol{u}^m)|\nabla \boldsymbol{u}^m|^2\;\mathrm{d}\mathbf{x}\,\mathrm{d}t = \int_0^\tau\int_\Omega F(\boldsymbol{u}^m)\cdot\boldsymbol{u}^m\,\mathrm{d}\mathbf{x}\,\mathrm{d}t + \frac{1}{2}\int_\Omega |\boldsymbol{u}_0(\mathbf{x})|^2\,\mathrm{d}\mathbf{x}.
\end{aligned}$$

Using (3.3.4), (3.3.2) and (3.3.6), we obtain

$$\begin{aligned}
&\frac{1}{2}\int_\Omega |\boldsymbol{u}^m(\tau,\mathbf{x})|^2\,\mathrm{d}\mathbf{x} + \sum_{i=1}^n \underline{d}_i\int_0^\tau\int_\Omega |\nabla u_i^m|^2\,\mathrm{d}\mathbf{x}\,\mathrm{d}t + \int_0^\tau\int_\Omega \max_{1\le i,j\le n}|\mathcal{A}_i^j(u_1^m,\dots,u_n^m)|\\
&\sum_{i=1}^n |\nabla u_i^m|^2\,\mathrm{d}\mathbf{x}\,\mathrm{d}t \le C_F\int_0^\tau\int_\Omega |\boldsymbol{u}^m(t,\mathbf{x})|^2\,\mathrm{d}\mathbf{x}\,\mathrm{d}t + \frac{1}{2}\int_\Omega |\boldsymbol{u}_0(\mathbf{x})|^2\,\mathrm{d}\mathbf{x} + C_F\,n\,T\,|\Omega|.
\end{aligned} \tag{3.3.19}$$

Setting $\Theta^m(\tau) = \displaystyle\int_\Omega |\boldsymbol{u}^m(\tau,\mathbf{x})|^2 dx$ in (3.3.19), we observe that

$$0 \le \Theta^m(\tau) \le \int_\Omega |\boldsymbol{u}_0(\mathbf{x})|^2\,\mathrm{d}\mathbf{x} + 2\,C_F\,n\,T\,|\Omega| + 2\,C_F\int_0^\tau \Theta^m(t)\,\mathrm{d}t.$$

Herein, we have used the positivity of the second and the third integrals in (3.3.19). Now, using Gronwall's inequality, we get

$$0 \le \Theta^m(\tau) \le \Big[\int_\Omega |\boldsymbol{u}_0(x)|^2 dx + 2\,C_F\,n\,T\,|\Omega|\Big]\exp(2\,C_F\,\tau), \quad \forall\tau\in(0,T).$$

This implies that

$$\int_\Omega |\boldsymbol{u}^m(\tau,x)|^2 dx \le C \quad \textit{for all } \tau\in(0,T).$$

Consequently

$$\sup_{\tau\in(0,T)}\int_\Omega |\boldsymbol{u}^m(\tau)|^2\,\mathrm{d}\mathbf{x}+\iint_{\Omega_T}|\nabla\boldsymbol{u}^m|^2\,\mathrm{d}\mathbf{x}\,\mathrm{d}t\le C, \tag{3.3.20}$$

where the constant $C>0$ depends only on T and $\boldsymbol{u}_0$.
Now, we take $\psi_v=\mathbf{v}^m$ in (3.3.17) and we integrate over $(0,\,\tau)$ with $\tau<T$ to obtain

$$\frac{1}{2}\int_\Omega|\mathbf{v}^m(\tau,\mathbf{x})|^2\,\mathrm{d}\mathbf{x}+\nu\int_0^\tau\int_\Omega|\nabla\mathbf{v}^m|^2\,\mathrm{d}\mathbf{x}\,\mathrm{d}t+\int_0^\tau\int_\Omega(\mathbf{v}^m\cdot\nabla)\mathbf{v}^m\cdot\mathbf{v}^m\,\mathrm{d}\mathbf{x}\,\mathrm{d}t$$
$$+\int_0^\tau\int_\Omega Q(\boldsymbol{u}^m)\nabla\phi\cdot\mathbf{v}^m\,\mathrm{d}\mathbf{x}\,\mathrm{d}t=\frac{1}{2}\int_\Omega|\mathbf{v}_0(\mathbf{x})|^2\,\mathrm{d}\mathbf{x}.$$

Since $\int_0^\tau\int_\Omega(\mathbf{v}^m\cdot\nabla)\mathbf{v}^m\cdot\mathbf{v}^m\,\mathrm{d}\mathbf{x}\,\mathrm{d}t=\mathbf{0}$, this implies

$$\frac{1}{2}\int_\Omega|\mathbf{v}^m(\tau,\mathbf{x})|^2\,\mathrm{d}\mathbf{x}\quad+\nu\int_0^\tau\int_\Omega|\nabla\mathbf{v}^m|^2\,\mathrm{d}\mathbf{x}\,\mathrm{d}t\le\frac{1}{2}\int_\Omega|\mathbf{v}_0(\mathbf{x})|^2\,\mathrm{d}\mathbf{x}-\int_0^\tau\int_\Omega Q(\boldsymbol{u}^m)\nabla\phi\cdot\mathbf{v}^m\,\mathrm{d}\mathbf{x}\,\mathrm{d}t. \tag{3.3.21}$$

Using (3.3.7) and Young inequality, we have

$$I:=\Big|\int_0^\tau\int_\Omega Q(\boldsymbol{u}^m)\nabla\phi\,\mathbf{v}^m\,\mathrm{d}\mathbf{x}\,\mathrm{d}t\Big|\le C_Q\Big(|\Omega_\tau|+\int_0^\tau\int_\Omega\big|\boldsymbol{u}^m(\tau,\mathbf{x})\nabla\phi\,\mathbf{v}^m\big|\,\mathrm{d}\mathbf{x}\,\mathrm{d}t\Big)$$
$$\le C_Q\Big(|\Omega_\tau|+\frac{d}{2(d+2)}\int_0^\tau\int_\Omega|\boldsymbol{u}^m|^{2\frac{d+2}{d}}\,\mathrm{d}\mathbf{x}\,\mathrm{d}t+\frac{1}{d+2}\int_0^\tau\int_\Omega|\nabla\phi|^{d+2}\,\mathrm{d}\mathbf{x}\,\mathrm{d}t+\frac{1}{2}\int_0^\tau\int_\Omega|\mathbf{v}^m|^2\,\mathrm{d}\mathbf{x}\,\mathrm{d}t\Big).$$

Thanks to Gagliardo-Nirenberg inequality, we get

$$\int_0^\tau\int_\Omega|\boldsymbol{u}^m|^{2\frac{d+2}{d}}\,\mathrm{d}\mathbf{x}\,\mathrm{d}t\le\Big(\sup_{\tau\in(0,T)}\int_\Omega|\boldsymbol{u}^m|^2\,\mathrm{d}\mathbf{x}\Big)^{\frac{1}{2}}\int_0^\tau\int_\Omega|\nabla\boldsymbol{u}^m|^2\,\mathrm{d}\mathbf{x}\,\mathrm{d}t.$$

Next, we use this to arrive

$$I\le C_Q\Big(|\Omega_\tau|+\frac{d}{2(d+2)}\Big(\sup_{\tau\in(0,T)}\int_\Omega|\boldsymbol{u}^m|^2\,\mathrm{d}\mathbf{x}\Big)^{\frac{1}{2}}\int_0^\tau\int_\Omega|\nabla\boldsymbol{u}^m|^2\,\mathrm{d}\mathbf{x}\,\mathrm{d}t+\frac{1}{d+2}\int_0^\tau\int_\Omega|\nabla\phi|^{d+2}\,\mathrm{d}\mathbf{x}\,\mathrm{d}t$$
$$+\frac{1}{2}\iint_{\Omega_\tau}|\mathbf{v}^m|^2\,\mathrm{d}\mathbf{x}\,\mathrm{d}t\Big).$$

Exploiting the assumption $\nabla\phi\in(\mathrm{L}^{d+2}(\Omega))^d$ and using estimate (3.3.20) in (3.3.21), we obtain

$$\frac{1}{2}\int_\Omega|\mathbf{v}^m(\tau,\mathbf{x})|^2\,\mathrm{d}\mathbf{x}+\nu\int_0^\tau\int_\Omega|\nabla\mathbf{v}^m|^2\,\mathrm{d}\mathbf{x}\,\mathrm{d}t\le\frac{C_Q}{2}\int_0^\tau\int_\Omega|\mathbf{v}^m(t,\mathbf{x})|^2\,\mathrm{d}\mathbf{x}\,\mathrm{d}t$$
$$+\frac{1}{2}\int_\Omega|\mathbf{v}_0(\mathbf{x})|^2\,\mathrm{d}\mathbf{x}+\tilde{C_Q}(T,\boldsymbol{u}_0,|\Omega|,\phi). \tag{3.3.22}$$

Similarly, setting $\chi^m(\tau)=\int_\Omega|\mathbf{v}^m(\tau,\mathbf{x})|^2\,\mathrm{d}\mathbf{x}$ in (3.3.22), we arrive at

$$0\le\chi^m(\tau)\le\int_\Omega|\mathbf{v}_0(\mathbf{x})|^2\,\mathrm{d}\mathbf{x}+2\tilde{C_Q}(T,\boldsymbol{u}_0,|\Omega|,\phi)+2\,C_Q\int_0^\tau\chi^m(t)\,\mathrm{d}t.$$

An application of Gronwall's inequality, we obtain

$$0\le\chi^m(\tau)\le\Big[\int_\Omega|\mathbf{v}_0(\mathbf{x})|^2\,\mathrm{d}\mathbf{x}+2\tilde{C_Q}(T,\boldsymbol{u}_0,|\Omega|,\phi)\Big]\exp(2\,C_Q\,\tau),\quad\forall\tau\in(0,T).$$

This implies that

$$\int_\Omega|\mathbf{v}^m(\tau,\mathbf{x})|^2\,\mathrm{d}\mathbf{x}\le C\quad\textit{for all }\tau\in(0,T).$$

Consequently, we deduce from this, (3.3.22) and we collect the previous results on $\boldsymbol{u}^m$ *to obtain*

$$\begin{aligned}
&\max_{0<\tau<T}\int_\Omega |\mathbf{v}^m(\tau,\mathbf{x})|^2\,\mathrm{d}\mathbf{x}+\nu\int_0^T\int_\Omega |\nabla\mathbf{v}^m|^2\,\mathrm{d}\mathbf{x}\le C,\\
&\max_{0<\tau<T}\int_\Omega |\boldsymbol{u}^m(\tau,\mathbf{x})|^2\,\mathrm{d}\mathbf{x}+\int_0^T\int_\Omega |\nabla\boldsymbol{u}^m|^2\,\mathrm{d}\mathbf{x}\le C,\\
&\int_0^T\int_\Omega \max_{1\le i,j\le n}|\mathcal{A}_i^{j,m}(u_1^m,\dots,u_n^m)|\sum_{i=1}^n|\nabla u_i^m|^2\,\mathrm{d}\mathbf{x}\le C.
\end{aligned}\tag{3.3.23}$$

Therefore, we deduce that $\mathbf{v}^m$ *is uniformly bounded in* $\mathrm{L}^\infty\big(0,T;\mathbf{H}\big)\cap\mathrm{L}^2\Big(0,T;\mathbf{V}\Big)$ *and* $\boldsymbol{u}^m$ *is uniformly bounded in* $\mathrm{L}^\infty\big(0,T;\mathbf{L}^2(\Omega)\big)\cap\mathrm{L}^2\Big(0,T;\mathbf{H}^1(\Omega)\Big)$. *Thus, we obtain the assertion of the lemma.*

Third step: passing to the limit. *The existence of a nonnegative weak solutions for system (3.2.29) will be shown by proving convergence of the solution of approximate problem. Using the sharp Sobolev embedding and thanks to (3.3.5) we observe that for* $i,\,j\in\{1,..,n\}$, $\mathcal{A}_i^{j,m}(u_1^m,\dots,u_n^m)$ *are bounded in* $\mathrm{L}^1(\Omega_T)$. *Moreover, the estimate (3.3.23) give the* $\mathrm{L}^2(\Omega_T)$ *estimate of* $\sqrt{|\mathcal{A}_i^{j,m}(u_1^m,\dots,u_n^m)|}\,\nabla u_i^m$. *By the Cauchy-Schwarz inequality we deduce uniform* $\mathrm{L}^1(\Omega_T)$ *estimate of* $\mathcal{A}_i^{j,m}(u_1^m,\dots,u_n^m)\,\nabla u_i^m$. *Moreover, from the assumption on* F, *we get easily the uniform bound of* $F(\boldsymbol{u}^m)$ *in* $\mathrm{L}^1(\Omega_T)$. *On the other hand, using estimate (3.3.18), we get*

$$\sup_{|\mu|\le\delta}\int_0^T\int_\Omega |u_i^m(\mathbf{x}+\mu)-u_i^m(\mathbf{x})|\,\mathrm{d}\mathbf{x}\,\mathrm{d}t\le\theta(\delta),\qquad \text{with } \theta(\delta)\to 0 \text{ as } \delta\to 0.$$

Thanks to the Kruzhkov compactness lemma (cf. [69]), we deduce that u_i^m *is relatively compact in* $\mathrm{L}^1(\Omega_T)$ *and there exists a subsequence will be noted* u_i^m *such that* u_i^m *converges strongly to* u_i *in* $L^1(\Omega_T)$ *and a.e. in* Ω_T.

From Lemma 3.3.3, we have $\mathbf{v}^m$ *is uniformly bounded in* $\mathrm{L}^\infty\big(0,T;\mathbf{H}\big)\cap\mathrm{L}^2\Big(0,T;\mathbf{V}\Big)$. *Therefore, there exists* $\mathbf{v}\in\mathrm{L}^\infty\big(0,T;\mathbf{H}\big)\cap\mathrm{L}^2\big(0,T;\mathbf{V}\big)$ *such as,* $m\to\infty$

$$\mathbf{v}^m\rightharpoonup\mathbf{v} \text{ weakly-}\star \text{ in } \mathrm{L}^\infty\big(0,T;\mathbf{H}\big) \text{ and } \mathbf{v}^m\rightharpoonup\mathbf{v} \text{ weakly in } \mathrm{L}^2\big(0,T;\mathbf{V}\big).$$

Moreover, thanks to the compacity Theorem of Aubin-Simon (see for e.g. [85]), the space

$$\{\mathbf{v}^m\in\mathrm{L}^2(0,T;\mathbf{V});\ \partial_t\mathbf{v}^m\in\mathrm{L}^1(0,T;\mathbf{V}')\}$$

is compactly injected in $\mathrm{L}^2(0,T;\mathbf{H})$. *Consequently, we have*

$$\mathbf{v}^m\to\mathbf{v}\quad \text{strongly in}\quad \mathrm{L}^2(0,T;\mathbf{H}).\tag{3.3.24}$$

In the next step, we pass to the limit in the weak approximate formulation. First, we have

$$\mathcal{A}_i^{j,m}(u_1^m,\dots,u_n^m)\,\nabla u_i^m\to\mathcal{A}_i^j(u_1,\dots,u_n)\,\nabla u_i\quad \text{weakly in}\quad (\mathrm{L}^1(\Omega_T))^d.\tag{3.3.25}$$

Indeed, using the Vitali theorem, we deduce that $\mathcal{A}_i^{j,m}(u_1^m,\dots,u_n^m)$ *converges to* $\mathcal{A}_i^j(u_1,\dots,u_n)$ *strongly in* $\mathrm{L}^1(\Omega_T)$. *Now we rewriting the cross-diffusion terms as*

$$sign\big(\mathcal{A}_i^{j,m}(u_1^m,\dots,u_n^m)\big)\sqrt{|\mathcal{A}_i^{j,m}(u_1^m,\dots,u_n^m)|}\,\Big(\sqrt{|\mathcal{A}_i^{j,m}(u_1^m,\dots,u_n^m)|}\,\nabla u_i^m\Big).$$

Thanks to the strong $\mathrm{L}^2(\Omega_T)$ *convergence of* $\sqrt{|\mathcal{A}_i^{j,m}(u_1^m,\dots,u_n^m)|}$ *to* $\sqrt{|\mathcal{A}_i^j(u_1,\dots,u_n)|}$, *we obtain (3.3.25). Using the optimal Sobolev embedding* $\mathbf{H}^1(\Omega)\subset\mathbf{L}^{2^\star}(\Omega)$, *we deduce that* $\boldsymbol{u}^m$ *is uniformly bounded in* $\mathrm{L}^2(0,T;\mathbf{L}^{2^\star(1+r/2)}(\Omega))$. *Then, thanks to the interpolation with* $\mathrm{L}^1(0,T;\mathbf{L}^2(\Omega))$, *we can take*

a higher value of r in (3.3.5). On the other hand, we have

$$\int_0^T \int_\Omega (\mathbf{v}^m \cdot \nabla)\boldsymbol{u}^m \cdot \psi_1 \, \mathrm{d}\mathbf{x}\, \mathrm{d}t = \int_0^T \int_\Omega \boldsymbol{u}^m (\mathbf{v}^m)^T \nabla \psi_1 \, \mathrm{d}\mathbf{x}\, \mathrm{d}t \longrightarrow \int_0^T \int_\Omega \boldsymbol{u}\mathbf{v}^T \nabla \psi_1 \, \mathrm{d}\mathbf{x}\, \mathrm{d}t. \tag{3.3.26}$$

Indeed,

$$II = \iint_{\Omega_T} (\boldsymbol{u}^m - \boldsymbol{u})(\mathbf{v}^m)^T \nabla \psi_1 \, \mathrm{d}\mathbf{x}\, \mathrm{d}t - \iint_{\Omega_T} \boldsymbol{u}(\mathbf{v}^m - \mathbf{v})^T \nabla \psi_1 \Big) \, \mathrm{d}\mathbf{x}\, \mathrm{d}t.$$

From the dominated convergence theorem of Lebesgue and the strong convergence (3.3.24), we have

$$II \leq \| \, (\boldsymbol{u}^m - \boldsymbol{u})^T \nabla \psi_1 \, \|_{\mathbf{L}^2(\Omega_T)} \| \, \mathbf{v}^m \, \|_{\mathbf{L}^2(\Omega_T)} + \| \, \mathbf{v}^m - \mathbf{v} \, \|_{\mathbf{L}^2(\Omega_T)} \| \, \boldsymbol{u}^T \nabla \psi_1 \, \|_{\mathbf{L}^2(\Omega_T)} \longrightarrow \mathbf{0}.$$

Now, we define $B(\mathbf{v}) := (\mathbf{v} \cdot \nabla)\mathbf{v}$, then equation (3.3.10) can be written as follows

$$\frac{d}{\mathrm{d}t}\langle \mathbf{v}, \psi \rangle = \langle -\nu \Delta \mathbf{v} + B(\mathbf{v}) + Q(\boldsymbol{u})\nabla \phi, \psi \rangle, \quad \forall \psi \in \mathbf{V}. \tag{3.3.27}$$

In the one hand, the operator $-\Delta : \mathbf{V} \to \mathbf{V}'$ is linear and continuous and $\mathbf{v} \in \mathrm{L}^2(0,T;\mathbf{V})$, this implies $-\Delta \mathbf{v} \in \mathrm{L}^2(0,T;\mathbf{V}')$. On the other hand, $Q(\boldsymbol{u})\nabla\phi \in \mathrm{L}^2(0,T;\mathbf{V}')$ and $b(\mathbf{v},\mathbf{v},w) = \langle B(\mathbf{v}), w\rangle$ is trilinear continuous on $\mathbf{V}$, see [86]. So that $\| \, B(\mathbf{v}) \, \|_{\mathbf{V}'} \leq \| \, \mathbf{v} \, \|_{\mathbf{V}}$, then $B(\mathbf{v}) \in \mathrm{L}^1(0,T,\mathrm{V}')$. Consequently, $\partial_t \mathbf{v} \in \mathrm{L}^1(0,T,\mathbf{V}')$.
Finally, we pass to the limit in (3.3.16) and (3.3.17), we obtain the weak formulation (3.3.9)-(3.3.10) in the sense of Definition 3.3.1. This completes the proof of Theorem 3.3.2.

The pressure. To introduce the pressure p, we set

$$V(t) = \int_0^t \mathbf{v}(s)\, ds, \; R(t) = \int_0^t (\mathbf{v} \cdot \nabla)\mathbf{v}(s)\, ds, \; K(t) = \int_0^t Q(\boldsymbol{u})(s)\nabla\phi \, ds.$$

It is clear that V, K, $R \in C(0,T;(\mathrm{H}^1(\Omega))')$. Integrating (3.3.27) over $[0,T]$ yields,

$$\langle \mathbf{v}(t) - \mathbf{v}_0 - \nu \Delta V(t) + R(t) + K(t), \psi \rangle = \mathbf{0}, \quad \forall t \in [0,T], \quad \forall \psi \in \mathbf{V}.$$

By application of the Rham Theorem [86], we find, for each $t \in [0,T]$, the existence of some function $P(t) \in \mathrm{L}^2_0(\Omega)$ such that

$$\mathbf{v}(t) - \mathbf{v}_0 - \nu \Delta V(t) + R(t) + K(t) + \nabla P = \mathbf{0},$$

where $\mathrm{L}^2_0(\Omega) = \Big\{ w \in \mathrm{L}^2(\Omega), \int_\Omega w \, \mathrm{d}\mathbf{x} = 0 \Big\}$. Therefore, $\nabla P \in C(0,T;\mathrm{H}^{-1}(\Omega))$, thus $P \in C(0,T;\mathrm{L}^2_0(\Omega))$. By derivation with respect to t in the sense of distributions, we obtain

$$\partial_t \mathbf{v} - \nu \Delta \mathbf{v} + (\mathbf{v} \cdot \nabla)\mathbf{v} + Q(\boldsymbol{u})\nabla\phi + \nabla p = \mathbf{0},$$

where $p = \partial_t P \in W^{-1,\infty}(0,T;\mathrm{L}^2_0(\Omega))$.

3.4 Computational analysis

In this section we develop and we propose an asymptotic preserving numerical schemes (AP). In other words, the uniform stability with respect to the parameter ε and the consistence with cross-diffusion-fluid limit. Simultaneously, we reproduce some interesting phenomena such as the formation of patterns induced by cross-diffusion terms, and convection of species caused by the fluid motion. Motivated by the obtained numerical simulation in 1D, we close this section with a various numerical tests in 2D.

3.4.1 A time semi-implicit discretization

Here, we present a time discretization of micro-macro formulation (3.2.11). Let denote by Δt a fixed time step and by $t_k := k\Delta t$ a discrete time where $k \in \mathbb{N}$. The approximations of $g_i(t,x,\xi)$,

$u_i(t,x)$, $\Phi_i(u_i)$, $\mathbf{v}(t,x)$ and $p(t,x)$ at the time step t_k are denoted, respectively, by $g_i^k := g_i(t_k,x,\xi)$, $u_i^k := u_i(t_k,x)$, $\Phi_i^k := \Phi_i(u_i^k)$, $\mathbf{v}^k := \mathbf{v}(t_k,x)$, and $p^k := p(t_k,x)$ for $i = 1,...,n$. We consider the semi-implicit scheme given by

$$\begin{cases} \dfrac{g_i^{k+1}-g_i^k}{\Delta t} + \dfrac{1}{\varepsilon^2}\xi M_i(\xi)\cdot\nabla_x(\Phi_i^k u_i^k) + \dfrac{1}{\varepsilon}(I-P_{M_i})(\xi\cdot\nabla_x(\Phi_i^k g_i^k)) = \dfrac{1}{\varepsilon^2}\mathcal{L}_i(g_i^{k+1}) \\ \quad + \dfrac{1}{\varepsilon^2}\mathcal{T}_i^2[M_1(\xi)u_1^k,...,M_{i-1}(\xi)u_{i-1}^k, M_{i+1}(\xi)u_{i+1}^k,...,M_n(\xi)u_n^k](M_i(\xi)u_i^k) \\ \quad + \dfrac{1}{\varepsilon}\mathcal{T}_1^2[M_1(\xi)u_1^k,...,M_{i-1}(\xi)u_{i-1}^k, M_{i+1}(\xi)u_{i+1}^k,...,M_n(\xi)u_n^k](g_i^k) \\ \quad + \dfrac{1}{\varepsilon^2}G_i^1(M_1(\xi)u_i^k,...,M_n(\xi)u_n^k,\xi,\mathbf{v}^k) + \dfrac{1}{\varepsilon}(I-P_{M_i})G_i^2(M_1(\xi)u_1^k,...,M_n(\xi)u_n^k,\xi,\mathbf{v}^k), \\ \dfrac{u_i^{k+1}-u_i^k}{\Delta t} + \langle\xi\cdot\nabla_x(\Phi_i^k g_i^{k+1})\rangle = \langle G_i^2(M_1(\xi)u_1^{k+1},...,M_{i-1}(\xi)u_i^{k+1}, M_i(\xi)u_i^k,...,M_n(\xi)u_n^k,\xi,\mathbf{v}^k)\rangle, \\ \dfrac{\mathbf{v}^{k+1}-\mathbf{v}^k}{\Delta t} - \nu\Delta\mathbf{v}^{k+1} + \mathbf{v}^{k+1}\cdot\nabla_x\mathbf{v}^k + \nabla_x p^{k+1} + Q(u_1^{k+1},...,u_n^{k+1})\nabla_x\phi = \mathbf{0}, \quad \mathrm{div}_x\,\mathbf{v}^{k+1} = 0. \end{cases} \tag{3.4.1}$$

Proposition 2 *The numerical scheme given by (3.4.1) is consistent with equations (3.2.16) when ε goes to 0.*

Remark 1 *In the micro equations of system (3.4.1), we have considered that only the turning operators $\mathcal{L}_i$ for $i = 1,...,n$ are implicit while other terms are explicit. Indeed, the objective is to ensure the stability as ε goes to 0. We refer the interested reader to [24] for the idea of the proof of Proposition 2.*

3.4.2 Computational analysis 1D

Here, we present our method in one dimension into the domain $[-a,a]$ for fixed $a \in \mathbb{R}_*^+$ by using the finite volume method. Fir this, we denote by $K_j =]x_{j-\frac{1}{2}}, x_{j+\frac{1}{2}}[$ the control volume where $x_j = \frac{1}{2}(x_{j-\frac{1}{2}} + x_{j+\frac{1}{2}})$ and its length is denoted by $h_j = x_{j+\frac{1}{2}} - x_{j-\frac{1}{2}}$ for $j = 1,...,N_x$, (N_x is the total number of cells). For the velocity space, we consider $\xi_\ell = \xi_{\min} + \ell\Delta\xi$ for $\ell = 0,...,N_\xi - 1$ where $\Delta\xi = \frac{1}{N_\xi}(\xi_{\max} - \xi_{\min})$ with $\xi_{\max} = -\xi_{\min}$. Our approach consists to compute the macroscopic densities in K_j while the microscopic quantities are computed on ∂K_j as follow

$$u_i(t_k,x)|_{K_j} \approx u_{i,j}^k, \quad \text{and} \quad g_i(t_k,x_{j+\frac{1}{2}},\xi_\ell)|_{\partial K_j} \approx g_{i,j+\frac{1}{2},\ell}^k, \quad \text{for } i = 1,...,n,\ j = 1,...,N_x,\ \ell = 1,...,N_\xi.$$

The rest terms in (3.2.11) are approximated by $\mathcal{L}_i \approx \mathcal{L}_{i,\ell}$, $M_i(\xi) \approx M_{i,\ell}$, $G_i^1 \approx G_{i,\ell}^1$ and $G_i^2 \approx G_{i,\ell}^2$. We mention that the fluid velocity $\mathbf{v}$ is a function depending only on the time variable t due to the incompressibility condition $\mathrm{div}\,\mathbf{v} = 0$ in 1D. Thus, we shall denote it by $v(t_k) \approx v^k$ in the rest of this section. The full discretization of micro-macro formulation (3.2.11) is given by the following

coupled system

$$\begin{cases} \dfrac{g^{k+1}_{i,j+\frac{1}{2},\ell}-g^{k}_{i,j+\frac{1}{2},\ell}}{\Delta t}+\dfrac{\Phi^k_i}{\varepsilon}(I-P_{M_{i,\ell}})\Big(\xi^+_\ell\dfrac{g^k_{i,j+\frac{1}{2},\ell}-g^k_{i,j-\frac{1}{2},\ell}}{h_j}+\xi^-_\ell\dfrac{g^k_{i,j+\frac{3}{2},\ell}-g^k_{i,j+\frac{1}{2},\ell}}{h_j}\Big) \\ \quad=\dfrac{1}{\varepsilon^2}\Big[\mathcal{L}_{i,\ell}(g^{k+1}_{i,j+\frac{1}{2},\ell})-\Phi^k_i\,\xi_\ell M_{i,\ell}\dfrac{u^k_{i,j+1}-u^k_{i,j}}{h_j}+G^1_{i,\ell}(M_{1,\ell}u^k_{1,j+\frac{1}{2}},...,M_{n,\ell}u^k_{n,j+\frac{1}{2}},\xi_\ell,v^k) \\ \quad+\mathcal{T}^2_{i,\ell}[M_{1,\ell}u^k_{1,j+\frac{1}{2}},...,M_{i-1,\ell}u^k_{i-1,j+\frac{1}{2}},M_{i+1,\ell}u^k_{i+1,j+\frac{1}{2}},...,M_{n,\ell}u^k_{n,j+\frac{1}{2}}](M_{i,\ell}u^k_{i,j+\frac{1}{2}})\Big] \\ \quad+\dfrac{1}{\varepsilon}\Big[\mathcal{T}^2_{i,\ell}[M_{1,\ell}u^k_{1,j+\frac{1}{2}},...,M_{i-1,\ell}u^k_{i-1,j+\frac{1}{2}},M_{i+1,\ell}u^k_{i+1,j+\frac{1}{2}},...,M_{n,\ell}u^k_{n,j+\frac{1}{2}}](g^k_i) \\ \quad+(I-P_{M_{i,\ell}})G^2_{i,\ell}(M_{1,\ell}u^k_{1,j+\frac{1}{2}},...,M_{n,\ell}u^k_{n,j+\frac{1}{2}},\xi_\ell,v^k)\Big], \\ \dfrac{u^{k+1}_{i,j}-u^k_{i,j}}{\Delta t}+\Big\langle\Phi^k_i\xi_\ell\dfrac{g^{k+1}_{i,j+\frac{1}{2},\ell}-g^{k+1}_{i,j-\frac{1}{2},\ell}}{h_j}\Big\rangle=\langle G^2_{i,\ell}(M_{1,\ell}u^k_{1,j},...,M_{i,\ell}u^k_{i,j},...M_{n,\ell}u^k_{n,j},\xi,v^k)\rangle, \\ \dfrac{v^{k+1}-v^k}{\Delta t}+\dfrac{p^{k+1}_{j+1}-p^{k+1}_j}{h_j}+Q(u^{k+1}_{1,j},...,u^{k+1}_{n,j})\dfrac{\phi_{j+1}-\phi_j}{h_j}=0, \end{cases} \tag{3.4.2}$$

for $i=1,...,n$, $j=1,...,N_x$ and $\ell=0,...,N_\xi-1$. The macroscopic quantities in ∂K_j computed as follows $u_{i,j+\frac{1}{2}}=\frac{u_{i,j}+u_{i,j+1}}{2}$ and $u_{i,j-\frac{1}{2}}=\frac{u_{i,j}+u_{i,j-1}}{2}$.
The micro-macro formulation scheme (3.4.2) is consistent with macroscopic system (3.2.16) in the limit thanks to the following proposition:

Proposition 3 *The time and space approximations (3.4.2) of micro-macro formulation (3.2.11) in the limit (ε goes to 0) satisfy the following discretization:*

$$\begin{cases} \dfrac{u^{k+1}_{i,j}-u^k_{i,j}}{\Delta t}+\dfrac{\Phi^k_i}{h_j}\Big\langle\xi_\ell\Big[\mathcal{L}^{-1}_{i,\ell}\Big(\xi_\ell M_{i,\ell}\dfrac{u^k_{i,j+1}-u^k_{i,j}}{h_j}\Big)-\mathcal{L}^{-1}_{1,\ell}\Big(\xi_\ell M_{i,\ell}\dfrac{u^k_{i,j}-u^k_{i,j-1}}{h_j}\Big)\Big]\Big\rangle \\ \quad+\frac{\Phi^k_i}{h_j}\Big\langle\xi_\ell\Big[\mathcal{L}^{-1}_{i,\ell}\Big(\mathcal{T}^2_{i,\ell}[M_{1,\ell}u^k_{1,j},...,M_{i-1,\ell}u^k_{i-1,j},M_{i+1,\ell}u^k_{i+1,j},...,M_{n,\ell}u^k_{n,j}](M_{i,\ell}u^k_{i,j+\frac{1}{2}})\Big) \\ \qquad-\mathcal{L}^{-1}_{i,\ell}\Big(\mathcal{T}^2_{i,\ell}[M_{1,\ell}u^k_{1,j},...,M_{i-1,\ell}u^k_{i-1,j},M_{i+1,\ell}u^k_{i+1,j},...,M_{n,\ell}u^k_{n,j}](M_{i,\ell}u^k_{i,j-\frac{1}{2}})\Big)\Big]\Big\rangle \\ \quad+\frac{\Phi^k_i}{h_j}\Big\langle\xi_\ell\Big[\mathcal{L}^{-1}_{i,\ell}\Big(G^1_{i,\ell}(M_{1,\ell}u^k_{i,j+\frac{1}{2}},...,M_{n,\ell}u^k_{n,j+\frac{1}{2}},v^k,\xi_\ell))\Big) \\ \qquad-\mathcal{L}^{-1}_{i,\ell}\Big(G^1_{i,\ell}(M_{1,\ell}u^k_{i,j-\frac{1}{2}},...,M_{n,\ell}u^k_{n,j-\frac{1}{2}},v^k,\xi_\ell))\Big)\Big]\Big\rangle \\ \qquad=\Big\langle G^j_{i,\ell 2}(M_{1,\ell}u^k_{i,j+\frac{1}{2}},...,M_{n,\ell}u^k_{n,j+\frac{1}{2}},\xi_\ell)\Big\rangle+O(\varepsilon), \\ \dfrac{v^{k+1}-v^k}{\Delta t}+\dfrac{p^{k+1}_{j+1}-p^{k+1}_j}{h_j}+Q(u^{k+1}_{1,j},...,u^{k+1}_{n,j})\dfrac{\phi_{j+1}-\phi_j}{h_j}=0, \end{cases} \tag{3.4.3}$$

for $i=1,...,n$, $j=1,...,N_x$ and $\ell=0,...,N_\xi-1$ is consistent with macroscopic system (3.2.16).

Boundary layers conditions

Here, we deals with the treatment of boundary conditions which is considered as one of the most important problems. For the numerical solution of kinetic-fluid equation (3.2.1), the following inflow boundary conditions are usually prescribed for the distribution functions

$$f_i(t,x_{\min},\xi)=f_{i,l}(\xi),\quad \xi>0 \qquad f_i(t,x_{\max},\xi)=f_{i,r}(\xi),\quad \xi<0,\ \text{for } i=1,...,n. \tag{3.4.4}$$

We define the inflow boundary conditions of the former from those described in (3.4.4) by

$$u_i(t,x_0)M_i(\xi)+\frac{\varepsilon}{2}(g_i(t,x_{\frac{1}{2}},\xi)+g_i(t,x_{-\frac{1}{2}},\xi))=f_{i,l}(\xi),\quad \xi>0, \tag{3.4.5}$$

$$u_i(t,x_{N_x})M_i(\xi)+\frac{\varepsilon}{2}(g_i(t,x_{N_x+\frac{1}{2}},\xi)+g_i(t,x_{N_x-\frac{1}{2}},\xi))=f_{i,r}(\xi),\quad \xi<0, \tag{3.4.6}$$

for $i = 1, ..., n$. For the other velocities, we consider the following artificial Neumann boundary conditions:

$$g_i(t, x_{\frac{1}{2}}, \xi_\ell) = g_i(t, x_{-\frac{1}{2}}, \xi_\ell), \quad \text{if } \xi_\ell < 0, \text{ and } g_i(t, x_{N_x+\frac{1}{2}}, \xi_\ell) = g_i(t, x_{N_x-\frac{1}{2}}, \xi_\ell), \quad \text{if } \xi_\ell > 0,$$

for $i = 1, ..., n$. Furthermore, using Eqs. (3.4.5) and (3.4.6) the ghost points can be computed as follows:

$$g^{k+1}_{i,-\frac{1}{2},\ell} = \begin{cases} \frac{2}{\varepsilon}(f_{1,l}(\xi_\ell) - u^{k+1}_{i,0} M_{i,\ell}) - g^{k+1}_{i,\frac{1}{2},\ell}, & \xi_\ell > 0, \\ g^{k+1}_{i,\frac{1}{2},\ell}, & \xi_\ell < 0; \end{cases} \tag{3.4.7}$$

$$g^{k+1}_{i,N_x+\frac{1}{2},\ell} = \begin{cases} \frac{2}{\varepsilon}(f_{i,r}(\xi_\ell) - u^{k+1}_{i,N_x} M_{i,\ell}) - g^{k+1}_{i,N_x-\frac{1}{2}}, & \xi_\ell < 0, \\ g^{k+1}_{i,N_x-\frac{1}{2},\ell}, & \xi_\ell > 0, \end{cases} \tag{3.4.8}$$

for $i = 1, ..., n$. Finally, using (3.4.2) to obtain for $i = 1, ..., n$

$$\begin{aligned} (1 + \Phi^k_i \tfrac{2\Delta t}{\varepsilon h_0} < \xi^+_\ell M_{i,\ell} >) u^{k+1}_{i,0} &= u^k_{i,0} - \Phi^k_i \tfrac{\Delta t}{h_0} \big\langle (\xi_\ell + \xi^+_\ell - \xi^-_\ell) g^{k+1}_{i,\frac{1}{2},\ell} - \tfrac{2\xi^+_\ell}{\varepsilon} f_{i,l}(\xi_\ell) \big\rangle \\ &\quad + \Delta t \big\langle G^2_{i,\ell}(M_{1,\ell} u^k_{1,0}, ..., M_{n,\ell} u^k_{n,0}) \big\rangle, \\ (1 - \Phi^k_i \tfrac{2\Delta t}{\varepsilon h_{N_x}} < \xi^-_\ell M_{i,\ell} >) u^{k+1}_{i,N_x} &= u^k_{i,N_x} - \Phi^k_i \tfrac{\Delta t}{h_{N_x}} \big\langle \tfrac{2\xi^-_\ell}{\varepsilon} f_{i,r}(\xi_\ell) - (\xi_\ell - \xi^+_\ell + \xi^-_\ell) g^{k+1}_{i,N_x-\frac{1}{2},\ell} \big\rangle \\ &\quad + \Delta t \big\langle G^2_{i,\ell}(M_{1,\ell} u^k_{1,N_x}, ..., M_{n,\ell} u^k_{n,N_x}) \big\rangle. \end{aligned} \tag{3.4.9}$$

Numerical simulations

We provide some numerical simulations to validate the asymptotic preserving scheme property, such as the uniform stability with respect to the parameter ε and the consistence with cross-diffusion-fluid limit. On the other hand, we show a comparison between local and nonlocal diffusion. Furthermore, we demonstrate cross-diffusion and also the fluid flow effects on the interacting species.

In our numerical simulations, we care out two different tests where the velocity space is $V = [-1; 1]$ with the number of grids $N_\xi = 164$ which can provide good enough accuracy for numerical simulations, see [29], and the time step is $\Delta t = 10^{-5}$.

Test 1: Two interacting populations. We investigate the numerical simulations of a system describing the evolution of two competing species living a medium governed by the incompressible Navier-Stokes flow. The aforesaid system can be written as follow

$$\begin{cases} \partial_t u_1 + \mathbf{v} \cdot \nabla_x u_1 - \operatorname{div}_x \left(d_{u_1} (\int_\Omega u_1 dx) \nabla_x u_1 + \mathcal{A}^1_1 \nabla_x u_1 + \mathcal{A}^2_1 \nabla_x u_2 \right) = F_1(u_1, u_2), \\ \partial_t u_2 + \mathbf{v} \cdot \nabla_x u_2 - \operatorname{div}_x \left(d_{u_2} (\int_\Omega u_2 dx) \nabla_x u_2 + \mathcal{A}^1_2 \nabla_x u_1 + \mathcal{A}^2_2 \nabla_x u_2 \right) = F_2(u_1, u_2), \\ \partial_t \mathbf{v} - \nu \Delta \mathbf{v} + (\mathbf{v} \cdot \nabla_x) \mathbf{v} + \nabla_x p + Q(u_1, u_2) \nabla_x \phi = \mathbf{0}, \ \operatorname{div}_x \mathbf{v} = 0. \end{cases} \tag{3.4.10}$$

In model (3.4.10) u_1 and u_2 denote densities of predator and prey, respectively. The cross-diffusion term matrix $\mathcal{A} = (\mathcal{A}^j_i)_{1 \le i,j \le 2}$ is defined by

$$\mathcal{A}(u_1, u_2) = \begin{pmatrix} 2\, a_{11}\, u_1 + a_{12}\, u_2 & a_{12}\, u_1 \\ a_{21}\, u_2 & a_{21}\, u_1 + 2 a_{22}\, u_2 \end{pmatrix}$$

where $a_{ij} > 0$ for $i, j = 1, 2$ is known as self and cross-diffusion rates. It is clear that the above cross-diffusion matrix satisfies condition (3.3.3). The ellipticity condition (3.3.4) is verified if $8 a_{11} a_{21} \ge a^2_{12}$ and $8 a_{22} a_{12} \ge a^2_{21}$, see [24]. We consider the following Lotka-Voltera terms

$$F_1(u_1, u_2) = u_1(a_1 - b_1 u_1 - c_1 u_2), \quad F_2(u_1, u_2) = u_2(a_2 - b_2 u_1 - c_2 u_2),$$

where a_1, a_2, b_1, b_2, c_1 and c_2 are the coefficients of intra- and inter-specific competitions. For the numerical simulations, we consider the following space domain $x = [-2, 2]$ with the number of cells $N_x = 200$ and the periodic boundary condition. Moreover, we adopt a set of parameters, namely the coefficients of intra- and inter-specific competitions, used in [84] (adopted also by [6, 24]): $a_1 = 0.61$, $a_2 = 0.82$, $b_1 = 0.4575$, $b_2 = 0.31$, $c_1 = 9.5$ and $c_2 = 8.2$. Furthermore, we choose $a_{11} = a_{21} = a_{22} = 0.5$ and $a_{12} = 1$ within which cross-diffusion matrix satisfies conditions (3.3.3) and (3.3.4). Finally, the initial densities correspond to the species densities u_1 and u_2 are given by

$$u_{1,0}(x) = 6, \quad u_{2,0}(x) = 3 - \sum_{z=1}^{3} (1 + \exp\left(-50(\sqrt{2(x + x_z)^2} - \sigma_z)\right))^{-1},$$

where $x_1 = 1$, $x_2 = 0.3$, $x_3 = -0.4$, $\sigma_1 = \sigma_3 = 0.25$ and $\sigma_2 = 0.2$. The initial distribution function is as follow $f_{i,0}(x, \xi) = \frac{u_{i,0}(x)}{|V|}$ for $i = 1, 2$. In order to compare local and nonlocal diffusion effects, we consider the choice of local diffusitive functions given by $\Phi_1 = \Phi_2 = 0.01$ and the choice of the following nonlocal diffusitive functions $d_{u_i}(z) = 0.01\, z^2$ for $i = 1, 2$.

In Figures 3.1 and 3.2, we show the obtained numerical simulations of micro-macro formulation scheme of local and nonlocal diffusitive functions with $\varepsilon = 10^{-k}$ where $k \in \{0, 1, 2, 3, 6, 9\}$ against local and nonlocal cross-diffusion macroscopic scheme respectively, at successive times $t = 0,\ 0.001,\ 0.003,\ 0.005,\ 0.007$. First, it is shown that our (AP) scheme is stable along the transition from kinetic to macroscopic regimes in the limit when $\varepsilon \to 0$ which illustrates the result in Proposition 3. Moreover, we can see that our (AP) scheme converges better in time. On the other hand, we observe the formation of patterns induced from the cross-diffusion terms. Finally, we notice that species have the tendency to stay in the crowded zones in the case of local diffusion while they have the tendency to leave crowded zones in case of nonlocal diffusitive functions.

In order to demonstrate the fluid flow effect on predator-prey interactions, we consider the same data as in the case of nonlocal diffusitive functions with a constant fluid velocity $v = 2.5$. Figure 3.3 provides the obtained results for micro-macro against cross-diffusion-fluid schemes at successive time $t = 0.001,\ 0.002,\ 0.003,\ 0.005$. It is shown that our (AP) scheme is stable and converges better in time. Moreover, we observe the previous reproduced phenomenon by the nonlocal cross-diffusion terms and that the two densities are transported in the direction of velocity sign.

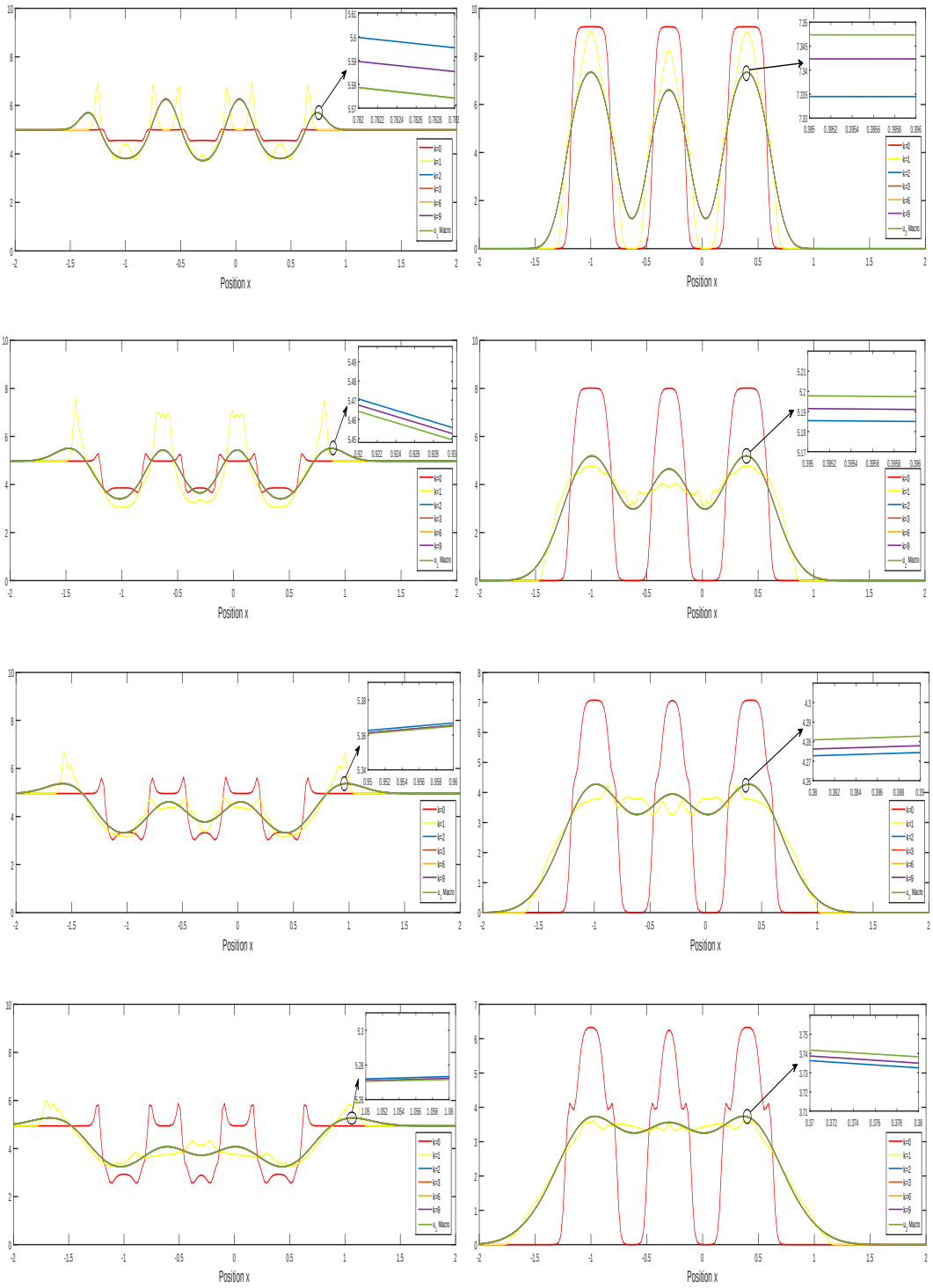

FIGURE 3.1: Test with local diffusitive functions: The first and second columns present, respectively, the dynamics of the densities $u_1(t;x)$ and $u_2(t;x)$ obtained from local micro-macro scheme with $\varepsilon = 10^{-k}$, $k = 0, 1, 2, 3, 6, 9$ against local cross-diffusion scheme with $v = 0$ at $t = 0.001, 0.003, 0.005, 0.007$.

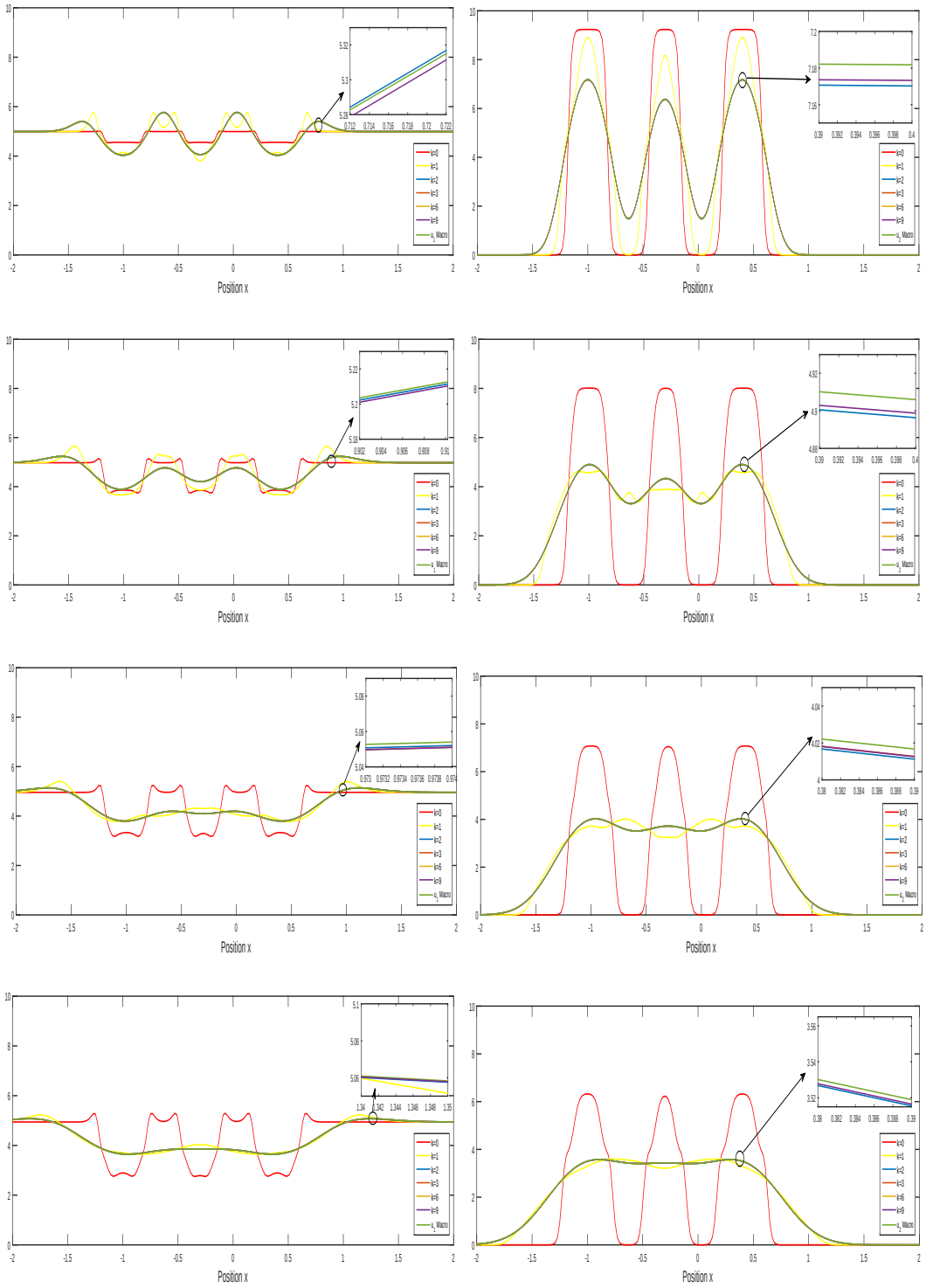

FIGURE 3.2: Test with nonlocal diffusitive functions: The first and second columns present, respectively, the dynamics of the densities $u_1(t;x)$ and $u_2(t;x)$ obtained from nonlocal micro-macro scheme with $\varepsilon = 10^{-k}$, $k = 0, 1, 2, 3, 6, 9$ against nonlocal cross-diffusion scheme with $v = 0$ at successive time
$t = 0.001, 0.003, 0.005, 0.007$.

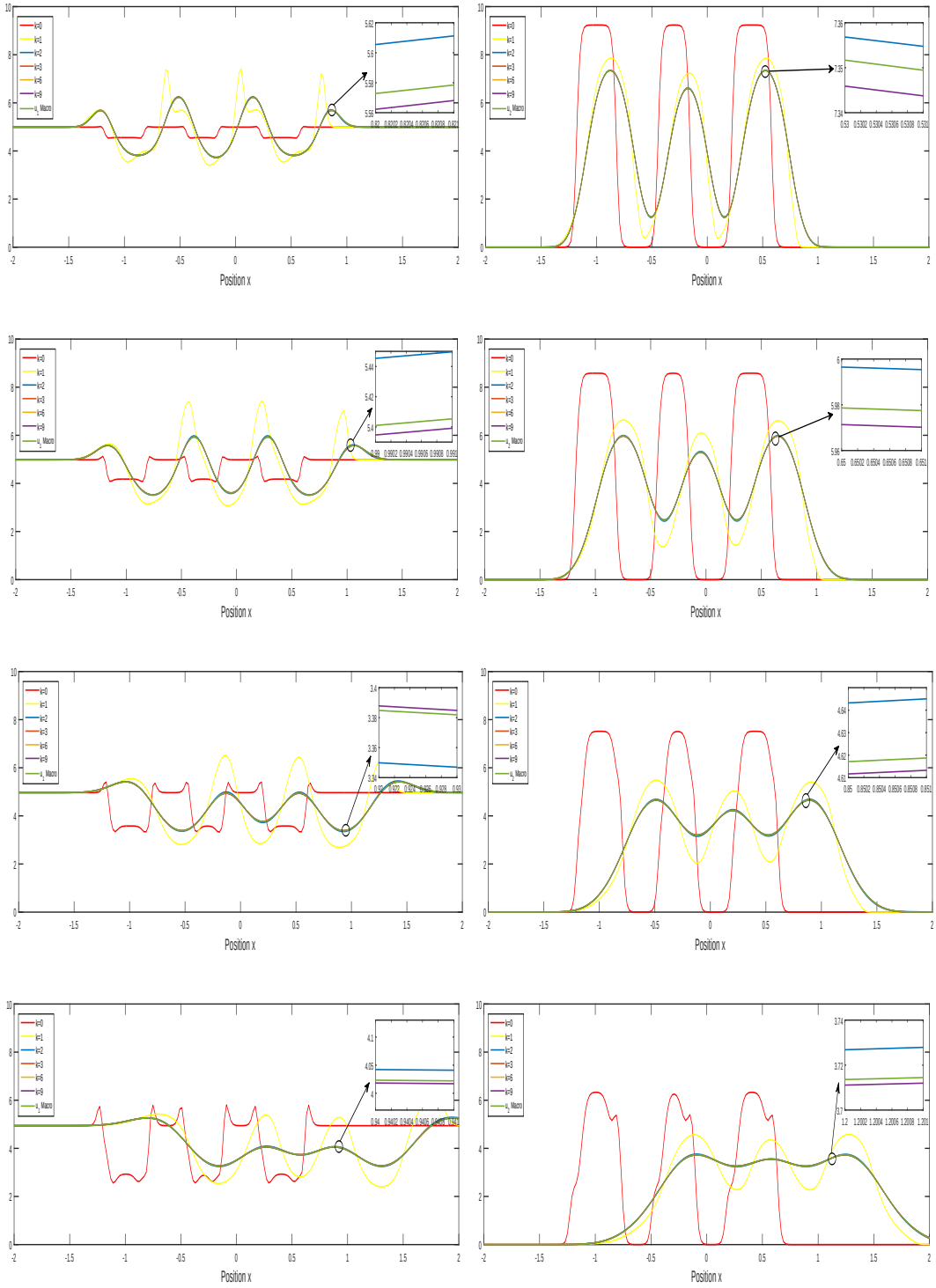

FIGURE 3.3: Test with fluid effect: The first and second columns present, respectively, the dynamics of the densities $u_1(t;x)$ and $u_2(t;x)$ obtained from local micro-macro scheme with $\varepsilon = 10^{-k}$, $k = 0, 1, 2, 3, 6, 9$ against local cross-diffusion-fluid scheme with $v = 2.5$ at successive time $t = 0.001, 0.002, 0.003, 0.005$.

Test 2: Three interacting populations. Here, we investigate the numerical simulations of a system describing the evolution of three interacting populations living in a fluid medium given by

$$\begin{cases} \partial_t u_1 + \mathbf{v}\cdot\nabla_x u_1 - \mathrm{div}_x\left(d_{u_1}(\int_\Omega u_1 dx)\nabla_x u_1 + \mathcal{A}_1^1\nabla_x u_1 + \mathcal{A}_1^2\nabla_x u_2\right) = F_1(u_1,u_2,u_3), \\ \partial_t u_2 + \mathbf{v}\cdot\nabla_x u_2 - \mathrm{div}_x\left(d_{u_2}(\int_\Omega u_2 dx)\nabla_x u_2 + \mathcal{A}_2^1\nabla_x u_1 + \mathcal{A}_2^2\nabla_x u_2 + \mathcal{A}_2^3\nabla u_3\right) = F_2(u_1,u_2,u_3), \\ \partial_t u_3 + \mathbf{v}\cdot\nabla_x u_3 - \mathrm{div}_x\left(d_{u_3}(\int_\Omega u_3 dx)\nabla_x u_3 + \mathcal{A}_3^2\nabla_x u_2 + \mathcal{A}_3^3\nabla_x u_3\right) = F_3(u_1,u_2,u_3), \\ \partial_t \mathbf{v} - \nu\Delta\mathbf{v} + (\mathbf{v}\cdot\nabla_x)\mathbf{v} + \nabla_x p + Q(u_1,u_2,u_3)\nabla_x\phi = \mathbf{0}, \ \ \mathrm{div}_x\,\mathbf{v} = 0, \end{cases} \tag{3.4.11}$$

where $u_1(t,x)$ is the population density of the species at the lowest level of the food chain (preys), $u_2(t,x)$ is the population density of the species that preys upon u_1 (predator), and $u_3(t,x)$ is the population density of the species that preys upon u_2 (superpredator). the cross-diffusion matrix $\mathcal{A} = (\mathcal{A}_i^j)_{1\le i,j\le 3}$ is defined as in [4]

$$\mathcal{A}(u_1,u_2,u_3) = \begin{pmatrix} \alpha_1 u_1 + u_2 & u_1 & 0 \\ u_2 & u_1 + \alpha_2 u_2 + u_3 & u_2 \\ 0 & u_3 & u_2 + \alpha_3 u_3 \end{pmatrix}$$

where $\alpha_1,\ \alpha_2, \alpha_3 > 0$ is known as self-diffusion rates. Note that the above cross-diffusion matrix $\mathcal{A}$ is uniformly nonnegative under the following conditions: $\alpha_1 > \frac{1}{2},\ \alpha_2 > 1$ and $\alpha_3 > \frac{1}{2}$, see [4]. The reaction terms take a nonlinear forms [55] as follows

$$\begin{cases} F_1(u_1,u_2,u_3) = (1-u_1)u_1 - \frac{a_1 u_1}{1+b_1 u_1}u_2, \\ F_2(u_1,u_2,u_3) = \frac{a_1 u_1}{1+b_1 u_1}u_2 - \frac{a_2 u_2}{1+b_2 u_2}u_3 - c_1 u_2, \\ F_3(u_1,u_2,u_3) = \frac{a_2 u_2}{1+b_2 u_2}u_3 - c_2 u_3, \end{cases} \tag{3.4.12}$$

where $a_1,\ a_2,\ b_1,\ b_2,\ c_1$ and c_2 are the coefficients of intra- and inter-specific competition. In our numerical simulations, we adopt the following set of parameters: $a_1 = a_2 = 80$, $b_1 = b_2 = 2$, $c_1 = 0.4$ and $c_2 = 0.01$. The cross-diffusion parameters are given by $\alpha_1 = 1,\ \alpha_2 = \alpha_3 = 1.5$. Finally, the nonlocal diffusion terms are given by $d_{u_i}(z) = d_i z$, for $i = 1,2,3$, where $d_1 = 0.1,\ d_2 = d_3 = 0.01$. The initial densities correspond to u_1, u_2 and u_3 are given by

$$u_{1,0}(x) = 3, \quad u_{2,0}(x) = 1 - \sum_{z=1}^{2}(1 + \exp\left(-50(\sqrt{2(x+x_z)^2} - \sigma_z)\right))^{-1}, \quad u_{3,0}(x) = 1,$$

where $x_1 = 0.25$, $x_2 = -0.25$, and $\sigma_1 = \sigma_2 = 0.18$,. The initial distribution function is as follow

$$f_{i,0}(x,\xi) = \frac{u_{i,0}(x)}{|V|} \quad i = 1,2,3.$$

In Figure 3.4, we present the obtained numerical results for three interacting species from micro-macro scheme against cross-diffusion scheme at successive time $t = 0.001,\ 0.005,\ 0.01,\ 0.06$. We observe that the densities u_1, u_2 and u_3 obtained from the two schemes have almost the same profiles in the limit when the mean free path $\varepsilon = 10^{-k}$, with $k = 0,1,2,3,6,9$, tend to zeros. This confirm that our (AP) scheme is uniformly stable along the transition from kinetic regime to macroscopic one. Moreover, we can see that our (AP) scheme converges better in time. On the other hand, we observe the effect of the nonlocal diffusion and of the cross-diffusion terms on the dynamic of the three populations. Specifically, superpredators moves toward the zones occupied by predators at the same time predators spread out to the areas where preys are located.

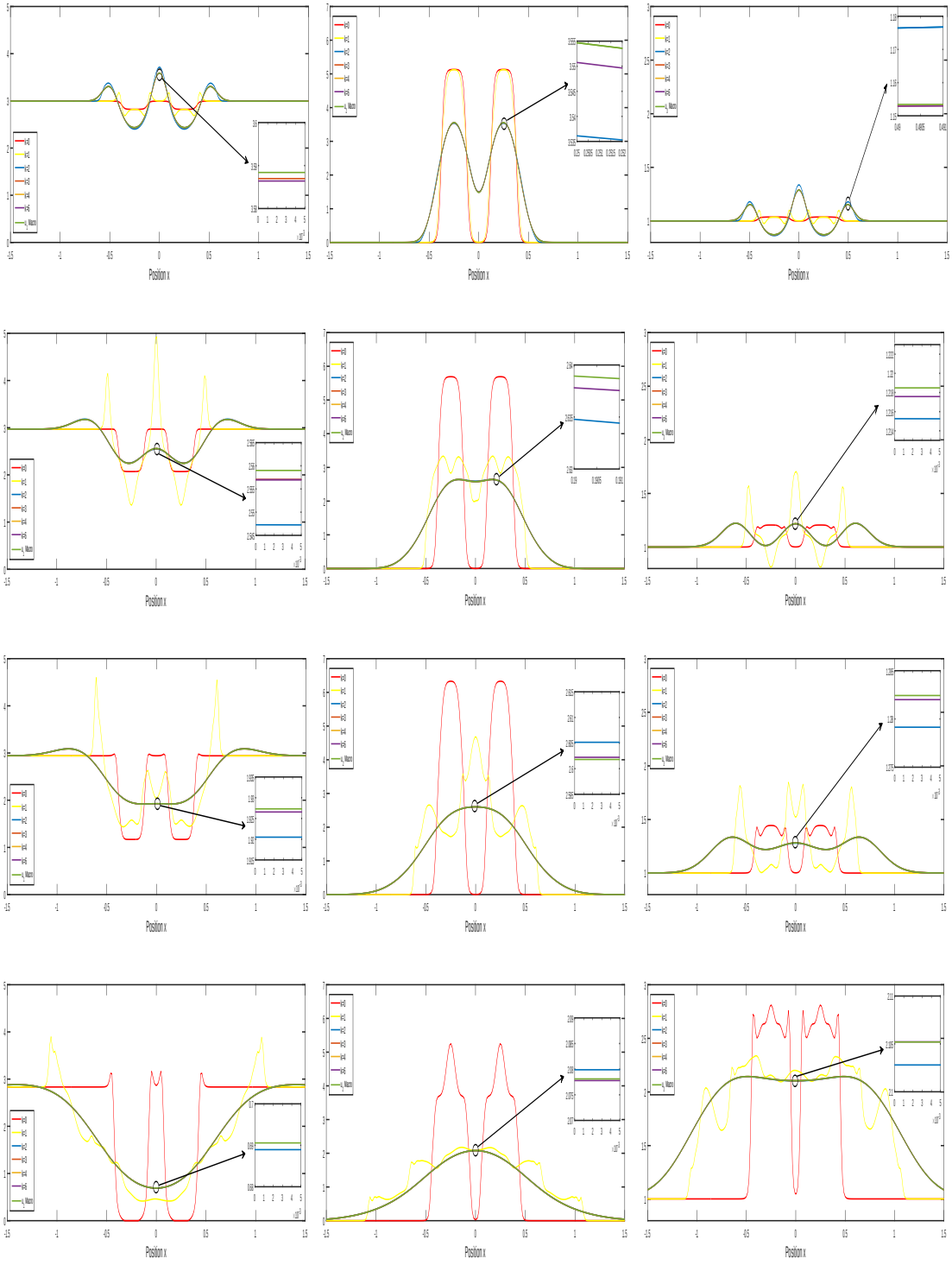

FIGURE 3.4: From left to right column, the obtained numerical solutions of u_1, u_2, u_3 from the nonlocal (AP) scheme with $\varepsilon = 10^{-k}$, $k = 0, 1, 2, 3, 6, 9$, against of the nonlocal cross-diffusion model with $v = 0$ at successive time $t = 0.001, 0.005, 0.01, 0.06$.

3.4.3 Computational analysis 2D

Motivated by the obtained numerical simulation in 1D, here we investigate two dimensions computational analysis of nonlocal cross-diffusion-fluid system (3.1.1) for three interacting populations. First, we numerically demonstrate the effect of nonlocal diffusion together with cross-diffusion, as well as fluid flow in an explicit form of the fluid velocity on the interactions of populations by using finite volume method. Secondly, we show the effect of external forces (obstacle interior de domain and the force of gravity) on the dynamic of fluid flow and simultaneously on the behavior of interacting populations by using finite element method.

Effect of the nonlocal cross-diffusion-fluid

We show the effect of nonlocal cross-diffusion and fluid flow in an explicit form of the fluid velocity on the distribution of the interacting populations. The system under consideration is written as follows implemented with initial and boundary conditions

$$\begin{cases} \partial_t u_1 + \mathbf{v}\cdot\nabla_x u_1 - \operatorname{div}_x\Big(d_{u_1}(\int_\Omega u_1 dx)\nabla_x u_1 + \mathcal{A}_1^1\nabla_x u_1 + \mathcal{A}_1^2\nabla_x u_2\Big) = F_1, & \text{in } \Omega_T,\\ \partial_t u_2 + \mathbf{v}\cdot\nabla_x u_2 - \operatorname{div}_x\Big(d_{u_2}(\int_\Omega u_2 dx)\nabla_x u_2 + \mathcal{A}_2^1\nabla_x u_1 + \mathcal{A}_2^2\nabla_x u_2 + \mathcal{A}_2^3\nabla_x u_3\Big) = F_2, & \text{in } \Omega_T,\\ \partial_t u_3 + \mathbf{v}\cdot\nabla_x u_3 - \operatorname{div}_x\Big(d_{u_3}(\int_\Omega u_3 dx)\nabla_x u_3 \mathcal{A}_3^2\nabla_x u_2 + \mathcal{A}_3^3\nabla_x u_3\Big) = F_3, & \text{in } \Omega_T,\\ \mathbf{v}(0,x) = \mathbf{v}_0, \quad u_1(0,x) = u_{1,0}, \quad u_2(0,x) = u_{1,0}, \quad u_3(0,x) = u_{3,0}, & \text{in } \Omega,\\ \dfrac{\partial u_1}{\partial \eta} = \dfrac{\partial u_2}{\partial \eta} = \dfrac{\partial u_3}{\partial \eta} = 0, \quad \mathbf{v} = \mathbf{0}, & \text{on } \Sigma_T. \end{cases} \tag{3.4.13}$$

In order to solve numerically system (3.4.13), we adopt the finite volume method in 2D. For that, we consider a family $\mathfrak{T}_h$ of admissible meshes of the domain Ω consisting of disjoint open and convex polygons called control volumes, see [46]. In the rest of this subsection, we shall use the following notation: the parameter h is the maximum diameter of the control volumes in $\mathfrak{T}_h$. K is a generic volume in $\mathfrak{T}$, $|K|$is the 2-dimensional Lebesgue measure of K and $N(K)$ is the set of the neighbors of K. Moreover, for all $L \in N(K)$, we denote by $\sigma_{K,L}$ the interface between K and L where L is a generic neighbor of K. $\eta_{K,L}$ is the unit normal vector to $\sigma_{K,L}$ outward to K. For an interface $\sigma_{K,L}$, $|\sigma_{K,L}|$ will denote its 1-dimensional measure. $d_{K,L}$ denote the distance between x_K and x_L, where the points x_K and x_L are respectively the center of K and L. On the other hand, we assume that a discrete function on the mesh $\mathfrak{T}_h$ is a set $(w_K)_K \in \mathfrak{T}$ and we identify it with the piecewise constant function w_h on Ω such that $w_h \ |_K = w_K$. Furthermore, we consider an admissible discretization of $(0,T)\times\Omega$ consisting of an admissible mesh $\mathfrak{T}_h$ of Ω and of a time step size $\Delta t_h > 0$ (both Δt_h and the size $\max_{K\in t_h} diam(K)$ tend to zero as $h \to 0$). Next, we define the discrete gradient $\nabla_h w_h$ as the constant per diamond $T_{K,L}$ function by

$$\Big(\nabla_h w_h\Big)|_{\mathfrak{T}_{K,L}} = \nabla_{K,L} w_h := \frac{w_L - w_K}{d_{K,L}}\eta_{K,L}.$$

Finally, we define the average of source terms $F_{i,K}^{n+1}$ by $F_{i,K}^{n+1} = F_i(u_1(t^n,x), u_2(t^n,x), u_3(t^n,x))$, for $i = 1,2,3$. And we make the following choice to approximate the diffuse terms $\mathcal{A}_{i,K,L}^{j,n+1}$

$$\mathcal{A}_{i,K,L}^{j,n+1} = \mathcal{A}\big(\min\{u_{1,K}^{n+1^+}, u_{1,L}^{n+1^+}\}, \min\{u_{2,K}^{n+1^+}, u_{2,L}^{n+1^+}, \min\{u_{3,K}^{n+1^+}, u_{3,L}^{n+1^+}\}\big),$$

where $u_{i,J}^{n+1^+} = \max(0, u_{i,J}^{n+1})$ for $i = 1,2,3$ and $J = K, L$. The computation starts from the initial cell averages $u_{i,0}^K = \frac{1}{|K|}\int_K u_{i,0}(x)\,dx$ for $i = 1,2,3$. In order to advance the numerical solution from t^n to $t^{n+1} = t^n + \Delta t$, we use the following implicit finite volume scheme: determine $u_{i,K}^{n+1}$ for

$K \in \mathfrak{T}$, $i = 1,2,3$ such that

$$
\begin{aligned}
&|K|\tfrac{u_{1,K}^{n+1}-u_{1,K}^{n}}{\Delta t} + \sum_{L\in N(K)} G(u_{1,K}^{n+1}, u_{1,L}^{n+1}; \mathbf{v}_{K,L}^{n+1}) - d_{u_1}\Big(\sum_{K_0\in\mathfrak{T}_h} m(K_0)u_{1,K_0}^{n}\Big)\sum_{L\in N(K)} \tfrac{|\sigma_{K,L}|}{d_{K,L}}(u_{1,L}^{n+1}-u_{1,K}^{n+1}) \\
&\quad - \sum_{L\in N(K)} \tfrac{|\sigma_{K,L}|}{d_{K,L}}\Big[\mathcal{A}_{1,K,L}^{1,n+1}(u_{1,L}^{n+1}-u_{1,K}^{n+1}) + \mathcal{A}_{1,K,L}^{2,n+1}(u_{2,L}^{n+1}-u_{2,K}^{n+1})\Big] = |K|F_{1,K}^{n+1}, \\
&|K|\tfrac{u_{2,K}^{n+1}-u_{2,K}^{n}}{\Delta t} + \sum_{L\in N(K)} G(u_{2,K}^{n+1}, u_{2,L}^{n+1}; \mathbf{v}_{K,L}^{n+1}) - d_{u_2}\Big(\sum_{K_0\in\mathfrak{T}_h} m(K_0)u_{2,K_0}^{n}\Big)\sum_{L\in N(K)} \tfrac{|\sigma_{K,L}|}{d_{K,L}}(u_{2,L}^{n+1}-u_{2,K}^{n+1}) \\
&\quad - \sum_{L\in N(K)} \tfrac{|\sigma_{K,L}|}{d_{K,L}}\Big[\mathcal{A}_{2,K,L}^{1,n+1}(u_{1,L}^{n+1}-u_{1,K}^{n+1}) + \mathcal{A}_{2,K,L}^{2,n+1}(u_{2,L}^{n+1}-u_{2,K}^{n+1}) + \mathcal{A}_{2,K,L}^{3,n+1}(u_{3,L}^{n+1}-u_{3,K}^{n+1})\Big] = |K|F_{2,K}^{n+1}, \\
&|K|\tfrac{u_{3,K}^{n+1}-u_{3,K}^{n}}{\Delta t} + \sum_{L\in N(K)} G(u_{3,K}^{n+1}, u_{3,L}^{n+1}; \mathbf{v}_{K,L}^{n+1}) - d_{u_3}\Big(\sum_{K_0\in\mathfrak{T}_h} m(K_0)u_{3,K_0}^{n}\Big)\sum_{L\in N(K)} \tfrac{|\sigma_{K,L}|}{d_{K,L}}(u_{3,L}^{n+1}-u_{3,K}^{n+1}) \\
&\quad - \sum_{L\in N(K)} \tfrac{|\sigma_{K,L}|}{d_{K,L}}\Big[\mathcal{A}_{3,K,L}^{2,n+1}(u_{2,L}^{n+1}-u_{2,K}^{n+1}) + \mathcal{A}_{3,K,L}^{3,n+1}(u_{3,L}^{n+1}-u_{3,K}^{n+1})\Big] = |K|F_{3,K}^{n+1},
\end{aligned}
\tag{3.4.14}
$$

for all $K \in \mathfrak{T}_h$, $n \in N_h$. The convective flux G is given by $G(w_K, w_L; \mathbf{v}_{K,L}) = \mathbf{v}_{K,L}^{+} w_K - \mathbf{v}_{K,L}^{-} w_L$ where $\mathbf{v}_{K,L}^{+}$ and $\mathbf{v}_{K,L}^{-}$ are positive and negative parts of $\mathbf{v}_{K,L}$, respectively. We take into account implicitly the homogeneous Neumann boundary condition. If $\mathbf{v}_{K,L} = 0$, we refer the reader to [6, 4] for more details. To solve the corresponding nonlinear system arising from the implicit finite volume scheme (3.4.14), we have used the Newton method. We mention that the linear systems involved in Newton's method are solved by the GMRES method.

In the next two tests, the initial densities u_1 and u_3 correspond to a constants $u_{1,0} = 0.75$, $u_{3,0} = 0.215$, while the initial density $u_{2,0}$ is concentrated in small pockets at two spatial points. The spatial domain corresponds to a simple square $\Omega = (-1,1)\times(-1,1)$ and uniform mesh is given by a Cartesian grid $N_x = N_y = 128$. Finally, we consider the same reaction terms F_i in (3.4.12) with a different choice of the coefficients $a_1 = 10$, $a_2 = 0.1$, $b_1 = b_2 = 2$, $c_1 = 0.4$ and $c_2 = 0.01$.

Test 1: the nonlocal cross-diffusion effect. Here, we are interested to show the effect of nonlocal cross-diffusion on the distributions of interacting populations. For that, we consider that they are depending linearly on the whole of each population in the domain. Specifically, the nonlocal functions are given by $d_{u_1}(z) = 0,1z$ and $d_{u_2}(z) = d_{u_3}(z) = 0.01z$, for all $z \in \mathbb{R}^+$. The cross-diffusion parameters are chosen as follows $\alpha_1 = 10$, $\alpha_2 = \alpha_3 = 1.5$, and the fluid velocity is neglected ($\mathbf{v} = \mathbf{0}$). Figure 3.5 provides the obtained numerical simulations of the three densities u_1, u_2, and u_3 at successive times $t = 0$, 0.2, 0.4, 0.6. Initially, we observe the effect of the nonlocal diffusion over the behavior of population and also the rapid movement of superpredators towards the regions occupied by predators. Moreover, we can see that predators spread out to the regions where preys are located. On the other hand, in order to well demonstrate the sensitivity with respect to the cross-diffusion matrix $\mathcal{A}_i^j$ for $i,j = 1,2,3$, on the behavior of three interacting populations, we consider different values of the cross-diffusion parameters α_1, α_2 and α_3.

Figure 3.6 shows the obtained numerical simulations for $T = 0.05$ with different values of α_i, $i = 1,2,3$. It is shown that the distribution of interacting populations and the spatial patterns are changing whenever we made different choices of cross-diffusion parameters.

Test 2: the nonlocal cross-diffusion-fluid effect. The objective of this test is to demonstrate the fluid effect on the interacting populations. For this, we consider sample choice of the fluid velocity $\mathbf{v}(x,y) = (1-x)(1+x)(1-y)(1+y)$. The made choice of the velocity fluid has a purpose to satisfy the theoretical assumption on it. We adopt the following set of parameters $\alpha_1 = 10$, $\alpha_2 = \alpha_3 = 1.5$ and the diffusitive functions d_{u_i} for $i = 1,2,3$ are chosen as in the first case in Test 1.

Figure 3.7 shows the influence of interacting populations in the presence of fluid flow. Moreover, it is clearly seen the effect of diffusion over the three populations.

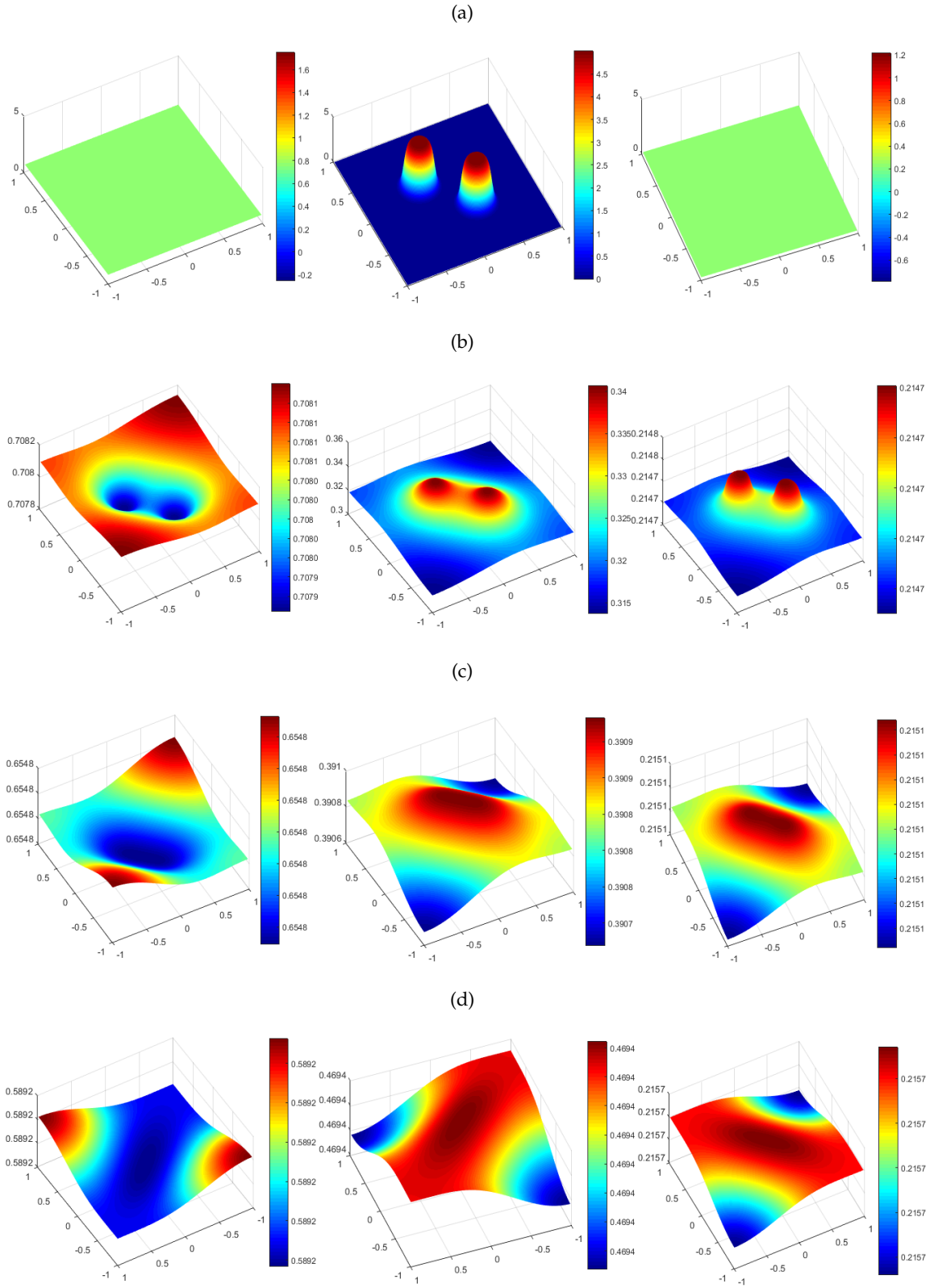

FIGURE 3.5: Test 1: snapshot of the three densities u_1, u_2 and u_3 at successive time $t = 0, 0.2, 0.4, 0.6$ with $\mathbf{v} = \mathbf{0}$.

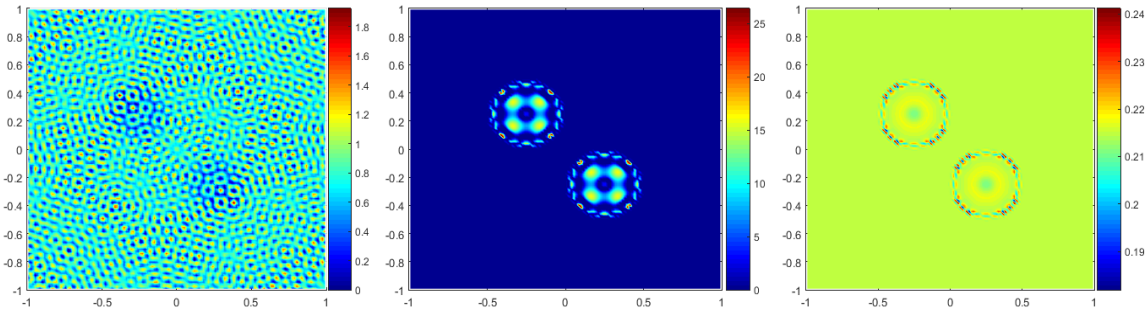

$\alpha_1 = 50,\ \alpha_2 = 50,\ \alpha_3 = 10$

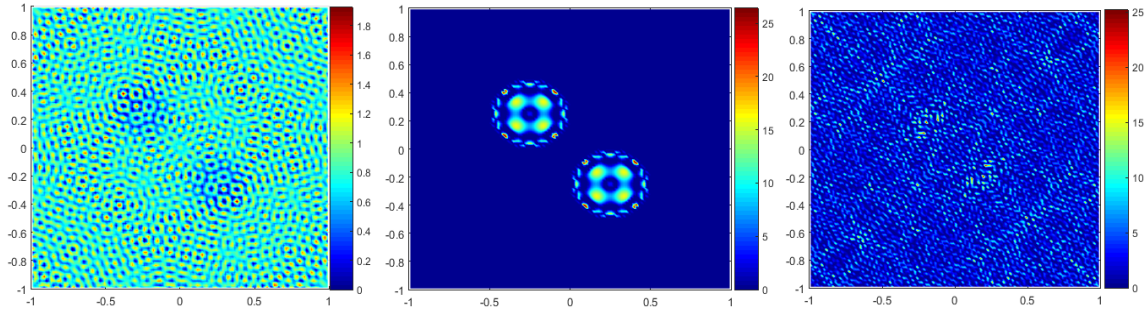

$\alpha_1 = 50,\ \alpha_2 = 50,\ \alpha_3 = 100$

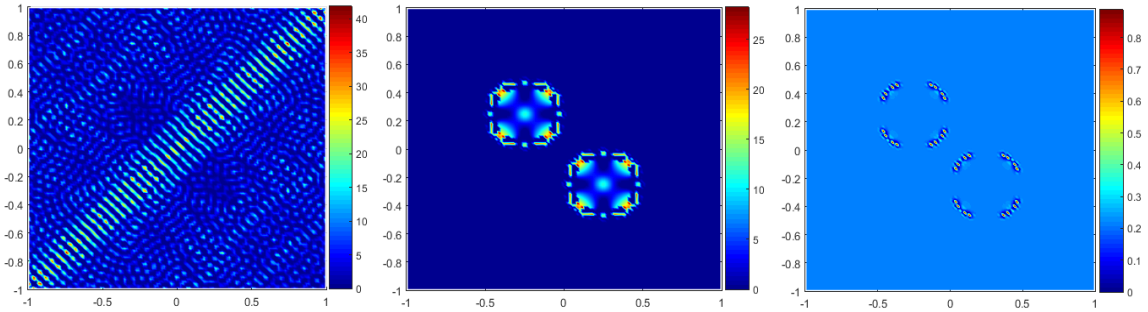

$\alpha_1 = 50,\ \alpha_2 = 100,\ \alpha_3 = 10$

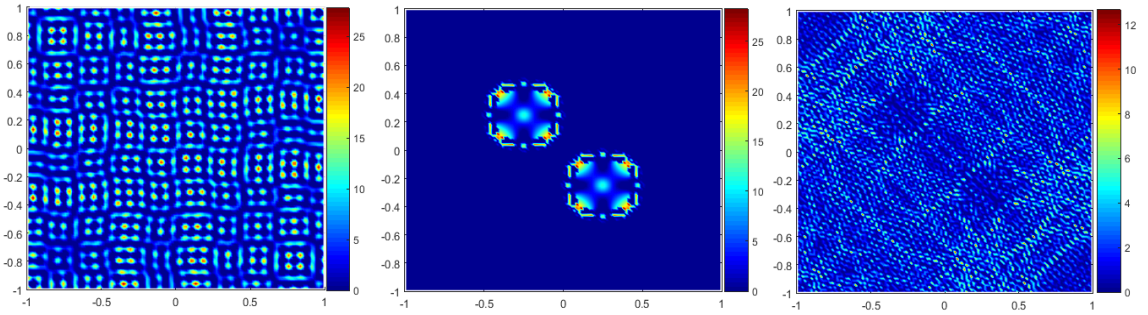

$\alpha_1 = 100,\ \alpha_2 = 100,\ \alpha_3 = 100$

FIGURE 3.6: Cross-diffusion effect: patterns of the three interacting populations with different cross-diffusion parameters at final time $t = 0.1$.

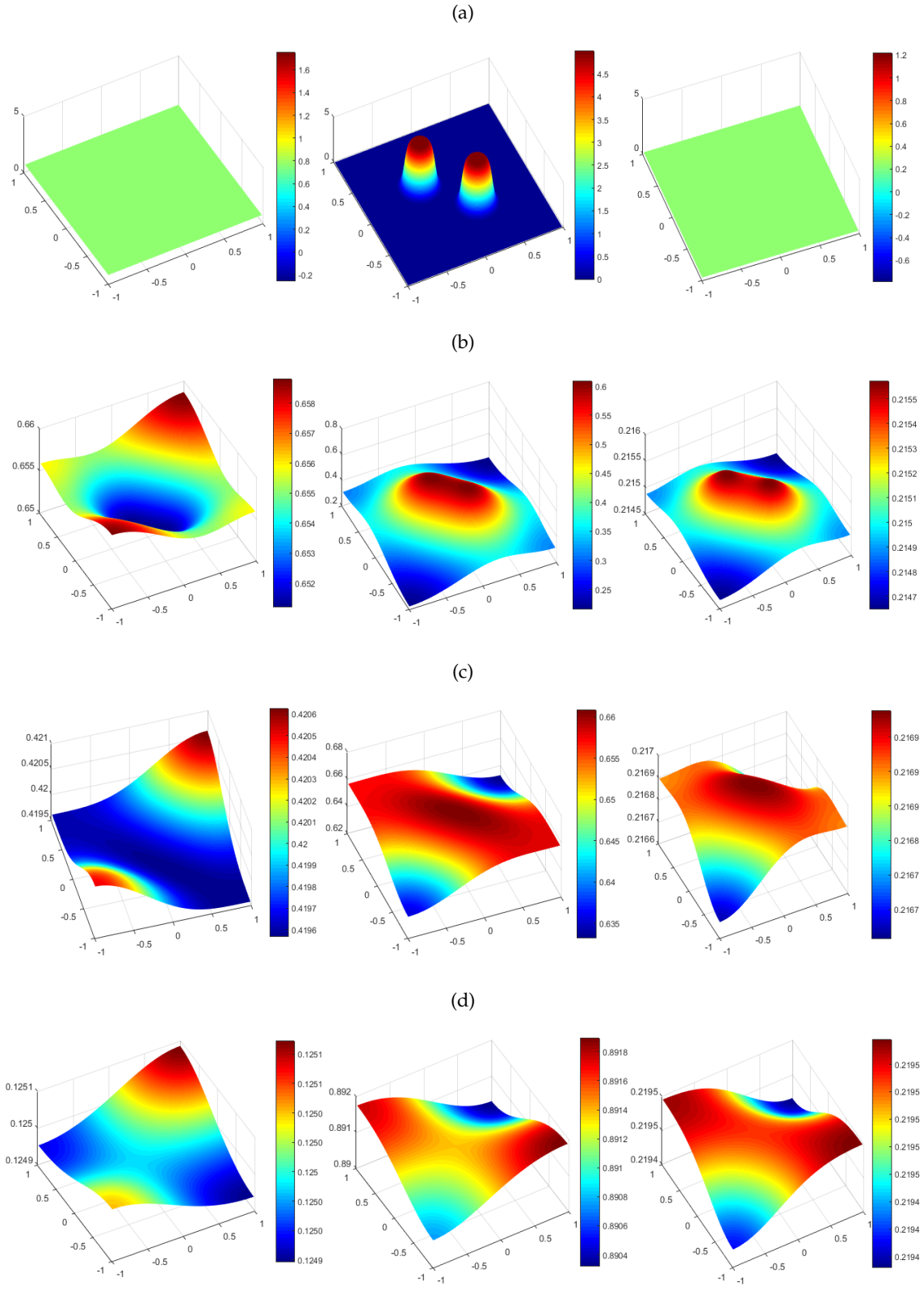

FIGURE 3.7: Test 2: snapshot of the three densities u_1, u_2 and u_3 at successive time $t = 0, 0.2, 0.4, 0.6$ with $\mathbf{v}(x, y) = (1 - x)(1 + x)(1 - y)(1 + y)$.

Effect of external forces on the fluid dynamic and on the distribution of populations

After showing the nonlocal cross-diffusion-fluid effects on the three interacting populations. Here, conversely we are interested to demonstrate the effect of gravity as an external forces on the fluid dynamic and on the behavior of the interacting populations. Moreover, we consider a spatial domain within obstacle. Thus, we are interested to solve numerically the following system implemented with initial and boundary conditions

$$\begin{cases} \partial_t \mathbf{v} - \nu\Delta\mathbf{v} + (\mathbf{v}\cdot\nabla)\mathbf{v} + \nabla p + \rho\,\nabla\phi = \mathbf{0}, \quad \operatorname{div}\mathbf{v} = 0, & \text{in } \Omega_T,\\ \partial_t u_1 + \mathbf{v}\cdot\nabla u_1 - \operatorname{div}\left(d_{u_1}\left(\int_\Omega u_1\,d\mathbf{x}\right)\nabla u_1\right) = \mu_1\,u_1(1-\rho) - \mu_2\,u_1\,u_2, & \text{in } \Omega_T,\\ \partial_t u_2 + \mathbf{v}\cdot\nabla u_2 - \operatorname{div}\left(d_{u_2}\left(\int_\Omega u_2\,d\mathbf{x}\right)\nabla u_2\right) = \mu_1\,u_2(1-\rho) - \mu_2\,u_2\,u_1, & \text{in } \Omega_T,\\ \partial_t u_3 + \mathbf{v}\cdot\nabla u_3 - \operatorname{div}\left(d_{u_3}\left(\int_\Omega u_3\,d\mathbf{x}\right)\nabla u_3\right) = \mu_1\,u_3(1-\rho) - \mu_2\,u_3\,u_2, & \text{in } \Omega_T,\\ \mathbf{v}(0,\mathbf{x}) = \mathbf{v}_0, \quad u_1(0,\mathbf{x}) = u_{1,0}, \quad u_2(0,\mathbf{x}) = u_{2,0}, \quad u_3(0,\mathbf{x}) = u_{3,0}, & \text{in } \Omega,\\ \dfrac{\partial u_1}{\partial\eta} = \dfrac{\partial u_2}{\partial\eta} = \dfrac{\partial u_3}{\partial\eta} = 0, & \text{on } \Gamma_1\cup\Gamma_2\cup\Gamma_3\cup\Gamma_4,\\ u_1 = u_2 = u_3 = 0, \quad \mathbf{v}(x,y) = (0,0)^T, & \text{on } \Gamma_5,\\ \mathbf{v}(x,y) = \left(\dfrac{\partial v}{\partial\eta} = 0\,,\,0\right)^T, & \text{on } \Gamma_1\cup\Gamma_3,\\ \mathbf{v}(x,y) = \left(0,\,\dfrac{\partial v}{\partial\eta} = 0\right)^T, & \text{on } \Gamma_2,\\ \mathbf{v}(x,y) = (4\,y\,(1-y),\,0)^T, & \text{on } \Gamma_4, \end{cases} \tag{3.4.15}$$

where μ_1 and μ_2 are the selection and reproduction rates, respectively and $\rho = u_1 + u_2 + u_3$ is the total population density, see [53] for more details about the modeling of used reaction terms. The spatial domain Ω corresponds to a rectangle $(0,12)\times(0,5)$ and contains an obstacle, see Figure 3.8.

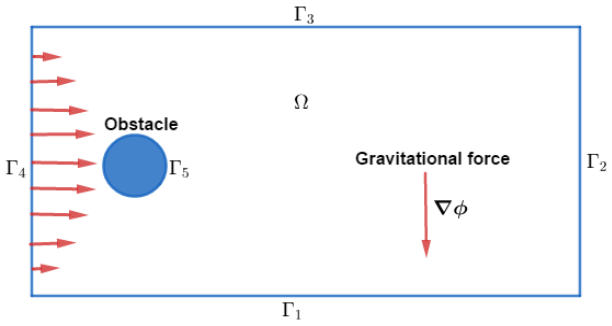

FIGURE 3.8: Schematic of the spatial domain Ω with boundary conditions.

Here, all computations have been implemented using the software package FreeFem++ [56]. The code uses a finite element method based on the weak formulation of the reaction diffusion system (3.4.15) in an iterative manner as follows

1) Solve Navier-Stokes equations $(3.4.15)_1$ and the incompressibility condition $(3.4.15)_2$ with the Characteristic Galerkin method. We mention that we have used a classical Taylor-Hood element technic, i.e. the fluid velocity $\mathbf{v}$ is approximated by P_2 finite elements and the pressure p is approximated by P_1 finite elements.

2) Approximate the densities u_1, u_2 and u_3 by P_2 finite elements and solve firstly equation $(3.4.15)_3$, then $(3.4.15)_4$ and finally $(3.4.15)_5$. We mention that have used UMFPACK package and θ-scheme with $\theta = 0.49$.

In all simulations bellow, we consider the following initial conditions:

$$u_{i,0} = 2.5\,\delta_i + 0.25, \quad i = 1,2,3, \quad \mathbf{v}_0 = (0,\,0)^T,$$

where δ_i is a random function for $i = 1, 2, 3$. The nonlocal diffusion terms and the fluid viscosity are chosen as follows $d_{u_1}(z) = 0.1\,z$, $d_{u_2}(z) = d_{u_3}(z) = 0.01\,z$ for all $z \in \mathbb{R}$ and $\nu = 10^{-3}$.

We recall that $\nabla\phi = V_s(\rho_s - \rho_f)\,g\,\overrightarrow{z}$ where V_s and ρ_s are, respectively, the volume and the density of populations, ρ_f is the fluid density and g is the gravitational force. In fact, the vector $-\nabla\phi$ is the resultant of gravity forces ($\overrightarrow{P} = -\rho_s V_s\, g\,\overrightarrow{z}$) and the Archimedes thrust ($\overrightarrow{F_a} = \rho_f V_s\, g\,\overrightarrow{z}$). In our tests, the populations are denser than the fluid and therefore a gravitational flow is created in the direction of the vector $-\overrightarrow{z}$. Herein, we investigate two different cases:

Case 1: absence of the gravitational force. In the first place, we illustrate the behavior of the nonlocal reaction-diffusion-fluid system (3.4.15) without the force gravity, i.e $\nabla_x\phi = (0, 0)$.

Figure 3.9 shows the obtained numerical simulations of the three interacting populations densities u_1, u_2 and u_3, and the dynamic of the fluid flow presented by the fluid velocity $\mathbf{v}$ and the pressure p. It's clear that populations are transported in the direction of the fluid. On the other hand, we observe that the fluid flow is not influenced by the presence of the populations in the medium. However, it is affected by the presence of the obstacle in the domain.

Case 2: the presence of gravitational force. In the second place, we illustrate the behavior of the nonlocal reaction-diffusion-fluid system (3.4.15) with the presence of the gravity force, i.e $\nabla_x\phi \neq (0, 0)$. Thus, we obtain the strong coupling system (3.4.15).

In Figure 3.10, we show the numerical simulations of the three densities u_1, u_2 and u_3 and the dynamic of the fluid flow. Clearly, we observe that the three interacting populations and the fluid are influenced by the presence of the gravitational force. We observe also the effect of the presence of the obstacle.

3.5 Conclusion

In this chapter, we have proposed a nonlocal cross-diffusion-fluid model for multi-interacting populations. The proposed model has been derived from a nonlocal kinetic-fluid model by using the micro-macro decomposition technic. Next, we have proved the existence of weak solutions for the proposed model by nonlinear Galerkin method. It has been shown that our proposed (AP) schemes are uniformly stable along the transition from kinetic to macroscopic regimes. At the same time, we have demonstrated the nonlocal diffusion, cross-diffusion and the fluid effects on two and three interacting populations. Finally, inspired by the obtained numerical simulation in 1D, we have provided various numerical simulations in 2D.

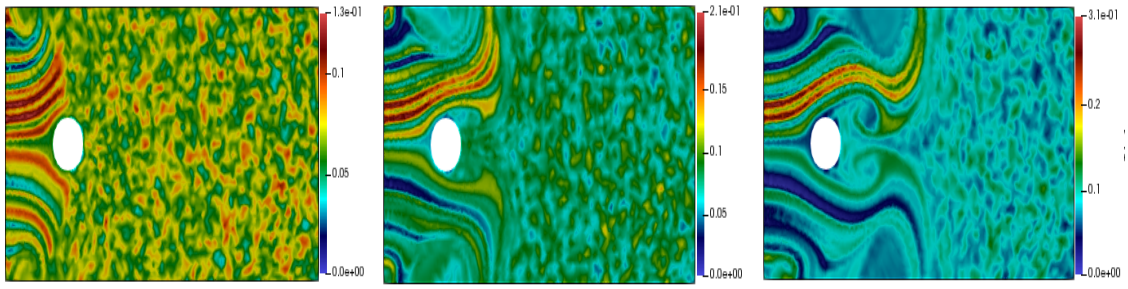

Evolution of the density u_1 at successive time $t = 5, 10, 15$.

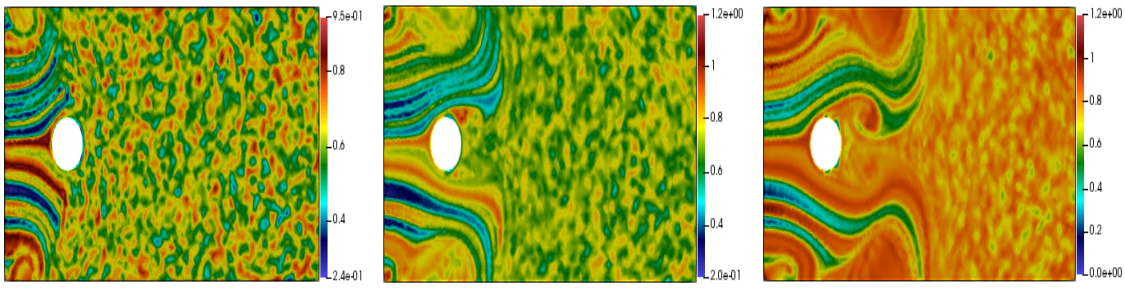

Evolution of the density u_2 at successive time $t = 5, 10, 15$.

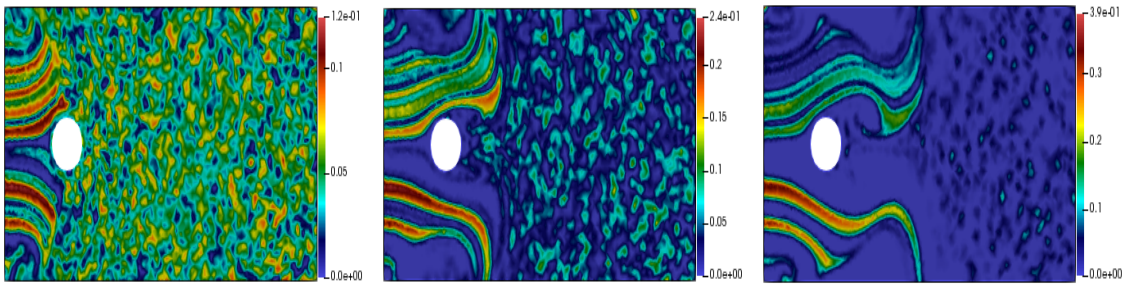

Evolution of the density u_3 at successive time $t = 5, 10, 15$.

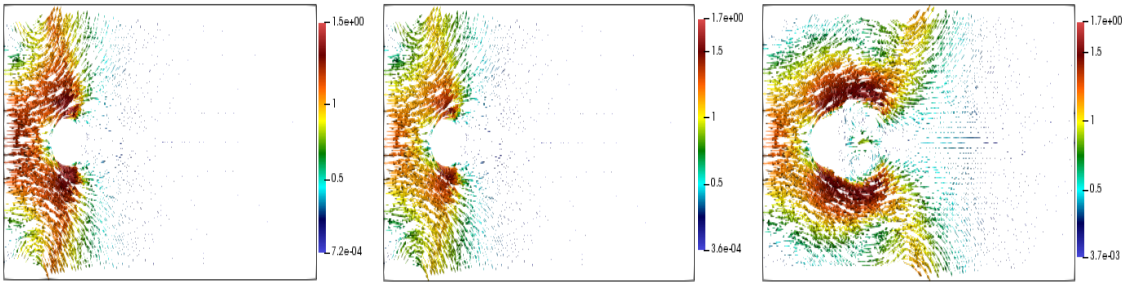

Snapshot of the fluid velocity $\mathbf{v}$ at successive time $t = 5, 10, 15$.

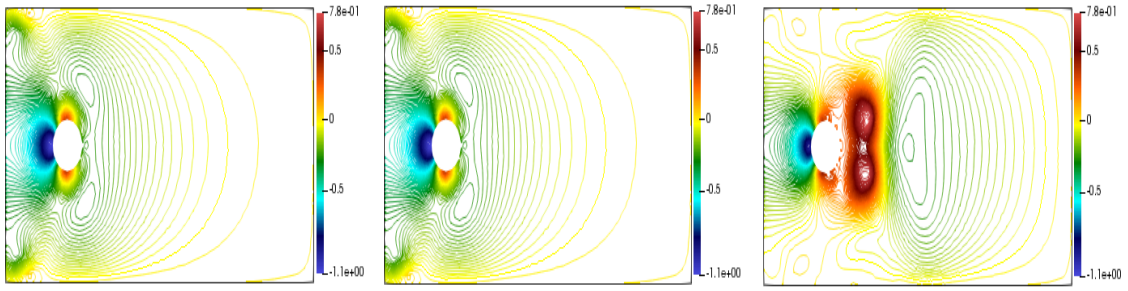

Snapshot of the pressure p at successive time $t = 5, 10, 15$.

FIGURE 3.9: Evolution of the three interacting populations and snapshot of the fluid velocity and the pressure in the case: $\nabla\phi = (0, 0)$.

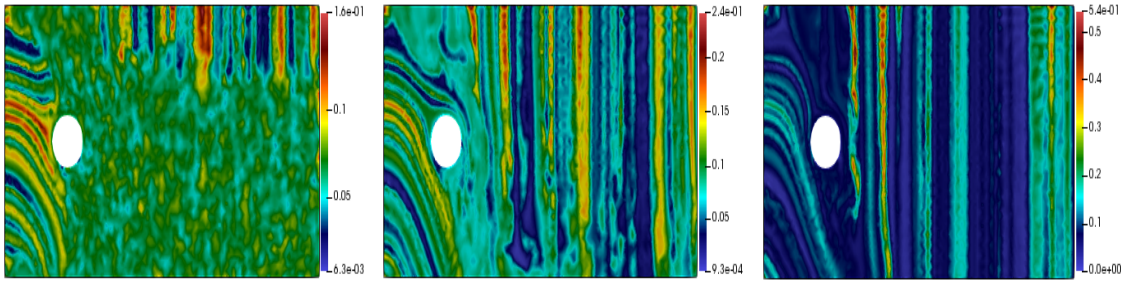

Evolution of the density u_1 at successive time $t = 5, 10, 15$.

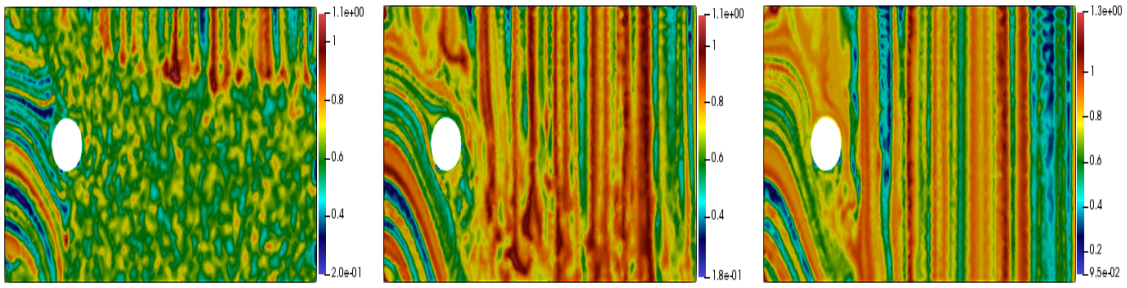

Evolution of the density u_2 at successive time $t = 5, 10, 15$.

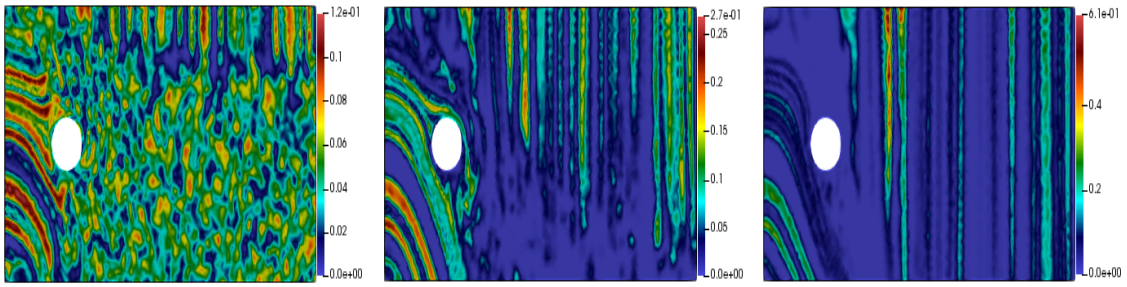

Evolution of the density u_3 at successive time $t = 5, 10, 15$.

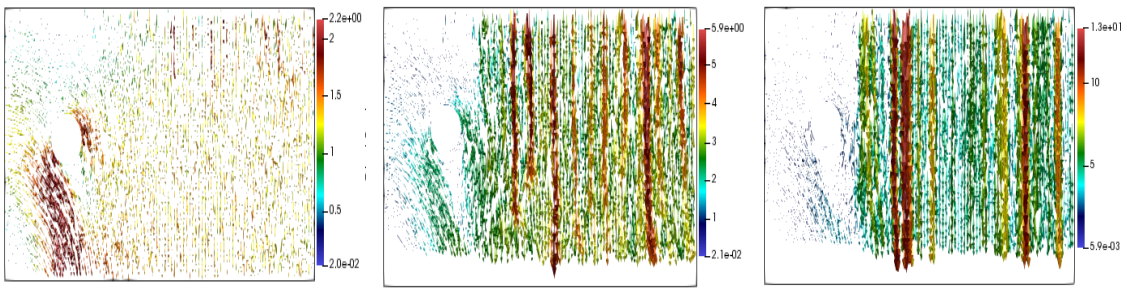

Snapshot of the fluid velocity $\mathbf{v}$ at successive time $t = 5, 10, 15$.

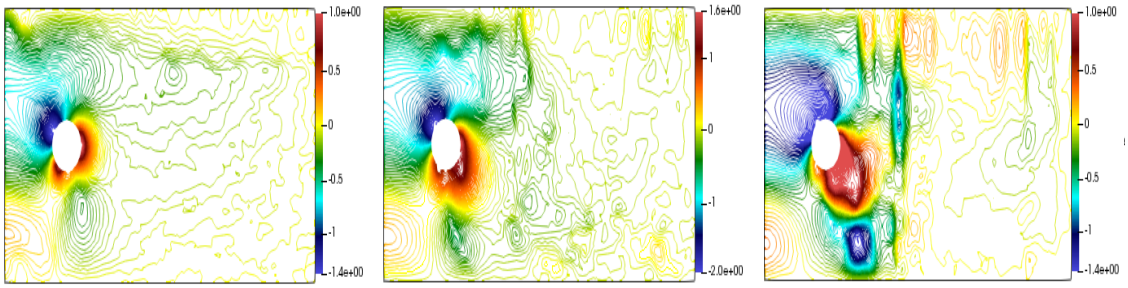

Snapshot of the pressure p at successive time $t = 5, 10, 15$.

FIGURE 3.10: Evolution of the three interacting populations and snapshot of the fluid velocity and the pressure in the case: $\nabla\phi = (0, 1)$.

Part II

Mathematical modeling of vehicular traffic by kinetic theory approach of active particles

Chapter 4

Representation and mathematical structures for one lane flow

This chapter is intended to give a brief overview of the basic mathematical structures for one lane vehicular traffic. It starts with the kinetic representation, in which we define the independent variables and dependent variables needed to describe the system. Then, macroscopic observable quantities can be obtained under suitable integrability assumption. Section 4.3 is devoted to state the mathematical structure of Boltzmann models with binary interaction, the models with Enskog-like interactions and Boltzmann models with averaged binary interactions. In section 4.4 we present discrete model by [43]. Section 4.5 is devoted to describe the kinetic theory for active particles. Specifically, the model by [21] where the authors take into account the behavior of the system driver-vehicle by adding the activity variable. The last section 4.6 aim to present the model by [47] where the authors propose a full discrete model.

4.1 Kinetic theory approach

Kinetic modeling in a Boltzmann framework applied to traffic flow was first initiated by [81]. Their model is based on local binary interactions framework with unidirectional flow and on the assumption that the driver is assumed willing to adjust the vehicle's velocity toward a certain desired velocity distribution. This model is only applicable in the situation of low traffic density. Indeed, in the inhomogeneous traffic flow situation, a serious drawback appears, for instance, since the velocities are positive, the traffic jams are not allowed to propagate backwards in negative direction, and this is in contrast to real traffic flow observations. Furthermore, the situation for kinetic equations in gas dynamics is completely different, because the velocity can be assumed positive and negative. Consequently, we can not expect to obtain a strict derivation of fluid dynamics equation from the aforesaid models. In order to correct this drawbacks, it is necessary to take in consideration the effects of the finite distance between the vehicles in analogy way to Enskog's theory for dense gas, see [68] where the authors used this argument in the context of microscopic interactions for the term of interactions.

After the pioneer work by [81], various contributions have been proposed by several authors starting from the critical analysis and substantial improvement proposed by [79] toward the most developments proposed, see for instance [76, 66, 67]. These models are based on a Boltzmann-type collision term in which the cross section, giving the probability of interaction between two particles, is replaced with a probability distribution depending on the local traffic conditions, see [76]. In contrast to work by [81], the equation proposed by [76] is strictly based on a microscopic model fulfilling the criterion of having a one parameter family of local equilibrium distributions depending only on the local density of cars. As in [76], the work by [66] derived a kinetic equation based on a microscopic model without going back to the phenomenological relation terms as in [81].

We would like to claim that the interactions integrals appeared in the models based in the continuous velocity typically do not provide the analytical expression of the equilibrium distribution and they are very demanding from computational point of view. To overtake these drawbacks, a several approaches has been proposed in literature. The first approach considered Vlasov-Fokker-Planck type model in which the integrals are replaced by differential operators, see [58] and recently [90]. The second one considered simplified kinetic models with a small number of velocities, namely based on the discrete-velocity [43, 21, 15].

It is attractive to state the two relevant complexity problems in the modeling of traffic flow by the engineer[40]. The first criticism observation is the assumption of continuity of the distribution function. Indeed, the number of vehicles is not large enough to justify this assumption. The second criticism observation is the assumption of homogeneity of the behavior of the system driver-vehicle. Indeed, the behavior of this system is not the same. Consequently, new models should take into account these criticisms observations. The method of discrete kinetic theory by [43] appears pertinent to avoid the first complexity problem. Indeed, the authors developed this method using the discreteness of the velocity variable, which allowed for a finite number of velocity only. In order to correct the second criticism observation, the paper by [21] proposed a mathematical structure based on the method of kinetic theory of active particles. This method on the one hand converts the Boltzmann's integral-differential equation into a set of partial differential equations. On the other hand it relaxes the continuum hypothesis and includes the granular nature of vehicular traffic. Recent work [82] proposed a spatially homogeneous model with discrete velocity by taking into account the heterogeneous nature of the flow of vehicles along a road. Namely, the authors considered mixture of two classes of populations instead of one class as in [21]. They considered the class of cars which is shorter and faster, and the class of trucks which is longer and slower.

More recently, the authors in [83] proposed a kinetic model based on continuous velocity space in the spatially homogeneous case with binary interactions. Their approach differs from the kinetic model proposed in [21] because they assumed continuous velocity spaces. The obtained result in their work suggest that a small number of velocities is sufficient for the kinetic modeling of traffic. Moreover, the acceleration remains controlled by the parameter Δv, in contrast to models based on a lattice of velocities, in which the possible outcomes of an interaction and the acceleration of vehicles depend on the particular lattice chosen [43, 21]. On the other hand, they found the explicit expression of the asymptotic distribution which leads to deriving new macroscopic equations using the closure provided by the kinetic model. We think that the most important result in their work is the derivation of the fundamental diagrams with a phase transition without the need of prescribing heuristic speed-density relations.

4.2 On the kinetic theory representation

In this section we are concerned about the kinetic theory representation where ee define the needed variables to state the mathematical structures. Let us consider a one-directional flow of vehicles along a road with length ℓ. We would like to mention that when the independent and dependent variables are in a suitable dimension form, they represent the relevant phenomena related to traffic flow and therefore some specific models will be described. Moreover, writing the model in terms of dimensionless variables is useful towards computational analysis and allows to extract suitable scaling parameters which can be properly used towards a qualitative understanding of the proprieties of the model.

In order to define dimensionless quantities, one has to identify characteristic time T and length of road ℓ, as well as maximum density ρ_M and maximum mean velocity V_M. Specifically,

- ρ_M is the maximum density of vehicles corresponding to bumper-to-bumper traffic jam.
- V_M is the maximum admissible mean velocity which may be reached by vehicles in the empty road.

It is spontaneous to assume $V_M T = \ell$, which means that T is the time necessary to cover the whole road length ℓ at the maximum mean velocity V_M. After the above preliminaries, we can now define dimensionless independent and dependent variables. The dimensionless independent variables are

- $t \in \mathbb{R}_+$ is the dimensionless time variable obtained by referring the real time to a suitable critical time T_c to properly be defined by a qualitative analysis of the differential model. Generally, it is convenient to identify the critical time T_c as the ratio between ℓ and V_M.
- $x = \dfrac{x_r}{\ell}$ is the dimensionless space variable obtained by dividing the real space by the length ℓ of the lane, where x_r is the real dimensional space.

Moreover, suitable reference variables can be introduced to define the dependent variables.

- Of course a fast isolated vehicle can reach velocities larger that V_M. In particular a limit velocity can be defined as
$$V_\ell = (1+\mu)V_M, \qquad \mu > 0,$$
taking into account that no vehicle can reach a velocity higher than V_ℓ, simply for mechanical reasons. Both V_M and μ may depend on the characteristics of the lane. Say, a country lane or a highway, as well as on the type of vehicles, for example, a slow car, a fast car, etc.

In the representation by kinetic theory methods, the whole system is defined by the statistical distribution function of position x and velocity v of the vehicles. This distribution function over the dimensionless microscopic state is defined by

$$f = f(t,x,v) : \mathbb{R}_+ \times [0,1] \times [0,1] \to \mathbb{R}_+.$$

$f(t,x,v)dxdv$ gives the number of vehicles which, at time t, is in the phase space domain $[x, x+dx] \times [v, v+dv]$. The distribution function f is normalized with respect to ρ_M so that all derived variables can be given in a dimensionless form.
In the kinetic representation, macroscopic observable quantities can be obtained, under suitable integrability assumptions, as momenta of the distribution f, normalized with respect to the maximum density ρ_M in order that all variables are given in a dimensionless form. Specifically,

- the dimensionless density is given by
$$\rho(t,x) = \int_0^{1+\mu} f(t,x,v)dv,$$
- the total number of vehicles at time t is computes as following
$$N(t) = \int_0^1 \int_0^{1+\mu} f(t,x,v)dvdx,$$
- the flux is giving by
$$q(t,x) = \int_0^{1+\mu} vf(t,x,v)dv,$$
- the dimensionless local mean velocity is
$$\xi(t,x) = \frac{q(t,x)}{\rho(t,x)}.$$
- Higher order momenta are related to other macroscopic variables, such as the average kinetic energy E and the variance of the velocity σ
$$E(t,x) = \frac{1}{2}\int_0^{1+\mu} v^2 f(t,x,v)dv, \qquad \sigma(t,x) = \frac{1}{\rho(t,x)}\int_0^{1+\mu} [v-\xi(t,x)]^2 f(t,x,v)dv.$$

4.3 Mathematical structures

Kinetic approach derivation follows lines similar to those of kinetic of gas-theory. Indeed, it needs the modeling of pair interactions at microscopic level. Let us consider pair interactions between a *test* vehicle with the state (x,v) and the *field* vehicle with state (y,w). As in the kinetic theory, different ways of modeling local interactions generate different types of evolution equations. The difference with respect to the classical theory is that interactions do not follow the rules of classical mechanics; but instead, the driving strategy is expressed by the vehicle-driver systems.

Models which are available in the literature have occasionally been derived by heuristic arguments. This section provides a description of some conceivable frameworks which can be used toward modeling of vehicular traffic. In particular, the following ones will be concisely described in the next subsections:

i) Boltzmann models with binary interactions,

ii) models with Enskog-like interactions,

iii) Boltzmann models with averaged binary interactions.

4.3.1 Boltzmann models with binary interactions

Localized binary interaction models are based on microscopic modeling, which assume binary interactions between the *test* and the *field* vehicles localized at point x of the field vehicle. The paper by [18] suggests the following formal structure

$$\begin{aligned} \frac{\partial f}{\partial t} + v\frac{\partial f}{\partial x} &= J[f,f](t,x,v) \\ &= \int_0^{1+\mu}\int_0^{1+\mu} \eta(v^*,v_*)\mathcal{A}(v^*,v_*;v)f(t,x,v^*)f(t,x,v_*)\,dv^*\,dv_* \\ &\quad -f(t,x,v)\int_0^{1+\mu}\eta(v,v_*)f(t,x,v_*)\,dv_*, \end{aligned} \tag{4.3.1}$$

where the right-hand side gives the difference between the inflow and outflow of vehicles in the control volume of the phase space. Moreover,

- $\eta(v^*,v_*)$ or $\eta(v,v_*)$ is *the encounter rate* between the test vehicle with velocity v^* and the field vehicle with velocity v_*. It gives the number of interactions between pairs of vehicles per unit time in the unit space.
- $\mathcal{A}(v^*,v_*;v)$ is *the transition probability density* that a candidate or test vehicle with velocity v^* interacting with a vehicle with velocity v_* ends up with velocity v. The density $\mathcal{A}$ must be equal to zero for $v \geqslant 1+\mu$.

The above description may lead to good results in homogeneous traffic flow situations; of course the description is satisfactory if the microscopic modeling is correct. If the above equation (4.3.1) are used for the description of inhomogeneous traffic flow situations, a serious drawback appears due to the positivity of the velocities v. There is no mechanism in the equations to allow perturbations to propagate backward in the negative-x direction. This can be seen by the following trivial argument: Considering a full space problem, the integral form of the kinetic equation is

$$f(t,x,v) = f(0,x-vt,v) + \int_0^t J[f,f](s,x+v(s-t),v)ds.$$

This shows that the distribution function f at x and t depends only on the distribution function at the values $x' \leqslant x$, $s \leqslant t$, since v is positive. A perturbation cannot propagate backward in the negative x direction. In particular, traffic jams occurring for dense traffic situations are not allowed to travel backward. This is in striking contrast to real traffic flow observations. Moreover, the above remark has consequences for the connection between kinetic and fluid dynamic traffic flow equations. Namely, one can not expect to obtain a strict derivation of fluid dynamic equations from the above kinetic equation (4.3.1). In general, to describe correctly the behavior of dense traffic with a kinetic equation and to obtain a consistent derivation of fluid dynamic equations. It is necessary to include the effects of the finite size extension of the vehicles. This can be done as we will show in the next subsection in analogy to Enskog's theory for a dense gas.

4.3.2 Models with Enskog-like interactions

Enskog-like models have a structure analogous to the Boltzmann-like models with binary interactions. The main difference is that the effects of the finite size of the vehicles are taken into account. Namely, the field vehicle is not localized in the same place x as the candidate or test vehicle, but at a certain distance from x that can be chosen depending on the velocities of the interacting pair. Moreover, the Enskog-type modeling introduces a pair correlation function depending on the local densities in the positions of the interacting pairs as follows, see [67]

$$f^{(2)}(t,x,v,y,w) \sim K(d_i(v,w),\rho(t,x))f(t,x,v)f(t,y,w), \tag{4.3.2}$$

where the function K is the correlation function between test and field vehicles depending, in a phenomenological way, on the reaction thresholds d_i of the driver, at least braking and accelerating thresholds. Interactions of the test vehicle are assumed to happen only when a threshold distance is crossed, and are supposed to be localized with a field vehicle in the position

$$y_i = y_i(v, w) = x + d_i(v, w).$$

The structure (4.3.1) can be rewritten in the following form

$$\begin{aligned}\frac{\partial f}{\partial t} + v\frac{\partial f}{\partial x} &= \sum_{i=1}^{2} J_i[f,f](t,x,v) \\ &= \sum_{i=1}^{2}\int_0^{1+\mu}\int_0^{1+\mu} \eta(v^*,w^*)\mathcal{A}_i(v^*,w^*;v) f^{(2)}(t,x,v^*,(x+d_i(v^*,w^*)),w^*)dv^*dw^* \\ &\quad -f(t,x,v)\sum_{i=1}^{2}\int_0^{1+\mu}\eta(v,w^*)f^{(2)}(t,x,v,(x+d_i(v,w^*)),w^*)dw^*. \end{aligned} \tag{4.3.3}$$

Reconsidering the arguments in Subsection 4.3.1, one obtains

$$f(t,x,v) = f(0,x-vt,v) + \int_0^t \sum_{i=1}^{2} J_i[f,f](s,x+v(s-t),v)ds.$$

In this case one observes, due to the definition of $J_i[f,f]$, that the distribution function at x, t depends not only on the distribution function at $x' \leqslant x$, $s \leqslant t$, but also on the distribution function at $x' > x$. Thus, this allows backward propagating disturbances.

4.3.3 Boltzmann models with averaged binary interactions

The review by [18] also introduces structure for models where a suitable function $\varphi(x,y)$ models the weight of the action on the driver of the test or candidate vehicle at x due to the field vehicle at y within the visibility area $D = [x-\delta r, x+\delta f]$ of the vehicle at x. Where δr and δf are, respectively, the rear and frontal visibility distance. For $y \in D$ the weight $\varphi(x,y)$ must be such that

$$y \uparrow \Rightarrow \varphi \downarrow, \qquad \int_D \varphi(x,y)dy = 1. \tag{4.3.4}$$

The corresponding mathematical structure is written as follows

$$\begin{aligned}\frac{\partial f}{\partial t} + v\frac{\partial f}{\partial x} &= \int_D\int_0^{1+\mu}\int_0^{1+\mu} \eta(v^*,v_*)\mathcal{A}(v^*,v_*;v) f(t,x,v^*)f(t,x,v_*)\varphi(x,y)\,dv^*\,dv_*\,dy \\ &\quad -f(t,x,v)\int_D\int_0^{1+\mu}\eta(v,v_*)f(t,x,v_*)\varphi(x,y)\,dv_*\,dy. \end{aligned} \tag{4.3.5}$$

It is immediate to show that Eq. (4.3.5), assuming that $\varphi(y) = \delta(y-x)$ (or $\varphi(y) = \delta(y-x+d)$), where δ denotes Dirac's delta function, gives a localized interaction models. Analogous reasoning can be applied to Enskog-type models.

It is worth stating that the above mathematical frameworks are criticized in [18]. Indeed, these mathematical frameworks did not take into account the complexity features. Precisely, as previously mentioned, the assumption of continuity of the distribution function and the assumption of homogeneity of the driver-vehicle systems. These critical analysis from an engineer's point of view on traffic phenomena modeling is given by the sharp paper of [40]. A few sentences can be extracted from this paper:

(i) Shock waves and particle flows in fluid dynamics refer to thousands of particles, while only a few vehicles are involved in traffic jams.

(ii) A vehicle is not a particle but a system linking driver and mechanics, so that one has to take into account the reaction of the driver, who may be aggressive, timid, prompt, etc. This criticism also applies to kinetic type models.

(iii) Increasing the complexity of the model increases the number of parameters to be identified.

The aim of the next sections is to take into account these criticism observations.

4.4 Discrete velocity models

The objective of this section is to overtake the first criticism (i). Namely, the continuity assumption of the function distribution. Indeed, continuity assumption can not be applied to vehicular flows considering that the inter-vehicular distances cannot be neglected, while methods of mathematical kinetic theory need a number of particles much greater than those involved in the road. To achieve this goal, it is pertinent to proceed by the discrete velocity methods which are based on the assumption that particles can only attain a finite number of velocities. Thus, developing discrete velocity models in kinetic theory appears to be particularly interesting, considering that vehicles are often observed to move along highways with group velocities, thus creating *clusters* of vehicles related to certain sets of velocities.

Referring to paper by [43], the authors observe that vehicles traveling along a road do not continuously span the whole set of admissible velocities; rather, they tend to move in clusters. This lead them to consider a mathematical structure that corresponds to average stochastic games. Technically, developing a discrete velocity model of traffic flow means selecting a discrete number of velocities as follows

$$I_v = \{v_0 = 0, ..., v_i, ..., v_n = 1\} \subset \ D_v = [0, 1],$$

where velocities have been divided by the maximal admitted velocity V_ℓ, D_v is the dimensionless velocity domain, and n is the number of points. In principle, the only requirement on n is that, it should be a positive integer different from zero i.e. $n \in \mathbb{N}$, $n > 0$. Each v_i is interpreted as a velocity classes encompassing a certain range of velocities v which are not individually distinguished. The discretization introduced above is not a simple mathematical procedure. Instead, it plays a specific role in the modeling of the system. Namely, it represents possible ways to consider the strongly granular nature of traffic. On the other hand, we observe that vehicles traveling along a road do not give rise to a continuous velocity distribution, since they tend to move in clusters which can be identified and distinguished from each other by a discrete set of speed values.
The corresponding discrete representation is obtained by linking the discrete distribution functions to each velocity v_i, $i = 1, ..., n$. Precisely, the distribution function f is expressed as a linear combination of Dirac functions in the variable v with coefficients depending on time t and space x.

$$f(t, x, v) = \sum_{i=1}^{n} f_i(t, x)\delta(v - v_i), \tag{4.4.1}$$

where $f_i(t, x) = f(t, x, v_i)$ gives the distribution of vehicles in the point x having at time t a velocity comprised in the i-th velocity class.

Naturally, the above discrete velocity approach implies that vehicles with velocity larger than V_ℓ can be disregarded. In other words, it is technically assumed that the presence of vehicles with velocity much larger than the maximum mean velocity corresponding to the given density is negligible. However, in a discrete velocity framework, such a detail is actually not very relevant, since vehicles are grouped and classified on the basis of velocity classes $\{v_i\}_{i=1}^n$. So that those which travel at speeds higher than V_M are simply included in the extreme class v_n. On the other hand, technically $v_1 = 0$ which coincides with the left endpoint of the interval D_v. The other classes are then recovered as

$$v_{i+1} = v_i + (\Delta v)_i, \qquad i = 1, ..., n - 1,$$

where $(\Delta v)_i$ represents the amplitude of the i-th velocity class. The authors have been consider an uniformly spaced velocity grid over D_v, which implies a constant step

$$\Delta v = \frac{|D_v|}{n - 1},$$

where $|D_v|$ is the length of the interval D_v. It results also that

$$v_i = (i-1)\Delta v, \qquad i = 1, ..., n,$$

with $v_n = |D_v|$. Note that if one takes $D_v = [0, 1+\mu]$ with μ sufficiently small, then the resulting amplitude $\Delta v = \frac{1+\mu}{n-1}$ of the velocity classes little differs from the case D_v, which produces $\Delta v = \frac{1}{n-1}$. Consequently, one can choose to refer to the unit dimensionless velocity domain $D_v = [0, 1]$ by simply assuming that vehicles possibly traveling at speeds higher than 1 are included in the extreme velocity class $v_n = 1$. The authors explicitly assumed a uniformly spaced velocity grid of the form

$$v_i = \frac{i-1}{n-1}, \qquad i = 1, ..., n$$

with the constant grid step $\Delta v = \dfrac{1}{n-1}$.
Using the representation of the distribution function f given by Eq. (4.4.1), the following expressions for the classical macroscopic average quantities are easily derived:

- the vehicle density
$$\rho(t, x) = \sum_{i=1}^{n} f_i(t, x);$$
- the vehicle flux
$$q(t, x) = \sum_{i=1}^{n} v_i f_i(t, x) = \rho(t, x)\xi(t, x),$$
where ξ is the mean velocity;
- the variance of the velocity
$$\sigma(t, x) = \frac{1}{\rho(t, x)} \sum_{i=1}^{n} [v_i - \xi(t, x)]^2 f_i(t, x).$$

The mathematical model by [43] is a set of evolution equations for the densities which can be formally written as follows

$$\begin{aligned} \frac{\partial f_i}{\partial t} + v_i \frac{\partial f_i}{\partial x} \quad = \quad & \sum_{h=1}^{n} \sum_{k=1}^{n} \int_{D_w} \eta[\mathbf{f}](t, y) \mathcal{A}^i_{h,k}[\mathbf{f}; \alpha](t, y) f_h(t, x,) f_k(t, y) w(x, y) dy \\ & - f_i(t, x) \sum_{k=1}^{n} \int_{D_w} \eta[\mathbf{f}](t, y) f_k(t, y) w(x, y) dy, \end{aligned} \tag{4.4.2}$$

for $i = 1, ..., n$, where $D_w = [x, x + L]$ is the visibility zone where $L > 0$, and $\mathbf{f} = (f_1, ..., f_n)$. Moreover,

- $\eta[\mathbf{f}]$ is the interaction rate, which gives the number of interactions per unit time among the vehicles,
- $\mathcal{A}^i_{h,k}[\mathbf{f}; \alpha]$ defines the table of games, which models the microscopic interactions among the vehicles by giving the probability that a vehicle with speed v_h adjusts its velocity to v_i after an interaction with a vehicle traveling at speed v_k.
- $w(x, y)$ represents the function weighting the interactions over the visibility zone; it is required to satisfy
$$w(x, y) \geq 0, \ \forall x \in [0, 1], y \in D_w, \quad \int_{D_w} w(x, y) dy = 1, \ \forall y \in D_w,$$
- α is phenomenological parameter, whose lower and higher values are related to bad and good road conditions respectively.

Furthermore, the authors assume that both the interaction rate and the table of games depend on the local density ρ with the following additional requirement

$$\mathcal{A}^i_{h,k}[\mathbf{f};\alpha] \geq 0, \qquad \sum_{i=1}^{n} \mathcal{A}^i_{h,k}[\mathbf{f};\alpha] = 1 \qquad \forall h,k \in \{1,...,n\}. \tag{4.4.3}$$

It is worth stating that numerical simulations of the spatially inhomogeneous problem have been carried out by addressing three representative cases, which highlight the ability of the model to reproduce correctly some interesting features of vehicular traffic flow. In particular, the merging of two clusters of vehicles with concomitant appearance of stop-and-go waves and the backward propagation of a queue, possibly in presence of a bottleneck, with a vehicle density profile which in this second case closely follows that of the bottleneck, and which in both cases never overcomes the maximum value fixed by the road capacity. Moreover, the above kinetic model (4.4.1) has been derived according to the generalized kinetic theory, where interactions at the microscopic level do not follow laws of classical mechanics. However, they are the same for all interacting vehicles. In other words, the behavior of the vehicle-driver system follows specific strategies that modify classical mechanical rules, but they are not heterogeneously distributed among the vehicles.

4.5 Kinetic Theory of Active Particles

The Kinetic Theory of Active Particles, hereafter sometimes abbreviated as KTAP, is a mathematical method that has been developed to model the dynamics of large living systems, see [12]. Motivations to use KTAP's methods to model vehicular traffic are offered by the criticisms (ii) and (iii) cited above in Subsection (2.3.3) by [40]. The basic idea of KTAP is to consider each driver-vehicle as an *active particle* of a large complex system, to model the heterogeneous behavior of the micro-systems that compose the overall system. As previously mentioned, [21] proceeded by the KTAP's method. The authors consider a modeling approach which takes into account not only the lack of continuity of the distribution function with respect to the velocity variable v but also with respect to the activity variable u. In order to describe this method, the authors discretized the variables v and u by introducing the following sets Iv and I_u

$$I_v = \{v_1 = 0, ..., v_i, ..., v_n = 1\}, \qquad I_u = \{u_1 = 0, ..., u_j, ..., u_m = 1\}.$$

where n and m are, respectively, the number of discretization points of the velocity v and the activity u.
The authors used a fixed uniform grids of velocity and activity defined as follows

$$v_i = \frac{i-1}{n-1}, \quad u_j = 1 - \frac{j-1}{m}, \qquad \forall i = 1, ..., n, \quad \forall j = 1, ..., m. \tag{4.5.1}$$

Moreover, the distribution function is defined as a sum of Dirac distributions in the variable v and u, with coefficients depending on t and x

$$f(t,x,v,u) = \sum_{i=1}^{n}\sum_{j=1}^{m} f_{ij}(t,x)\delta(v-v_i)\delta(u-u_j), \tag{4.5.2}$$

where $f_{ij}(t,x) = f(t,x,v_i,u_j)$.
Thus, according to this mathematical representation, the following expressions for the classical macroscopic average quantities are easily derived

- the dimensionless local density

$$\rho(t,x) = \sum_{i=1}^{n}\sum_{j=1}^{m} f_{ij}(t,x),$$

- the dimensionless mean velocity and flow

$$\xi(t,x) = \frac{1}{\rho(t,x)} \sum_{i=1}^{n} \sum_{j=1}^{m} v_i f_{ij}(t,x),$$

and

$$q(t,x) = \xi(t,x)\rho(t,x).$$

- while the local speed variance is given by

$$\sigma(t,x) = \frac{1}{\rho(t,x)} \sum_{i=1}^{n} \sum_{j=1}^{m} [v_i - \xi(t,x)]^2 f_{ij}(t,x).$$

- Similarly, one can compute the local mean value and variance of the activity variable

$$a(t,x) = \frac{1}{\rho(t,x)} \sum_{i=1}^{n} \sum_{j=1}^{m} u_j f_{ij}(t,x),$$

and

$$Var(a) = \frac{1}{\rho(t,x)} \sum_{i=1}^{n} \sum_{j=1}^{m} [u_j - a(t,x)]^2 f_{ij}(t,x).$$

The authors introduce the discrete probability density

$$\mathcal{A}^{ij}_{hk,pq}(v_h \to v_i, u_k \to u_j | v_h, v_p, u_k, u_q, \rho(t,y)), \tag{4.5.3}$$

which denotes the probability density that the candidate particle (v_h, u_k) falls into the state (v_i, u_j) of the test particle after an interaction with a field particle (v_p, u_q), with the property that

$$\sum_{i=1}^{n} \sum_{j=1}^{m} \mathcal{A}^{i,j}_{hk,pq} = 1, \qquad \forall h, p \in \{1, ..., n\} \quad \forall k, q \in \{1, ..., m\}. \tag{4.5.4}$$

The evolution of the system is ruled by nonlinearly additive interactions described by stochastic games. The corresponding mathematical structure by [21] is written as follows

$$\begin{aligned} \frac{\partial f_{ij}}{\partial t} + v_i \frac{\partial f_{ij}}{\partial x} \quad = \quad & \sum_{h,p=1}^{n} \sum_{k,q=1}^{m} \int_x^{x+L} \eta[\rho(t,y), x] \\ & \times \mathcal{A}^{ij}_{hk,pq}(v_h \to v_i, u_k \to u_j | v_h, v_p, u_k, u_q, \rho(t,y)) f_{hp}(t,x,) f_{kq}(t,y) dy \\ & - f_{ij}(t,x) \sum_{p=1}^{n} \sum_{q=1}^{m} \int_x^{x+L} \eta[\rho(t,y), x] f_{pq}(t,y) dy, \end{aligned} \tag{4.5.5}$$

where $L > 0$ is the visibility zone length, and

- $\eta[\rho(t,y), x]$ is the encounter rate. The authors consider the following expression

$$\eta[\rho(t,y), x] = \Psi[\rho(t,y)] w(x,y),$$

where $w(x,y)$ is the weighted function; it is required to satisfy

$$w(x,y) \geq 0, \ \int_{D_w} w(x,y) dy = 1, \ \forall x \in [0,1], \ \forall y \in [x, x+L],$$

and

$$\Psi[\rho(t,y)] = 1 + \frac{1}{\alpha}\rho^2,$$

- α is a phenomenological parameter modeling the traffic condition. Technically, $\alpha \to 0$ models bad condition and $\alpha \to 1$ models good condition.

- $u \in [0,1]$ is the activity variable, which identifies the quality of the driver-vehicle micro-system. $u = 0$ corresponds to the worst quality and $u = 1$ corresponds to the best quality.

The authors presented some numerical simulations in the case of the spatially homogeneous and inhomogeneous problems that show the ability of the above model (4.4.1) to reproduce some empirical data. Namely, in the first case, the numerical simulations are devoted to reproduce the so called fundamental diagrams [63]. Such diagrams relate the density of cars to either their average speed or their flux, this way providing synthetic insights into the gross phenomenology of vehicular traffic flow expected in stationary conditions. In the second case, the authors consider a special case of merging of two clusters.

To make it short, the idea of the aforesaid models by [43] and [21] is to relax the hypothesis that the speed distribution is continuous by introducing in the domain D_v a lattice of discrete speeds. Consequently, the granular character of the car flow is at least partially taken into account from the point of view of the speed distribution. We will propose a deep revisiting of the paper by [21] in the Chapter 5.

4.6 A fully-discrete-state kinetic model by Fermo and Tosin

This section is devoted to introduce a mathematical framework starting from the discrete velocity kinetic method. In order to accomplish the program of a fully-discrete-state kinetic theory of vehicular traffic, we refer to the paper by [47], in which the position x and velocity v are discrete. The authors follow line of aforesaid framework [43] for the discretization of the velocity v. The basic idea is to introduce a partition of the spatial domain. It is worth anticipating that partitioning the spatial domain D_x in a number of cells of finite size is a more realistic way to detect the positions of the vehicles along the road. Indeed, it is consistent with the intrinsic granularity of the flow, which does not allow for a statistical description of their spatial distribution more accurate than a certain minimum level of details. In addition, it enables one to account easily for some effects due to the finite size of the vehicles even in a context where the actual representation is not focused on each of them. Technically, a useful partition of the spatial domain D_x is in pairwise disjoint cells I_i, whose union is $D_x = [0, L]$, where $L > 0$ is the length of the road. Namely,

$$D_x = \bigcup_{i=1}^{m} I_i, \qquad I_{i_1} \cap I_{i_2} = \emptyset, \qquad \forall i_1 \neq i_2, \tag{4.6.1}$$

where $m \in \mathbb{N}$ is the number of cells I_i needed for covering D_x, which depends on the size ℓ_i of each I_i. Moreover, cells assumed have a constant size ℓ, chosen in a such a way that $\frac{L}{\ell} \in \mathbb{N}$, therefore $m = \frac{L}{\ell}$.

The authors consider $f_{ij} = f_{ij}(t)$ the distribution function of vehicles that, at time t, are located in the i-th cell with a speed in the j-th class. The total number N_{ij} of vehicles in I_i with speed v_j is $N_{ij} = f_{ij} l$. Then, the total number N_i of vehicles in I_i is

$$N_i = \sum_{j=1}^{n} N_{ij} = \ell \sum_{j=1}^{n} f_{ij}.$$

One can get the total number N of vehicles along the road by further summing over i,

$$N = \sum_{i=1}^{m} N_i = \ell \sum_{i=1}^{m} \sum_{j=1}^{n} f_{ij}.$$

The system is described by a distribution function

$$f(t, x, v) = \sum_{i=1}^{m} \sum_{j=1}^{n} f_{ij}(t) \chi_{I_i}(x) \delta(v - v_j), \tag{4.6.2}$$

χ_{I_i} being the characteristic function of the cell I_i $\left(\chi_{I_i}(x) = 1 \text{ if } x \in I_i, \chi_{I_i}(x) = 0 \text{ if } x \notin I_i\right)$. In practice, f is an atomic distribution with respect to the variable v, like in the discrete velocity framework, and is piecewise constant with respect to the variable x. Particularly, this latter characteristic implies that vehicles are thought of as uniformly distributed within each cell.
Usual macroscopic variables of traffic, such as the vehicle density ρ, flux q, and average speed ξ are obtained from Eq. (4.6.2) as distributional moments of f with respect to v: the density, the flux and the mean velocity quantities are defined by

$$\rho(t,x) = \sum_{i=1}^{n}\Big(\sum_{j=1}^{m} f_{ij}(t)\Big)\chi_{I_i}(x), \quad q(t,x) = \sum_{i=1}^{n}\Big(\sum_{j=1}^{m} f_{ij}(t)\Big)\chi_{I_i}(x), \quad \xi(t,x) = \frac{q(t,x)}{\rho(t,x)}.$$

According to [47], the corresponding model is written as follows

$$\frac{df_{ij}}{dt} + v_i\left(\phi_{i,i+1}f_{ij}(t) - \phi_{i-1,i}f_{i-1,j}(t)\right) = \sum_{h,k=1}^{n}\eta_{hk}(i)\mathcal{A}^{j}_{hk}(i)f_{ih}(t)f_{ik}(t) - f_{ij}(t)\sum_{k=1}^{n}\eta_{jk}(i)f_{ik}(t) \quad (4.6.3)$$

where

1. if $2 < i < m-1$, the equation are well defined;
2. if $i = 1$, $\phi_{0,1}$, $f_{0,1}$ are provided as left boundary conditions;
3. if $i = m$, $\phi_{m,m+1}$ has to be the right conditions.

Moreover,

- $\phi_{i,i+1}$ is the flux limiters, which limits the number of vehicles that can actually travel across the cells on the basis of the occupancy of the destination cells.

$$\phi_{i,i+1} = \begin{cases} \frac{1-\rho_{i+1}}{\rho_i}, & \text{if } \rho_i + \rho_{i+1} > 1, \\ 1, & \text{if } \rho_i + \rho_{i+1} \leq 1, \end{cases}$$

  where ρ_i is the density of the i-th cell.

- $\eta_{hk}(i)$, $\eta_{jk}(i)$ are the encounter rate, they present frequency interaction between (I_i, v_h) and (I_i, v_k)

$$\eta_{hk}(i) = \eta_0\rho_i, \text{ with } \eta_0 = \text{constant}.$$

- $\mathcal{A}^{j}_{hk}(i)$ is the table of games, it presents the probability that (I_i, v_h) interacting with (I_i, v_k) becomes (I_i, v_j). the following conditions must hold

$$\mathcal{A}^{j}_{hk}(i) \geq 0, \qquad \sum_{j=1}^{n}\mathcal{A}^{j}_{hk}(i) = 1, \qquad \forall h,j,k \in \{1,...,n\} \quad \forall i \in \{1,...,m\}.$$

It is worth anticipating that the resulting model Eq. (4.6.3) is not a cellular automaton in spite of the discreteness of the space state. In fact, vehicles are not assimilated to fictive particles jumping from their current site to a neigh-boring one with prescribed probability. They actually flow through the cells with their true speed according to a transport term duly implemented in the time evolution equations of their distribution functions. So that finally the evolution of the system is not seen as a stepwise algorithmic update of the lattice of microscopic states.
The validity of the above model (4.6.3), and indirectly also that of the methodological approach which generated it, can be assessed through exploratory numerical simulations addressing typical phenomena of vehicular traffic. For this reason, the authors consider the case of space dynamics at traffic lights and the case of space dynamics for road works.

Chapter 5

Multiscale continuum-velocity kinetic model for vehicular traffic with local and mean field interactions

This chapter is devoted to summarize our paper [28]. In this paper, we deals with the modeling of vehicular traffic according to a kinetic theory approach, where the microscopic state of vehicles is described by position, velocity and activity, namely a variable suitable to model the quality of the driver-vehicle micro-system. Interactions at the microscopic scale are modeled by methods of game theory, thus leading to the derivation of mathematical models within the framework of the kinetic theory. Short and long range interactions are modeled to depict change of velocity related to passing and clustering phenomena.

5.1 Introduction

This chapter specifically refers to [21], where a kinetic type model has been proposed with the following main features:

1. The approach is developed at the mesoscopic scale to account for the heterogeneous behavior of the driver-vehicle micro-system;
2. The velocity variable is assumed to be discrete to overcome the difficulty that the number of micro-systems might not large enough to assure continuity of the probability distributions over the microstates;
3. The quality of the road-environment conditions is modeled by a parameter that has an influence on the dynamics of interactions. Such parameter takes values in the interval $[0, 1]$, where the extremes of the domain correspond to worst and best conditions respectively.

The paper by [28] is based on the kinetic theory for active particles [19] and starts from the achievements obtained in [21], which are definitely interesting, such as the ability to reproduce the fundamental diagrams, namely mean velocity and flow versus local density, as well as clustering phenomena of vehicles with closed speeds. This work aims at providing further developments of interest for the applications. In more detail, the following modeling topics are treated: *Interactions, both local and long distance, between vehicles accounting on perceived (rather than real ones) quantities of the flow of vehicles, role of variable road conditions, and dynamics under external actions such as presence of tollgates. In addition, we consider a continuous velocity distribution rather than discrete velocities.* Discrete velocities, our approach, can be introduced only for computational purposes.

These new modeling features introduced in this work make it as a deep revisiting of that proposed in [21].

More precisely, the contents are as follows: Section 5.2 derives a new mathematical structure suitable to include the aforementioned features in addition to those already included in [21]; Section 5.3 shows how specific models can be derived by inserting in the said structure models of interactions obtained by a detailed phenomenological interpretation of physical reality. Section 5.4 presents a number of sample simulations which aim at exploring the ability of the model to predict emerging behaviors that appear in the complexity of vehicular traffic.

5.2 Mathematical structures

The derivation of models according to the kinetic theory of active particles is in two steps: The first step consists in deriving a mathematical structure suitable to capture the most important features of the system under consideration, while the second step consists in deriving specific models of vehicular traffic by inserting into the said structure models of interactions at the microscopic scale.

This section develops an approach to the first step by deriving a new general structure appropriate to include the specific features defined in Section 5.1. The overall content is presented through a sequence of subsections from the representation of the system to the derivation of the structure which is innovative with respect to the existing literature [21] as it includes modeling local and long distance interactions, as well as the interaction with external actions. This structure is deemed to offer the conceptual basis for the derivation of specific models.

5.2.1 Representation

Let us consider a one dimensional flow of vehicles along a road of length ℓ. Dimensionless position and velocity variables are denoted by x and v and are referred to ℓ and v_ℓ, respectively, where v_ℓ is a limit velocity such that no vehicle, simply for mechanical reasons, can pass it even in favourable environmental conditions. Moreover, it is useful to introduce a dimensionless time variable t obtained by dividing the real time by the time t_c needed by the fastest vehicle to move along the whole length of the road $t_c = \ell/v_\ell$. Dimensionless variables are used also for macroscopic gross quantities. For instance, the local number density $\rho = \rho(t,x)$ is obtained by dividing the real density by ρ_M, which is the maximum density of vehicles, corresponding to bumper-to-bumper traffic jam.

The analysis developed in what follows is based on the assumption that the state of the driver-vehicle subsystem is defined, at the microscopic scale, by the variables $(x,v,u) \in [0,1]^3$, where u, according to the kinetic theory of active particles [19], is a variable which denotes the quality of the micro-system. More precisely $u = 0$ corresponds to the worst quality, namely motion is prevented, while $u = 1$ to the best quality corresponding to an experienced driver operating in a high quality vehicle.

According to [19], the driver-vehicle subsystem is an *active particle*, while the internal variable is heterogeneously distributed over the active particles. In addition, the quality of the road, including environmental conditions, are accounted for by a parameter $\alpha \in [0,1]$ such that $\alpha = 0$ corresponds to the worst quality that prevents motion, while $\alpha = 1$ corresponds to the best conditions. In general α can depend on space $\alpha = \alpha(x)$ to account for the presence of curves, local restrictions, speed limits, etcetera.

The overall state of the system is described by the distribution function over the state at the microscopic scale:

$$f = f(t,x,v,u): \quad \mathbb{R}_+ \times [0,1] \times [0,1] \times [0,1] \to \mathbb{R}_+, \tag{5.2.1}$$

which is made to refer to ρ_M so that, if f is locally integrable, $f(t,x,v,u)\,dx\,dv\,du$ denotes the dimensionless density of vehicles which, at time t, are in the phase elementary domain $[x, x+dx] \times [v, v+dv] \times [u, u+du]$. In particular, the local density, also referred to ρ_M, is given by

$$\rho(t,x) = \int_0^1 \int_0^1 f(t,x,v,u)\,dv\,du, \tag{5.2.2}$$

while the total number of vehicles at time t is computed by integration over space. Precisely,

$$N(t) = \int_0^1 \int_0^1 \int_0^1 f(t,x,v,u)\,dx\,dv\,du. \tag{5.2.3}$$

In the same way, the local dimensionless mean velocity and the flow can be computed, respectively, as follows:

$$\xi(t,x) = \frac{1}{\rho(t,x)} \int_0^1 \int_0^1 v f(t,x,v,u)\,dv\,du \tag{5.2.4}$$

and

$$q(t,x) = \xi(t,x)\rho(t,x). \tag{5.2.5}$$

Moreover, higher order momenta such as the average kinetic energy E and the variance of the velocity σ can be computed, respectively, as follows:

$$E(t,x) = \frac{1}{2}\int_0^1 \int_0^1 v^2 f(t,x,v,u)\, dv\, du \tag{5.2.6}$$

and

$$\sigma(t,x) = \frac{1}{\rho(t,x)}\int_0^1 \int_0^1 \big[v - \xi(t,x)\big]^2 f(t,x,v,u)\, dv\, du. \tag{5.2.7}$$

Similarly, one can compute the local mean value and variance of the activity variable:

$$a(t,x) = \frac{1}{\rho(t,x)}\int_0^1 \int_0^1 u f(t,x,v,u)\, dv\, du \tag{5.2.8}$$

and

$$Var(a) = \frac{1}{\rho(t,x)}\int_0^1 \int_0^1 [u - a(t,x)]^2 f(t,x,v,u)\, dv\, du. \tag{5.2.9}$$

The derivation of models might be based on the assumption that interactions do not modify the variable u, namely the probability distributions over the mechanical variables and over u are independent:

$$f = f(t,x,v,u) \cong f(t,x,v)\, g(u), \quad \text{where} \quad \int_0^1 g(u)\, du = 1. \tag{5.2.10}$$

However, the dynamics of the mechanical variable depends on the activity variable.

5.2.2 Interaction domains and perceived quantities

The car-driver subsystem, namely the active particles, has a visibility zone $\Omega_v = \Omega_v(x) = [x, x + \ell_v]$, where ℓ_v is the visibility length on front of the vehicle, that depends on the quality of the environment, namely on $\alpha = \alpha(x)$. In more detail, we assume $\ell_v = \alpha L$, where $L << \ell$ is the visibility length in the case of best quality of the road, namely $\alpha = 1$.

In addition, it has a sensitivity zone, $\Omega_\ell = [x, x + \ell_s]$, necessary to perceive the flow conditions in Ω_ℓ. In general $\Omega_\ell \subseteq \Omega_v$. However also the opposite case has to be taken into account whenever local conditions of the road prevent visibility. This matter will be discussed in the critical analysis of the last section, while calculations are here developed assuming that the visibility zone includes the sensitivity zone. In general, Ω_ℓ can depend on f, which induces an additional nonlinearity.

The driver develops its driving strategy by taking into account perception of the state of the other vehicles both in Ω_ℓ and in a much shorter domain, say Ω_s within which active particles are supposed to perceive an approximate estimate of the local gradients $\partial_x \rho$, and hence of a perceived density $\rho^p[f]$ higher than the real one in the presence of positive gradients, and lower than the real one in the presence of negative gradients. We define *long range interactions* in the former case and *short range interactions* in the latter case.

In general, the approach of the kinetic theory for active particles is such that interactions are modeled by evolutionary stochastic games. Three types of particles are involved, namely *candidate* particles (vehicles) with the micro-state $\{x, v_*, u_*\}$, *field* particles (vehicles) with the state $\{x^*, v^*, u^*\}$, and the *test* particle which is representative of the whole system. Candidate particles are localized in x and can acquire, in probability, the state of the test particle, while field particles are localized in Ω_s for short range interactions and in Ω_ℓ for long range interactions.

The rationale toward modeling proposed in the following is based on the assumption that the activity variable of candidate and test particles is not modified by interactions.

5.2.3 Mean field interactions

The test vehicle is subject to an action of the vehicles in its sensitivity zone which can induce a consensus toward a common velocity, as an example the mean speed within the visibility domain

as well as a clustering effect. The test vehicle is sensitive to these actions if the distance between its speed and the common velocity is below a certain critical threshold.

In general, mean field interactions can be modeled by individual based *acceleration term* $\varphi(x, x^*, v, v^*, u, u^*)$ that is applied to the *test* vehicle (x, v, u) by a *field* vehicle (x^*, v^*, u^*) in the sensitivity domain Ω_ℓ of the test vehicle. Therefore, the overall acceleration of all vehicles is obtained by integration corresponding to the action of all vehicles in Ω_ℓ. Hence:

$$\mathcal{F}[f](t, x, v|u) = \int_\Lambda \varphi(x, x^*, v, v^*|u) f(t, x^*, v^*, u^*)\, dx^*\, dv^*\, du^*, \tag{5.2.11}$$

where $\Lambda = \Omega_\ell \times [0, 1] \times [0, 1]$.

5.2.4 Short range interactions

Short range interactions occur, as mentioned, in a small domain Ω_s sufficient for a candidate particle to perceive the density gradients ρ^p. Moreover, it is assumed that the probability distribution of field particles can be approximated by the probability distribution in x. Therefore, the state of candidate, test, and field particles is as follows:

$$f = f_* = f(t, x, v_*, u), \qquad f = f(t, x, v, u), \qquad f = f^* = f(t, x, v^*, u^*). \tag{5.2.12}$$

The description of short range interactions requires the modeling of two additional quantities:

- *The encounter rate* $\eta[f]$: which models the number of interactions per unit time between candidate and test particles with field particles.
- *The transition probability density* $\mathcal{A}[f](v_* \to v|u)$ which defines the probability density that a candidate particle falls into the state of with the field particles.

The actual modeling of short range interactions is based on the assumption that these quantities depend not only on the microscopic state of the interacting particles, but also on the distribution function f. This dependence induces a nonlinearity in models of interactions at the microscopic scale, which is put in evidence by square brackets. This dependence involves, as we shall see, both f and gradients of f. In addition, these interaction terms are allowed to depend on the quality of the road modeled by a parameter $\alpha \in [0, 1]$, where $\alpha = 0$ corresponds to the worse conditions that prevent motion and $\alpha = 1$ to the best conditions.

In addition $\mathcal{A}$ is required to satisfy the *probability density* condition:

$$\mathcal{A}[f; \alpha] \geq 0, \quad \int_{[0,1]} \mathcal{A}[f; \alpha](v_* \to v|v_*, v^*, u) dv = 1, \tag{5.2.13}$$

for all possible inputs v_*, v^*, u.

5.2.5 Interactions with the external actions

The test vehicle can be subject to external actions which control its velocity. As an example tollgates indicate the maximal speed when the vehicle approaches to the tollgate. Similarly the exit from the tollgate indicates how the speed can increase to the standard values.

The simplest way to model this term consists in using a BGK-type trend:

$$\mathcal{T}[f](t, x, v|u) = \mu[\rho]\big(f_e(x, v_e(x)) - f(t, x, v|u)\big), \tag{5.2.14}$$

where $\mu[\rho]$ models the intensity of the action, which increases with ρ, while $v_e(x)$ is the speed imposed by the external action.

A more general alternative would be modeling this action as by the term Eq. (5.2.11). However, this task does not appear practical as empirical data on this matter are not available.

5.2.6 A mathematical structure toward modeling

This subsection shows how all models of actions that have been described above can be inserted into a proper mathematical structure deemed to offer the conceptual basis for the derivation of

models. This structure is obtained by a balance of particles in the elementary volume of the space of the microscopic state which includes position, velocity (namely the variables of the phase space) and the activity. This balance of particles includes the free transport term, the transport due to long range interactions, the dynamics of short range interaction, and the trend to the speed required by the external actions. The dynamics of short range interactions include a "gain" term of vehicles that enter in the aforementioned elementary volume and a "loss" term of vehicles that leave it. The resulting structure can be written, at a formal level, as follows:

$$\partial_t f + v\,\partial_x f + F[f] = J[f] + \mathcal{T}[f], \tag{5.2.15}$$

where $f = f(t,x,v,u)$ and $v\partial_x f$ is the free flow transport term, while F, J, and $\mathcal{T}$ correspond, respectively, to mean field interactions, short range interactions, and interaction with external actions.

Classical calculation of the kinetic theory leads to the following result

$$\begin{aligned}
&\partial_t f(t,x,v,u) + v\partial_x f(t,x,v,u) + \partial_v(\mathcal{F}[f](t,x,v,u) f(t,x,v,u)) \\
&\quad = \int_{[0,1]^3} \eta[f]\mathcal{A}[f;\alpha](v_* \to v|v_*,v^*,u)\, f(t,x,v_*,u)\, f(t,x,v^*,u^*) dv_*\, dv^*\, du^* \\
&\qquad -f(t,x,v,u) \int_{[0,1]^2} \eta[f]\, f(t,x,v^*,u^*) dv^*\, du^* \\
&\qquad\quad +\mu[f]\big(f_e(x,v_e(x)) - f(t,x,v,u)\big).
\end{aligned} \tag{5.2.16}$$

5.2.7 Critical analysis

The mathematical structure proposed in this work include the features of the complex system under consideration which, according to the authors' opinion, appear to be the most important aspects of the dynamics to be retained by the modeling approach. Namely heterogeneity of the driver-vehicle subsystem, aggregation dynamics for vehicles with closed each other velocity, passing probability, variable properties of the road-environment where the dynamics occur and role of the external actions.

The structure can operate as a general framework for the derivation of models which can be obtained by inserting into the structure models of interaction at the microscopic scale. These models can be obtained by a phenomenological interpretation of empirical data. The most important reference to this aim is the book by Kerner [63], see also [64], which provides an interesting variety of empirical data valid in uniform flow conditions as well as in transient conditions. The main difficulty is that empirical data are available in steady flow conditions, while individual behaviors in unsteady conditions are quite different from those in steady conditions. However, a sharp interpretation of data can hopefully lead to models that can be validated by the information delivered by empirical data.

Validation is generally understood as the ability of models to reproduce quantitatively steady flow conditions, in particular the fundamental diagrams, and emerging behaviors at a qualitative level.

5.3 From mathematical structures to models

This section develops a possible approach to the derivation of specific models of vehicular traffic by inserting into the structure (5.2.16) models of interactions at microscopic scale. This objective is pursued by looking at the modeling of the interaction terms that characterize such structure, namely φ, η, $\mathcal{A}$, μ and f_e, such that a good agreement with empirical data, concerning both the fundamental diagram and the emerging behaviors in unsteady flow conditions, is provided.

5.3.1 Modeling accelerations

The acceleration term φ in Eq. (5.2.11) accounts for mean field interactions, where the test vehicle is subject to an action of the vehicles in its sensitivity zone Ω_ℓ which can induce a consensus

toward a common velocity v^*. A phenomenological interpretation of reality is as follows: *The test vehicle is sensitive to these actions if the distance between its speed and the common velocity is below a certain critical threshold d_c; it decays with the distance between the test and field vehicle; takes the sign of $v^* - v$ and depends on u and on the quality of the road α.*

A simple formalization of the formalization given above yields:

$$\begin{cases} |v^* - v| \leq d_c : & \varphi(x, x^*, v, v^*|u) = \dfrac{\alpha}{\ell_v}\, u(x^* - x)(v^* - v), \\ |v^* - v| > d_c : & \varphi(x, x^*, v, v^*|u) = 0. \end{cases} \tag{5.3.1}$$

Since $x^* \in \Omega_\ell$, one has $x \leq x^* \leq x + \ell_v$, then $0 \leq \dfrac{x^* - x}{\ell_v} \leq 1$. Now, taking $z^* = \dfrac{x^* - x}{\ell_v}$, yields

$$\mathcal{F}[f](t, x, v|u) = \ell_v \int_0^1 \int_0^1 \int_0^1 \varphi(x, \ell_v z^* + x, v, v^*) f(t, \ell_v z^* + x, v^*, u^*) dz^*\, dv^*\, du^*.$$

$$\begin{aligned} \mathcal{F}[f](t, x, v|u) &= \alpha\, u\, \ell_v \int_0^1 \int_0^1 \int_0^1 z^*(v^* - v) f(t, \ell_v z^* + x, v^*, u^*) dz^*\, dv^*\, du^* \\ &= \alpha\, u\, \ell_v\, \left(I_1(t, x) - v\, I_2(t, x)\right), \end{aligned} \tag{5.3.2}$$

where

$$I_1(t, x) = \int_0^1 \int_0^1 \int_0^1 z^* v^* f(t, \ell_v z^* + x, v^*, u^*) dz^*\, dv^*\, du^*,$$

and

$$I_2(t, x) = \int_0^1 \int_0^1 \int_0^1 z^* f(t, \ell_v z^* + x, v^*, u^*) dz^*\, dv^*\, du^*.$$

Computing the derivative of $\mathcal{F}$ with respect to v, yields

$$\partial_v(\mathcal{F}[f])(t, x|u) = -\alpha\, u\, \ell_v\, I_2(t, x). \tag{5.3.3}$$

5.3.2 Modeling the perceived density

The concept of perceived density was introduced in [41], where it was suggested that this quantity is greater (smaller) than the real one whenever positive (negative) density gradients appear. The following expression can be adopted according to [15]:

$$\rho^p[f] = \rho + \frac{\partial_x \rho}{\sqrt{1 + (\partial_x \rho)^2}} \left[(1 - \rho)\, H(\partial_x \rho) + \rho\, H(-\partial_x \rho)\right], \tag{5.3.4}$$

where $H(\cdot)$ is the heaviside function $H(\cdot \geq 0) = 1$, while $H(\cdot < 0) = 0$. Thus, the perceived density, positive gradients increase the value of ρ^p from ρ to the maximum admissible value $\rho = 1$, while negative gradients decrease it from ρ to the lowest admissible value $\rho = 0$ such that

$$\partial_x \rho \to +\infty \Rightarrow \rho^p \to 1, \quad \partial_x \rho = 0 \Rightarrow \rho^p = \rho, \quad \partial_x \rho \to -\infty \Rightarrow \rho^p \to 0.$$

5.3.3 Modeling the encounter rate

The encounter rate $\eta[f]$ refers the rate of interactions per unit time between candidate and test particles with field particles. One can assume that this term grows with the local perceived density starting from a minimal value corresponding to driving in vacuum conditions η_0. The following expression can be proposed:

$$\eta[f] = \eta_0\, (1 + \gamma_\eta\, \rho^p[f]), \tag{5.3.5}$$

where γ_η is the growth coefficient and ρ^p is the perceived density.

5.3.4 Modeling short range interactions

Let us now consider the term $\mathcal{A}$ which models short range interactions. This term defines the probability density that a candidate particle with the state $\{x, v_*, u\}$ falls into the state of the test particle $\{x, v, u\}$ after interaction with the field particles with the state $\{x, v^*, u^*\}$. These notations indicate that the activity variable is not modified by the interaction which, however, modifies the speed.

The modeling approach proposed in our work is based on the following assumptions:

1. Short range interactions do not modify the activity variable, but only the speed.
2. $\mathcal{A}$ depends on the velocities of the interacting pairs, on the perceived density, on the activity, and on the quality of the road, $\mathcal{A}[f](v_* \to v|v_*, v^*, u, \alpha, \rho^p)$, where the dynamics is enhanced by $\alpha\, u$, while it is limited by the perceived density. In addition, it is totally prevented if $\rho^p = 1$.
3. We assume that the candidate particle after interacting with the field particle reach new velocity $v \in [v_m, v_M]$ where v_m and v_M, respectively, are the minimum and the maximum velocities given by

$$v_m = \max\{0, \min\{v_*, v^*\} - \kappa(1 - \alpha u)\rho^p(|v_* - v^*| + \exp(-|v_* - v^*|))\},$$

$$v_M = \min\{1, \max\{v_*, v^*\} + \kappa\alpha u(1 - \rho^p)(|v_* - v^*| + \exp(-|v_* - v^*|))\}$$

where $\kappa = \frac{1}{200}$ is a constant allowed to make v_m close to the $\min\{v_*, v^*\}$ and v_M close to the $\max\{v_*, v^*\}$. Note that these choices of v_m and v_M guaranteed the condition $v_M - v_m > 0$ even if $v_* = v^*$.

It is natural that we have the following two cases to distinguish:

Interaction with faster particles

If $v_* \leq v^*$, the candidate particle has a trend, in probability, to increase its speed. This probability decreases with $v - v_m$ with $v \in [v_m, v_M]$. We propose the following probability density, which generalize the table of games defined in [21] where the velocity and the activity variables are discrete,

$$\mathcal{A}[f](v_* \to v) = (1 - \alpha u(1 - \rho^p))\frac{e^{-\frac{|v-v_*|^2}{\sigma_1}}}{\int_{v_m}^{v_M} e^{-\frac{|v-v_*|^2}{\sigma_1}} dv} + \alpha u(1 - \rho^p)\frac{(v_M - v)^2}{\int_{v_m}^{v_M}(v_M - v)^2 dv} \tag{5.3.6}$$

where σ_1 is a small constant given by $\sigma_1 = \kappa\alpha u(1 - \rho^p)$. Note that the probability density (5.3.6) has the same nonlinear behavior as of the table of games in [21]. More precisely, in good road conditions α and good activity u, the candidate particle has attendance to accelerate and reach new velocities greater than its pre-interaction velocity v_*. On the other hand, decreasing the value of α or u decreases the probability to accelerate (see Figure 5.1).

Interaction with slower particles

If $v_* > v^*$, the candidate particle has a trend, in probability, to decrease its speed. In order to get the similar behavior as in the discrete table of games by [21], we propose that our probability distribution is a dichotomy function which can be written as follows:

$$\mathcal{A}[f](v_* \to v) = \alpha u(1 - \rho^p)\frac{e^{-\frac{|v-v_*|^2}{\sigma_2}}}{\int_{v_m}^{v_M} e^{-\frac{|v-v_*|^2}{\sigma_2}} dv} + (1 - \alpha u(1 - \rho^p))\frac{v_M - v}{\int_{v_m}^{v_M}(v_M - v) dv}, \tag{5.3.7}$$

where σ_2 is a small constant given by $\sigma_2 = \kappa(1 - \alpha u(1 - \rho^p))$. Note that if α or u tend to zeros, the probability to decelerate is greater than the probability to maintain the velocity. On the contrary,

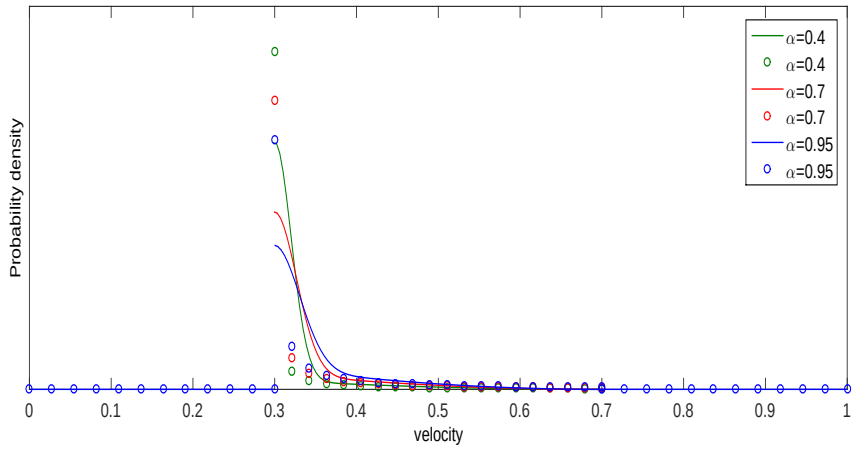

FIGURE 5.1: The probability density (discrete velocity) proposed by [21] vs our probability density (continuous velocity) in the case: $0.3 = v_* < v^* = 0.7$, $u = 1$ and $\rho^p = 0.6$.

if α and u tend to maximum value, the candidate particle has tendency to maintain it velocity (see Figure 5.2).

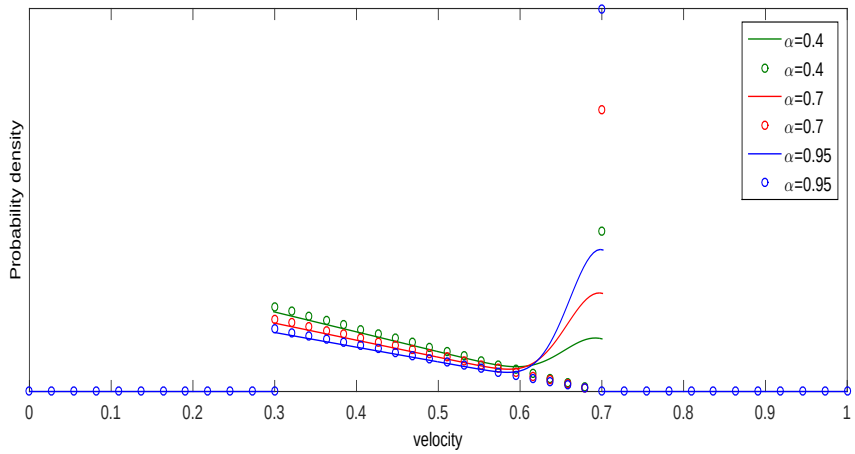

FIGURE 5.2: The probability density (discrete velocity) proposed by [21] vs our probability density (continuous velocity) in the case: $0.7 = v_* > v^* = 0.3$, $u = 1$ and $\rho^p = 0.6$.

Bearing in mind these two cases, the probability density is defined as follows:

$$\mathcal{A}[f](v_* \to v \in [v_m, v_M]) = \begin{cases} (1-P)\dfrac{e^{-\frac{|v-v_*|^2}{\sigma_1}}}{\int_{v_m}^{v_M} e^{-\frac{|v-v_*|^2}{\sigma_1}} dv} + P\dfrac{(v_M - v)^2}{\int_{v_m}^{v_M}(v_M - v)^2 dv}, & v_* \leq v^* \\ P\dfrac{e^{-\frac{|v-v_*|^2}{\sigma_2}}}{\int_{v_m}^{v_M} e^{-\frac{|v-v_*|^2}{\sigma_2}} dv} + (1-P)\dfrac{v_M - v}{\int_{v_m}^{v_M}(v_M - v) dv}, & v_* > v^* \end{cases} \tag{5.3.8}$$

where $P = \alpha u(1-\rho^p)$. Accordingly, the probability density (5.3.8) can be rewrites as follows

$$\mathcal{A}[f](v_* \to v) = \Big(H(v^* - v_*)\Big((1-P)\frac{e^{-\frac{|v-v_*|^2}{\sigma_1}}}{\int_{v_m}^{v_M} e^{-\frac{|v-v_*|^2}{\sigma_1}} dv} + P\frac{(v_M - v)^2}{\int_{v_m}^{v_M}(v_M - v)^2 dv}\Big)$$

$$+ (1 - H(v_* - v^*))\Big(P\frac{e^{-\frac{|v-v_*|^2}{\sigma_2}}}{\int_{v_m}^{v_M} e^{-\frac{|v-v_*|^2}{\sigma_2}} dv} + (1-P)\frac{v_M - v}{\int_{v_m}^{v_M}(v_M - v) dv}\Big)\Big)\chi_{[v_m, v_M]}(v). \tag{5.3.9}$$

5.3.5 Modelling external action

Let us now consider the modeling of external action which indicate a prescribed speed as it occurs, as an example, in the presence of tollgates. The structure of this term is reported in Eq. (5.2.14), where f_e is a given function (for instance a step-wise function) of the prescribed velocity $v_e = v_e(x)$. Therefore, the simplicity of Eq. (5.2.14) simply means that only the rate μ needs to be modelled. Following the same rationale applied to η, the following can be used:

$$\mu[f] = \eta_0\,(1 + \gamma_\mu\,\rho^p[f]), \tag{5.3.10}$$

where γ_μ is the growth coefficient and ρ^p is the perceived density.

5.3.6 Parameters and critical analysis

This section has proposed a simple modeling of the interaction terms to be implemented into the structure delivered by Eq. (5.2.16). The model includes the following parameters which related to specific different phenomena in vehicular traffic flows:

- α which models the quality of the road-weather conditions;
- ℓ_v which is length of the sensitivity zone Ω_ℓ. It depends on quality of the road-weather conditions α ($\ell_v = \alpha L$);
- η_0 which is the minimal value corresponding to driving in vacuum conditions;
- γ_η and γ_μ which are, respectively, the growth coefficients of the encounter rate η and the intensity of the action μ.

Bering the proposed modeling of the interaction terms in mind, one gets the following derived model

$$\begin{aligned}
&\partial_t f(t,x,v|u) + v\partial_x f(t,x,v|u) + \mathcal{F}[f](t,x,v|u)\partial_v(f(t,x,v|u)) \\
&\quad = \int_{[0,1]^3} \eta[f]\mathcal{A}[f](v_* \to v)\, f(t,x,v_*,u)\, f(t,x,v^*,u^*) dv_*\, dv^*\, du^* \\
&\quad - f(t,x,v|u)\int_{[0,1]^2} \eta[f]\, f(t,x,v^*,u^*) dv^*\, du^* + \alpha\, u\, \ell_v\, f(t,x,v|u)\, I_2(t,x) \\
&\qquad + \mu[f]\big(f_e(x, v_e(x)) - f(t,x,v|u)\big).
\end{aligned} \tag{5.3.11}$$

It is worth mentioning that in this work we proposed a generalized probability density (5.3.9) by taking inspiration on the table of games with the discrete variables of velocity and activity case proposed by [21]. Moreover, we considered the nonlinear interactions by taking into account the perceived density ρ^p and the mean field interactions, which are one of the paradigms of the complexity in vehicular traffic field. We would like to stress that only a few works can be found in the field proposing a modeling of the probability density based on the continuous velocity variable. Namely, the authors in [83] proposed two models of $\mathcal{A}$: the first is the quantified acceleration model, in which the post-interactions after an acceleration is obtained by a velocity jump. The second model is actually based on the paper by [67] which assumed that the interaction result between the candidate and field particles is uniformly distributed in a velocity interval.

5.4 Simulations toward validation of models

This section is devoted to the computational analysis toward validation of spatially homogeneous and inhomogeneous problems. In the first subsection, after the description of numerical scheme of the spatially homogeneous problem, we will reproduce Kerner's fundamental diagrams for different values of the road conditions. The second subsection aims to reproduce some numerical simulations for the spatially inhomogeneous problem, namely we will show emerging of two clusters in the case of good and bad road conditions.

5.4.1 Spatially homogeneous problem

The spatially homogeneous problem provides some information on the trend of the system toward the equilibrium state (called fundamental diagrams), which can be duly compared with the measurements performed under uniform flow conditions (see e.g. [64]). We account for the spatial homogeneity by assuming that the kinetic distribution function is independent of the variable representing the space x. Consequently $\partial_x f = 0$, this implies $\rho^p = \rho$. Moreover, we neglect the mean field interactions and the external forces. Thus, the distribution function f is given by

$$f = f(t, v, u) : [0, T] \times [0, 1] \times [0, 1] \longrightarrow \mathbb{R}^+.$$

Under the above assumptions, model 5.3.11 is reduced to the following ordinary differential equation implemented with initial condition:

$$\begin{cases} \dfrac{df}{dt} = \eta[\rho]\Big(\displaystyle\int_{[0,1]^3} \mathcal{A}[\rho]\, f(t, v_*, u)\, f(t, v^*, u^*) dv_*\, dv^*\, du^* - f(t, v, u) \int_{[0,1]^2} f(t, v^*, u^*)\, dv^*\, du^* \Big) \\ f(0, v, u) = f_0(v, u) \in \mathbb{R}_+. \end{cases} \tag{5.4.1}$$

Recalling the probability density propriety (5.2.13), the above model (5.4.1) satisfies the ``mass conservation'' hypothesis, i.e. $\frac{d\rho}{dt} = 0$, as it is required in spatially homogeneous conditions. Consequently, model (5.4.1) can be written as follows

$$\begin{cases} \dfrac{df}{dt} = \eta[\rho_0]\Big(\displaystyle\int_{[0,1]^3} \mathcal{A}[\rho_0]\, f(t, v_*, u)\, f(t, v^*, u^*) dv_*\, dv^*\, du^* - f(t, v, u)\, \rho_0 \Big) \\ f(0, v, u) = f_0(v, u) \in \mathbb{R}_+. \end{cases} \tag{5.4.2}$$

For the existence and uniqueness of the solution of the spatially homogeneous model (5.4.2), we refer the reader to the Appendix A.
As it is mentioned above, the numerical simulations of Eq. (5.4.2) have been carried out to obtain the fundamental diagrams relating the flux $q(\rho)$, the kinetic energy $E(\rho)$ and the average velocity $\xi(\rho)$ to the vehicle density ρ at the equilibrium. We divide the velocity and activity variables into a certain number of cells and calculate the transition rates between the cells given by the above ordinary differential equation. We assume that the velocities and activities grid points are chosen uniformly:

$$v_i = \frac{i}{n}, \quad u_j = \frac{j}{m}, \quad i = 0, ..., n-1,\ j = 0, ..., m-1.$$

The discrete scheme over the variables v and u of model (5.4.2) is given by

$$\begin{cases} \dfrac{df_{i,j}}{dt} = \eta[\rho_0]\Big[\dfrac{1}{n^3\, m^2} \displaystyle\sum_{h,p=0}^{n-1} \sum_{k=0}^{m-1} \mathcal{A}^{ij}_{hp,k} f_{h,j}(t) f_{p,k}(t) - \frac{1}{n^2\, m} f_{i,j}(t) \rho_0 \Big], \\ \\ f_{i,j}(0) = f^0_{i,j}, \end{cases}$$

for $i = 0, ..., n-1$, $j = 0, ..., m-1$. $\mathcal{A}^{ij}_{hp,k}$ is the discrete passing probabilities calculate in each average of cells. Thus, it given by

$$\mathcal{A}^{i,j}_{hp,k} = n^3\, m^2 \int_{(\frac{i}{n}, \frac{h}{n}, \frac{p}{n})}^{(\frac{i+1}{n}, \frac{h+1}{n}, \frac{p+1}{n})} \int_{(\frac{j}{m}, \frac{k}{m})}^{(\frac{i+1}{m}, \frac{k+1}{m})} \mathcal{A}(v, v_*, v^*, u, u^*)\, dv\, dv_*\, dv^*\, du\, du^*.$$

The scheme under consideration has been numerically solved by using Runge-Kutta of order 4 method. We adopt the following set of variables: $u = 1$, $n = 31$, $\eta_0 = 1$, $\gamma_\eta = \frac{1}{\alpha}$. Moreover, we perform a different situations of road conditions by choosing different values of α. Namely, we consider $\alpha_1 = 0.95$, $\alpha_2 = 0.7$ and $\alpha_3 = 0.2$.

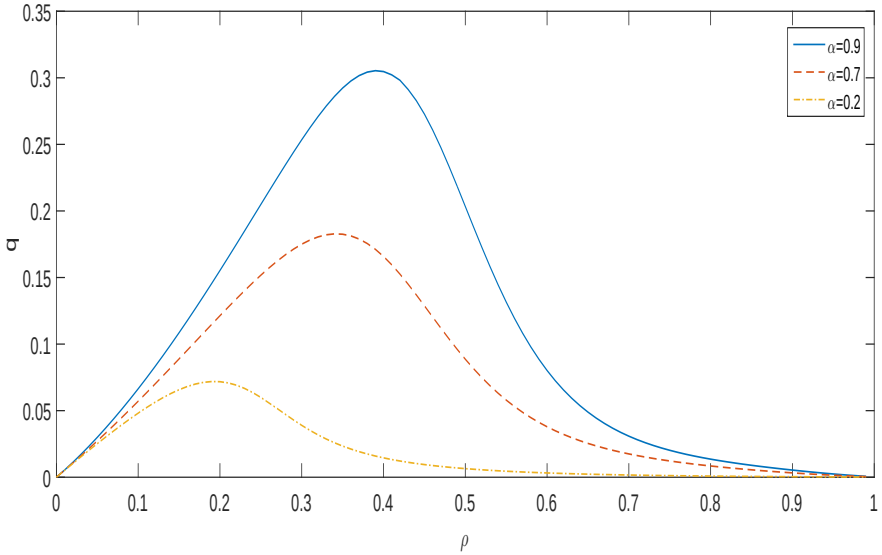

FIGURE 5.3: Fundamental diagram: flux q vs density ρ.

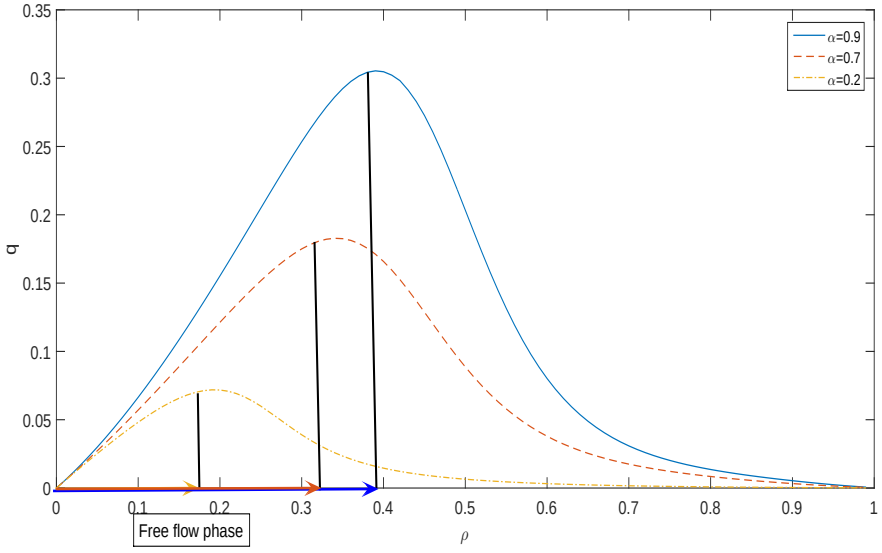

FIGURE 5.4: Free flow phase and fundamental diagram: flux q vs density ρ.

Figure 5.3 shows the obtained numerical results for different values of road conditions ($\alpha = 0.95,\ 0.7,\ 0.2$) for the density ρ against the flux q. We notice that for low density, the flux exhibits linear behaviour. While for high density, it decreases to zero and shows a critical change known as phase transition between the free and congested flow regime as it has been described experimentally by [64]. Finally, it is clear that the free flow phase reduces as the environmental conditions worsen, see Figure 5.4.

In Figure 5.5, we present the obtained numerical results for different values of road conditions ($\alpha = 0.95,\ 0.7,\ 0.2$) for the density ρ against the kinetic energy E. We observe that the kinetic

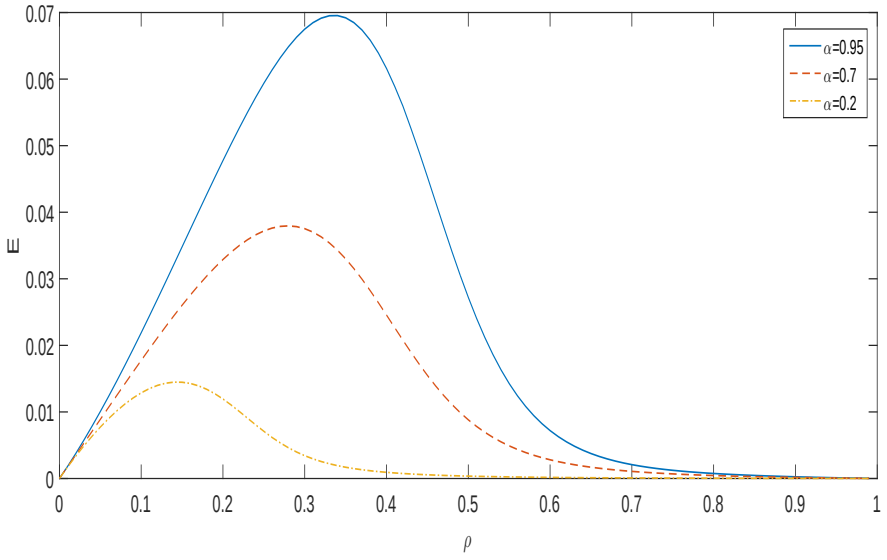

FIGURE 5.5: Fundamental diagram: kinetic energy E vs density ρ.

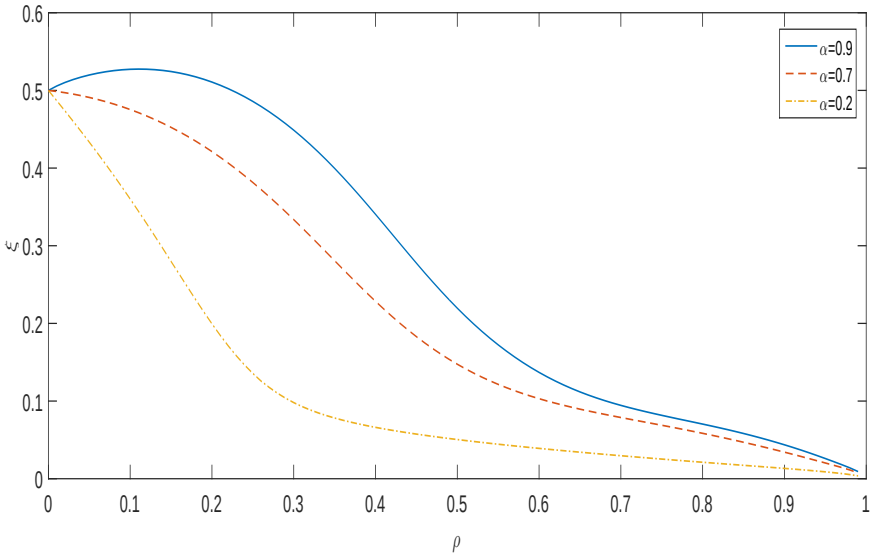

FIGURE 5.6: Fundamental diagram: mean velocity ξ vs density ρ.

energy increasing linearly in free flow situation. It decreases nonlinearly to zeros in the congested flow.

Figure 5.6 shows the obtained numerical results for different values of road conditions ($\alpha = 0.95,\ 0.7,\ 0.2$) for the density ρ against the mean velocity ξ. The average speed takes the maximum value for the low density. As the density increases, the average speed decreases in a nonlinear way to zeros which corresponds to the traffic jam.

We would like to mention the primordial role of road conditions α in the proposed probability density (5.3.9), which has been modelled to depict the quality of the environment. It has been considered one of the paradigms of the complexity in vehicular traffic field (see [21]). On the other hand, the obtained results are achieved without artificial insertion of the velocity diagram into the model itself ([38]).

5.4.2 Spatially inhomogeneous problem

In order to show the ability of our model to depict some phenomena in vehicular traffic flow field. Here, we are interested to the numerical method of the spatially inhomogeneous problem, where the mean field interactions is neglected. Thus, the model (5.3.11) is reduced to the following advection equation implemented with initial condition and the periodic boundary condition:

$$\begin{cases} \partial_t f(t,x,v,u) + v\partial_x f(t,x,v,u) = J[f,f] = G[f,f] + fL[f] + \mathcal{T}[f] \\ \quad = \int_{[0,1]^2} \eta[\rho^p(t,x)]\mathcal{A}[\rho^p(t,x)]\, f(t,x,v_*)\, f(t,x,v^*) dv_*\, dv^* \\ \qquad\qquad -f(t,x,v)\int_0^1 \eta[\rho^p(t,x)]\, f(t,x,v^*) dv^* \\ \qquad\qquad +\mu[\rho^p](f_e(x,v(e)) - f(t,x,v,u)), \\ f(t=0,x,v,u) = f_0(x,v,u), \quad f(t,0,v,u) = f(t,1,v,u), \end{cases} \tag{5.4.3}$$

where η and $\mathcal{A}$ this time depend on the perceived density ρ^p. μ is the intensity of the action given by Eq. (5.3.10) and f_e is a given function.

We introduce the following gridpoints:

$$x_i = i\, dx, \quad v_j = \frac{j+0.5}{N_v}, \quad u_s = \frac{s+0.5}{N_u}, \quad t^n = n\, dt, \quad dt = CFL\, dx,$$

for $i = 1,...,N_x$, $j = 0,...,N_v-1$, $s = 0,...,N_u-1$. Where CFL is Courant-Friedrichs-Lewy condition.
The full discrete scheme of inhomogeneous model (5.4.3) is given by

$$\begin{cases} \dfrac{f^{n+1}_{ijs} - f^n_{ijs}}{dt} + \dfrac{\Phi^n_{i,j,s} - \Phi^n_{i-1,j,s}}{dx} = G^n_{i,j,s} - f^n_{ijs} L^n_{i,j,s} + \mathcal{T}^n_{i,j,s} \\ f(t=0,x_i,v_j,u_s) = f^n_{ijs}, \quad f(t,0,v_j,u_s) = f(t,1,v_j,u_s), \end{cases}$$

for $i = 1,...,N_x$, $j = 1,...,N_v$, $s = 1,...,N_u$ and $n = 1,...,T$. The discrete distribution function is given by $f^n_{ijs} = f(t^n,x_i,v_j,u_s)$. The discritized gain and lose terms are given by

$$G^n_{i,j,s} = \sum_{h,p=1}^{N_v}\sum_{k=1}^{N_u} \eta^n_i[\rho^p]\, \mathcal{A}^n_{i,j,h,p,s,k}[\rho^p]\, f^n_{ihs} f^n_{ipk}\, dv^2\, du, \quad L^n_{i,j,s} = \sum_{p=1}^{N_v}\sum_{k=1}^{N_u} \eta^n_i[\rho^p]\, f^n_{ips}\, dv\, du,$$

where

$$\mathcal{A}^n_{i,j,h,p,s,k} = N_v^3 N_u^2 \int_{(\frac{j}{N_v},\frac{h}{N_v},\frac{p}{N_v})}^{(\frac{j+1}{N_v},\frac{h+1}{N_v},\frac{p+1}{N_v})} \int_{(\frac{s}{N_u},\frac{k}{N_u})}^{(\frac{s+1}{N_u},\frac{k+1}{N_u})} \mathcal{A}^n(v,v_*,v^*,u,u^*)\, dv\, dv_*\, dv^*\, du\, du^*,$$

and

$$\mathcal{T}^n_{i,j,s} = \mu^n_i[\rho^p]((f_e)_{ij} - f^n_{ijs}).$$

The flux Φ is chosen in order to get the conservation of mass and it given as follow

$$\Phi^n_{i,j,s} = v_j(f^n_{i-1,j,s} - f^n_{i-2,j,s}) + v_j \frac{dx}{2}\left(1 - \frac{v_j\, dt}{dx}\right)(\Psi_1 - \Psi_2),$$

where

$$\Psi_1 = \frac{f^n_{i,j,s} - f^n_{i-1,j,s}}{dx}\frac{f^n_{i-1,j,s} - f^n_{i-2,j,s}}{f^n_{ijs} - f^n_{i-1,j,s}}\phi, \quad \Psi_2 = \frac{f^n_{i-1,j,s} - f^n_{i-2,j,s}}{dx}\frac{f^n_{i-2,j,s} - f^n_{i-3,j,s}}{f^n_{i-1,j,s} - f^n_{i-2,j,s}}\phi,$$

where ϕ is the flux-limiter [73]. In our case, we consider Superbee flux-limiter defined by

$$\phi(\theta) = \max(\max(0, \min(1, 2\theta)), \min(\theta, 2)).$$

Parameters	Values
Activity u	1
Road conditions α	0.3, 0.95
Number of space points N_x	101
Number of velocity cells N_v	31
CFL condition	0.7
Growth coefficients of the encounter rate γ_η	$1/\alpha$

TABLE 5.1: Values of the used parameters.

Application: emerging of two clusters

In this example, we aim to reproduce the numerical simulations of the emerging of two clusters of vehicles travelling with different speeds on a closed road and having different density. We assume that there is no external force and that the first cluster travels with the maximum velocity $v_M = 1$, and has the following initial density

$$\rho(0, x) = 100 \sin^2(10\pi(x - 0.2)(x - 0.3)), \quad x \in [0.2, 0.3],$$

the other one travels with the velocity $v_M - 3\,dv$ and has the following initial density

$$\rho(0, x) = 50 \sin^2(10\pi(x - 0.5)(x - 0.6)), \quad x \in [0.5, 0.6].$$

Figure 5.7 shows the result of simulation in bad road conditions ($\alpha = 0.2$). We notice that the fast group of vehicles after have reached the slow ones (Figure 5.7(b)), have a mixing period (Figure 5.7(c)). Finally, two groups merge and transport as a one group (Figure 5.7(d)).

We show in Figure 5.8 the numerical results in good road conditions ($\alpha = 0.95$). We observe that fast group of vehicles reach the slow ones, as indicated in (Figure 5.7(b)), having a mixing period (Figure 5.7(c)). Finally, fast group overtake the slow ones (Figure 5.7(d)).

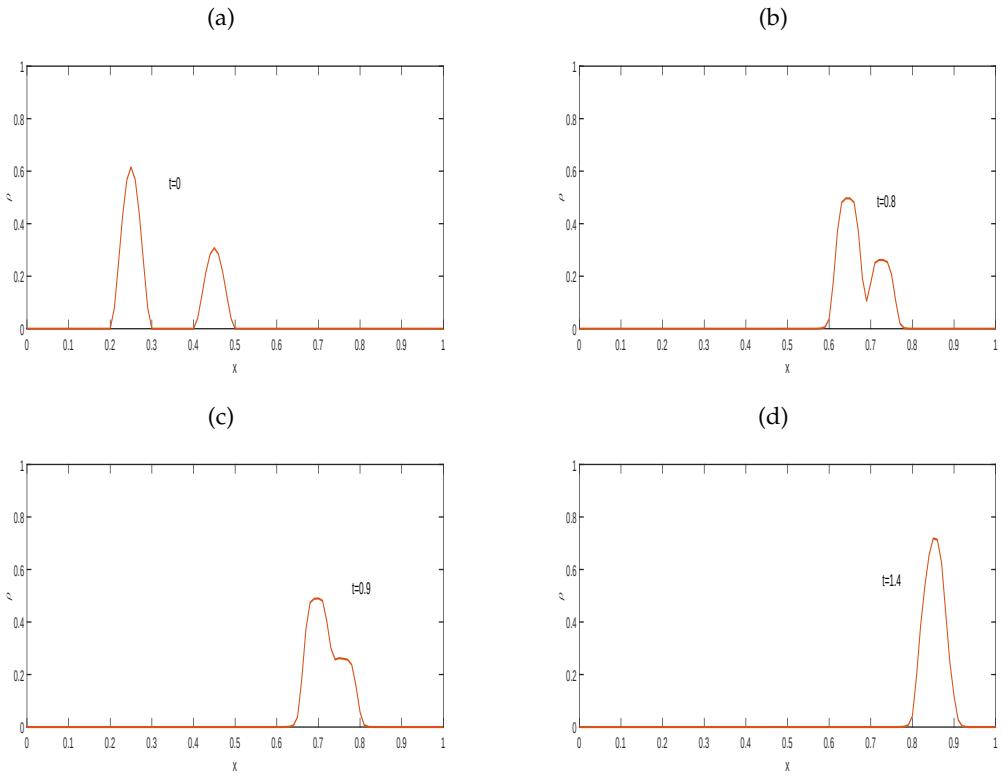

FIGURE 5.7: Evolution of two clusters in the case of bad road condition ($\alpha = 0.3$).

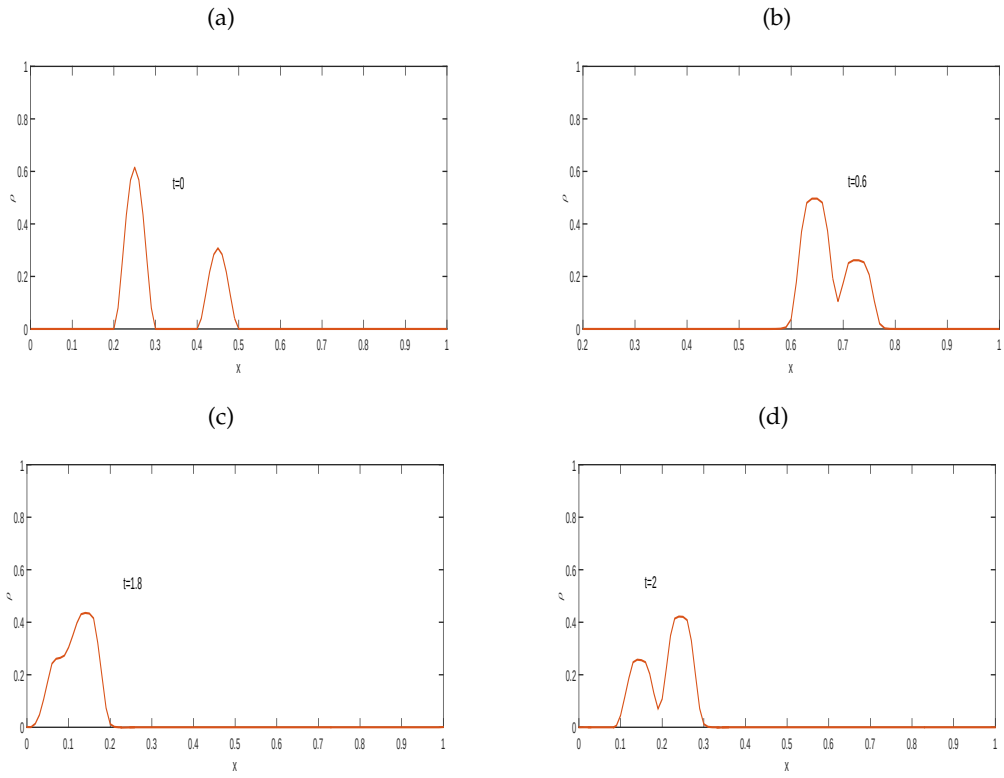

FIGURE 5.8: Evolution of two clusters in the case of good road condition ($\alpha = 0.95$).

Chapter 6

Conclusion and perspectives

6.1 Summary

This thesis has been devoted to the modeling and mathematical analysis of complex systems in biology and vehicular traffic on the basis of kinetic theory and macroscopic-fluid approaches. The aims were to propose and to study a new mathematical models which improve some interesting characteristics of already existing models. On the other hand, these proposed models are suitable for mathematical modeling investigations. In the first part, we successfully proposed two new macroscopic systems and two new kinetic-fluid models describing the interacting biological species living in complex medium. The second part of this thesis dealt with vehicular traffic flow on the basis of kinetic theory of active particles. Here also, we are successfully proposed and studied a new general mathematical structure according to a kinetic theory approach. It includes the features of the complex system under consideration which appear to be the most important aspects of the dynamics to be retained by the modeling approach. Namely heterogeneity of the driver-vehicle subsystem, aggregation dynamics for vehicles with closed each other velocity, passing probability, variable properties of the road-environment where the dynamics occur and role of the external actions. The most important achievements in this thesis can be summarized as follows:

• **Kinetic-fluid derivation and mathematical analysis of cross-diffusion-Brinkman system**. We have proposed a new nonlinear cross-diffusion system coupled to a stationary fluid. The micro-macro decomposition has been applied to derive this system from kinetic-fluid model. Moreover, we have proved the existence of weak solutions of the derived system by using Schauder fixed-point theory. Finally, it has shown that the presented numerical scheme enjoys the asymptotic preserving property. In other words, when Knudsen parameter ε is small, our scheme is asymptotically equivalent to a standard numerical scheme of the derived cross-diffusion-fluid system.

• **Kinetic-fluid derivation and mathematical analysis of nonlocal cross-diffusion-fluid system**. We have proposed a new generalized nonlocal cross-diffusion model for multi-interacting populations coupled to non-stationary fluid. The proposed model has been derived from an improved nonlocal kinetic-fluid model by using the micro-macro decomposition technique. On the basis of nonlinear Galerkin method, we have proved the existence of weak solutions for the proposed system. Moreover, we have developed an asymptotic preserving numerical schemes (AP). Simultaneously, we have reproduced some interesting phenomena such as the pattern-formation induced by cross-diffusion terms and convection of species caused by the fluid motion. Motivated by the obtained numerical simulation in 1D, we shown the effect of nonlocal diffusion together with cross-diffusion, as well as fluid flow in an explicit form of the fluid velocity on the interactions of populations. Finally, we have demonstrated the effect of external forces (obstacle interior de domain and the force of gravity) on the dynamic of fluid flow and simultaneously on the behavior of interacting populations.

• **Multiscale continuum-velocity kinetic model for vehicular traffic with local and mean field interactions**. We have proposed a mew mathematical structure on the basis of the kinetic theory for active particles. The purpose was to provide further developments of interest for the applications and to treat the following modeling topics: Interactions, both local and long distance,

between vehicles accounting on perceived (rather than real ones) quantities of the flow of vehicles, role of variable road conditions, and dynamics under external actions such as presence of tollgates.

6.2 Looking ahead for perspectives

In our opinion, this thesis opens up several research perspectives.

• **Development of asymptotic preserving numerical schemes in 2D.** A natural extension of our presented works in chapters 2-3 would be the development of an asymptotic preserving numerical schemes in 2D. We think that our proposed numerical schemes en the basis of the finite volume method can be extended to this aim, one only has to well choose the meshes. However, one has to overtake the drawback of the computational cost.

• **Anisotropic model with degenerate diffusion.** In fact, we have in mind many models that can be studied by an improved developed techniques. The future works include the derivation and mathematical analysis of the following anisotropic model with degenerate diffusion

$$\begin{cases} \partial_t u_1 - \operatorname{div}\Big(a(x)\nabla u_1 + b(x)\,\nabla u_2\Big) = H_1(u_1,u_2), \\ \\ \partial_t u_2 - \operatorname{div}\Big(c(x)\nabla u_1 + d(x)\,\nabla u_2\Big) = H_2(u_1,u_2). \end{cases}$$

• **Other numerical applications for vehicular traffic flow.** A natural extension of our work in chapter 5 would be the development of other numerical applications. As it mentioned, our proposed model (5.2.16) brings together all the following modeling topics: Interactions, both local and long distance, between vehicles accounting on perceived (rather than real ones) quantities of the flow of vehicles, role of variable road conditions, and dynamics under external actions such as presence of tollgates. We have successfully reproduced the fundamental diagrams in the homogeneous case and the emerging of two clusters. However, we think that it is so interesting to seek for other applications such as the bottleneck, tallgates and stop and go waves phenomena. We stress that one has to reduce the complexity of the numerical cost.

• **On the modeling of multilane traffic flow by kinetic theory for active particles [61].** Another possible extension of the kinetic model proposed in chapter 5 is the derivation of new models being able to describe the multilane traffic flow. This was the aim of an article in preparation where we propose the following model

$$\begin{aligned} &\partial_t f_{ij}^{\ell}(t,x) + v_i \partial_x f_{ij}^{\ell}(t,x) = J_{ij}^{\ell}[f](t,x) \\ &= \sum_{r,s=1}^{L}\sum_{h,p=1}^{n}\sum_{k,q=1}^{m}\int_x^{x+\xi} \eta^r[\rho_r(t,x^*),x]\mathcal{A}_{hk,pq,rs}^{i,j,\ell} f_{h,k}^r(t,x) f_{p,q}^s(t,x^*)dx^* \\ &\quad - f_{ij}^{\ell}(t,x)\sum_{s=1}^{L}\sum_{p=1}^{n}\sum_{q=1}^{m}\int_x^{x+\xi}\eta^{\ell}[\rho_{\ell}(t,x^*),x] f_{p,q}^s(t,x^*)dx^*, \end{aligned}$$

for $i = 1,\dots,n,\ j = 1,\dots,m$, and $\ell = 1,\dots,L$. In the proposed model above

- $x^* \in J_\xi = [x, x+\xi]$, with J_ξ represents the visibility zone;
- $\eta^{\ell}[\rho_{\ell}(t,x^*),x]$ is the encounter rate, it depends on the probability distributions by means of the density ρ_ℓ in the $\ell-$lane.
- $\mathcal{A}_{hk,pq,rs}^{i,j,\ell}[v_h \to v_i, u_k \to u_j, y_r \to y_l | v_h, v_p, u_k, u_q, y_r, y_s, \rho_\ell(t,x^*)]$ defines the table of games, which denotes the probability density that the candidate particle (v_h, u_k, y_r) falls into the state (v_i, u_j, y_l) of the test particle after an interaction with a field particle (v_p, u_q, y_s).

Appendix A

Mathematical analysis of the spatially homogeneous problem

In this appendix, we prove the existence and uniqueness of solution in the spatially homogeneous case associated to model (5.2.16). Thus, the distribution function f is given by

$$f = f(t,v) : [0,T] \times [0,1] \longrightarrow \mathbb{R}.$$

Consequently, the Initial Value Problem (IVP) is given by

$$\begin{cases} \dfrac{df}{dt} = \eta[\rho_0]\Big(\displaystyle\int_0^1 \int_0^1 \mathcal{A}[\rho_0](v_* \to v|\alpha,u)\, f(t,v_*)\, f(t,v^*) dv_*\, dv^* - f(t,v)\rho_0 \Big) \\ f(0,v) = f_0(v) \in \mathbb{R}_+. \end{cases} \tag{A.0.1}$$

Remarks:

- The distribution function f is independent of the variable x. Consequently $\partial_x f = 0$, which gives $\rho^p = \rho$. Moreover, by integrating over v the IVP (A.0.1) once get the integral of source term equals 0, then gets $\rho(t) = \rho_0$.
- The encounter rate is defined by $\eta[\rho_0] = \eta_0(1 + \gamma_\eta \rho_0)$. Then, there exists a constant C_η such that
$$0 < \eta[\rho_0] \leq C_\eta.$$
- The probability density is defined by

$$\begin{aligned} \mathcal{A}[\rho_0](v_* \to v) \quad = \quad & \Bigg(H(v^* - v_*)\Big((1-P) \frac{e^{-\frac{|v-v_*|^2}{\sigma_1}}}{\int_{v_m}^{v_M} e^{-\frac{|v-v_*|^2}{\sigma_1}} dv} + P \frac{(v_M - v)^2}{\int_{v_m}^{v_M} (v_M - v)^2 dv} \Big) \\ & + (1 - H(v_* - v^*))\Big(P \frac{e^{-\frac{|v-v_*|^2}{\sigma_2}}}{\int_{v_m}^{v_M} e^{-\frac{|v-v_*|^2}{\sigma_2}} dv} + (1-P) \frac{v_M - v}{\int_{v_m}^{v_M} (v_M - v) dv} \Big) \Bigg) \chi_{[v_m, v_M]}(v) \end{aligned}$$

  where $P = \alpha u(1-\rho_0), \sigma_1 = \alpha u(1-\rho_0)/200, \sigma_2 = (1 - \alpha u(1-\rho_0))/200, v_m = \max\{0, \min\{v_*, v^*\} - (1-\alpha u)\rho_0(|v_* - v^*| + \exp(-|v_* - v^*|))/200\}$ and $v_M = \min\{1, \max\{v_*, v^*\} + \alpha u(1 - \rho_0)(|v_* - v^*| + \exp(-|v_* - v^*|))/200\}$.

We introduce the following space $X_T = C([0,T]; \mathrm{L}^1([0,1]))$ for some $T > 0$, equipped with the norm

$$||f|| = \sup_{t \in [0,T]} ||f(t,.)||_1 = \sup_{t \in [0,T]} \int_0^1 |f(t,v)| dv.$$

A.1 Local existence

Theorem A.1.1 *Let $\rho_0 \in [0,1]$ Then there exists a unique function f solution to the IVP (3.4.12) such that f is non-negative and such that*

$$||f(t,.)||_1 = ||f_0(.)||_1 = \rho_0, \quad \forall t \in [0,T]. \tag{A.1.1}$$

Proof A.1.1 *In the sequel we denoted the term source by $Q[f,f]$ defined by*

$$Q[f,f](t,v) = \eta[\rho_0]\Big(\int_0^1\int_0^1 \mathcal{A}[\rho_0](v_* \to v|\alpha,u)\, f(t,v_*)\, f(t,v^*)dv_*\, dv^* - f(t,v)\rho_0\Big).$$

The proof of this theorem is based on the two following Lemmas:

Lemma A.1.1 *There exists a constant $C > 0$ such that*

$$||Q[f,f](t,.)||_1 \leq C||f(t,.)||_1^2, \tag{A.1.2}$$

$$||Q[f,f](t,.) - Q[g,g](t,.)||_1 \leq C\Big(||f(t,.)||_1 + ||g(t,.)||_1\Big)||f(t,.) - g(t,.)||_1. \tag{A.1.3}$$

Let $R(f)(t,v) = \int_0^t Q[f,f](s,v)ds$, then one have the following Lemma

Lemma A.1.2 *The operator R is continuous map from X to X. Moreover, $\exists C > 0$ such that*

$$||R(f)|| \leq CT||f||^2, \tag{A.1.4}$$

$$||R(f) - R(g)|| \leq CT\Big(||f|| + ||g||\Big)||f - g||. \tag{A.1.5}$$

After integrating Eq.(3.4.12) over the interval $[0,t]$, $t \in [0,T]$, it can be written in the form of integral equation

$$f = N(f)$$

where

$$N(f)(t,v) = f_0(v) + \int_0^t Q[f,f](s,v)ds.$$

From the Lemma A.1.2, we have the following estimates

$$||N(f)|| \leq ||f_0(.)||_1 + CT||f||^2, \tag{A.1.6}$$

$$||N(f) - N(g)|| \leq CT\Big(||f|| + ||g||\Big)||f - g||. \tag{A.1.7}$$

In order to apply the Banach fixed point method, the operator N should verify the following estimates

$$||N(f)|| \leq ||f||, \tag{A.1.8}$$

$$||N(f) - N(g)|| \leq L||f - g||, \qquad L \in [0,1[. \tag{A.1.9}$$

By comparing the estimates $(9) - (11)$, the solution of the following equation

$$||f_0(.)||_1 + CT||f||^2 - ||f|| = 0$$

Assume that $\Delta = 1 - 4CT|f_0(.)||_1 > 0$ that implies the condition on T

$$T \leq \frac{1}{4C|f_0(.)||_1}$$

In the oder hand, one can choose to solve

$$CT2r = \frac{1}{2} \Rightarrow r = \frac{1}{4CT} \geq ||f||.$$

The operator N is a contraction on a ball in X_T of radius r, then there exists a unique local solution f of Eq. (3.4.12) on $[0,T]$.

In order to finish to proof of the theorem it remains the positivity of the solution. After multiplying Eq.(3.4.12) by $\exp(R)$ and integrating over $[0,t]$, we get

$$N(f)(t,v) = f(t,v) = \exp(-\eta[\rho_0]\rho_0 t)f_0(v) + \int_0^t \exp(\eta[\rho_0]\rho_0(s-t))\eta[\rho_0]$$

$$\cdot \int_0^1 \int_0^1 \mathcal{A}[\rho_0](v_* \to v) f(s,v_*) f(s,v^*)\, dv_*\, dv^* ds.$$

The operator N maps X_T^+ into itself if $f_0(v)$ is positive. That closed the proof of the theorem.

A.2 Global existence

Thanks to the existence of local solution in time and the estimate (A.1.2), we can prove the existence of global solution in time to our problem (3.4.12).

Theorem A.2.1 *The problem (3.4.12) admits a unique nonnegative global solution $f \in C([0,+\infty); \mathrm{L}^1([0,1])$ satisfying the estimate (A.1.2).*

Proof A.2.1 *It suffices to apply the same reasoning developed in the proof of Theorem 1 on the interval $(T,2T]$, taking $f(T,v)$ as new initial condition. Since $f(T) \geq 0$ and moreover $\int_0^1 f(T,v)dv = \rho_0 \in [0,1]$ we are in the same hypotheses of Theorem 4.1, hence we can conclude on the existence and uniqueness of a local solution on $[T,2T]$ satisfying the estimate*

$$||f(t,.)||_1 = ||f(T,.)||_1, \qquad \forall t \in (T,2T]$$

Therefore a unique solution $f(t,v)$ to the problem (3.4.12) in the whole interval $(0,2T]$ is found. Iterating this procedure on all intervals of the form $(kT,(k+1)T]$, $k \in N$, we can construct the global solution on $\mathbb{R}_+$.

Bibliography

[1] V. Anaya, M. Bendahmane, D. Mora, R Oyarzúa, and R. Ruiz-Baier. A priori and a posteriori error analysis of a fully-mixed scheme for the brinkman problem. *Numer. Math.*, 133(4):781–817, 2016.

[2] V. Anaya, M. Bendahmane, D. Mora, and R. Ruiz-Baier. On a vorticity-based formulation for reaction-diffusion-Brinkman systems. *Netw. Heterog. Media*, 13(1):69–94, 2018.

[3] V. Anaya, M. Bendahmane, and M. Sepúlveda. A numerical analysis of a reaction-diffusion system modelling the dynamics of growth tumors. *Math. Models Methods Appl. Sci.*, 20(5):731–756, 2010.

[4] V. Anaya, M. Bendahmane, and M. Sepúlveda. Numerical analysis for a three interacting species model with nonlocal and cross diffusion. *ESAIM Math. Model. Numer. Anal.*, 49(1):171–192, 2015.

[5] V. Anaya, G. N. Gatica, D. Mora, and R. Ruiz-Baier. An augmented velocity-vorticity-pressure formulation for the Brinkman equations. *Internat. J. Numer. Methods Fluids*, 79(3):109–137, 2015.

[6] B. Andreianov, M. Bendahmane, and R. Ruiz-Baier. Analysis of a finite volume method for a cross-diffusion model in population dynamics. *Math. Models Methods Appl. Sci.*, 21(2):307–344, 2011.

[7] A. Atlas, M. Bendahmane, F. Karami, D. Meskine, and M. Zagour. Kinetic-fluid derivation and mathematical analysis of nonlocal cross-diffusion-fluid system. *Submitted*, 2018.

[8] J. Banasiak and M. Lachowicz. *Methods of small parameter in mathematical biology*. Modeling and Simulation in Science, Engineering and Technology. Birkhäuser/Springer, Cham, 2014.

[9] J. W. Barrett and J. F. Blowey. Finite element approximation of a nonlinear cross-diffusion population model. *Numer. Math.*, 98(2):195–221, 2004.

[10] N. Bellomo and A. Bellouquid. On the onset of non-linearity for diffusion models of binary mixtures of biological materials by asymptotic analysis. *International Journal of Non-Linear Mechanics*, 41(2):281–293, 2006.

[11] N. Bellomo, A. Bellouquid, and N Chouhad. From a multiscale derivation of nonlinear cross-diffusion models to keller-segel models in a navier-stokes fluid. *Math. Models Methods Appl. Sci.*, 26:2041–2069, 2016.

[12] N. Bellomo, A. Bellouquid, L. Gibelli, and N. Outada. *A quest towards a mathematical theory of living systems*. Springer, 2017.

[13] N. Bellomo, A. Bellouquid, J. Nieto, and J. Soler. Multiscale biological tissue models and flux-limited chemotaxis for multicellular growing systems. *Math. Models Methods Appl. Sci.*, 20(7):1179–1207, 2010.

[14] N. Bellomo, A. Bellouquid, J. Nieto, and J. Soler. On the asymptotic theory from microscopic to macroscopic growing tissue models: an overview with perspectives. *Math. Models Methods Appl. Sci.*, 22(1):1130001, 37, 2012.

[15] N. Bellomo, A. Bellouquid, J. Nieto, and J. Soler. On the multiscale modeling of vehicular traffic: from kinetic to hydrodynamics. *Discrete Contin. Dyn. Syst. Ser. B*, 19(7):1869–1888, 2014.

[16] N. Bellomo, A. Bellouquid, Y. Tao, and M. Winkler. Toward a mathematical theory of Keller-Segel models of pattern formation in biological tissues. *Math. Models Methods Appl. Sci.*, 25(9):1663–1763, 2015.

[17] N. Bellomo, M. Delitala, and V. Coscia. On the mathematical theory of vehicular traffic flow. I. Fluid dynamic and kinetic modelling. *Math. Models Methods Appl. Sci.*, 12(12):1801–1843, 2002.

[18] N. Bellomo and C. Dogbé. On the modeling of traffic and crowds: a survey of models, speculations, and perspectives. *SIAM Rev.*, 53(3):409–463, 2011.

[19] N. Bellomo, D. Knopoff, and J. Soler. On the difficult interplay between life, "complexity", and mathematical sciences. *Math. Models Methods Appl. Sci.*, 23(10):1861–1913, 2013.

[20] A. Bellouquid. On the asymptotic analysis of the BGK model toward the incompressible linear Navier-Stokes equation. *Math. Models Methods Appl. Sci.*, 20(8):1299–1318, 2010.

[21] A. Bellouquid, E. De Angelis, and L. Fermo. Towards the modeling of vehicular traffic as a complex system: a kinetic theory approach. *Math. Models Methods Appl. Sci.*, 22(suppl. 1):1140003, 35, 2012.

[22] A. Bellouquid and J. Tagoudjeu. An asymptotic preserving scheme for kinetic models for chemotaxis phenomena. *Communications in Applied and Industrial Mathematics*, (1):ahead–of–print, 2018.

[23] M. Bendahmane. Weak and classical solutions to predator-prey system with cross-diffusion. *Nonlinear Anal.*, 73(8):2489–2503, 2010.

[24] M. Bendahmane, F. Karami, and M. Zagour. Kinetic-fluid derivation and mathematical analysis of the cross-diffusion-brinkman system. *Math. Meth. Appl. Sci.*, 41:6288–6311, 2018.

[25] M. Bendahmane and M. Langlais. A reaction-diffusion system with cross-diffusion modelling the spread of an epidemic disease. *Journal of Evolution Equations*, 10(4):883–904, 2010.

[26] M. Bennoune, M. Lemou, and L. Mieussens. An asymptotic preserving scheme for the Kac model of the Boltzmann equation in the diffusion limit. *Contin. Mech. Thermodyn.*, 21(5):401–421, 2009.

[27] D. Burini and N. Chouhad. Hilbert method toward a multiscale analysis from kinetic to macroscopic models for active particles. *Math. Models Methods Appl. Sci.*, 27(7):1327–1353, 2017.

[28] J. Calvo, J. Nieto, and M. Zagour. Multiscale continuum-velocity kinetic model for vehicular traffic with local and mean field interactions. *In preparation*, 2018.

[29] J. A. Carrillo and B. Yan. An asymptotic preserving scheme for the diffusive limit of kinetic systems for chemotaxis. *Multiscale Model. Simul.*, 11(1):336–361, 2013.

[30] F. A. C. C. Chalub, P. A. Markowich, B. Perthame, and C. Schmeiser. Kinetic models for chemotaxis and their drift-diffusion limits. *Monatsh. Math.*, 142(1-2):123–141, 2004.

[31] M. Chamoun, G. Saad and R. Talhouk. A coupled anisotropic chemotaxis-fluid model : The case of two sidedly degenerate diffusion. *Comput. Math. Appl.*, 68:1052–1070, 2014.

[32] N. H. Chang and M. Chipot. Nonlinear nonlocal evolution problems. *RACSAM. Rev. R. Acad. Cienc. Exactas Fıs. Nat. Ser. A Mat*, 97(3):423–445, 2003.

[33] L. Chen and A. Jüngel. Analysis of a multi-dimensional parabolic population model with strong cross diffusion. *SIAM J. Math. Anal.*, 36:301–322, 2004.

[34] L. Chen and A. Jüngel. Analysis of a parabolic cross-diffusion population model without self-diffusion. *J. Differential Equations*, 224(1):39–59, 2006.

[35] L. Chen and A. Jüngel. Analysis of a parabolic cross-diffusion population model without self-diffusion. *J. Differential Equations*, 224(1):39–59, 2006.

[36] X. Chen, E.S. Daus, and A Jüngel. Global existence analysis of cross-diffusion population systems for multiple species. *Arch. Rational Mech. Anal.*, 227:715–747, 2018.

[37] M. Chipot and B. Lovat. Existence and uniqueness results for a class of nonlocal elliptic and parabolic problems. *Dynamics of Cont. discrt. and Impul. Syst.*, 8(1):35–52, 2001.

[38] R. M. Colombo. Hyperbolic phase transitions in traffic flow. *SIAM J. Appl. Math.*, 63(2):708–721, 2002.

[39] N. Crouseilles, H. Hivert, and M. Lemou. Numerical schemes for kinetic equations in the anomalous diffusion limit. Part I: The case of heavy-tailed equilibrium. *SIAM J. Sci. Comput.*, 38(2):A737–A764, 2016.

[40] C. F. Daganzo. Requiem for second-order fluid approximations of traffic flow. *Transportation Research Part B: Methodological*, 29(4):277–286, 1995.

[41] E. De Angelis. Nonlinear hydrodynamic models of traffic flow modelling and mathematical problems. *Math. Comput. Modelling*, 29(7):83–95, 1999.

[42] P. Degond, J. G. Liu, and L. Mieussens. Macroscopic fluid models with localized kinetic upscaling effects. *Multiscale Model. Simul.*, 5(3):940–979, 2006.

[43] M. Delitala and A. Tosin. Mathematical modelling of vehicular traffic: A discrete kinetic theory approach. *Math. Models Methods Appl. Sci.*, 17:901–932, 2006.

[44] L. Desvillettes, T. Lepoutre, and A. Moussa. Entropy, duality, and cross diffusion. *SIAM J. Math. Anal.*, 46(1):820–853, 2014.

[45] J. Deteix, A. Jendoubi, and D. Yakoubi. A coupled prediction scheme for solving the navier-stokes and convection-diffusion equations. *SIAM J. Numer. Anal.*, 52(5):2415–2439, 2014.

[46] R. Eymard, T. Gallout, and R. Herbin. *Finite volume methods.In: Handbook of Numerical Analysis*, volume vol. VII of *Biomathematics*. North-Holland, Amsterdam, 2000.

[47] Luisa Fermo and Andrea Tosin. A fully-discrete-state kinetic theory approach to modeling vehicular traffic. *SIAM J. Appl. Math.*, 73(4):1533–1556, 2013.

[48] F. Filbet, P. Laurençot, and B. Perthame. Derivation of hyperbolic models for chemosensitive movement. *J. Math. Biol.*, 50:189–207, 2005.

[49] G. Gambino, M. C. Lombardo, and M. Sammartino. A velocity-diffusion method for a Lotka-Volterra system with nonlinear cross and self-diffusion. *Appl. Numer. Math.*, 59(5):1059–1074, 2009.

[50] G. N. Gatica. *A simple introduction to the mixed finite element method. Theory and applications*. Springer, Briefs in Mathematics, Springer, Cham Heidelberg New York Dordrecht London, 2014.

[51] M. Gaultier and J. Lezaun. Equations de navier-stokes couplées à des équations de la chaleur: résolution par une méthode de point fixe en dimension infinie. *Ann. Sci. Math.*, 13:1–17, 1989.

[52] F. Golse, S. Jin, and C. D. Levermore. A domain decomposition analysis for a two-scale linear transport problem. *M2AN Math. Model. Numer. Anal.*, 37(6):869–892, 2003.

[53] D. Grošelj, F. Jenko, and E. Frey. How turbulence regulates biodiversity in systems with cyclic competition. *Phys. Rev. E*, 91:033009, 2015.

[54] P. Hartman and A. Wintner. Asymptotic integrations of linear differential equations. *Amer. J. Math.*, 77(1):45–86, 1955.

[55] A. Hasting and T. Powell. Chaos in a three-species food chain. *Ecology*, 72:896–903, 1991.

[56] F. Hecht. New development in freefem++. *J. of Numer. Math.*, 20:251–265, 2013.

[57] Dirk Helbing. Traffic and related self-driven many-particle systems. *Rev. Mod. Phys.*, 73:1067–1141, 2001.

[58] M. Herty and L. Pareschi. Fokker-Planck asymptotics for traffic flow models. *Kinet. Relat. Models*, 3(1):165–179, 2010.

[59] A. Jüngel. Diffusive and nondiffusive population models. In *Mathematical modeling of collective behavior in socio-economic and life sciences*, Model. Simul. Sci. Eng. Technol., pages 397–425. Birkhäuser Boston Inc. Boston MA, 2010.

[60] A. Jüngel. *Entropy Methods for Diffusive Partial Differential Equations*. Springer Briefs in Mathematics, 2016.

[61] F. Karami and M. Zagour. On the modeling of multilane traffic flow by kinetic theory for active particles. *In preparation*.

[62] E.F. Keller and L.A. Segel. The keller-segel model of chemotaxis. *J. Theor. Biol.*, 26:399–415, 1970.

[63] B. S. Kerner. *The physics of traffic*. Springer, New York, Berlin, 2004.

[64] B. S. Kerner. A theory of traffic congestion at heavy bottleneck. *J. of Phys. A*, 41(215101), 2008.

[65] A. Klar. Asymptotic-induced domain decomposition methods for kinetic and drift diffusion semiconductor equations. *SIAM J. Sci. Comput.*, 19(6):2032–2050, 1998.

[66] A. Klar, R. D. Kühne, and R. Wegener. Mathematical models for vehicular traffic. *Surveys Math. Indust.*, 6(3):215–239, 1996.

[67] A. Klar and R. Wegener. Enskog-like kinetic models for vehicular traffic. *J. Statist. Phys.*, 87(1-2):91–114, 1997.

[68] A. Klar and R. Wegener. Kinetic derivation of macroscopic anticipation models for vehicular traffic. *SIAM J. Appl. Math.*, 60(5):1749–1766, 2000.

[69] S. N. Kruzhkov. Results concerning the nature of the continuity of solutions of parabolic equations and some of their applications. *Mathematical Notes of the Academy of Sciences of the USSR*, 6(1):517–523, 1969.

[70] O. A. Ladyzhenskaya. *Mathematical theory of viscous incompressible flow*. Gordon and Breach Science Publishers Inc., 1968.

[71] M. Lemou and L. Mieussens. A new asymptotic preserving scheme based on micro-macro formulation for linear kinetic equations in the diffusion limit. *SIAM J. Sci. Comput.*, 31(1):334–368, 2008.

[72] P. Lenarda, M. Paggi, and R. Ruiz-Baier. Partitioned coupling of advection-diffusion-reaction systems and Brinkman flows. *J. Comput. Phys.*, 344:281–302, 2017.

[73] R. J. LeVeque. *Numerical methods for conservation laws*. Lectures in Mathematics ETH Zürich. Birkhäuser Verlag, Basel, second edition, 1992.

[74] J.L. Lions. *Quelques méthodes de r ésolution des problèmes aux limites non linéaires*. unod, Paris D, 1969.

[75] A. Lorz. Coupled chemotaxis fluid model. *Math. Models Methods Appl. Sci.*, 20(6):987–1004, 2010.

[76] P. Nelson. A kinetic model of vehicular traffic and its associated bimodal equilibrium solution. *Transp. Theory Stat. Phys.*, 24:383–409, 1995.

[77] A. Okubo. *Diffusion and ecological problems: mathematical models*, volume 10 of *Biomathematics*. Springer-Verlag, Berlin-New York, 1980. An extended version of the Japanese edition, ıt Ecology and diffusion, Translated by G. N. Parker.

[78] N. Outada, N. Vauchelet, T. Akrid, and M. Khaladi. From kinetic theory of multicellular systems to hyperbolic tissue equations: asymptotic limits and computing. *Math. Models Methods Appl. Sci.*, 26(14):2709–2734, 2016.

[79] S. L. Paveri Fontana. On boltzmann like treatments for traffic flow. *Transp. Res.*, 9:225–235, 1975.

[80] D. Poyato and J. Solar. Euler-type equations and commutators in singular and hyperbolic limits of kinetic cucker–smale models. *Math. Models Methods Appl. Sci.*, 27(6):1089–1152, 2017.

[81] I. Prigogine and R. Herman. *Kinetic Theory of Vehicular Traffic*. Elsevier, New York, 1971.

[82] G. Puppo, M. Semplice, A. Tosin, and G. Visconti. Analysis of a multi-population kinetic model for traffic flow. *Commun. Math. Sci*, 5(2):379–412, 2017.

[83] G. Puppo, M. Semplice, A. Tosin, and G. Visconti. Kinetic models for traffic flow resulting in a reduced space of microscopic velocities. *Kinet. Relat. Models*, 10(3):823–854, 2017.

[84] N. Shigesada and K. Kawasaki. *Biological invasions: theory and practice*. Oxford University Press, 1997.

[85] J. Simon. Compact sets in the space $l^p(0;t;b)$. *Ann. Mat. Pura Appl.*, 4:65–96, 1987.

[86] R. Temam. *Navier-Stokes Equations: Theory and Numerical Analysis*, volume 3rd edition of *North-Holland, Amsterdam*. reprinted in the AMS Chelsea series, AMS, Providence, 2001.

[87] C. Tian, Z. Lin, and M. Pedersen. Instability induced by cross-diffusion in reaction-diffusion systems. *Nonl. Anal.: Real World Appl.*, 11:1036–1045, 2010.

[88] I. Tuval, L. Cisneros, C. Dombrowski, C. W. Wolgemuth, J. O. Kessler, and R. E. Goldstein. Bacterial swimming and oxygen tansport near contact lines. *Proc. Natl. Acad. Sci. USA*, 102:2277–2282, 2005.

[89] P.S. Vassilevski and U. Villa. A mixed formulation for the brinkman problem. *SIAM J. Numer. Anal.*, 52(1):258–281, 2014.

[90] G. Visconti, M. Herty, G. Puppo, and A. Tosin. Multivalued fundamental diagrams of traffic flow in the kinetic Fokker-Planck limit. *Multiscale Model. Simul.*, 15(3):1267–1293, 2017.

[91] V. A. Volper. *Elliptic Partial Differential Equations*, volume vol. 104 of *Volume 2: Reaction-Diffusion Equations*. Monographs in Mathematics Birkhäuser, Basel, 2014.

[92] Z. Wen and S. Fu. Global solutions to a class of multi-species reaction-diffusion systems with cross-diffusions arising in population dynamics. *J. Comp. Appl. Math.*, 230:34–43, 2009.

[93] M. Winkler. Global weak solutions in a three-dimensional chemotaxis-navier-stokes system. *Ann. Henri Poincaré*, 33(5):1329–1359, 2016.

[94] M. Winkler. Stabilization in a two-dimensional chemotaxis-navier-stokes system. *Arch. Ration. Mech. Anal.*, 33:1329–1352, 2016.